NUREG/IA-0462

International Agreement Report

Uncertainty and Sensitivity Investigations with TRACE-SUSA and TRACE-DAKOTA by Means of Post-test Calculations of NUPEC BFBT Experiments

Prepared by:
Wadim Jaeger, Victor Hugo Sanchez Espinoza*
Francisco Javier Montero Mayorga, Cears Queral**

*Karlsruher Institute of Technology (KIT)
Institute for Neutron Physics and Reactor Technology (INR)
Hermann-von-Helmholtz-Platz 1
76344, Eggenstein-Leopoldshafen, Germany

**Universidad Politecnica de Madrd,
Departmento de Sistemas Energeticos ETSI Minas
28003 Madrid, Alenza 4, Spain

Kirk Tien, NRC Project Manager

Division of Systems Analysis
Office of Nuclear Regulatory Research
U.S. Nuclear Regulatory Commission
Washington, DC 20555-0001

Manuscript Completed: January 2014
Date Published: August 2017

Published by
U.S. Nuclear Regulatory Commission

AVAILABILITY OF REFERENCE MATERIALS IN NRC PUBLICATIONS

NRC Reference Material

As of November 1999, you may electronically access NUREG-series publications and other NRC records at the NRC's Public Electronic Reading Room at http://www.nrc.gov/reading-rm.html. Publicly released records include, to name a few, NUREG-series publications; *Federal Register* notices; applicant, licensee, and vendor documents and correspondence; NRC correspondence and internal memoranda; bulletins and information notices; inspection and investigative reports; licensee event reports; and Commission papers and their attachments.

NRC publications in the NUREG series, NRC regulations, and Title 10, "Energy," in the *Code of Federal Regulations* may also be purchased from one of these two sources.

1. **The Superintendent of Documents**
   U.S. Government Publishing Office
   Mail Stop SSOP
   Washington, DC 20402-0001
   Internet: http://bookstore.gpo.gov
   Telephone: 1-866-512-1800
   Fax: (202) 512-2104

2. **The National Technical Information Service**
   5301 Shawnee Road
   Alexandria, VA 22161-0002
   http://www.ntis.gov
   1-800-553-6847 or, locally, (703) 605-6000

A single copy of each NRC draft report for comment is available free, to the extent of supply, upon written request as follows:

U.S. Nuclear Regulatory Commission
Office of Administration
Publications Branch
Washington, DC 20555-0001
E-mail: distribution.resource@nrc.gov
Facsimile: (301) 415-2289

Some publications in the NUREG series that are posted at the NRC's Web site address http://www.nrc.gov/reading-rm/doc-collections/nuregs are updated periodically and may differ from the last printed version. Although references to material found on a Web site bear the date the material was accessed, the material available on the date cited may subsequently be removed from the site.

Non-NRC Reference Material

Documents available from public and special technical libraries include all open literature items, such as books, journal articles, transactions, *Federal Register* notices, Federal and State legislation, and congressional reports. Such documents as theses, dissertations, foreign reports and translations, and non-NRC conference proceedings may be purchased from their sponsoring organization.

Copies of industry codes and standards used in a substantive manner in the NRC regulatory process are maintained at—

The NRC Technical Library
Two White Flint North
11545 Rockville Pike
Rockville, MD 20852-2738

These standards are available in the library for reference use by the public. Codes and standards are usually copyrighted and may be purchased from the originating organization or, if they are American National Standards, from—

American National Standards Institute
11 West 42nd Street
New York, NY 10036-8002
http://www.ansi.org
(212) 642-4900

Legally binding regulatory requirements are stated only in laws; NRC regulations; licenses, including technical specifications; or orders, not in NUREG-series publications. The views expressed in contractor-prepared publications in this series are not necessarily those of the NRC.

The NUREG series comprises (1) technical and administrative reports and books prepared by the staff (NUREG-XXXX) or agency contractors (NUREG/CR-XXXX), (2) proceedings of conferences (NUREG/CP-XXXX), (3) reports resulting from international agreements (NUREG/IA-XXXX), (4) brochures (NUREG/BR-XXXX), and (5) compilations of legal decisions and orders of the Commission and Atomic and Safety Licensing Boards and of Directors' decisions under Section 2.206 of NRC's regulations (NUREG-0750).

NUREG/IA-0462

International Agreement Report

Uncertainty and Sensitivity Investigations with TRACE-SUSA and TRACE-DAKOTA by Means of Post-test Calculations of NUPEC BFBT Experiments

Prepared by:
Wadim Jaeger, Victor Hugo Sanchez Espinoza*
Francisco Javier Montero Mayorga, Cears Queral**

*Karlsruher Institute of Technology (KIT)
Institute for Neutron Physics and Reactor Technology (INR)
Hermann-von-Helmholtz-Platz 1
76344, Eggenstein-Leopoldshafen, Germany

**Universidad Politecnica de Madrd,
Departmento de Sistemas Energeticos ETSI Minas
28003 Madrid, Alenza 4, Spain

Kirk Tien, NRC Project Manager

Division of Systems Analysis
Office of Nuclear Regulatory Research
U.S. Nuclear Regulatory Commission
Washington, DC 20555-0001

Manuscript Completed: January 2014
Date Published: August 2017

Published by
U.S. Nuclear Regulatory Commission

ABSTRACT

Uncertainty and sensitivity investigations are performed with TRACE-SUSA and with TRACE-DAKOTA for thermal hydraulic simulations of selected BWR related experimental scenarios based on the NUPEC BFBT data base. Steady state as well as transient scenarios are selected to conduct a comprehensive investigation of BWR like phenomena. The steady state investigations include single and two phase flow pressure drop analyses, axial void fraction profiles and critical power predictions. The pressure losses and the void fractions are also predicted during two postulated BWR transients; a turbine trip and a trip of a re-circulation pump. The average error for the pressure losses, the void fractions and the critical power scenarios is in the order of ± 5 %. Parameters of the input and of the source code are selected for the uncertainty and sensitivity study. By means of sensitivity coefficients, a quantitative way of evaluating the system response is given. The analysis shows that even small variations can cause a rather large spread of the output parameter(s). The investigations show also that the width of the predicted uncertainty band is a function of parameters like the inlet sub cooling or the hydraulic diameter. In addition, shortcomings of the thermal hydraulic code/modeling or of the uncertainty and sensitivity tool(s) are given in order to help to improve the prediction capabilities.

FOREWORD

This assessment report deals with the application of the system code TRACE in combination with SUSA and DAKOTA for the quantification of uncertainties related to input and boundary conditions and empirical models. The subject of this report is the post-test analyses of experiments performed within the NUPEC BFBT benchmark which is related to BWRs. The results predicted by TRACE are in code agreement to the experiments and the associated uncertainty and sensitivity study quantifies the importance of the input and source code parameters on selected output parameters. Such studies help to identify areas for improvement of the system code but also help to better understand the physical feedbacks between different parameters.

CONTENTS

FIGURES

TABLES

EXECUTIVE SUMMARY

The scope of this report is to present TRACE results related to the post-test analyses of the NUPEC BWR Full-size Fine mesh Bundle Test (BFBT) benchmark. First of all, the investigations are valuable for the ongoing validation process of the best estimate system code. Second, the application of uncertainty and sensitivity methods together with TRACE helps to identify which parameters have the highest influence on the system behavior during various test scenarios. Therefore, the tools SUSA and DAKOTA are used for the quantification of input and boundary uncertainties as well as uncertainties related to source code parameters.

The quantification of uncertainties in the process of safety related investigations with best estimate thermal hydraulic codes is the latest step on the path to enhance the safety of nuclear installations. By means of best estimate codes more realistic values can be predicted for safety relevant parameters like the peak cladding temperature or the DNB. With the help of uncertainty analyses the influence of input parameter uncertainties can be considered (material properties, decay heat curve, temperature and mass flow rate profiles, etc.). Instead of one calculation as with conservative codes or best estimate codes without uncertainty, several calculations are necessary to show that not only the reference or best estimate case is within acceptance limits but also the combination of extremes (lowest mass flow rate possible combined with highest power possible).

In the context of this report several stationary and transient scenarios have been evaluated. A short summary of the investigation and findings is given hereafter

- Steady state scenarios:
    - Single-phase pressure drop: During this investigation 36 different combinations of system pressure, mass flow rate and inlet temperature have been investigated to evaluate the single-phase pressure drop. Thereby, typical BWR conditions are considered (70 bar, 560 K) as well as low pressure (2 bar) low temperature (310 K) cases. The overall evaluation yields an average error of less than 7 %. The largest discrepancies are found for the cases with the lowest mass flow rate. Deviations of up to 35 % are found. But in these cases the pressure drop is extremely small and amounts to just 1000 Pa. The most important parameters for the uncertainty and sensitivity analysis are related to geometrical uncertainties (exact hydraulic diameter of the bundle, form loss coefficients).
    - Two-phase flow pressure differences: Concerning the two-phase flow cases, 33 combinations of pressure, inlet sub-cooling, mass flow rate and assembly power are studied. The overall error is smaller as for the single phase cases and is less than 5 %. The reason for the lower deviation in two-phase flow then in single-phase flow might be origin from the different formalism. For single phase flow it is the pressure drop with considered geodetic height change while for the two-phase flow cases it is just the pressure difference between inlet and outlet. Therefore, also higher values are reported than for single phase flow and the problem of low pressure drop measurement is not pronounced. Parameters like the inlet temperature and the hydraulic diameter have the highest influence on the two-phase flow pressure difference.Void fraction:

- Critical power: 79 parameter combinations (pressure, inlet sub-cooling and mass flow rate) are taken into account in this exercise. The comparison results in an average error of less than 4 %. One finding is that with increasing critical power, the deviations between experiment and calculations are getting lower. Main parameter of interest for the uncertainty and sensitivity study is the inlet temperature and the mass flow rate. Even though the error is less than 4 % the investigation/results must be treated with caution. During the uncertainty analysis the coefficient of determination (R^2) is calculated and serves, to some extent, as a figure of merit. For the three previous sub-tasks, this value is close to unity, indicating the quality of the investigation. For the critical power cases, values between 0.15 and 0.8 are found. Furthermore, some of the critical powers could not have been calculated with TRACE due to code failure.

- Transient scenarios

  - Turbine trip: By means of variation of the inlet temperature, bundle mass flow rate, outlet pressure and assembly power, a postulated turbine trip in a BWR is simulated. The turbine isolation valve is closed and the pressure increases immediately. The pressure wave propagates through the core and results in a decrease of the void fraction. Due to the better moderation the power increases. To minimize the consequences of such an event the pump speed is reduced. Less mas flow rate results in an increase of the void fraction. The higher void (lower density) causes the power to drop. The calculated void fraction as a function of the transient time is compared to the experimental data for three axial elevations. The comparison shows a good agreement.

  - Re-circulation pump trip: During this simulated accident the pump speed is reduced that the mass flow rate decreases to 1/3 of the nominal mass flow. This will cause an increase of the void fraction which will, in turn, causes the power to drop due to the lower moderation. The mass flow rate is reset to the nominal value after approximately 30 seconds. The void fraction comparison shows a relatively good agreement to the experiment.

The performed investigation proofed that TRACE is very well able to model BWR fuel assemblies during different stationary and transient scenarios. The comparison to the experimental data showed a general good agreement. The applied uncertainty and sensitivity methods are in good agreement to each other, which is mainly due to their identical approach. These studies helped to quantifiy the influence of the input parameters on the output parameters. This information is valuable for the further development of the TRACE system code.

ACKNOWLEDGMENTS

This work has been performed during a collaboration of the Karlsruhe Institute of Technology and the Universidad Politecnica de Madrid. The authors like to thank to the Program "Nuclear Safety Research" of KIT for the financial support of the Research Topic "Multiphysics Methodologies for Reactor Dynamics and Safety" and the Deutscher Akademischer Austauschdienst (DAAD), which provided the funding for the exchange of UPM scientists to KIT.

Furthermore, the authors highly appreciate the help and support of Nico Trost, Jorge Perez, Uwe Imke, and Javier Jimenez Escalante. A special thanks goes to Professor Rafael Macián-Juan for providing modules and routines for the data manipulation in the context of SUSA application.

Parts of this work have been submitted to international conferences and journals prior to the compilation of the present document. These are:

W. Jaeger, J. Perez Manes, U. Imke, J. Jimenez Escalate and V. Sanchez Espinoza, “Validation and comparison of two-phase flow modeling capabilities of CFD, sub channel and system codes by means of post-test calculations of BFBT transient tests”. Nuclear Engineering and Design, Vol 263, pp 313-326, 2013.

W. Jaeger, V. Sanchez Espinoza, F. Montero Mayorga und C. Queral, „Uncertainty and Sensitivity Studies with TRACE-SUSA and TRACE-DAKOTA by means of steady state BFBT Data“.Science and Technology of Nuclear Installations, Vol 2013, Article ID 610598, 2013.

W. Jaeger, V. Sanchez Espinoza, F. Montero Mayorga und C. Queral, „Uncertainty and Sensitivity Studies with TRACE-SUSA and TRACE-DAKOTA by means of transient BFBT Data“.Science and Technology of Nuclear Installations, Vol 2013, Article ID 565246, 2013.

F. Montero Mayorga, W. Jaeger and V. Sanchez Espinoza, “Análisis de Incertidumbre y Sensibilidad con TRACE-SUSA y TRACE-DAKOTA - Aplicación a NUPEC BFBT” (in spanish). Annual Meeting of the Spanish Nuclear Society, Caceres, Spain, October 17-19, 2012.

ABBREVIATIONS

AEAW	Atomic Energy Authority Winfrith
BFBT	BWR Full-size Fine mesh Bundle Test
BWR	Boiling Water Reactor
CAMP	Code Application and Maintenance Program
CHF	Critical Heat Flux
CSAU	Code Scaling, Applicability and Uncertainty
CT	Computer Tomography
DAAD	Deutscher Akademischer Austausch Dienst
DAKOTA	Design Analysis Kit for Optimization and Terascale Application
DBA	Design Basis Accident
DRM	Deterministic Realistic Method
ENUSA	Empresa Nacional del Uranio, SA
GRS	Gesellschaft fuer Anlagen- und Reaktorsicherheit mbH
IAEA	International Atomic Energy Agency
INR	Institute for Neutron physics and Reactor technology
IPSN	Institut de Protection et de Sûreté Nucléaire
KIT	Karlsruhe Institute of Technology
LOCA	Loss Of Coolant Accident
LWR	Light Water Reactor
METI	Japanese Ministry of Economy, Trade and Industry
NEA	Nuclear Energy Agency
NUPEC	Nuclear Power Engineering Corporation
OECD	Organization for Economic Co-operation and Development
PCC	Partial Correlation Coefficient
PCT	Peak Cladding Temperature
PDF	Probability Density Function
PSA	Probabilistic Safety Assessment
PWR	Pressurized Water Reactor
RELAP	Reactor Excursion and Leak Analysis Program
SETS	Stability-Enhancing Two Step
SNAP	Symbolic Nuclear Analysis Package
SRC	Standardized Regression Coefficient
SUSA	Software system for Uncertainty and Sensitivity Analysis
TDMA	Tri-Diagonal Matrix Algorithm
TH	Thermal Hydraulics
TRACE	TRAC/RELAP Advanced Computational Engine
UMAE	Uncertainty Methodology based on Accuracy Extrapolation
UPM	Universidad Politecnica de Madrid
US NRC	US Nuclear Regulatory Commission

NOMENCLATURE

Symbol	Name of quantity	Value	Unit
A	Area	-	m^2
Cov	Covariance	-	-
E	Expected value	-	-
F	Force term	-	-
N	Sample size	-	-
Nu	Nusselt number, Nu = f(Re, Pr)	-	-
P	Pressure ratio	-	-
P	Probability	-	-
Pe	Peclet number, Pe = Re·Pr	-	-
Pr	Prandtl number, Pr = $cp \cdot \eta \cdot k^{-1}$	-	-
R	Rank	-	-
R^2	Coefficient of determination	-	-
Re	Reynolds number, Re = $\rho \cdot v \cdot l \cdot \eta^{-1}$	-	-
St	Stanton number, St = $Nu \cdot Re^{-1} \cdot Pr^{-1}$	-	-
T	Temperature	-	K
V	Volume	-	m^3
X	Input variable	-	-
X	Random variable	-	-
Y	Output variable	-	-
c	Drag coefficient	-	-
c_p	Specific heat	-	$J \cdot kg^{-1} \cdot K^{-1}$
d	Diameter	-	m
e	Internal Energy	-	W
f	Friction factor	-	-
g	Acceleration of Gravity	-	$m \cdot s^{-2}$
h	Enthalpy	-	$kJ \cdot kg^{-1}$
h	Heat transfer coefficient	-	$W \cdot m^{-2} \cdot K^{-1}$
h_0	Reference heat transfer coefficient, Eq. (4.14)	5600	$W \cdot m^{-2} \cdot K^{-1}$
i	Index	-	-
j	Index	-	-
k	Thermal conductivity	-	$W \cdot m^{-1} \cdot K^{-1}$
p	Pressure	-	Pa
p	Pitch	-	m
p	Probability content	-	-
q	Heat flux	-	$W \cdot m^{-2}$
q_0"	Reference heat flux, Eq. (4.14)	20000	$W \cdot m^{-2}$
r	Pearson's product momentum correlation coefficient	-	-
s	Standard deviation	-	-
s^2	Variance	-	-
t	Time	-	s
v	Velocity	-	$m \cdot s^{-1}$
y	Output	-	-
$\bar{y}$	Mean	-	-
ΔT_{liquid}	$T_{wall} - T_{liquid}$	-	K
$\Delta T_{saturation}$	$T_{wall} - T_{saturation}$	-	K

Greek

Γ	Mass transfer rate	-	-
Δ	Wall roughness	-	m
α	Void fraction	-	-
β	Confidence interval	-	-
β	Blomqvist's medial correlation coefficient	-	-
η	Dynamic viscosity	-	Pa·s
ρ	Density	-	$kg \cdot m^{-3}$
ρ	Spearman's rank correlation coefficient	-	-
σ	Standard deviation	-	-
σ^2	Variance	-	-
μ	Mean	-	-
τ	Kenadall's tau	-	-

Subscript

dg	Droplet-to-gas
dl	Droplet-to-liquid
g	Gas
i	Interface
i	index
ig	Interface-to-gas
il	Interface-to-liquid
l	Liquid
r	Reduced
wg	Wall-to-gas
wl	Wall-to-liquid
x	Related to an input quantity
y	Related to an output quantity

1 INTRODUCTION

1.1 Motivation

Uncertainty and sensitivity (U+S) analysis related to nuclear design and safety investigations gain more and more importance. That is a necessary step since the codes which are used in combination with U+S analysis have been changed from conservative codes to best estimate codes. Conservative codes used conservative approaches in order to account for shortcomings and uncertainties of the used models. Best estimate codes are now using the best empirical models. But these models are nevertheless affected by uncertainties and inaccuracies. These uncertainties are related to material properties, input and boundary conditions and as well as physical models. Therefore, it is necessary to account for them by means of combined U+S when using best estimate codes. The methods to be used to perform that kind of analysis are at a mature level and the community reached a certain experience in order to provide realistic and reliable results. Besides the fact that the application of thermal hydraulic best estimate codes with the purpose of licensing issues has to be accompanied by the quantification of uncertainties, these studies help also to identify areas of further research. In addition, it can be determined to which extend certain models are sensitive to variations of e.g. input and boundary conditions. This information is helpful to address improvement of these models and to show how the computational implementation of empirical models is performing.

A prerequisite for best estimate + uncertainty quantification is the validation and verification of the best estimate simulation tool. Since best estimate tools are based, usually, on empirical correlations within a computational framework, it is mandatory to proof that the used correlations and models are implemented in a proper way and that they are only applied if the simulation condition fit with their range of validity. Verification can be therefore defined, with simple words, as the assessment whether a given correlation is implemented/solved correctly. This is an issue for the mathematical/computational quality management of computer codes. Validation can simply be defined as the test whether or not the correct correlation is used. This is a check of the physical nature of the problem to be investigated and the correlation which is used for (parts of) the simulation. Usually, both tasks go hand in hand since the process of validation requires sometimes to improve or to replace models since they are wrong or obsolete. In case new models need to be implemented or existing models are about to get updated, the verification is one major part of such tasks.

Besides the best estimate codes, the applied uncertainty method must be also checked for appropriateness. One major difference is that the results of thermal hydraulic obtained during validation and verification can be compared to experimental or analytical data. Each of the major thermal hydraulic best estimate code like TRACE has its validation matrix. Such a matrix consists of several hundred experiments. These experiments cover small scale single effect test but also large scale integral plant tests. For the uncertainty methods, no validation matrix or qualification procedure exists.

In the present report, the thermal hydraulic best estimate code TRACE is used for the post test analysis of experiments related to BWR fuel assembly. Results of these experiments are provided by the NUPEC in the frame of the BFBT (BWR Full-Size Fine Mesh Bundle Test) endorsed by the OECD/NEA. TRACE is well validated for the present simulation conditions and therefore can be applied as is without performing validation and verification work prior to the study. Concerning

the U+S analysis, the programs SUSA and DAKOTA are used. SUSA is chosen on the one hand because it has been used successfully in the past and provides a reference tool in order to be compared with a new one such as DAKOTA. On the other hand DAKOTA is used as a second reference in order to perform a code-to-code comparison. Moreover, DAKOTA has been provided with a graphical user interface which is used for the input generation, manipulation and execution of TRACE simulations. Therefore, an automatized interaction already exists. Furthermore, the application of one best estimate code with two U+S analysis tools has the advantage that the user effect related to the modeling of the BWR fuel assembly can be excluded. Usually, the application of different thermo hydraulic codes or even the same code by different users will result in different representations of the object to be investigated. That, by itself, can cause differences and inaccuracies in the model results. Additional, with the application of the same code the influence of e.g. different physical models or material properties is excluded from the analysis. The only reason for different results presented in this report will arise from the different U+S tools and their interaction with TRACE.

1.2 Scope of the Report

The scope of this report can be divided into two major tasks. Task 1 is to provide an overview of uncertainties and related consideration especially when dealing with thermal hydraulic system codes like TRACE. In addition, the presented working methodology for the TRACE-SUSA study and the TRACE-DAKOTA study can be used as a guide book for future investigations.

The second task is to present the results related to the post test calculations of BFBT experiments for pressure losses, void fraction and critical power during steady state and transient conditions.

1.3 Structure and Content of the Report

The report is divided into several sections. The second section deals with the uncertainties, their origin and methods to account for them. Section three gives an overview on the BFBT benchmark. The experimental facility is explained in detail as well as the different measurement devises installed for the different experiments. The fourth section covers the codes and programs which are used. In particular, the structure of the TRACE code is given and the theoretical fundamentals of the SUSA/DAKOTA are explained. Section five presents the applied uncertainty methodologies. This section can be considered as a guidebook for future U+S analysis with SUSA and with DAKOTA. The sixth section presents the actual U+S analysis. Results are presented for 1) steady state single and two phase flow pressure drops, void fraction and critical power measurements and 2) for transient void fraction and pressure drop measurements following two representative BWR transients.

2 UNCERTAINTIES IN NUCLEAR SAFETY INVESTIGATIONS

2.1 Generalities

Uncertainties are the lack of certainties which are caused by inappropriate data and missing information. In general, uncertainties can be divided into two groups: stochastic or statistical uncertainties and epistemic or systematic uncertainties.

Stochastic or statistical uncertainties are results of a random variability of the values of the variable that describe the system and its boundary conditions, also known as input variables to the model, and the lack of precision of the code's physical models.

Epistemic or systematic uncertainties are related due to the lack of knowledge, whether realized or not by the analyst. For instance, the real degree of variability of the input variables are not completely known, and an approximation is necessary, or that the physical models lack the description of some process or mechanism with more or less relevance in the quality of the predictions of the model.

2.2 Conservative Approach versus Best Estimate Plus Uncertainties

In the frame of safety related investigations of nuclear installations it has to be demonstrated that during normal and off-normal operation: the reactivity can be controlled, the heat can be removed from the system and that no radioactivity is released into the environment. The demonstration is done by simulation of the actual plant during normal and off-normal operation.
With the development of nuclear technology, computer programs have been developed to describe the phenomena taking place in a nuclear reactor. But since some of these phenomena are of complex physical nature and elude from a comprehensive description, the models of the computer programs are afflicted with uncertainties or with a bias. In order to avoid a too optimistic prediction of vital safety parameters, safety factors have been introduced into the programs. These codes follow a conservative approach.

Since the beginning of the nuclear safety simulation tools development the knowledge concerning the involved phenomena has increased, the computational capabilities are growing and the measurement and instrumentation techniques have improved. Hence, the conservatism in the codes has been reduced step by step. The actual safety analysis tools related to thermal hydraulic are nowadays best estimate codes referring to the fact that the best available empirical model is used to describe a certain phenomenon. A qualitative comparison of a peak cladding temperature as a function of time during a LOCA transient is depicted in Figure 1.

Nevertheless, the models are afflicted by uncertainties since the experiments which have been used to derive the models are itself subject of uncertainties. About the sources of uncertainties please see the next sub section. That will ultimately lead to values which are characterized by an uncertainty band.

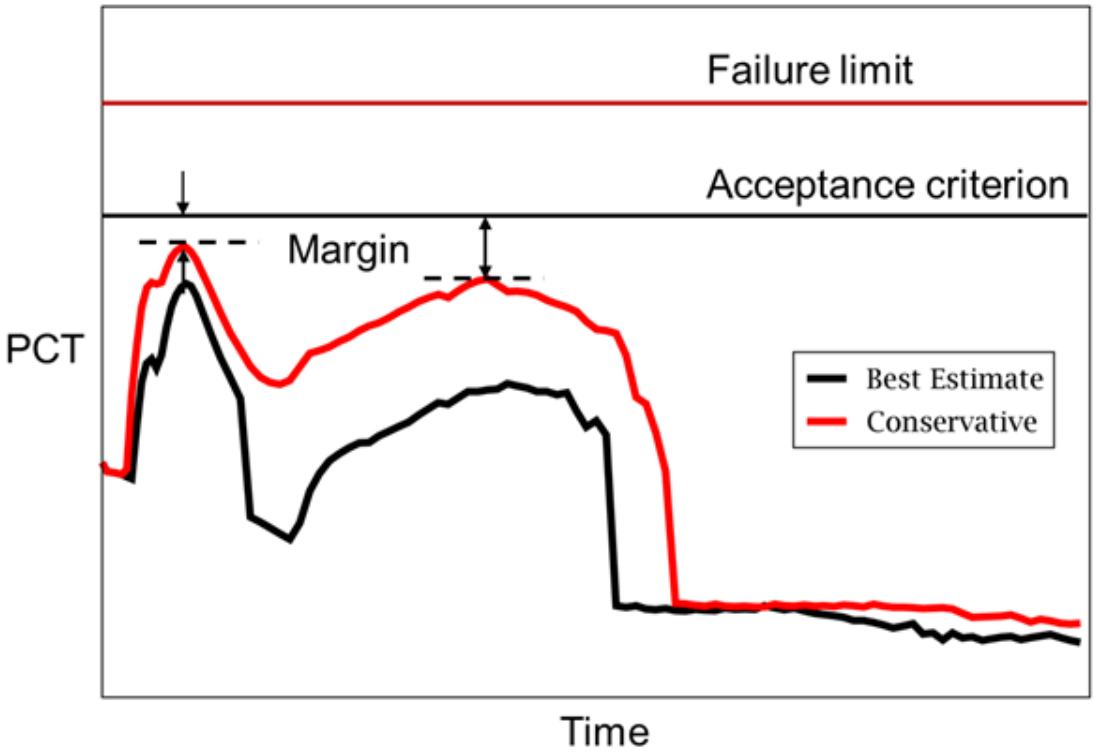

Figure 1 Conservative Calculation versus Best Estimate

Figure 2 is a more general overview of conservative and best estimate calculations and their margins to acceptance and failure criteria. As one can see, the best estimate result is expressed as a range of possible solutions. It is the purpose of uncertainty studies to prove that the upper or lower band limits are not exceeding or undershooting the acceptance limits.

The remaining margin between the conservative prediction and the upper (or lower) value of the best estimate plus uncertainty investigation to the acceptance criterion is called margin. Intentionally, it is the aim to reduce that margin to its minimum. The safety is guaranteed by maintaining the margin which is defined as the distance between the failure limit, e.g. cladding fragilisation, and the acceptance criterion. That margin does not only consider a “safe distance” to failure but also the uncertainty which comes along with determining the failure limit(s).

In case the conservative and best estimate plus uncertainty investigation would aim for the same, e.g., peak cladding temperature the conservative investigation would be characterized by e.g., a lower linear heating rate, meaning lower power level since the distance to the acceptance limit is smaller for the conservative code.

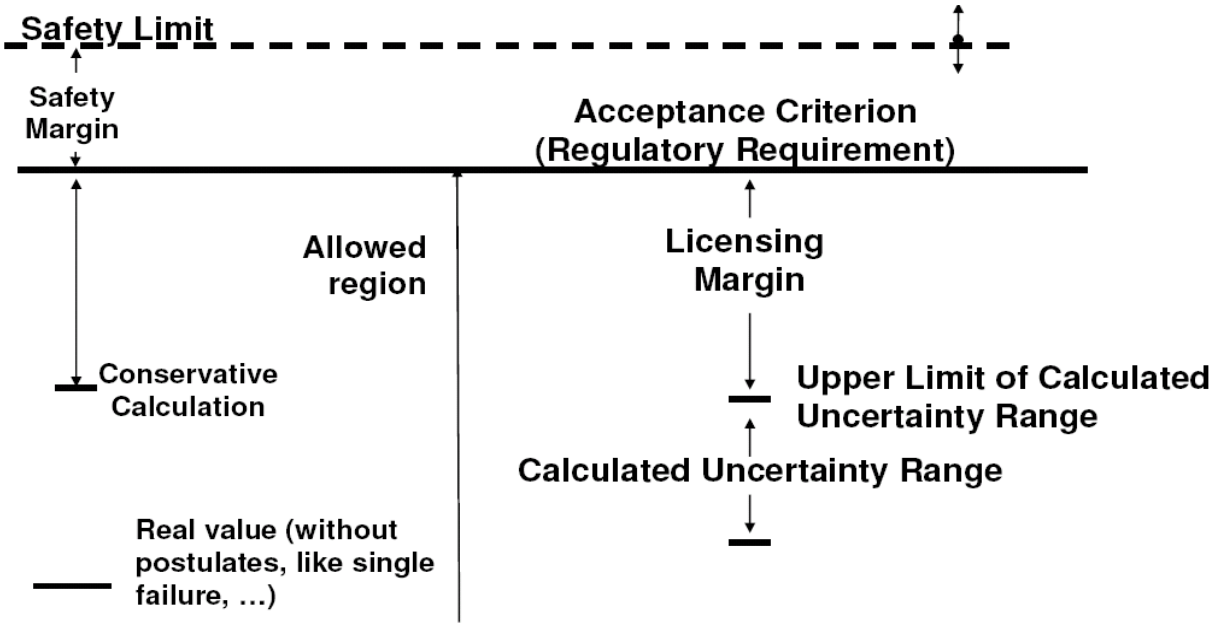

Figure 2 Safety Margins

The IAEA [1] defines the safety margins as:

> *"Safety Margins are the differences in physical units between the established safety limits/criteria of assigned parameters associated with failures or changes of a system or component or with a phenomenon under consideration, and the calculated values of those parameters. Safety limits may be the limiting value used in the design or established for plant operation. Safety limits ... shall not be exceeded during normal operations including anticipated operational occurrences. The terminology safety criterion is generally associated with the assigned parameter for design basis accidents (DBAs). The values of acceptance limits or criteria are stipulated by national regulatory bodies, not to be exceeded during DBAs. The regulatory limits or criteria may be the same or more restrictive than what the plant is designed for. Therefore, for practical purposes, the safety margin is usually understood as the difference in physical units between the regulatory acceptance criteria and the results provided by the calculation of the relevant plant parameter. ..."*

and

> *"…The probabilistic safety margins may be defined as the difference between the established probabilistic safety targets acceptable to the regulatory body and the calculated value of the risk parameter taking into account uncertainties in failure data, modeling of common cause failures, human actions etc. and other uncertainties in knowledge. ..."*

Since the computer codes underwent a transition from conservative to best estimate the safety analysis with respect to licensing purposes changes, too.
Table 1 gives an overview about the different approaches [1].

Table 1 Safety Analysis Options for Licensing Purposes

Applied Code	Input and boundary conditions	Assumptions on system availability	Approach
Conservative	Conservative	Conservative	Deterministic
Best estimate	Conservative	Conservative	Deterministic
Best estimate + uncertainty	Realistic + uncertainty	Conservative	Deterministic
Best estimate + uncertainty	Realistic + uncertainty	PSA based	Deterministic + probabilistic

The option assuming a best estimate code and conservative assumptions regarding the initial and boundary conditions as well as the system availability is the preferred option for safety analyses. The safety of a system can be demonstrated with a single calculation. Recently, the option with a realistic input taking also into account the uncertainties is considered more frequently since the other analyses are too conservative and in some cases and due to e.g. power upgrades the acceptance criteria can be reached. This requires several calculations to demonstrate safety for a given condition. Option two is used in Germany while in the USA either option one or option three must be applied [2]. Most times it is a question of time and money whether option one or three is followed.

2.3 Sources of Uncertainties

According to the IAEA safety report no. 52 [2], the origin of the uncertainties can be divided into five groups: Code or model uncertainties, representation uncertainties, scaling uncertainties, plant uncertainties and user effects.

The code or model uncertainties are related to the field equations and the corresponding empirical closure laws. Furthermore, uncertainties can be attributed to: the correlations or physical models (e.g. the wall to fluid heat transfer or the interface friction), material data (e.g. thermal conductivity, dynamic viscosity of coolants or of structure materials), or geometrical averaging at a cross section or volume scale (one value per cell or cell interface).

The uncertainties related and caused by the modeling of the facility or plant to be investigated are called representative uncertainties. A real set-up has to be transferred into a code readable input deck. Most codes have several components available allowing the description of the plant in great detail. Nevertheless, a 1-to-1 copy from a real system into an input deck is not possible. This can be related to the geometrical representation. For instance, asymmetries can hardly be modeled since the nodalization approaches are rigid. Another example is the representation of the pressure losses which is done by form loss coefficients. These are based on empirical formulations, tabulated for different parameter combinations.

The third group considers the uncertainties related to scaling issues. The model or experiment is usually of smaller geometrical size than the real plant. In addition, boundary and initial conditions like temperature or pressure might be different in the experiment and the plant. The underlying physical phenomena are the same but the aforementioned differences introduce uncertainties.

The uncertainties with respect to initial and boundary conditions are called plant uncertainties. Not all data of a nuclear power plant are available for setting up a model. But the missing information, however, can alter the results dramatically. Besides the pure operational parameters

such as water level in the pressurizer or radial mass flow rate distributions at the core inlet geometrical parameters are unknown. These could be the pin and pellet dimensions in hot state. Moreover, parameters such as the gap conductance and the fuel composition after a certain burn-up are also subject of uncertainties. Especially during transients, these parameters have an influence on e.g. the peak cladding temperature.

The user effect is the last group of uncertainties. These uncertainties can be caused by different approaches users follow, which will yield different results even if both/all users made no mistakes and their assumptions are reasonable. Nevertheless, due to the user knowledge and experience the users can do mistakes while creating a model. To build a full plant model several hundreds of components and control blocks are required. Each of these components or controllers requires various information and multiple numbers have to be entered. It is likely that mistakes appear, causing not necessarily the code to crush but to predict wrong numbers.

Based on the mentioned sources of uncertainties it is impossible that predictions with best estimate system codes are free of uncertainties.

2.4 Uncertainty Methods

The majority of the practical and applied uncertainty methods follow either an input error propagation approach or an output error extrapolation approach. An overview of selected uncertainty methods is given in Figure 3.

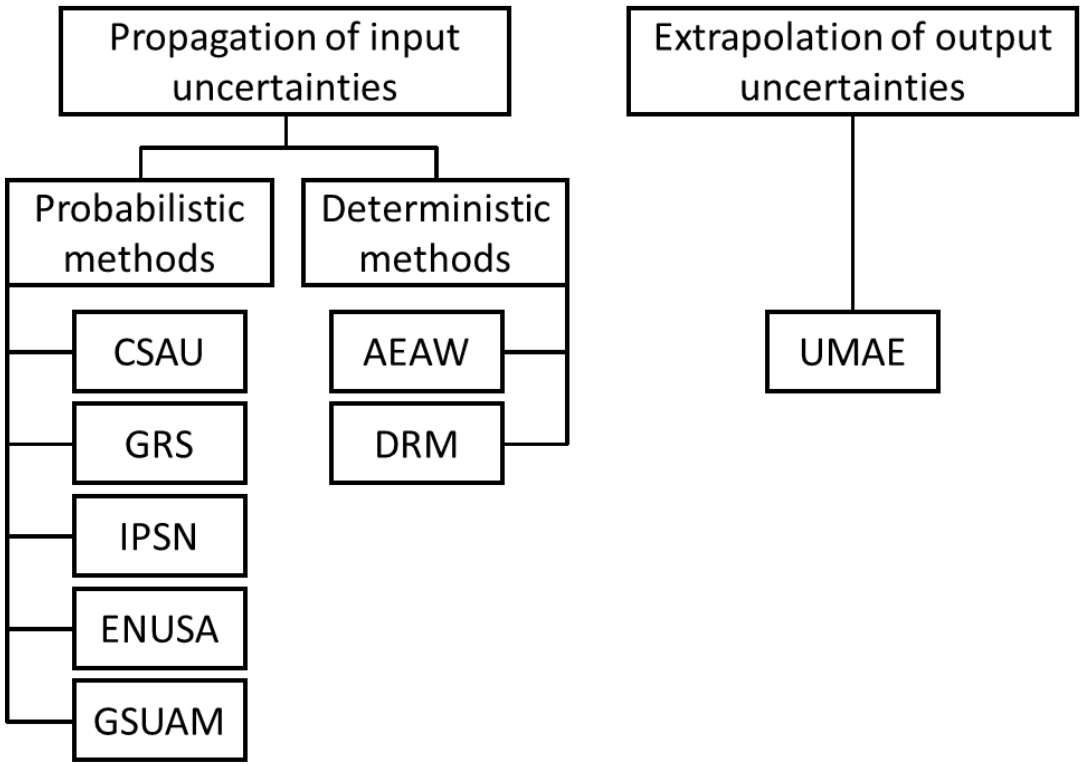

Figure 3 Uncertainty Methods

The input error propagation approach considers the uncertainties of, e.g., initial and boundary conditions, the geometry, the material data and the physical models. These uncertainties will be propagated through the code calculation and will cause, for their part, the uncertainties of the output. A graphical sketch is shown in Figure 4. That requires detailed information about the uncertainty of each and single parameter (e.g. uncertainty range, distribution, correlation between two or more parameters).

The output error extrapolation approach does not consider the uncertainties of specific parameters. Instead, it extrapolates the uncertainties of relevant output parameters from an experiment to a real plant. That requires a comprehensive data base of experiments, which are focused on the same specific phenomena as during the investigation of the plant (e.g. reflood after LOCA). An illustration of that approach is given in Figure 5.

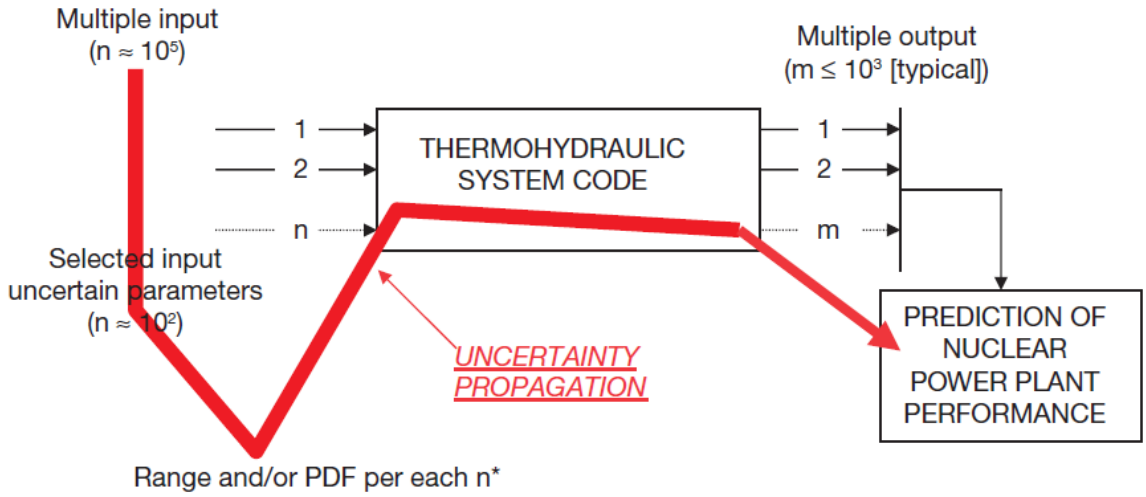

Figure 4 Propagation of Input Errors [2]

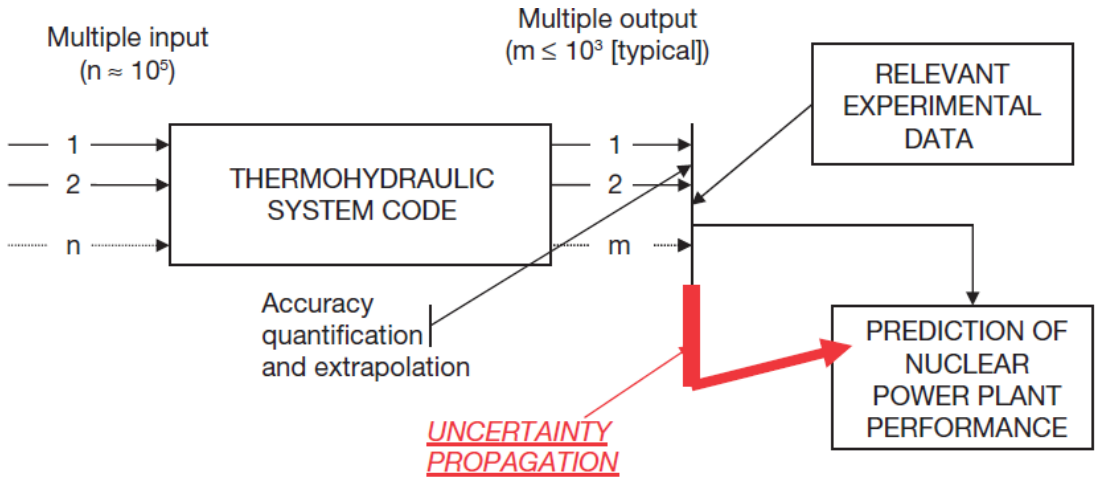

Figure 5 Output Error Extrapolation [2]

3 NUPEC BFBT BENCHMARK

3.1 General Remarks

The objective of the OECD/NRC BWR Full-size Fine-Mesh Bundle Test (BFBT) benchmark is to understand the phenomena taking place during two-phase flow and to improve two-phase flow models needed for sub channel analysis [3]. In the frame of an international project the data base of the NUPEC has been made available to benchmark participants. The benchmark team consists of international experts in the field of modeling and validation as well as two-phase flow. Figure 6 shows the organization team formed by NUPEC Nuclear Power Engineering Corporation), JNES (Japan Nuclear Energy Safety organization) and the Pennsylvania State University. That benchmark has been approved as an international project by METI (Japanese Ministry of Economy, Trade and Industry), OECD/NEA and the U.S. NRC (United States Nuclear Regulatory Commission).

By means of the NUPEC database, benchmark participants can assess the two-phase flow models of their codes. Based on the results, the models can be modified in order to represent the experimental data. In addition, the results obtained with the different codes can be compared to each other. Thereby, the different physical models can be compared and conclusions can be drawn regarding the appropriateness of the models.

The benchmark is divided into two phases with the following sub division.

- Phase I – Void distribution benchmark
    - Exercise 1 – Steady-state sub-channel grade benchmark, where sub-channel, meso- and microscopic approaches can be used;
    - Exercise 2 – Steady-state microscopic grade benchmark, where meso- and microscopic approaches and molecular dynamics can be utilized;
    - Exercise 3 – transient macroscopic grade benchmark, where a sub-channel approach can be applied;
    - Exercise 4 – uncertainty analysis of the void distribution benchmark.
- Phase II – Critical power benchmark
    - Exercise 0 – Steady-state pressure drop benchmark;
    - Exercise 1 – Steady-state benchmark, which applies a one-dimensional approach with BT correlations and a sub-channel mechanistic approach;
    - Exercise 2 – transient benchmark, which applies a one-dimensional approach with BT correlations and a sub-channel mechanistic approach.

The advantage of the NUPEC database related to BWRs is that full-size mock-ups of current BWR fuel assemblies have been used during the experimental phase, conducted from 1987 to 1995 in Japan.

Pictures and drawings showing the test facility, the test section, the assembly, etc. are taken from the specifications [3].

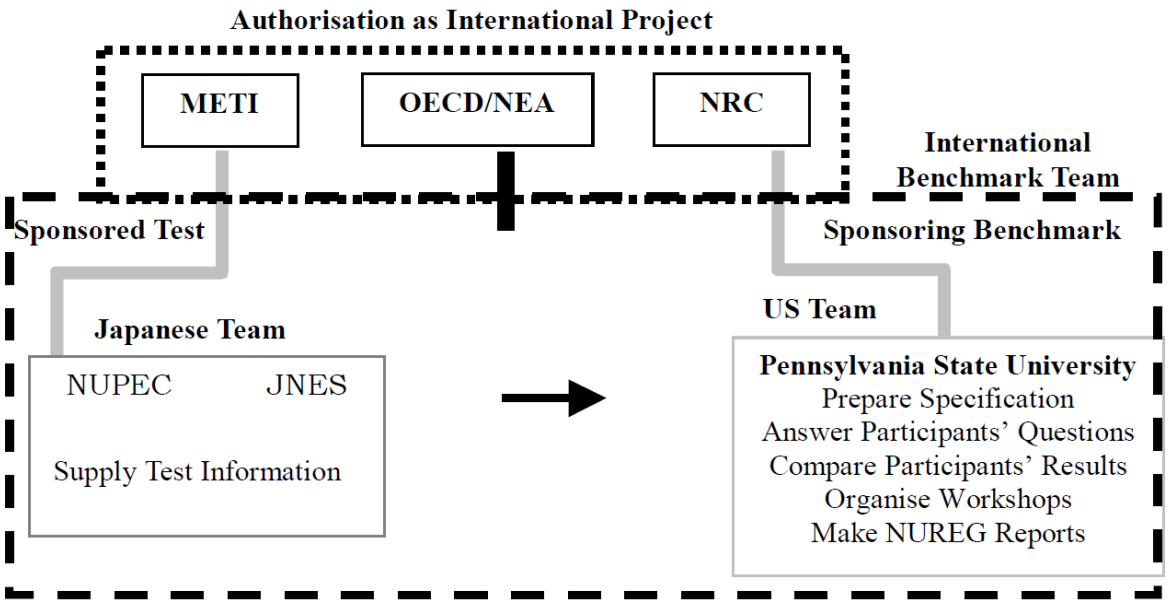

Figure 6 NUPEC BFBT Benchmark Organization

3.2 Test Facility

The test facility is shown in Figure 7. The description of the test facility is taken verbatim from the specifications [3]. The test section which holds the mock-ups of the BWR fuel assemblies is shown in Figure 8.

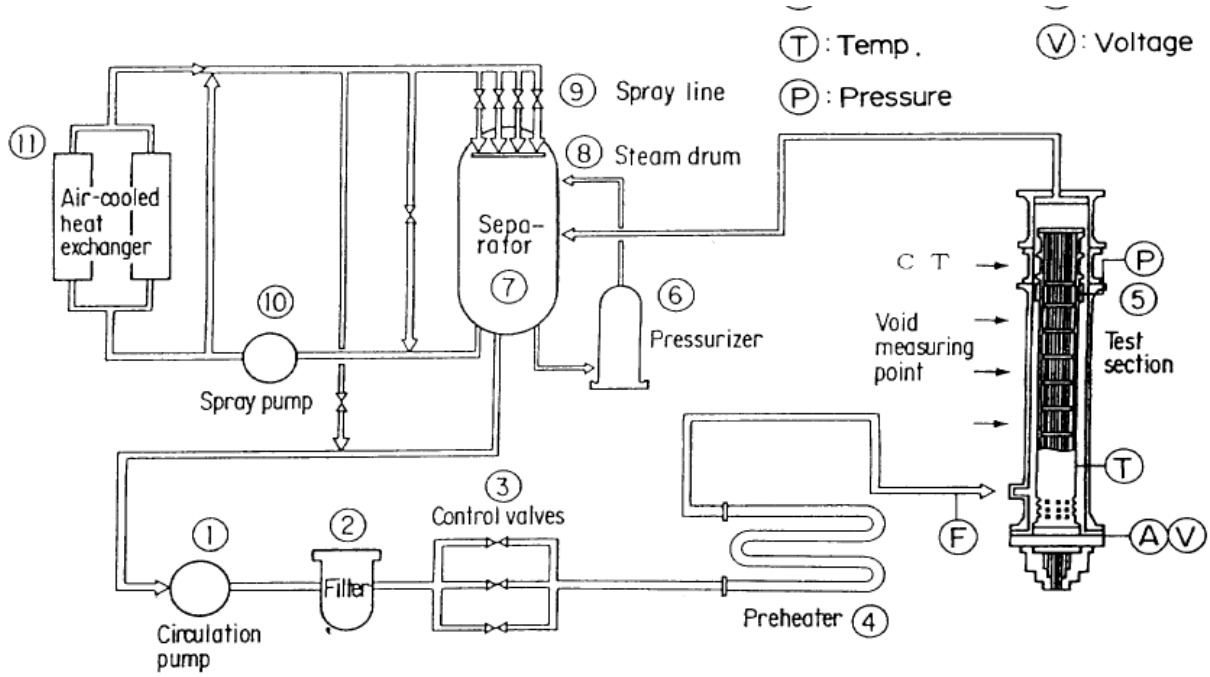

Figure 7 Schematic Diagram of the Test Facility

Water is circulated by the circulation pump (1) and the coolant flow rate is controlled by the three valves (3) of different sizes. The inlet fluid temperature for the test section (5) is controlled by a direct-heating tubular pre-heater (4). Sub-cooled coolant flows upward into the test bundle (5), where it is heated and becomes a two-phase mixture. The steam is separated from the steam-water mixture in the separator (7) and is condensed using a spray of sub-cooled water in the steam drum (8). The condensed water is then returned to the circulation pump (1). The system pressure in both steady and transient state is controlled by spray lines (9), which have four different-sized valves. The pressurizer (6) controls the system pressure when the test assembly power is low. The spray pump (10) forces a spray into the steam-drum after water is cooled with two air-cooled heat exchangers (11). With the test facility operational conditions of up to 10.3 MPa, 315°C, 12 MW and 75 t/h could have been realized.

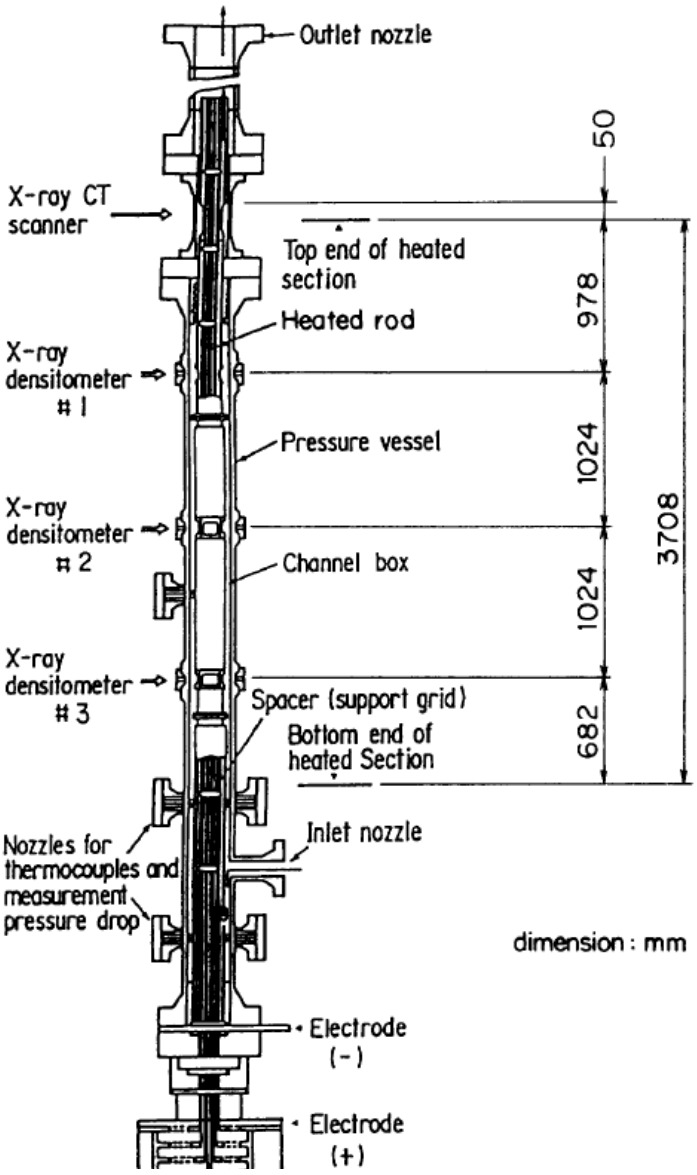

Figure 8 Cross Section of the BWR Fuel Assembly Test Section

3.3 Assembly and Heat Rod Design

In general, two different types of fuel assemblies can be investigated, a current (1980s) 8X8 and a high burn-up 8X8 assembly. The mock-ups consist of electrically heated rods which are arranged like in an 8X8 fuel assembly. Geometrical data of the fuel assemblies are given in Table 2. Assembly type four with a uniform axial power profile is used for the stationary investigations related to pressure drop, void fraction and critical power. For the transient analyses, assembly type C2A with a cosine shaped axial power profile is used.

A drawing of the fuel assembly layout of the considered assemblies is given on the left side of Figure 9 along with the radial power profile, right side. The axial power profile can be found in Figure 10.

Table 2 Geometrical Data of the Considered Fuel Assembly Types

Parameter [unit]	Value	
Assembly type [-]	4	C2A
Investigation condition	steady state	transient
Number of fuel rods [-]	60	
Outer diameter [mm]	12.3	
Rod pitch [mm]	16.2	
Heated length [mm]	3708 (100%)	
Number of water rods [-]	1	
Channel box inner width [mm]	132.5	
Channel box corner radius [mm]	8	
In channel flow area [mm²]	9463	
Number of spacers [-]	7	
Spacer type [-]	Ferrule	
Spacer form loss coefficient [-]	1.2	
Spacer location (from bottom) [mm]	455, 967, 1479, 1991, 2503, 3015, 3527	
Heater outer diameter [mm]	7.3	
Heater material [-]	Nichrome	
Insulator outer diameter [mm]	9.7	
Insulator material [-]	Boron nitride	
Cladding thickness [mm]	1.3	
Cladding material [-]	Inconel 600/beryllium	
Axial power profile [-]	uniform	cosine

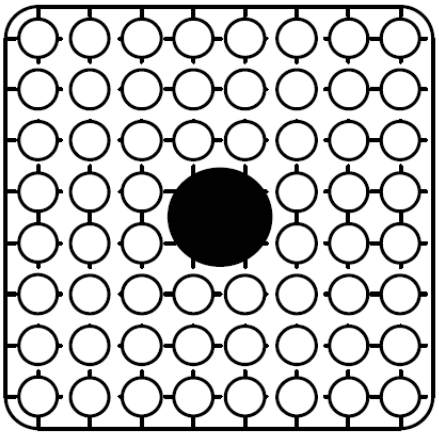

1.15	1.30	1.15	1.30	1.30	1.15	1.30	1.15
1.30	0.45	0.89	0.89	0.89	0.45	1.15	1.30
1.15	0.89	0.89	0.89	0.89	0.89	0.45	1.15
1.30	0.89	0.89			0.89	0.89	1.15
1.30	0.89	0.89			0.89	0.89	1.15
1.15	0.45	0.89	0.89	0.89	0.89	0.45	1.15
1.30	1.15	0.45	0.89	0.89	0.45	1.15	1.30
1.15	1.30	1.15	1.15	1.15	1.15	1.30	1.15

Figure 9 Fuel Assembly 4/C2A and Radial Power Profile

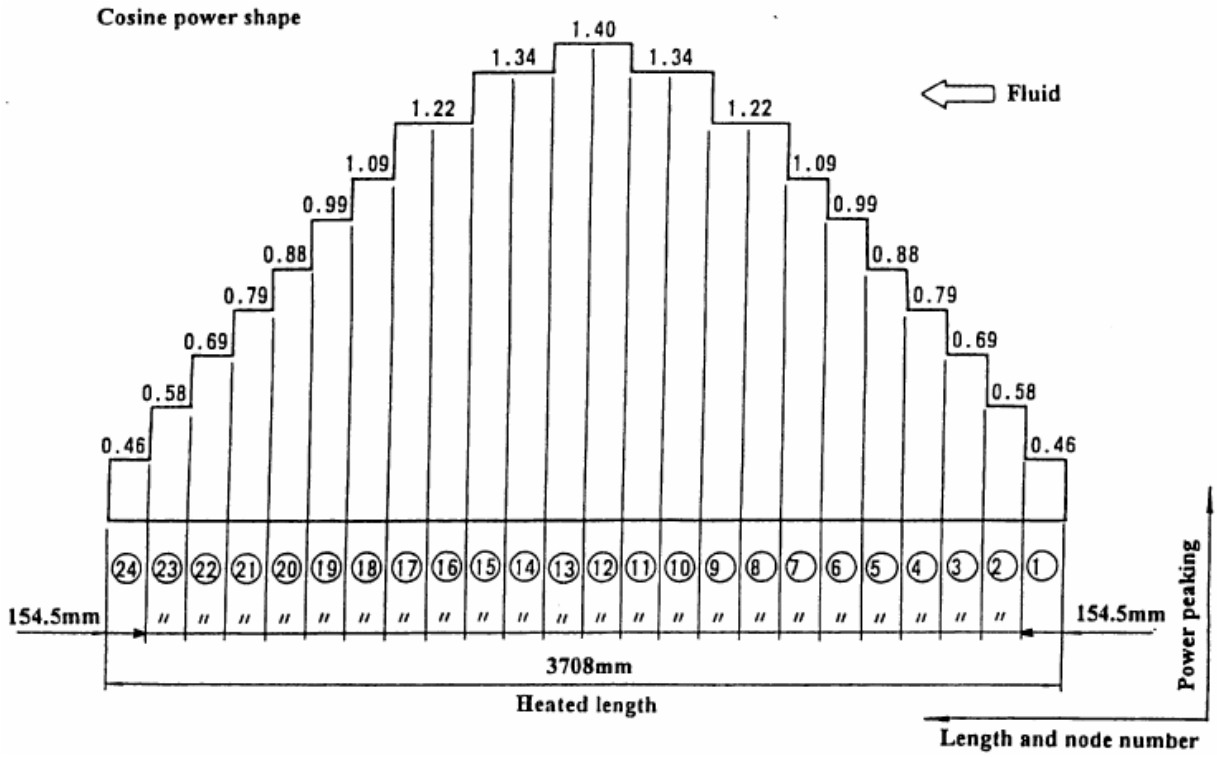

Figure 10 Axial Power Profile for Assembly C2A

The heat rod design and structure is depicted in Figure 11. The dimensions of the heater rods are identical to regular fuel rods. The heater rods consist of three layers. The central one is the heater layer made from Nichrome. The middle layer is made from boron nitride and has the function of an insulator. The last and outer layer is made of Inconel.

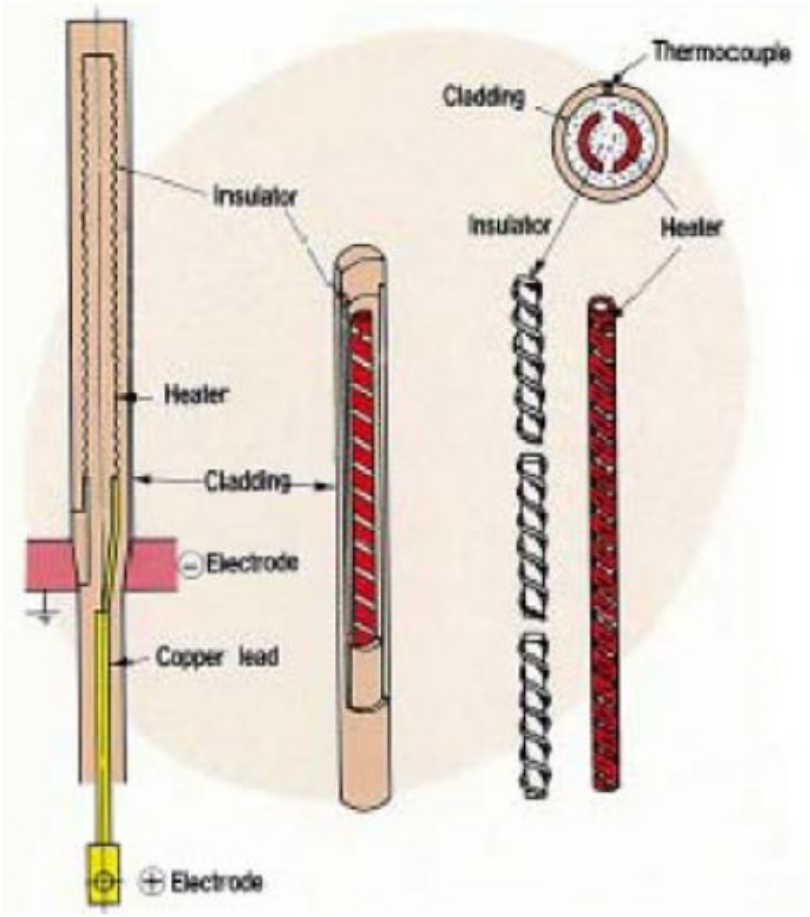

Figure 11 Heater Rod Design

3.4 Pressure Drop Evaluation

During the exercise 3 of phase 1 and exercise 0 of phase 2, absolute and differential pressures were measured. Diaphragm transducers have been used in both cases. The locations of the pressure taps are shown in Figure 12. Nine differential pressure tabs are installed to measure the pressure drop e.g. across the spacer grids, dpT1, dpT2, dpT6 and dpT8, or of the whole bundle, dpT9. These taps have been employed for exercise 0 of phase 2. During exercise 3 of phase 1, the absolute pressure sensors, PTN010 and PTN007, are used and the difference between them is taken as the pressure loss.

During exercise 0 of phase 2, prior to the critical power measurements, several single and two-phase flow conditions have been analyzed with respect to the pressure loss. During the transient scenarios in exercise 3 of phase 1 only two-phase flow pressure losses have been investigated.

As Figure 12shows, 7 spacer grids are installed along the heated length of 3708 mm. A ferrule type spacer grid, Figure 13, is used for the high burn up 8x8 assemblies (4 and C2A). The form loss coefficient is 1.2 according to the specifications.

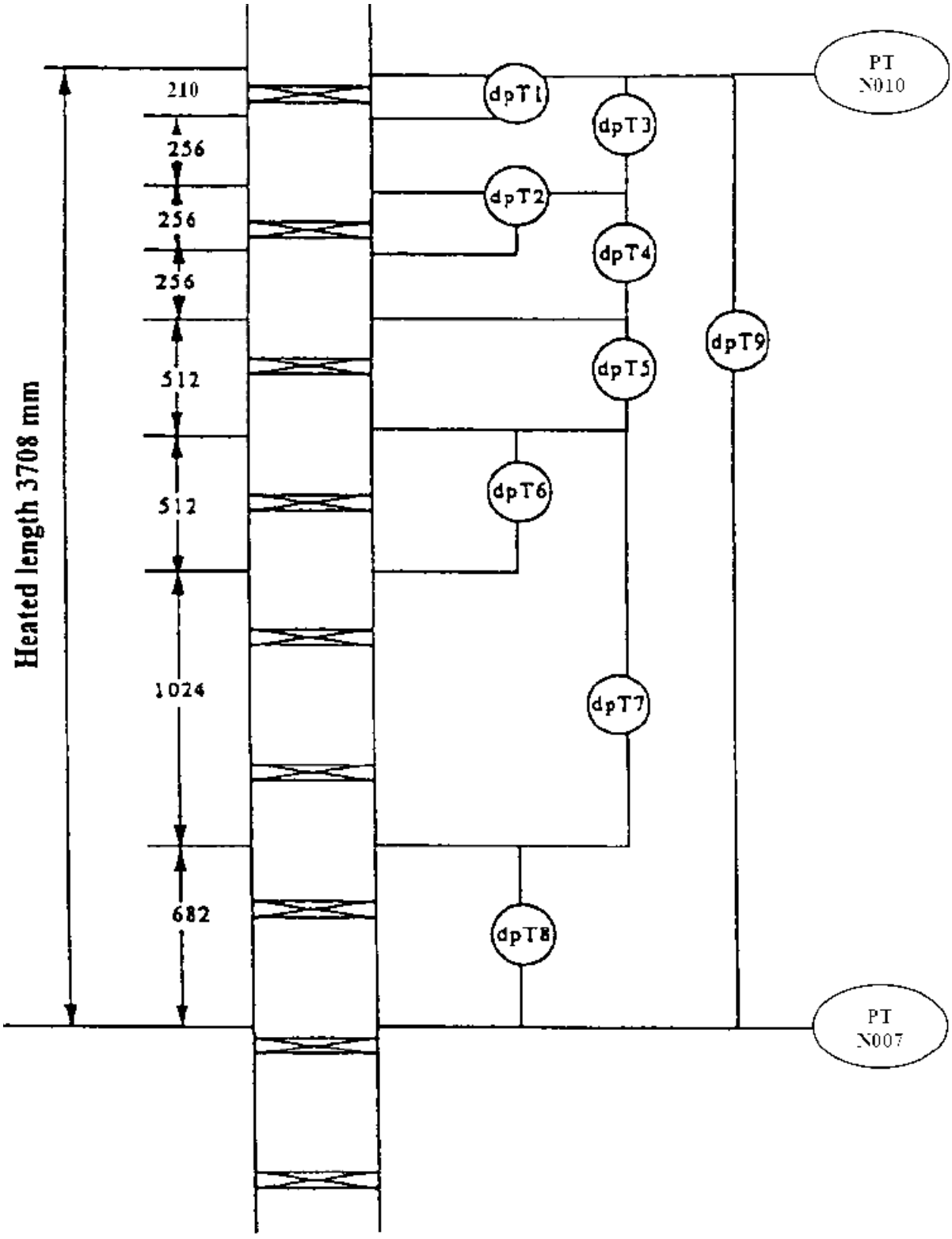

Figure 12 Location of the Pressure Sensors

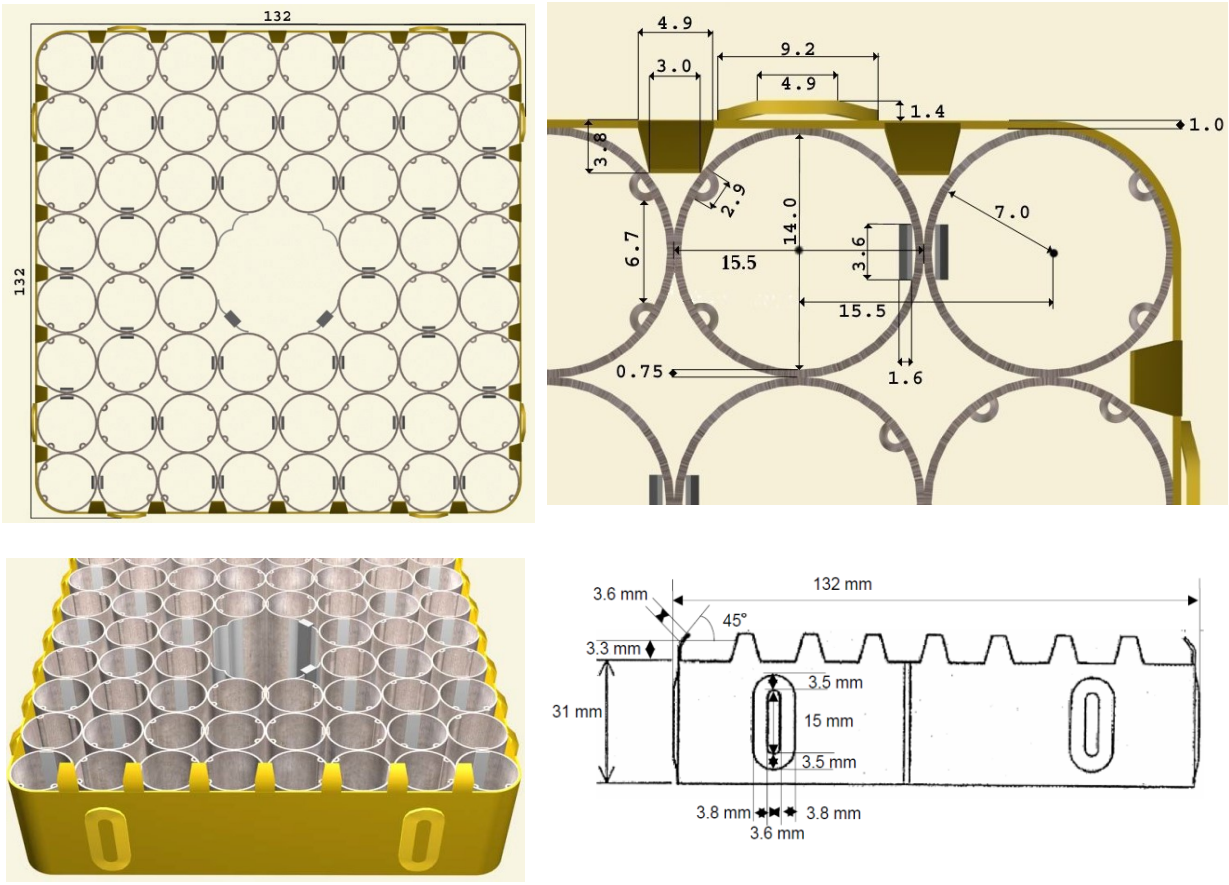

Figure 13 Ferrule Spacer Type (Top Left: Top View; Bottom Left: 3D View; Top Right: Radial Dimensions; Bottom Right Axial Dimensions

3.5 Void Fraction Evaluation

The void fraction at various combinations of pressure, mass flow rate, inlet sub-cooling and power has been recorded during all exercises of phase 1. Figure 14 indicates the positions of the void fraction measurement devices. Two different types have been use. The first one is an X-ray CT (computational tomography) scanner which consists of an X-ray tube and 512 detectors, located at 3758 mm (850 mm above the top of the heated section). The whole arrangement can be rotated around the bundle. With this detector and the applied measurement technique a spatial resolution of 0.3 x 0.3 mm was achieved. These fine mesh results have been exclusively provided for the steady state scenarios where it was possible to rotate the detector in order to precisely measure the void fraction. During transient conditions, the X-ray CT scanner has been used too but it has not been rotated in order to repeat the measurements to obtain fine mesh data. These data are called chordal averaged void fraction.

The second device consists of one X-ray tube and one detector. Three of these devices have been placed at 682, 1706 and 2730 mm. The X-ray tube and the arrangements have been moved in lateral direction since only a thin beam is penetrating the test section. Cross-sectional averaged void fractions have been recorded during the transients where the device was not moved.

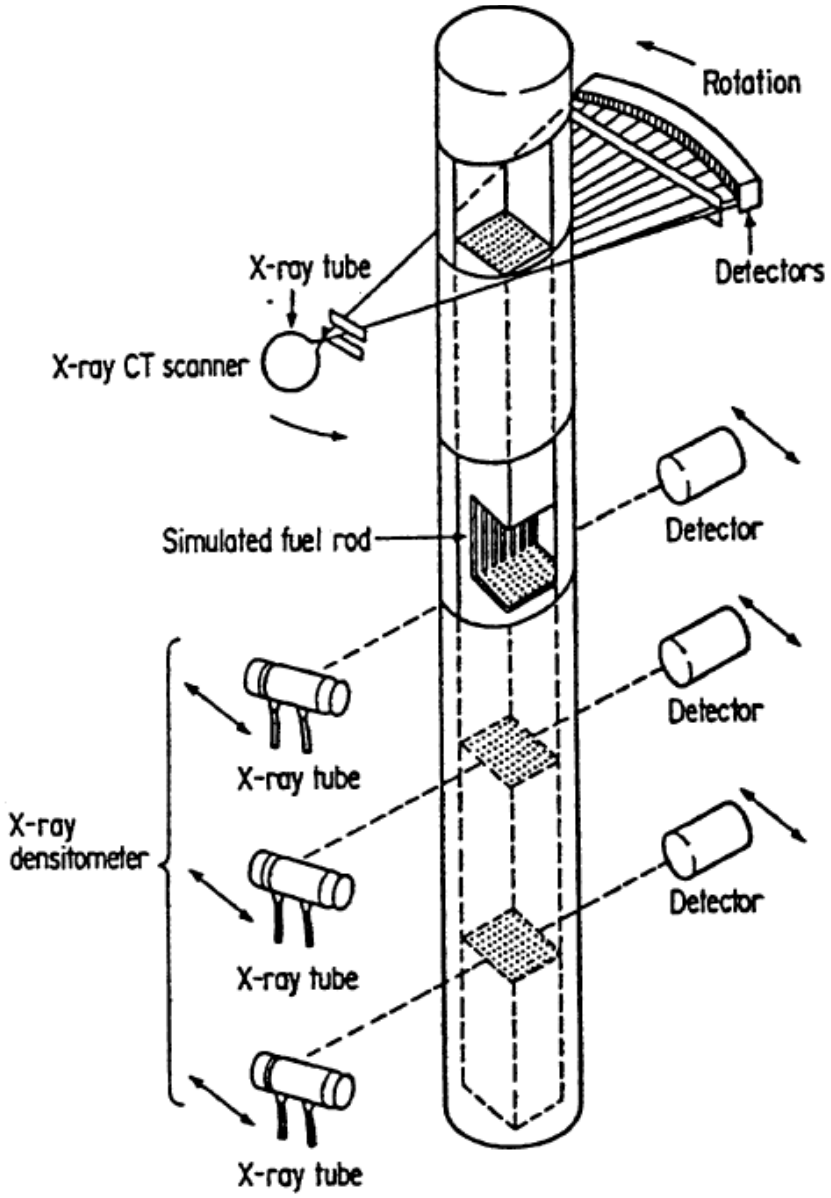

Figure 14 Arrangement of the Void Fraction Measurement Devices

3.6 Critical Power Evaluation

During phase 2, critical power measurements were taken. The assembly power has been increased slowly and the surface temperatures of the rods were monitored, making it a quasi-transient experiment. The positions of the thermo couples are shown in Figure 15. About the definition when critical power was reached the specification states the following:

> *"The critical power was defined when the peak rod surface temperature became 14°C higher than the steady-state temperature level before the dry-out occurred. The dry-out was observed in the peak power rod located at the peripheral row*

adjacent to the channel box. The boiling transition was always observed just upstream of the spacer."

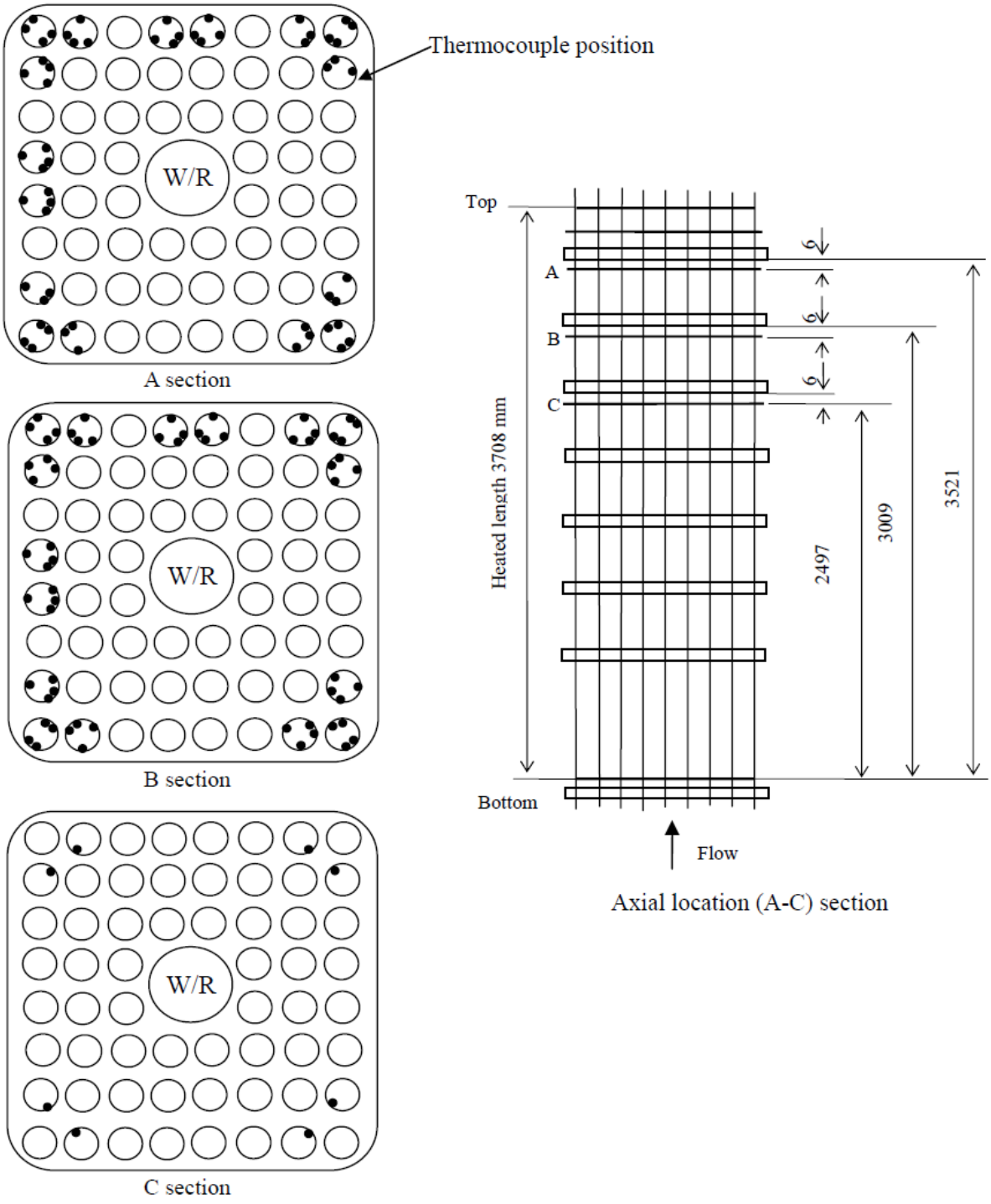

Figure 15 Thermocouple Position during Critical Power Measurement

4 CODES AND PROGRAMS

4.1 TRACE

The explanations and discussion that follow in this sub section have been pulled, almost entirely verbatim, from the Ph.D. thesis of W. Jäger [4].

4.1.1 General Remarks and Main Features

The system code TRACE (TRAC/RELAP Advanced Computational Engine) is one of the latest developments for the investigations of the thermal hydraulic of light water reactors (LWR) and the current thermo-hydraulic reference code of the U.S. NRC. The span of application ranges from investigations of normal operation behavior to the analyses of accidental scenarios (e.g., loss of flow or loss of coolant). TRACE has also been used to design and evaluate experimental test-rigs supporting the research related to LWR's. For this application range TRACE has been widely used in the nuclear community but nevertheless the validation, as well as the developing process, is still ongoing to increase the confidence of the code calculation.

In the frame of an international project - Code Application and Maintenance Program (CAMP) - codes of the U.S. NRC (e.g., TRACE, RELAP5) are distributed to the CAMP partners, to assess their capabilities. TRACE combines the capabilities of four major system codes (TRAC-P, TRAC-B, RELAP5 and RAMONA) and is envisaged to replace them in the near future. The U.S. NRC describes TRACE as follows [5]:

> *"TRACE has been designed to perform best-estimate analysis of loss-of-coolant accidents (LOCAs), operational transients, and other accident scenarios in pressurized light-water reactors (PWRs) and boiling light-water reactors (BWRs). It can also model phenomena occurring in experimental facilities designed to simulate transients in reactor systems. Models used include multidimensional two-phase flow, non equilibrium thermo-dynamics, generalized heat transfer, re flood, level tracking, and reactor kinetics. Automatic steady-state and dump/restart capabilities are also provided."*

The main numerical features of TRACE are:

- Partial differential equations for two-phase flow and heat transfer are solved using a finite volume method.
- Heat transfer equations use a semi-implicit time differencing procedure.
- Fluid-dynamics equations in the components (1D or 3D) use either a multi-step time differencing procedure or a semi-implicit time differencing procedure.
- The coupled, nonlinear equations for the hydrodynamic phenomena using finite difference equations are solved by the Newton-Raphson iteration method.
- Resulting linearized equations are solved by direct matrix inversion.

TRACE follows a component-based approach to model a reactor system or an experimental facility. Nearly all components employed in a reactor system are represented in TRACE. The component itself can be nodalized as demanded by the user. Also, several types of the component are available. The following components can be used in TRACE: BREAK (pressure boundary), CHAN (BWR FAs), CONTAN (containment), EXTERIOR (needed for parallel execution of TRACE), FILL (mass flow and temperature boundary condition), FLPOWER (fluid power), HEATR (feed water heater), HTSTR (heat structure), JETP (jet pumps), PIPE (piping system), PLENUM, POWER, PRIZER (pressurizer), PUMP, RADENC (radiation enclosure), SEPD (separator), TEE, TURB (turbine), VALVE and VESSEL (3D). The VESSEL component can be used to model components where 3D phenomena take place like the reactor pressure vessel (RPV) or a storage tank. The VESSEL can also be separated into RPV typical components like downcomer, lower and upper plenum, and the core.

4.1.2 Numerical Methodology

A comparison between numerical methods used for current legacy codes like TRACE and future code systems are given by Nourgaliev [6], see Table 3. The numerical architecture of codes like TRACE and RELAP corresponds to the state-of-the-art of the 1970/80. Nowadays, more advanced mathematical methods are available to handle time and space discretization problems. Also new developments concerning program languages have been made by means of object oriented programming. Therefore, it is foreseen that the existing codes will be replaced by codes based on advanced physical, numerical and computational methods. The closure relations in the current TH system codes needed to solve the field equations are based on empirical models derived from experiments. Due to the complexity of certain experimental investigations, the derived correlations are valid for a narrow range of parameters only. Examples are the flow regime maps in the system and sub channel codes. For each flow regime (depending on mass flux and void fraction) a set of correlations is needed. In system codes, the size of the control volume is rather big ranging from centimeter to meter. Hence, some small scale physical phenomena (e.g., turbulence, boiling effects) cannot be taken into account because of time and space averaging techniques in the codes. To describe these phenomena, models based on first principles are needed. Instead of empirical correlations, the phenomena will be described by mechanistic models, i.e. based on nature laws if feasible.

4.1.3 Field Equations

The set of equations in TRACE are based on single-phase Navier-Stokes equation for each phase and additional jump conditions between the phases. The set of two-fluid, two-phase conservation equations are obtained by time and volume averaging techniques. Six partial differential equations, to describe the mass, energy and momentum conservation for the liquid and the gas field, are implemented into TRACE. Concerning non-condensables in the gas phase, a single momentum and a single energy conservation equation for the gas mixture is used. For the conservation of mass, one equation for each component of the gas field is used [5].

Table 3 Numerical Differences between Legacy Codes like TRACE and Future Code Systems

Legacy codes	New developments	Remarks
	Time discretization	
Semi-implicit Nearly-implicit SETS Operator split 1st order	Fully implicit L-stable Runge-Kutta High order	1st order does not allow to quantify numerical discretization uncertainties
	Space discretization	
Staggered-grid Donor-cell Upwind 1st order	Finite-volume Finite-elements Discontinuous Galerkin Godunov based Collocated grid	1st order does not allow to quantify numerical discretization uncertainties
	Linear algebra	
Direct solvers Sparse Gaussian elimination TDMA Scale as ≈ N^3	Efficient iterative linear and nonlinear solvers Krylov method Multigrid Scale as ≈ N·log (N)	
	Programming	
Serial FORTRAN legacy	Parallel (MPI) Object-oriented (C++, Java	

The six partial differential equations for mass, energy and momentum conservation in the TRACE code are given below whereas the equations for the mass conservation are [5].

$$\frac{\partial[(1-\alpha)\cdot\rho_l]}{\partial t}+\nabla[(1-\alpha)\cdot\rho_l\cdot\vec{v_l}]=-\Gamma \tag{1}$$

$$\frac{\partial[\alpha\cdot\rho_g]}{\partial t}+\nabla[\alpha\cdot\rho_g\cdot\vec{v_g}]=\Gamma \tag{2}$$

The conservation of energy is based on a formulation with the internal energy

$$\frac{\partial\left[(1-\alpha)\cdot\rho_l\cdot\left(e_l+\frac{v_l^2}{2}\right)\right]}{\partial t}+\nabla\left[(1-\alpha)\cdot\rho_l\cdot\left(e_l+\frac{p}{\rho_l}+\frac{v_l^2}{2}\right)\cdot\vec{v_l}\right] = q_{il}+q_{wl}+q_{dl}+(1-\alpha)\cdot\rho_l\cdot\vec{g}\cdot\vec{v_l}-\Gamma\cdot h_l'+\left(\vec{F_l}+\overrightarrow{F_{wl}}\right)\cdot\vec{v_l} \tag{3}$$

$$\frac{\partial\left[\alpha\cdot\rho_g\cdot\left(e_g+\frac{v_g^2}{2}\right)\right]}{\partial t}+\nabla\left[\alpha\cdot\rho_g\cdot\left(e_g+\frac{p}{\rho_g}+\frac{v_g^2}{2}\right)\cdot\vec{v_g}\right] = q_{ig}+q_{wg}+q_{dg}+\alpha\cdot\rho_g\cdot\vec{g}\cdot\vec{v_g}-\Gamma\cdot h_g'+\left(\vec{F_g}+\overrightarrow{F_{wg}}\right)\cdot\vec{v_g} \tag{4}$$

Conservation of momentum for the two phases writes as follows

$$\frac{\partial[(1-\alpha)\cdot\rho_l\cdot\vec{v_l}]}{\partial t}+\nabla(1-\alpha)\cdot\rho_l\cdot\vec{v_l}\cdot\vec{v_l}+(1-\alpha)\cdot\nabla p = \vec{F_i}+\overrightarrow{F_{wl}}+(1-\alpha)\cdot\rho_l\cdot\vec{g}-\Gamma\cdot\vec{v_i} \tag{5}$$

$$\frac{\partial[\alpha\cdot\rho_g\cdot\vec{v_g}]}{\partial t}+\nabla\alpha\cdot\rho_g\cdot\vec{v_g}\cdot\vec{v_g}+\alpha\cdot\nabla p=-\vec{F_i}+\overrightarrow{F_{wg}}+\alpha\cdot\rho_g\cdot\vec{g}-\Gamma\cdot\vec{v_i} \tag{6}$$

The force terms F_i, F_{wl} and F_{wg} rely on friction coefficients f_i, f_{wl} and f_{wg}, and are cast in the following equations.

$$F_i=f_i\cdot(\vec{v_g}-\vec{v_l})\cdot|\vec{v_g}-\vec{v_l}| \tag{7}$$

$$F_{wl}=-f_{wl}\cdot\vec{v_l}\cdot|\vec{v_l}| \tag{8}$$

$$F_{wg}=-f_{wg}\cdot\vec{v_g}\cdot|\vec{v_g}| \tag{9}$$

4.1.4 Closure Relations

As one can see, it is necessary to provide additional information to close the above given correlations. Therefore, 10 parameters have been defined. These parameters are: the interfacial area, the interfacial mass transfer rate, the interfacial drag coefficient, the wall drag coefficient for both phases, the interfacial heat transfer coefficient for both phases, the heat transfer coefficient for the liquid-to-gas sensible heat transfer, and the wall heat transfer coefficients for both phases. Table 4 gives an overview of the flow and heat transfer regime dependent parameters required for solving the field equations. The relationship between the field equations and the closure parameters is illustrated in Figure 16 - Figure 18.

Table 4 Required Parameters for the Closure of the Field Equations [7]

Par.	Mass		Energy		Momentum	
	Liquid	Gas	Liquid	Gas	Liquid	Gas
Ai	X	X	-	X	X	X
Γ	X	X	-	X	X	X
ci	-	-	-	-	X	X
cwl	-	-	-	-	X	-
cwg	-	-	-	-	-	X
hil	X	X	-	X	X	X
hig	X	X	-	X	X	X
hgl	-	-	-	X	-	-
hwl	X	X	X	X	X	X
hwg	-	-	X	X	-	-

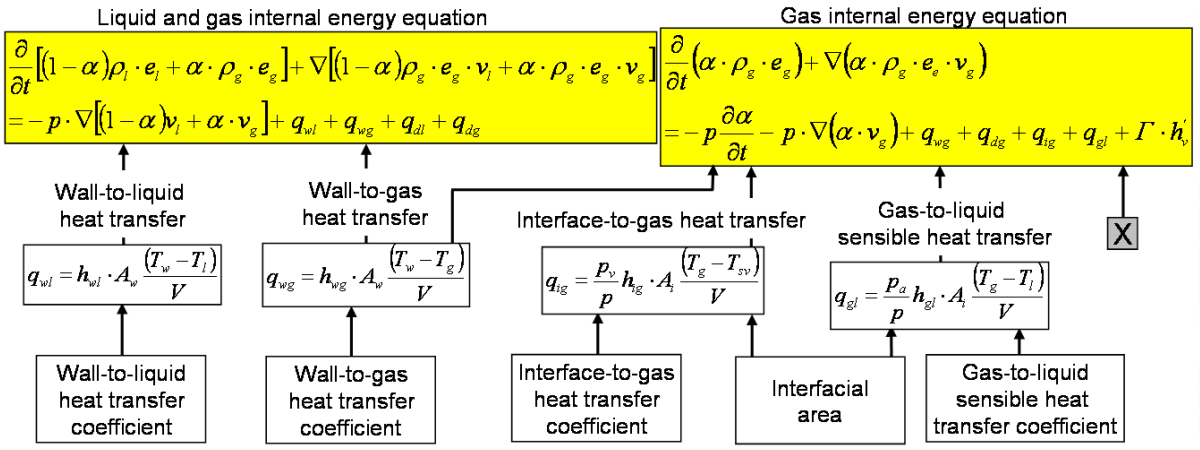

Figure 16 Mapping of the Regime Dependent Parameters for Energy Conservation [7]

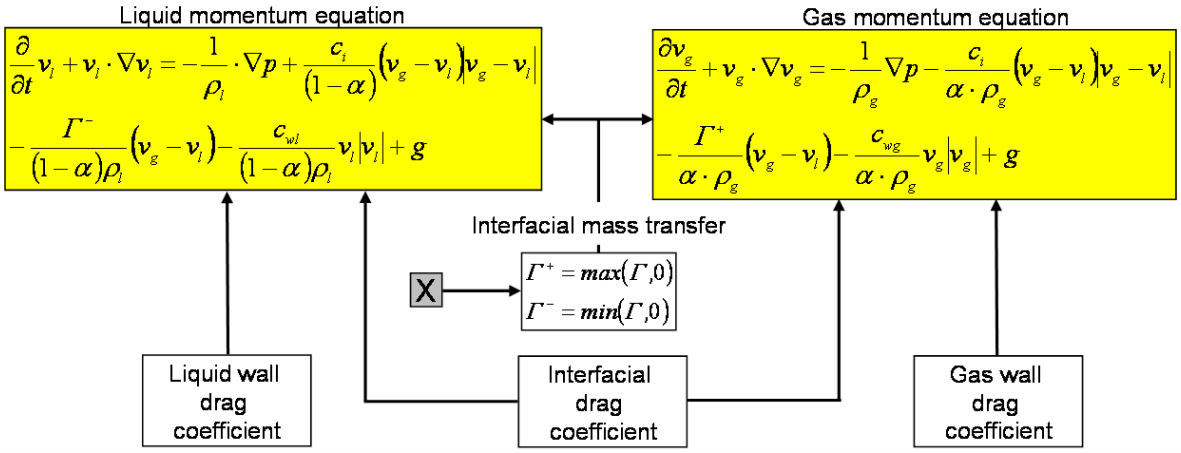

Figure 17 Mapping of the Regime Dependent Parameters Momentum Conservation [7]

For the present investigation the heat transfer regime is pre-CHF more precisely nucleate boiling. The selection logic for pre-CHF scenarios is given in Figure 19. Depending on the void fraction and the bulk and wall temperatures, the position on the boiling curve is determined and the corresponding correlations/models are called. The nucleate boiling model takes into account pool boiling, based on Gorenflo [8] and forced convection flow, based on El-Genk [9]. For the sake of completeness, the considered physical models are given hereafter.

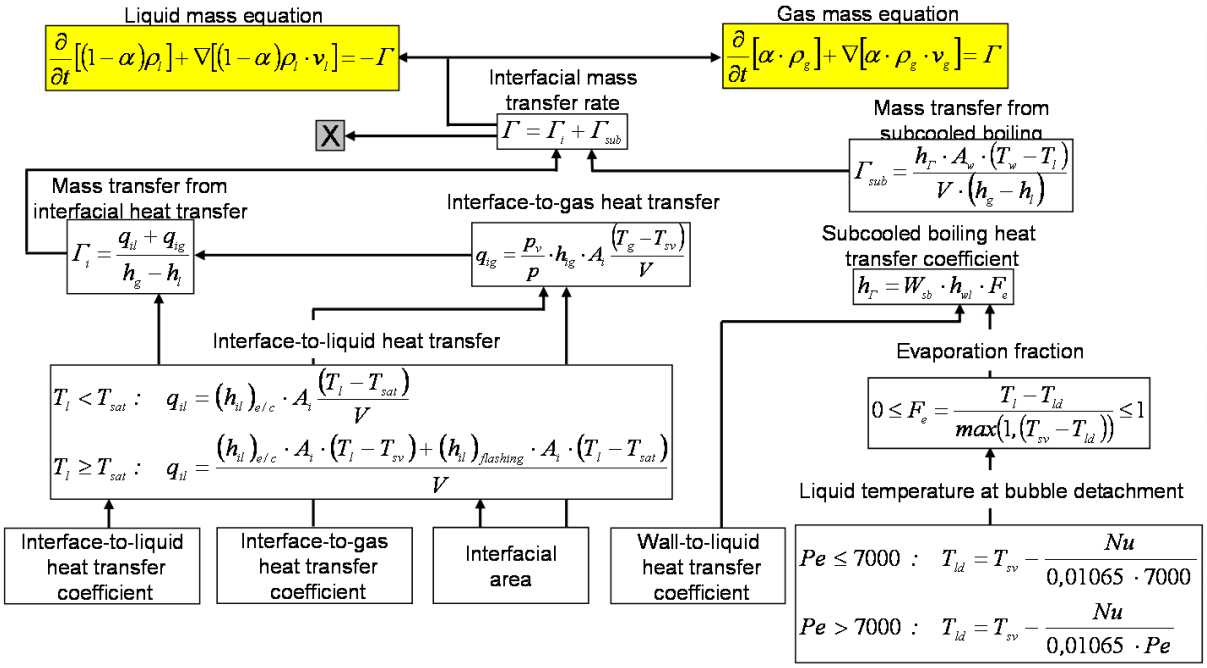

Figure 18 Mapping of the Regime Dependent Parameters for Mass Conservation [7]

$$q''_{\text{nucleate boiling}} = \left(q''_{\text{forced convection}}{}^{3} + \left(q''_{\text{pool boiling}} - q''_{\text{boiling initiation}}\right)^{3}\right)^{\frac{1}{3}} \tag{10}$$

$$q''_{\text{forced convection}} = h_{\text{forced convection}} \cdot \Delta T_{\text{liquid}} \tag{11}$$

$$h_{\text{forced convection}} = \left(\frac{k}{d_{\text{hydraulic}}}\right) \cdot \left[0.028 \cdot \left(\frac{p_{\text{pin}}}{d_{\text{pin}}}\right) - 0.006\right] \cdot \text{Re}^{0.8} \cdot \text{Pr}^{0.4} \tag{12}$$

$$q''_{\text{pool boiling}} = h_{\text{pool boiling}} \cdot \Delta T_{\text{saturation}} \tag{13}$$

$$h_{\text{pool boiling}} = \left(\frac{h_0 \cdot F_p}{q''_0}\right)^{\left(\frac{1}{1-n}\right)} \cdot \Delta T_{\text{saturation}}{}^{\left(\frac{n}{1-n}\right)} . \tag{14}$$

with

$$F_p = 1.73 \cdot P_r{}^{0.27} + \left(6.1 + \frac{0.68}{1 - P_r}\right) \cdot P_r{}^{2} \tag{15}$$

$$n = 0.9 + 0.3 \cdot P_r{}^{0.15} \tag{16}$$

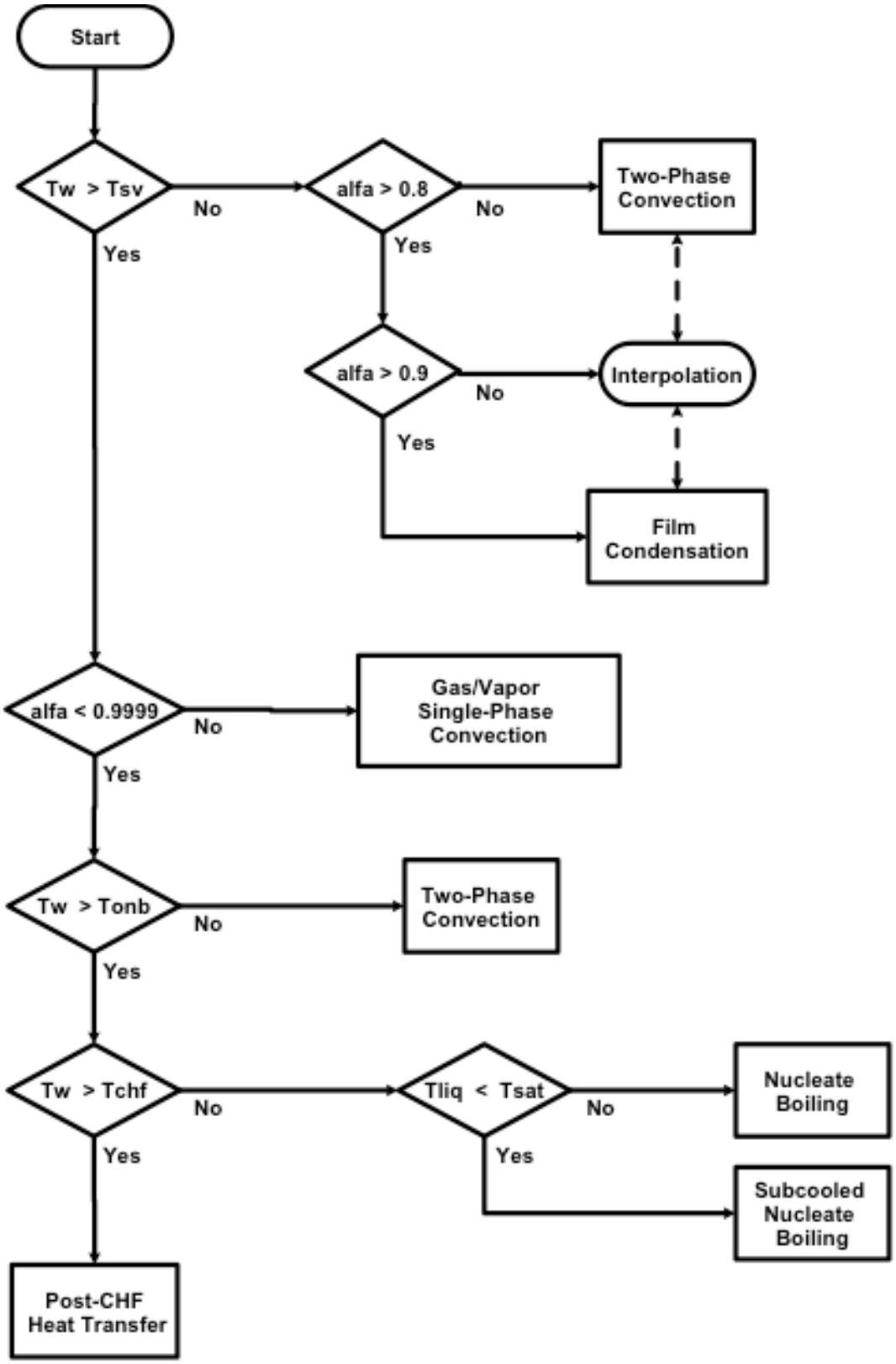

Figure 19 Pre-CHF Heat Transfer Selection Logic in TRACE [5]

where h_0 is a reference heat transfer coefficient (5600 W/m²·K), q_0'' is a reference heat flux (20000 W/m²) and P_r is the reduced pressure quantity ($P_r = {}^{p}/_{p_{critical}}$)

$$q''_{\text{boiling initiation}} = q''_{\text{pool boiling}}(T_{\text{onset nucleate boiling}}) \tag{17}$$

The wall heat transfer coefficient for subcooled boiling is calculated with the same models as for nucleate boiling but with a vapor generation fraction by means of temperatures.

$$h_{\text{liquid boiling}} = \frac{f_{\text{sub cooled}} \cdot \left(q''_{\text{nucleate boiling}} - q''_{\text{forced convection}}\right)}{\Delta T_{\text{saturation}}} \tag{18}$$

$$h_{\text{wall}} = \frac{q''_{\text{forced convection}} + (1 - f_{\text{sub cooled}}) \cdot q''_{\text{nucleate boiling}}}{\Delta T_{\text{liquid}}} \tag{19}$$

$$f_{\text{sub cooled}} = \text{MAX}\left(0, \frac{T_{\text{liquid}} - T_{\text{bubble detachment}}}{T_{\text{saturation}} - T_{\text{bubble detachment}}}\right) \tag{20}$$

$$T_{\text{bubble detachment}} = T_{\text{saturation}} - \frac{q''_{\text{nucleate boiling}} - d_{\text{hydraulic}}}{Pe \cdot St} \tag{21}$$

where Pe is the Peclet number which is the maximum of either 70000 or the product of Reynolds number and Prandtl number, St is the Stanton number which is considered to be 0.0065 for sub cooled boiling $T_{\text{bubble detachment}}$ is the temperature at which bubble detachment occurs.

In addition, TRACE uses flow regime dependent wall drag models. For void fractions lower than 0.8 the bubbly/slug flow regime with nucleation is used to determine the wall drag coefficient.

$$C_{\text{wall}\rightarrow\text{liquid}} = f \cdot \frac{2 \cdot \rho_{\text{liquid}}}{d_{\text{hydraulic}}} \cdot \left(1 + C_{\text{nucleate boiling}}\right)^2 \tag{22}$$

where f is the single-phase friction factor based on Churchill [10] and (1+Cnucleate boiling)² is the two phase flow multiplier related to nucleate boiling.

$$f_{\text{single-phase}} = 2 \cdot \left[\left(\frac{8}{Re}\right)^{12} + \frac{1}{(a+b)^{1.5}}\right]^{\frac{1}{12}} \tag{23}$$

$$a = \left\{2.457 \cdot \ln\left[\frac{1}{\left(\frac{7}{Re}\right)^{0.9} + 0.27 \cdot \left(\frac{\Delta}{d_{\text{hydraulic}}}\right)}\right]\right\}^{16} \tag{24}$$

$$b = \left(\frac{37530}{Re}\right)^{16} \tag{25}$$

$$C_{\text{nucleate boiling}} = \text{MIN}\left\{2.0, 155 \cdot \left(\frac{d_{\text{bubble}}}{d_{\text{hydraulic}}}\right) \cdot [\alpha \cdot (1-\alpha)]^{0.62}\right\} \tag{26}$$

4.1.5 Validation Process

Since TRACE is a tool for the analysis of LWRs, an assessment matrix, as well as a validation matrix, has been developed to improve and validate TRACE. The development process of TRACE related to LWRs is summarized in Figure 20 [11]. Many experimental facilities exist and the results have been used for the purpose of assessment and validation. Figure 21 shows the assessment matrix of the U.S. NRC and the assessment matrix consists of more than 400 individual experiments [11].

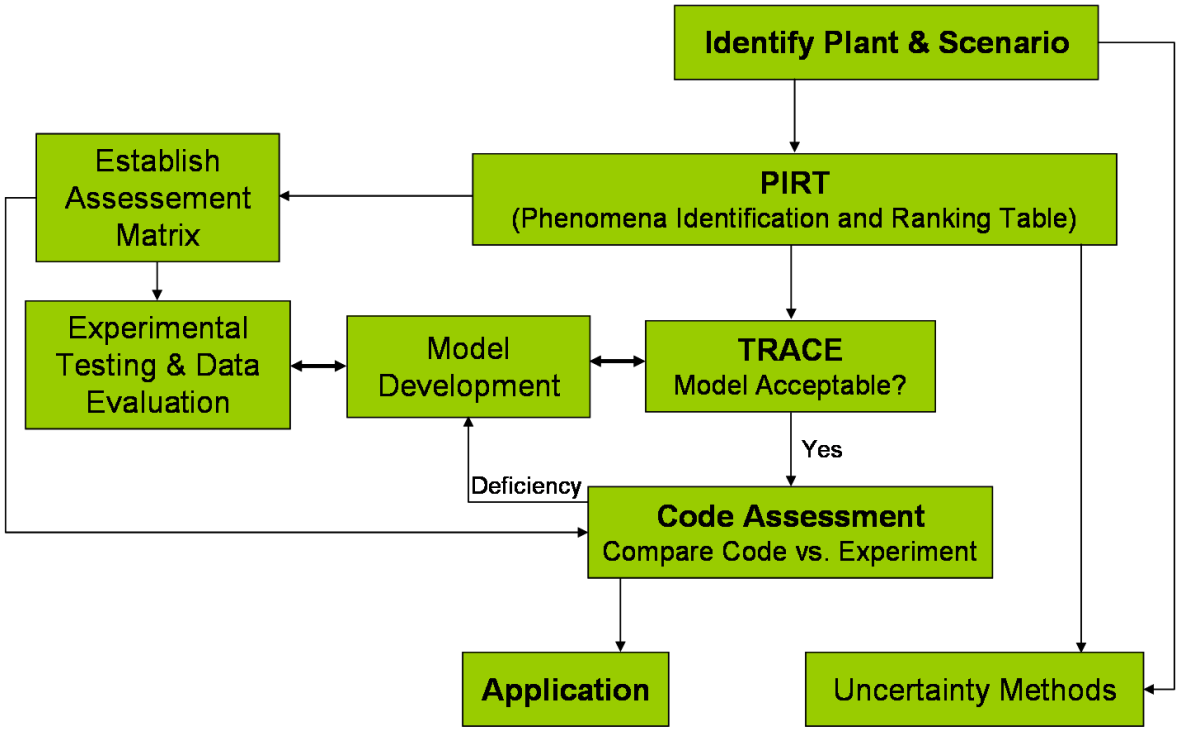

Figure 20 Flowchart of the TRACE Development Process for LWRs

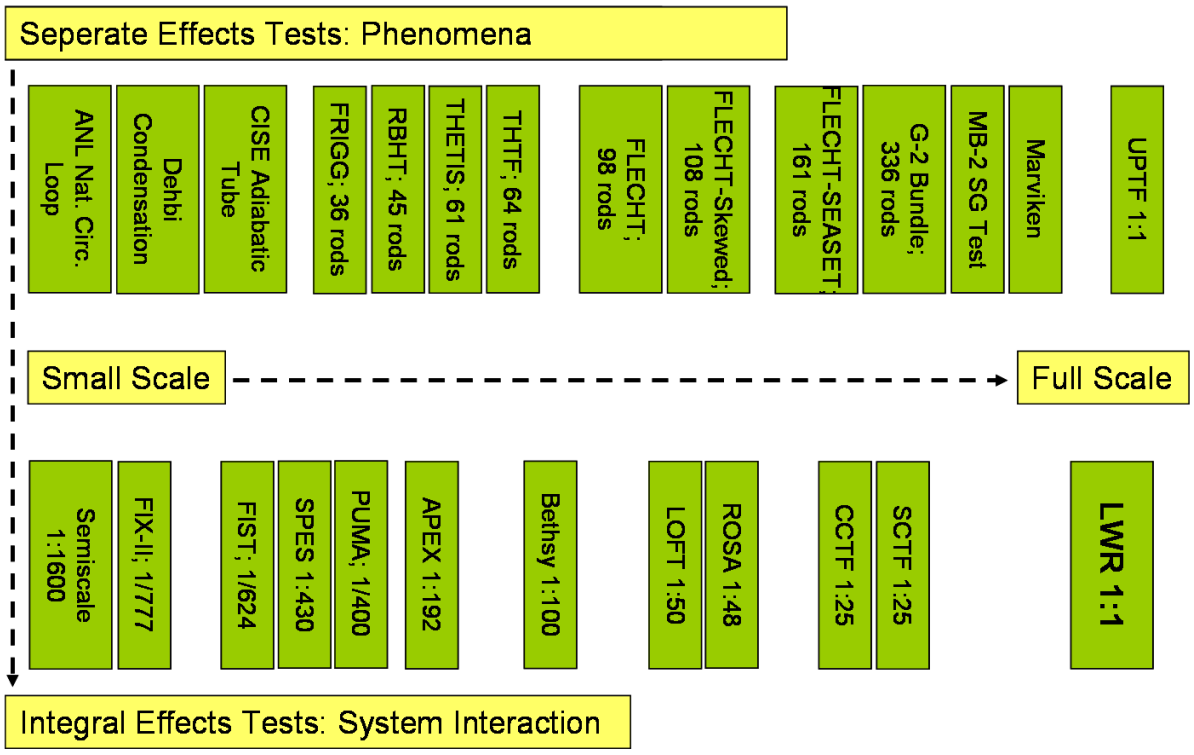

Figure 21 TRACE Validation Matrix for LWRs

4.2 SUSA

4.2.1 Generalities

The program system SUSA (Software for Uncertainty and Sensitivity Analysis) of the GRS (Gesellschaft fuer Anlagen- und Reaktorsicherheit mbH) [12, 13] can be used in general to evaluate the uncertainty of results and the sensitivity concerning input and boundary parameter variations. In particular, with respect to the uncertainty evaluation, SUSA can provide the range of output parameters and margins of upper and lower bounds to acceptance limits or safety criteria. For the sensitivity evaluation, SUSA can be used to identify important parameters based on sensitivity coefficients and corresponding ranks. Furthermore, these results can be used as feedback to code and physical model developments and to experimental investigations. Due to its programming in Visual Basic as an Add-on for Microsoft Excel, SUSA can be used for various problems including thermal hydraulics and neutron physics.

SUSA follows the input error propagation approach. The uncertainties in the input deck or the source code of any program (assuming source code is accessible) will be treated as stochastic variables. The deterministic code transforms the stochastic input into a stochastic output. Thereby, the uncertainties in the input will be propagated to the output. By means of statistical methods uncertainty information of selected output parameters will be extracted from the output. A mathematical formulation of this paragraph is given in the following equation [14].

Input sample of size N | **Input multivariate k stochastic input variables** | **Input variables for N code executions** | **N code executions**

$$\begin{pmatrix}(X)_1\\(X)_2\\\vdots\\(X)_N\end{pmatrix}=\begin{pmatrix}(X_1,\dots,X_k)_1\\(X_1,\dots,X_k)_2\\\vdots\\(X_1,\dots,X_k)_N\end{pmatrix}\rightarrow\begin{pmatrix}(x_1,\dots,x_k)_1\\(x_1,\dots,x_k)_2\\\vdots\\(x_1,\dots,x_k)_N\end{pmatrix}\rightarrow\begin{pmatrix}\mathrm{Code}[(x_1,\dots,x_k)_1]\\\mathrm{Code}[(x_1,\dots,x_k)_2]\\\vdots\\\mathrm{Code}[(x_1,\dots,x_k)_N]\end{pmatrix}\rightarrow\dots$$

$$\dots\rightarrow\begin{pmatrix}(y_1,\dots,y_m)_1\\(y_1,\dots,y_m)_2\\\vdots\\(y_1,\dots,y_m)_N\end{pmatrix}=\begin{pmatrix}\mathrm{Code}[(X)_1]\\\mathrm{Code}[(X)_2]\\\vdots\\\mathrm{Code}[(X)_N]\end{pmatrix}\rightarrow\begin{pmatrix}(Y)_1\\(Y)_2\\\vdots\\(Y)_N\end{pmatrix}\tag{27}$$

Output multivariate m stochastic output variables | **Output sample of size N**

4.2.2 Probability Density Function and Other Statistical Parameters

For a comprehensive understanding of the SUSA methodology some statistical parameters will be introduced and explained. Reference of this section can be given, if not indicated otherwise to [15]. First, a function is defined that assigns a real number to a point in a sample space. That function is called random variable. The probability of a random variable which corresponds to the individual values assumed by the random variable equals the sum of the probability associated with the values of the set which is:

$$P(a<X<b)=\sum_{a<x<b}P(X=x)\tag{28}$$

The random variable can be described by the probability density function (PDF) and writes as follows

$$f(x)=\begin{cases}P(X=x), & \{x\in\mathbb{Z}|-\infty\le x\le\infty\}\\P(x-dx<X<x+dx), & \{x\in\mathbb{R}|-\infty\le x\le\infty\}\end{cases}\tag{29}$$

The PDF is the derivative of the cumulative distribution function which is the probability that a random variable (X) is less or equal to any integer or real number (x) and is given by the following equation

$$F(x)=P(X\le x)=\begin{cases}\sum_{t\le x}f(t) & \{t\in\mathbb{Z}|-\infty\le t\le x\}\\\int_{-\infty}^{x}f(t)dt & \{t\in\mathbb{R}|-\infty\le t\le x\}\end{cases}\tag{30}$$

Furthermore, the expected value or the population mean (μ), the population variance (σ^2) and the standard deviation (σ) can be expressed by means of the PDF.

$$\mu = E(X) = \begin{cases} \sum_{x} x \cdot f(x) & \{x \in \mathbb{Z} | -\infty \leq x \leq \infty\} \\ \int_{-\infty}^{\infty} x \cdot f(x) dx & \{x \in \mathbb{R} | -\infty \leq x \leq \infty\} \end{cases} \tag{31}$$

$$\sigma^2 = E[(X-\mu)^2] \begin{cases} \sum_{t} (x-\mu)^2 \cdot f(x) & \{x \in \mathbb{Z} | -\infty \leq x \leq \infty\} \\ \int_{-\infty}^{\infty} (x-\mu)^2 \cdot f(x) dx & \{x \in \mathbb{R} | -\infty \leq x \leq \infty\} \end{cases} \tag{32}$$

$$\sigma = \sqrt{\sigma^2} = \sqrt{E[(X-\mu)^2]} = \begin{cases} \sqrt{\sum_{x} x \cdot f(x)} & \{x \in \mathbb{Z} | -\infty \leq x \leq \infty\} \\ \sqrt{\int_{-\infty}^{\infty} (x-\mu)^2 \cdot f(x) dx} & \{x \in \mathbb{R} | -\infty \leq x \leq \infty\} \end{cases} \tag{33}$$

The above given formulas express statistical parameters of the input parameters with infinite boundary conditions but are identical for the analysis of output parameter with limited variation. The mean of the output parameter with limited numbers of samplings is expressed as $\bar{y}$, and the sample variance, s^2, can be written:

$$\bar{y} = \frac{1}{N} \cdot \sum_{i=1,N} y_i \tag{34}$$

$$s^2 = \frac{1}{N-1} \cdot \sum_{i=1,N} (y_i - \bar{y})^2 \tag{35}$$

The equations above are valid for the scalar case meaning that the output parameter has no special or temporal dependency (index dependent) which is not part of the actual uncertainty analysis. In case the output parameter is a function of time (like the peak cladding temperature during LOCA transients) the mean and the sample variance can be calculated according to the hereafter given equations

$$\bar{y}(t) = \frac{1}{N} \cdot \sum_{i=1,N} [y(t)]_i \tag{36}$$

$$[s(t)]^2 = \frac{1}{N-1} \cdot \sum_{i=1,N} \{[y(t)]_i - \bar{y}(t)\}^2 \tag{37}$$

The standard deviation can be calculated by

$$s = \begin{cases} \sqrt{s^2} \\ \sqrt{[s(t)]^2} \end{cases} \tag{38}$$

After the number of samples is defined, the distribution type must be specified. Based on the information known, e.g., the minimum and maximum, quantiles, the expected value, the standard deviation or the parameters of the untruncated distribution, distribution types such as the normal, log-normal, uniform, log-uniform, triangular, etc. can be selected. The normal distribution type will be chosen for a random number to demonstrate how known information can influence the distribution trend and subsequent the values which will be generated. For the normal distribution, given in Eq. (39), the reference value (= 3.0), the minimum (= 1.0), the maximum (= 5.0) and two quantiles are known. The quantiles are 2.0 with a probability of 10 % and 4.5 with a probability of 90%

$$F(x) = P(a \le X \le b) = \int_a^b \frac{1}{\sqrt{2 \cdot \pi \cdot \sigma}} \cdot e^{-\frac{1}{2}\left(\frac{x-\mu}{\sigma}\right)^2} dx \tag{39}$$

The density function for the above given example is plotted in Figure 22.

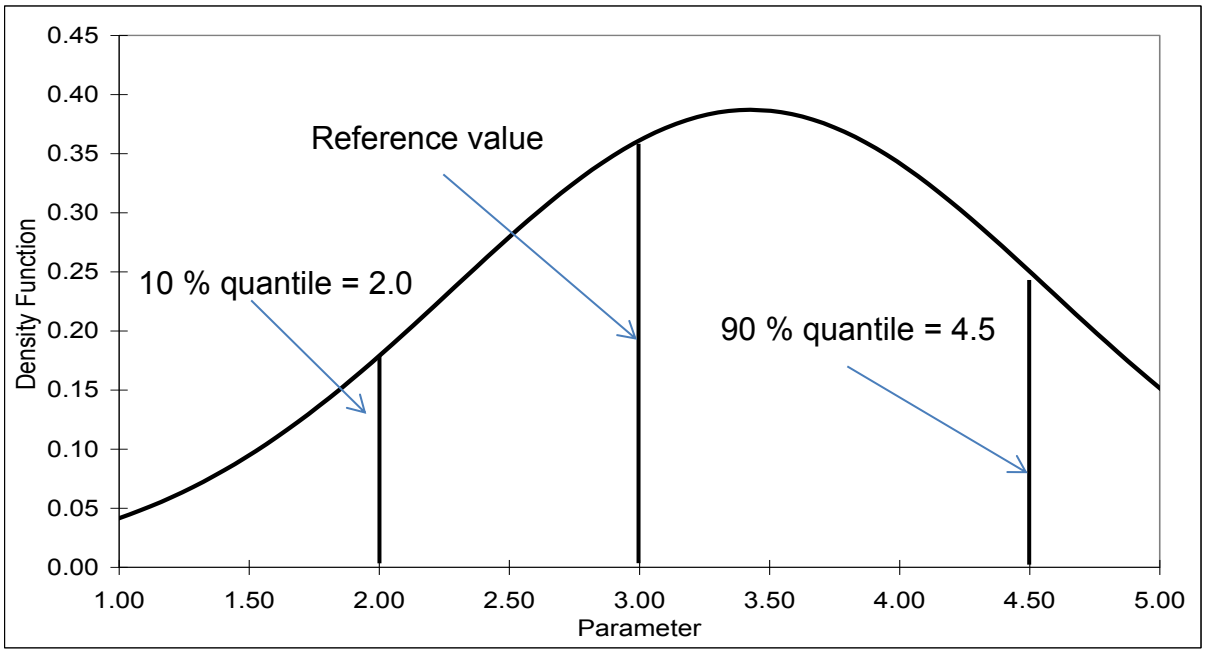

Figure 22 Normal Distribution with 2 Known Quantiles

4.2.3 Number of Samples

As shown in Eq. (27) each selected input and source code parameter will be sampled according to the statistical fidelity which is required (e.g. 95 %/95 %) and N values for each parameter will be generated. Afterwards, these N values will be written in N inputs and the N inputs will be executed yielding N outputs. Before the parameter sampling is performed, the size of N, the distribution of the N values between the minimum and maximum must be known and the type of sampling needs to be specified. Unfortunately, the distribution (PDF) is usually unknown. Sometimes only information about maximum and minimum are known. But information about PDF's can be obtained from empirical distribution functions and estimators. Quantiles are useful estimators. A quantile of a random variable is a point in the sample space of the distribution of the random variable.

$$P \leq \begin{cases} p & \{X < x_p\} \\ 1-p & \{X > x_p\} \end{cases} \tag{40}$$

With that definition the tolerance interval can be introduced. The tolerance interval, with L as lower and U as upper interval limit is an estimate of a random variable which contains a fraction of the variable probability, p, with a specified level of confidence, β, which expresses that p is overestimated conservatively with a certain probability (e.g. 95 %) by the (p, β) tolerance limit. That means that the probability of having a sample of the random variable between the lower and upper interval is exactly p and β expresses how sure one is about this, see Figure 23. The confidence level accounts for the limited number of samples (or experimental data).

For practical reasons one can write for the first one-sided tolerance limit

$$P\left(x_p \leq X^{N+1-l}\right) \geq \beta \tag{41}$$

$$P\left(x_p \leq X^{N+1-l}\right) \geq \sum_{i=0}^{N-m} \binom{N}{i} \cdot p^i \cdot (1-p)^{N-i} \tag{42}$$

Rewriting the left side of Eq. (42), which is possible since the sum of the binomial probabilities yield unity, and changing the index, j = N – i, will result to the following equation.

$$\sum_{i=0}^{N-l} \binom{N}{i} \cdot p^i \cdot (1-p)^{N-i} = 1 - \sum_{i=N-l+1}^{N} \binom{N}{i} \cdot p^i \cdot (1-p)^{N-i} \tag{43}$$

$$\sum_{i=0}^{N-l} \binom{N}{i} \cdot p^i \cdot (1-p)^{N-i} = 1 - \sum_{j=0}^{l-1} \binom{N}{j} \cdot p^{N-j} \cdot (1-p)^j \tag{44}$$

which yields

$$1 - \sum_{j=0}^{l-1} \binom{N}{j} \cdot p^{N-j} \cdot (1-p)^{j} \geq \beta \tag{45}$$

The second one-sided tolerance limit can be written as follows:

$$1 - \sum_{i=0}^{u-1} \binom{N}{i} \cdot p^{N-i} \cdot (1-p)^{i} \geq \beta \tag{46}$$

After the aid of the calculus the two-sided tolerance limit can be written:

$$1 - \sum_{i=0}^{l+u-1} \binom{N}{i} \cdot p^{N-i} \cdot (1-p)^{i} \geq \beta \tag{47}$$

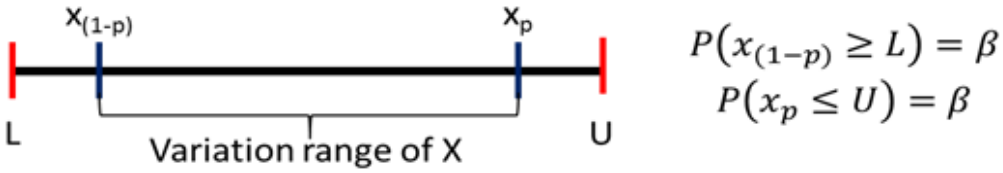

Figure 23 Definition of the Tolerance Interval

In case the sum of the integers l + u = 1, the one-sided tolerance limit is used. If l + u = 2, the two-sided tolerance limit is used. Solving the binomial Eq. (47) it yield the following two equations which is known as the Wilk's formula [16] for one-side tolerance limit, Eq. (48) and two-sided tolerance limit, Eq. (49).

$$\beta = 1 - p^{N} \tag{48}$$

$$\beta = 1 - p^{N} - N \cdot (1-p) \cdot p^{N-1} \tag{49}$$

As it can be seen from Eq. (48) and Eq. (49), the number of samples depends only on the probability content and on the level of confidence but not on the number of input and source code parameters. Values of N are tabulated in Table 5 and Table 6 for various p and β combinations. The highlighted numbers correspond to a confidence level of 95 % and a probability content of 95 %. These numbers are accepted in (nuclear) engineering as being satisfactory in terms of statistical fidelity, see part 50, paragraph 46 of [17].

Table 5 Minimum Sample Size (N) for the One-sided Tolerance Limit (l + u = 1)

β	p									
	0.500	0.700	0.750	0.800	0.850	0.900	0.950	0.975	0.980	0.990
0.500	1	2	3	4	5	7	14	28	35	69
0.700	2	4	5	6	8	12	24	48	60	120
0.750	2	4	5	7	9	14	28	55	69	138
0.800	3	5	6	8	10	16	32	64	80	161
0.850	3	6	7	9	12	19	37	75	94	189
0.900	4	7	9	11	15	22	45	91	144	230
0.950	5	9	11	14	19	29	59	119	149	299
0.975	6	11	13	17	23	36	72	146	183	368
0.980	6	11	14	18	25	38	77	155	194	390
0.990	7	13	17	21	29	44	90	182	228	459

Table 6 Minimum Sample Size (N) for the Two-sided Tolerance Limit (l + u = 2)

β	p									
	0.500	0.700	0.750	0.800	0.850	0.900	0.950	0.975	0.980	0.990
0.500	3	6	7	9	11	17	34	67	84	168
0.700	5	8	10	12	16	24	49	97	122	244
0.750	5	9	10	13	18	27	53	107	134	269
0.800	5	9	11	14	19	29	59	119	149	299
0.850	6	10	13	16	22	33	67	134	168	337
0.900	7	12	15	18	25	38	77	155	194	388
0.950	8	14	18	22	30	46	93	188	236	473
0.975	9	17	20	26	35	54	110	221	277	555
0.980	9	17	21	27	37	56	115	231	290	581
0.990	11	20	24	31	42	64	130	263	330	662

4.2.4 Sampling

After the probability density function has been characterized for each uncertain parameter and the number of code calculations has been calculated the sampling process can be performed. In the present case 93 numbers (or any other number) will be generated following the trend of the probability density function. In SUSA, two different ways of sampling are available. The first one is the simple random sampling, the second one is the Latin hypercube sampling.

Random sampling is the simplest approach of sampling numbers of a particular subset. Each sample value is generated independently of the other sample values (rolling a die) by means of Monte-Carlo algorithm. Therefore, it is possible that a sample value is not going to be generated from a subset which might be of interest for the analysis. The sensitivity studies point out which of the parameter must be evaluated with special care.

It is furthermore possible that sample values with a low probability but high consequences (like peak power or minimal mass flow rate) are missed. Considering a normal distribution and a limited number of 93 samples per parameter it is rather unlikely that, e.g., the highest power, the lowest mass flow rate and the lowest gas gap conductivity will be sampled at the same time. The

combination of these, and other extreme cases, would be of high interest if analyzing the peak cladding temperature during different scenarios.
In order to avoid the missing of extreme cases or more precisely the combination of extreme cases a different sampling technique is available in SUSA. For the present investigation, the Latin Hypercube Sampling (LHS) method is not applied. Therefore, only a brief introduction will be given here. Detailed information about Latin hypercube sampling can be found in [18] and [19].

In LHS n values of *k* parameters (X_1, X_2, …, X_k) are selected. The range of variation is split into *n* intervals which are non-overlapping and are of equal probability. One value from each interval is selected at random with respect to the probability density in the interval. The *n* values for X_1 are paired randomly with the *n* values for X_2. The *n* pairs are combined with the *n* values for X_3, continuing in this manner until *nk* tuplets are formed [20]. In a matrix of (*n* x k) dimensions it will guarantee that in each column (*n*) and each row (*k*) only one sample can be found. In random sampling the distribution of the samples is independent of the previous sample. That means that some columns, which represent an interval on the parameter range, will remain empty. With the above given explanations the sampling can be performed and a pre-selected number of samples will be generated according to the chosen PDF.

The so generated values for each parameter must be implemented in an existing code calculation strategy. The way such incorporation of *n* samples per *k* input parameters is done is given in sub-section 5.2. Following the execution of the code(s) selected results will be transferred to SUSA to evaluate the uncertainty and the sensitivity.

4.2.5 Statistical Measures

During the sensitivity study with SUSA input and output parameters are checked if they are correlating in a linear manner. This can be expressed by the covariance between parameter *x* (input variable) and parameter *y* (output variable). The covariance is defined as follows.

$$\mathrm{Cov}(\mathrm{x},\mathrm{y}) = \frac{\sum(\mathrm{x_i} - \mu_\mathrm{x}) \cdot (\mathrm{y_i} - \mu_\mathrm{y})}{\mathrm{N}} \tag{50}$$

In case the covariance is calculated to be zero no linear dependence exists between the two selected parameters. However, a correlation following a different function, e.g. polynomial, exponential, might be existing. The calculated value might be large but it is not possible to find out whether the relation between the parameters is strong or not [21]. In order to remove the dependency of the scale from the covariance it is divided by the standard deviation of the selected parameters.

	n_1	n_2	n_3	n_4
k_1			**X**	
k_2	**X**			
k_3		**X**		
k_4				**X**

	n_1	n_2	n_3	n_4
k_1	**X**			
k_2			**X**	
k_3			**X**	
k_4				**X**

Figure 24 Comparison of Latin Hypercube Sampling (left side) and Random Sampling (right side) Regarding the Sampling Distribution

This approach is working if both parameters can be expressed in quantitative units, meaning physical values. In that case one is referring to parametric correlations. An example is the Pearson's product momentum correlation coefficient. If at least one of the parameters is expressed in form of a ranking system non-parametric (monotonic) correlations will be used. If one parameter is a numerical value and the second one is based on ranks, the numerical values will be converted to ranks. Spearman's rank correlation coefficient, Kendall's tau and Blomqvist's medial correlation coefficient are non-parametric correlation measures. The four named correlation measures are available in SUSA and will be shortly described in the following.

One of the most used sensitivity measure is the product momentum correlation coefficient of Pearson (*r*) which is defined as:

$$r = \frac{\sum_{i=1}^{N}(x_i - \mu_x)\cdot(y_i - \mu_y)}{\left[\sum_{i=1}^{N}(x_i - \mu_x)^2 \cdot \sum_{i=1}^{N}(y_i - \mu_y)^2 \cdot\right]^{\frac{1}{2}}} \tag{51}$$

The rank correlation coefficient of Spearman, denoted as ρ is writes as follows:

$$\rho = \frac{\sum_{i=1}^{N} R(x_i)\cdot R(y_i) - N\cdot\left(\frac{N+1}{2}\right)^2}{\left[\sum_{i=1}^{N} R(x_i)^2 - N\cdot\left(\frac{N+1}{2}\right)^2\right]^{\frac{1}{2}}\cdot\left[\sum_{i=1}^{N} R(y_i)^2 - N\cdot\left(\frac{N+1}{2}\right)^2\right]^{\frac{1}{2}}} \tag{52}$$

where *R* denotes the rank of the selected parameter. A simplified form can be used if no ties exist

$$\rho = \frac{6\cdot\sum_{i=1}^{N}[R(x_i) - R(y_i)]^2}{N\cdot(N^2-1)} \tag{53}$$

A different approach is used by Kendall for his non-parametric correlation measure called tau [22]. In this measure, simulation results are grouped in concordant (n_c) and discordant (n_d) pairs. A pair is concordant if the values of one calculation are greater than the respective values of a second calculation. τ is defined as follows:

$$\tau = \frac{2\cdot(n_c - n_d)}{N\cdot(N-1)} \tag{54}$$

For the sake of clarity, a small example will be used to illustrate the underlying methodology of Kendall's tau. Assume that two persons have to rank the n = 4 parameters [a, b, c, d] in a certain way. Person number one ranks the parameters as follows [a, b, c, d] = [1, 2, 3, 4] while the second person ranks it in the following order [a, b, c, d] = [1, 3, 2, 4]. Based on that ranking six ordered pairs can be derived. For person number one {[1, 2], [1, 3], [1, 4], [2, 3], [2, 4], [3, 4]} are the pairs and the six pairs for person number two are {[1, 3], [1, 2], [1, 4], [3, 2], [3, 4], [2, 4]}. 5 of the ordered pairs appear for both persons {[1, 2], [1, 3], [1, 4], [2, 4] and [3, 4]. These pairs are the concordant pairs (n_c = 5). One pair per person is not represented in the sequence of the other

person, [2, 3] for person 1 and [3, 2] for person 2. Therefore, the number of discordant pairs is 1 (n_d = 1). With these numbers Kendall's tau can be rewritten as.

$$\tau = \frac{2 \cdot (5-1)}{4 \cdot (4-1)} = \frac{8}{12} = 0.667 \tag{55}$$

The last sensitivity measure is the medial correlation coefficient of Blomqvist, commonly referred to beta [23]. Let (x_1, y_1) … (x_n, y_n) be a sample of a 2D population and m_x, m_y the medians of the sample. The 2D plane spanned by x and y will be divided into four regions by introducing the lines $x = m_x$ and $y = m_y$. With the number of sample points in the different sectors a correlation between x and y can be obtained. The following formula shows Blomqvist's β with two sample numbers where each number represents the sample numbers of two sectors.

$$\beta = \frac{\mathrm{N}_1 - \mathrm{N}_2}{\mathrm{N}_1 + \mathrm{N}_2} = \frac{2 \cdot \mathrm{N}_1}{\mathrm{N}_1 + \mathrm{N}_2} - 1 \tag{56}$$

These four coefficients have in common that the result will be between -1.0 and +1.0. Based on the number and its algebraic sign the strength and the direction of the correlation are indicated. The strength is determined by the value. Values close to -1.0 or +1.0 indicate a very strong correlation while values close to zero indicate low or no correlation. The direction is indicated by the algebraic sign. A positive value means that with increasing *X* (input) value the *Y* (output) value is increasing, too. A negative sign means that if *X* is increasing *Y* is decreasing. Table 7 gives a qualitative overview whether the correlation is strong or not and Figure 25 illustrates the meaning of the calculated coefficient.

The plots in the diagonal represent a coefficient of +1.0. The values on the abscissa are increasing and the ordinate is following. The number 0.025 in the upper right corner indicates a very low dependency which can be already called independent. The corresponding plot in the lower left corner shows that the points are scattered across the whole plot and no correlation can be deduced.

Table 7 Dependency of Correlation as Function of the Sensitivity Coefficient

Correlation	Positive	Negative
Independent	0.0	
Weak	+ 0.29 … + 0.10	- 0.29 … - 0.10
Medium	+ 0.49 … + 0.30	- 0.49 … - 0.30
Strong	+ 1.00 … + 0.50	- 1.00 … - 0.50

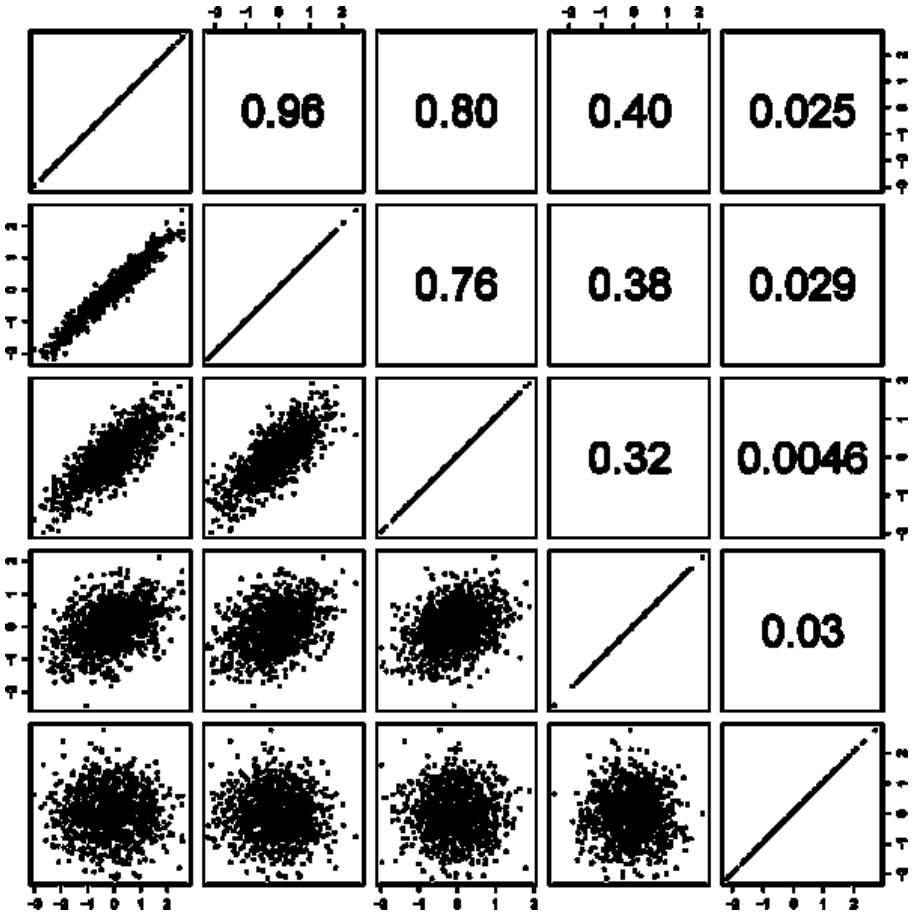

Figure 25 Meaning of Statistical Correlation [14]

Besides the ordinary correlation coefficients, two other coefficients can be calculated. These are the partial correlation coefficient (PCC) and the standardized regression coefficient (SRC). The presented measures correlate the linear relationship between two random variables. In cases several random variables are involved these variables can influence each other in a way that the influence of one random variable on a second random variable might bias the results. With the PCC that perturbation is eliminated so that only the influence of variable 1 on variable 2 is evaluated. This can also be a disadvantage because it is possible that a parameter with an actual low correlation compared to another parameter can obtain a high sensitivity coefficient, meaning that its importance is over estimated.

For the Pearson product momentum correlation the PCC is denoted as follows (if $N = 3$),

$$r_{12.3} = \frac{r_{12} - r_{13} \cdot r_{23}}{\sqrt{(1 - r_{13}^2) \cdot (1 - r_{23}^2)}} \tag{57}$$

where r_{ij} is the regular Pearson product moment correlation coefficient evaluated between X_i and X_j. In the same way the PCC of e.g. Kendall's tau can be calculated

$$\tau_{12.3} = \frac{\tau_{12} - \tau_{13} \cdot \tau_{23}}{\sqrt{(1 - \tau_{13}^2) \cdot (1 - \tau_{23}^2)}} \tag{58}$$

The SRC is similar to the PCC since the influence of non-selected random variables will be eliminated. But in the SRC the linear influence of the other parameters will be erased. In addition, SUSA also offers importance measures like correlation ratios and correlation ratios on ranks.

A figure of merit for the significance of the analysis (or how well fits a model the data) can be the coefficient of determination, R^2 which is determined as follows:

$$R^2 = 1 - \frac{RSS_{model}}{RSS_{0-model}} \tag{59}$$

It is the comparison of the residual sums of squares for the model and the 0-model which is the reference of comparison. This model describes a horizontal line at the level of the mean of the y values, which is the simplest possible model that could be fitted to any set of data [21].

To avoid confusion about the terminology “being of importance” or “being sensitive to” it must be clarified that the coefficients calculated consider the parameter variation and not only the parameter. During an uncertainty and sensitivity analysis the most important parameters for the peak cladding temperature might be the mass flow rate or the coolant inlet temperature while the power is evaluated to be of low or no importance. That is somehow violating the general understanding that the power is a dominant factor for the evaluation of the peak cladding temperature. The calculated values, however, are only valid for the selected case within the applied parameter range. If the power is changed only marginal but the mass flow rate and the inlet temperature show a high variation their variation has a bigger impact on the results than the small variation of the power.

4.3 DAKOTA

DAKOTA (Design Analysis Kit for Optimization and Terascale Applications) is under development by the Sandia National Laboratories. It is intended to be a multilevel parallel object-oriented framework for design optimization, parameter estimation, uncertainty quantification, and sensitivity analysis [24]. DAKOTA has been implemented into the Symbolic Nuclear Analysis Package (SNAP) which is the graphical interface for using NRC codes such as TRACE (refer to section 4.4).

The general theory behind DAKOTA concerning the sampling, the uncertainty quantification and the sensitivity analysis is identical to SUSA. In addition, DAKOTA employs also the formula of Wilk. The data flow between TRACE and DAKOTA is similar to the one of TRACE and SUSA as depicted in Figure 26 with the exception that the data extracted is automatized and no actions from the user are required. Since everything is done in SNAP, the user does not need to write scripts for the data transfer. One only needs to select the input parameters, the uncertainty band with the corresponding distribution, the number of samples, the type of sampling and the desired output parameters. The disadvantage of this process is that only parameters can be selected which are made available to DAKOTA in SNAP.

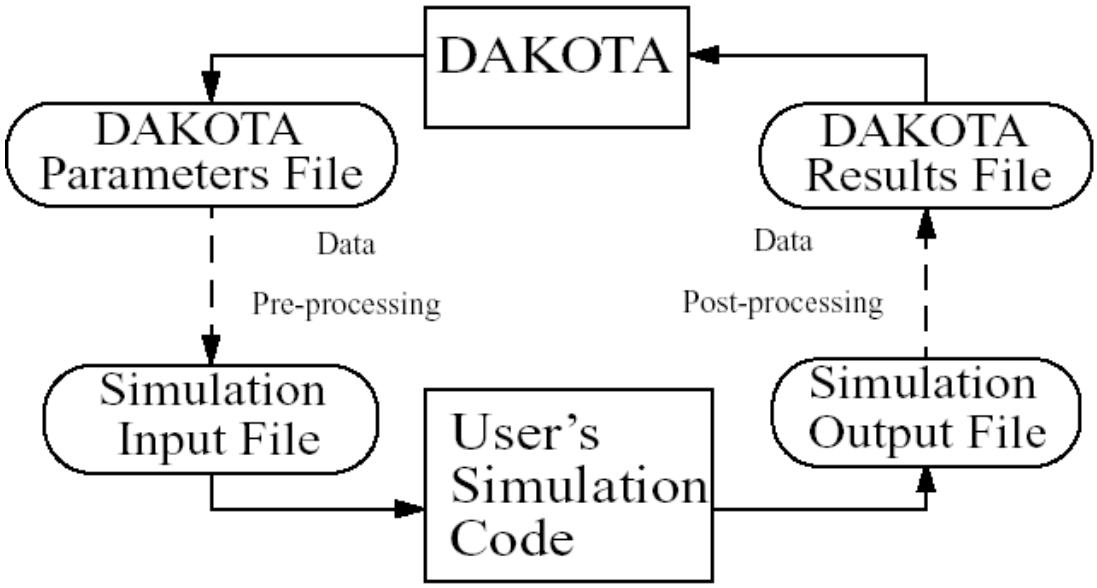

Figure 26 Coupling Scheme between DAKOTA and a Simulation Code

Currently, not all parameters of the input deck are available for uncertainty analysis, see the following section. Moreover, the parameters which can be selected are limited to the input deck. Physical model parameters cannot be selected yet even if all necessary uncertain parameters are known.

4.4 SNAP

SNAP, the Symbolic Nuclear Analysis Package, is a graphical user interface which is under development by Applied Programing Technology, Inc [25]. The main purpose of SNAP is to simplify the analysis process related to engineering orientated simulations and modeling. By means of the Common Application Framework for Engineering Analysis (CAFEAN), a very flexible framework for creating, editing and processing input decks of several engineering codes is utilized. The major U.S. NRC codes for the evaluation and simulation of LWRs are incorporated into SNAP via java based plugins, among them TRACE, COBRA, RELAP5, MELCOR, PARCS and CONTAIN. The architecture, see Figure 27, is divided in client and server applications where a client application is the one which is performed on a local machine and provides a graphical user interface while the server application runs in the background and on a different machine [25]. Besides the main analysis tools, other programs can be used like DAKOTA to perform the uncertainty analysis or AptPlot to allow the graphical representation of results.

Moreover, SNAP consists of a suite of integrated applications including the Model Editor, the Configuration Tool and the Job Status.

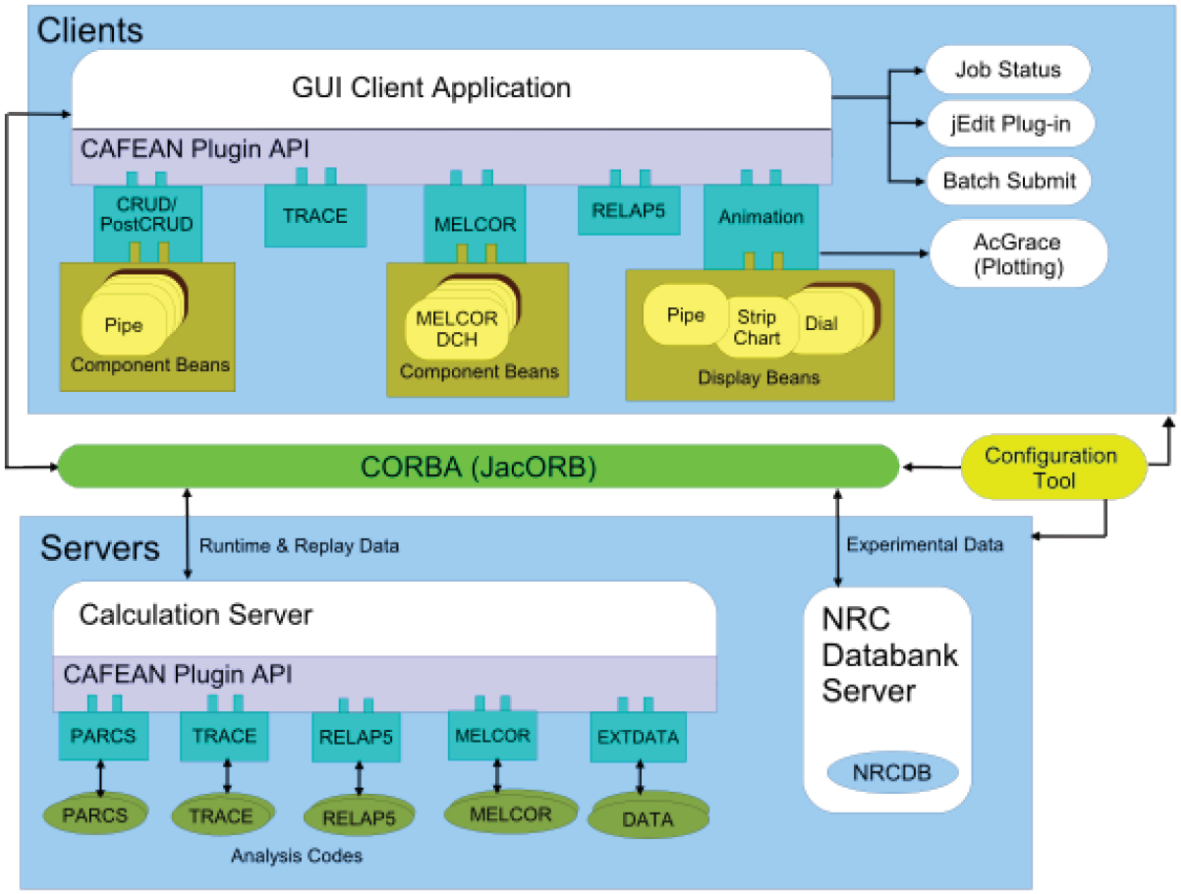

Figure 27 SNAP Architecture [25]

The Model Editor is the actual graphical user interface used for client applications. It is used for the development and modification of the input deck of the considered code(s). Within the model editor the components of the different codes can be presented and arranged to improve the modeling process. In addition, the modeled components/loops/plants can be animated to visualize the results. A screenshot of the Model Editor is given in Figure 28. The Model Editor itself is divided into five components or windows. At the Toolbar the main operations (safe, load, etc.) can be performed. It can also be used to create a new component. In the navigator window the different components and model options can be selected. These components will then appear in the Property View window where the modification of selected parameters can be done. The view/Dock view visualizes the component. In that window, the components can be connected to each other and arranged in loops to allow a better understanding on the behavior. The Message window keeps the user informed about the last actions performed.

The Configuration Tool is used to define the global settings of the client application. With it, new applications, e.g., a new TRACE or DAKOTA model, can be created. It is also used to connect the executables of the involved programs (TRACE, JAVA, AptPlot, etc.) with the applications, Figure 29.

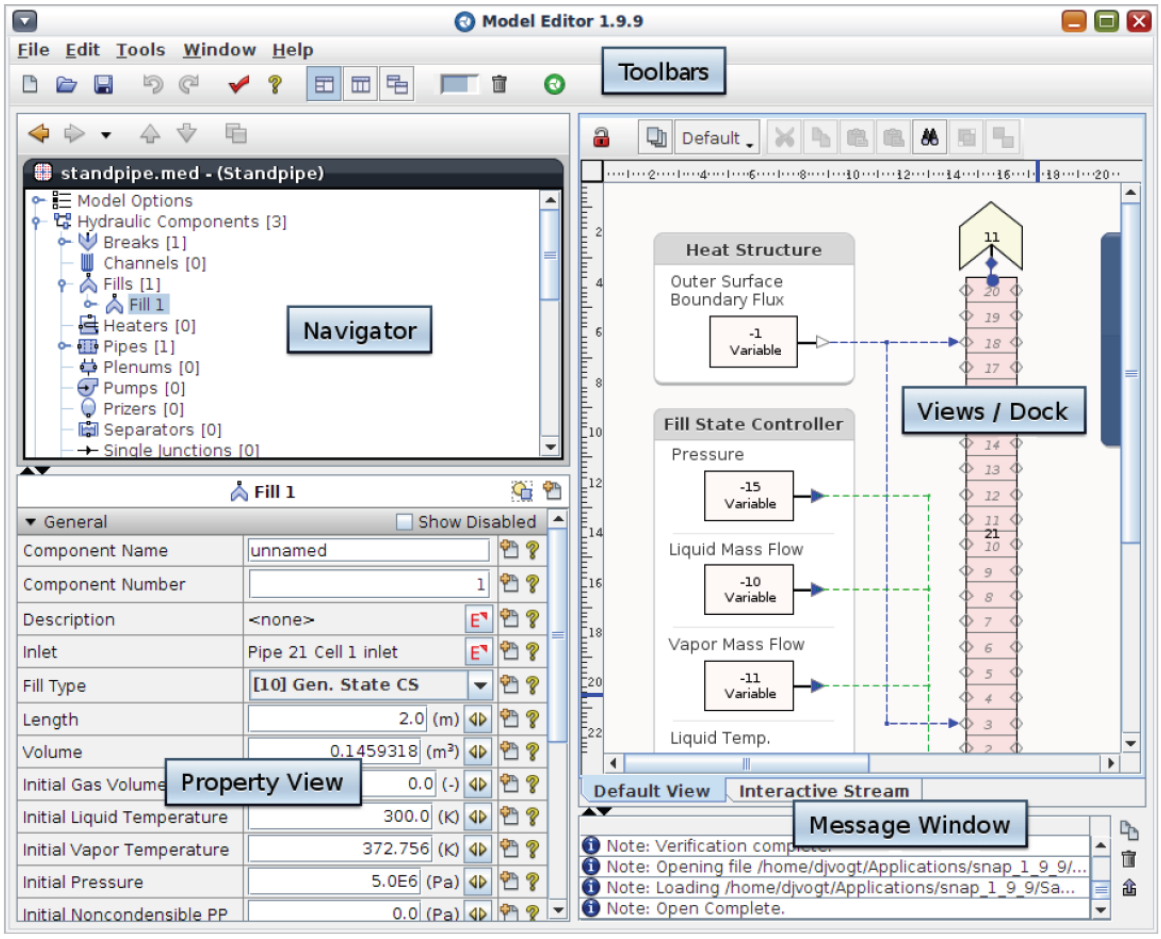

Figure 28 Model Editor

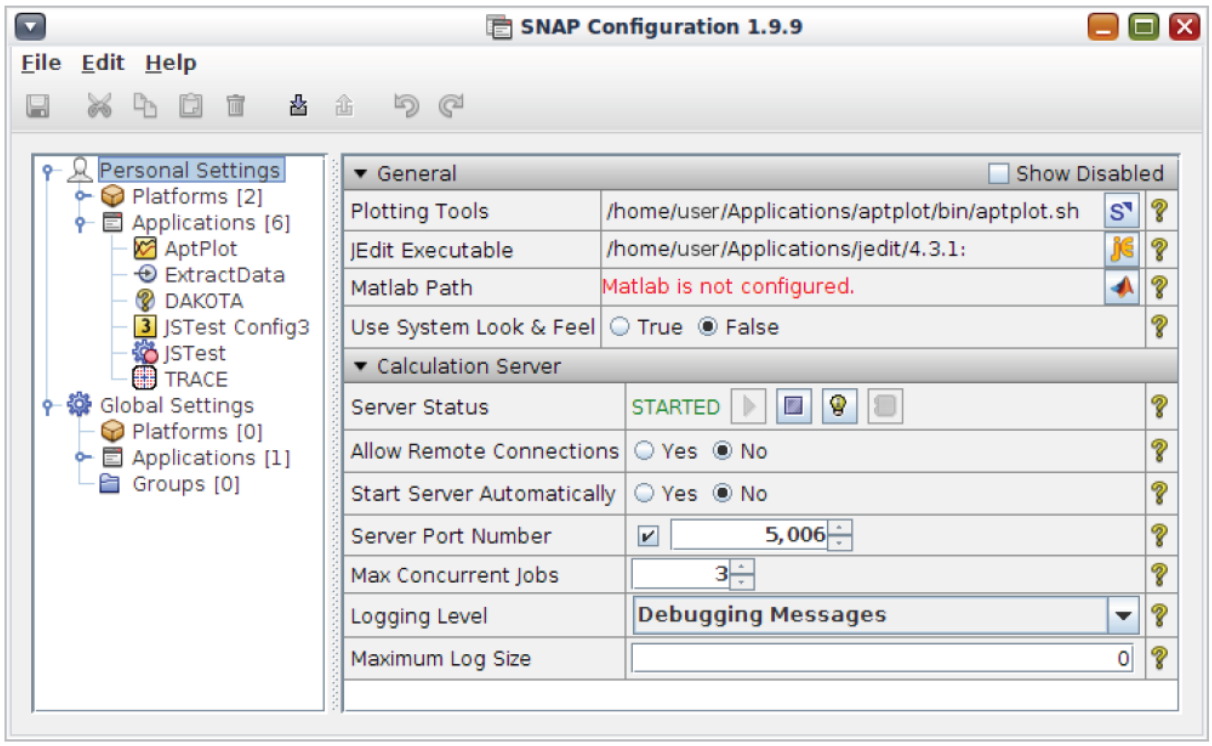

Figure 29 Configuration Tool

The last integrated application is the Job Status which monitors the progress and status of each simulation. Besides that, local files can be imported as new jobs, Figure 30.

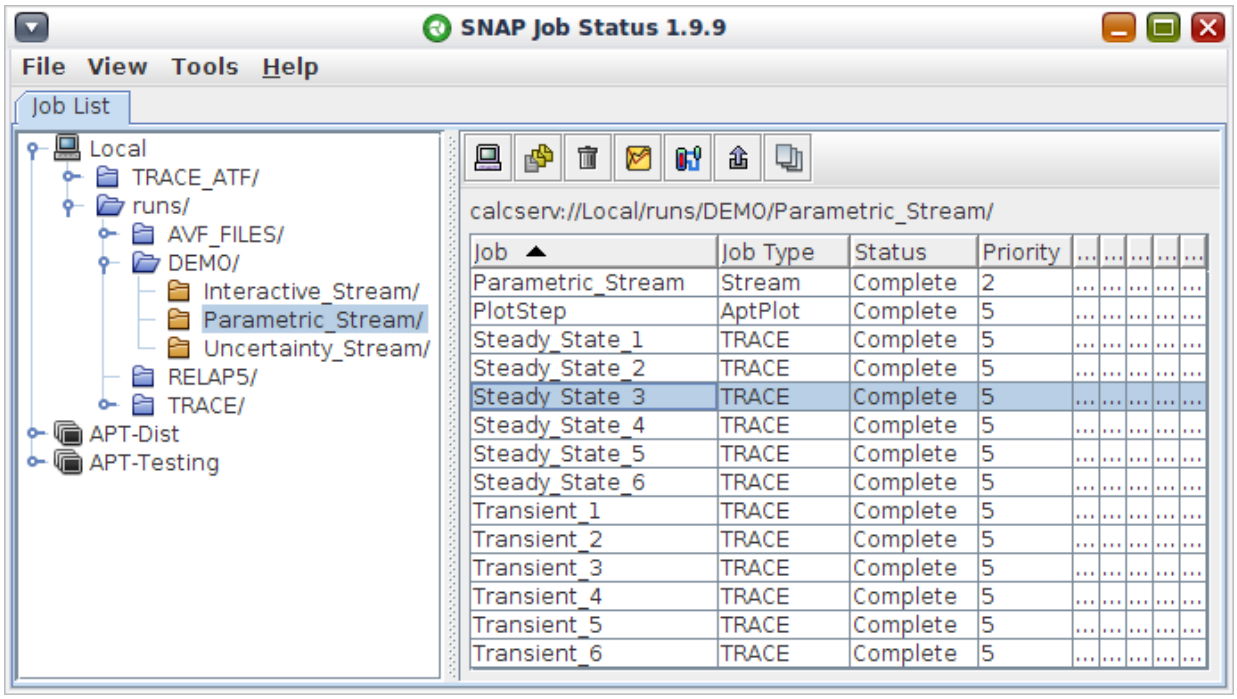

Figure 30 Job Status

5 APPLIED UNCERTAINTY AND SENSITIVITY METHODOLOGY

5.1 General Remarks

To select parameters for the uncertainty and sensitivity study, the input and boundary conditions and the physical models need to be evaluated with respect to their impact on the output parameter of interest.

The following sub sections are aimed to provide the reader the information necessary to perform similar investigations with TRACE-SUSA and TRACE-DAKOTA and can be used as a guideline. In case only the results of these investigations are of interest, this section can be skipped.

To perform U+S studies two codes/programs are needed. The first code is to perform the analyses of interest, in the present case thermal-hydraulic evaluation of the BFPT benchmark. The tool of choice is TRACE. In order to evaluate the results regarding uncertainty and sensitivity constrains, a different code must be applied. In the first case it is SUSA (sub section 5.2) and in the second case it is DAKOTA (sub section 5.3).

5.2 Uncertainty and Sensitivity Study with TRACE-SUSA

5.2.1 General Procedure

A flow chart of the information processing is given in Figure 31. It consists of two separate SUSA applications and of one TRACE application. The presented steps are not done automatically but scripts have to be written to connect the different files. That is one of the main disadvantages of the TRACE and DAKOTA approach; everything has to be done manually. But it can also be considered as an advantage since every parameter, variable, number in the TRACE input file can be altered and with general scripts future investigations can be performed time and resources efficient.

At the beginning of any U+S analysis stays the reference input of TRACE, or any other code which is designed to do thermal-hydraulic, mechanical, chemical, etc. analysis. It is evaluated regarding potential parameters, variables, input and boundary conditions which might be afflicted with uncertainty. In certain cases, physical models can also be afflicted with uncertainties. These parameters can be included in the analysis if access to the source code is possible. As mentioned in section 4.2, the number of runs is independent of the number of uncertain parameters. Therefore, it does not matter whether 10 or 20 parameters will be selected for the uncertainty and sensitivity analysis. Hence, in case it is not clear if an input parameter will influence an output parameter, it is reasonable to include it anyway.

After the uncertain parameters have been selected the range of uncertainty must be known or should at least be estimable. The information can be taken out of measurements of the experiments which is subject of the investigation. In case the documentation of the experiment does not include measurement uncertainties, similar experiments have to be taken and their uncertainty ranges can be adopted. Also, in some cases, manufacturer of components provide this kind of information. In case no information is known or available engineering judgment based

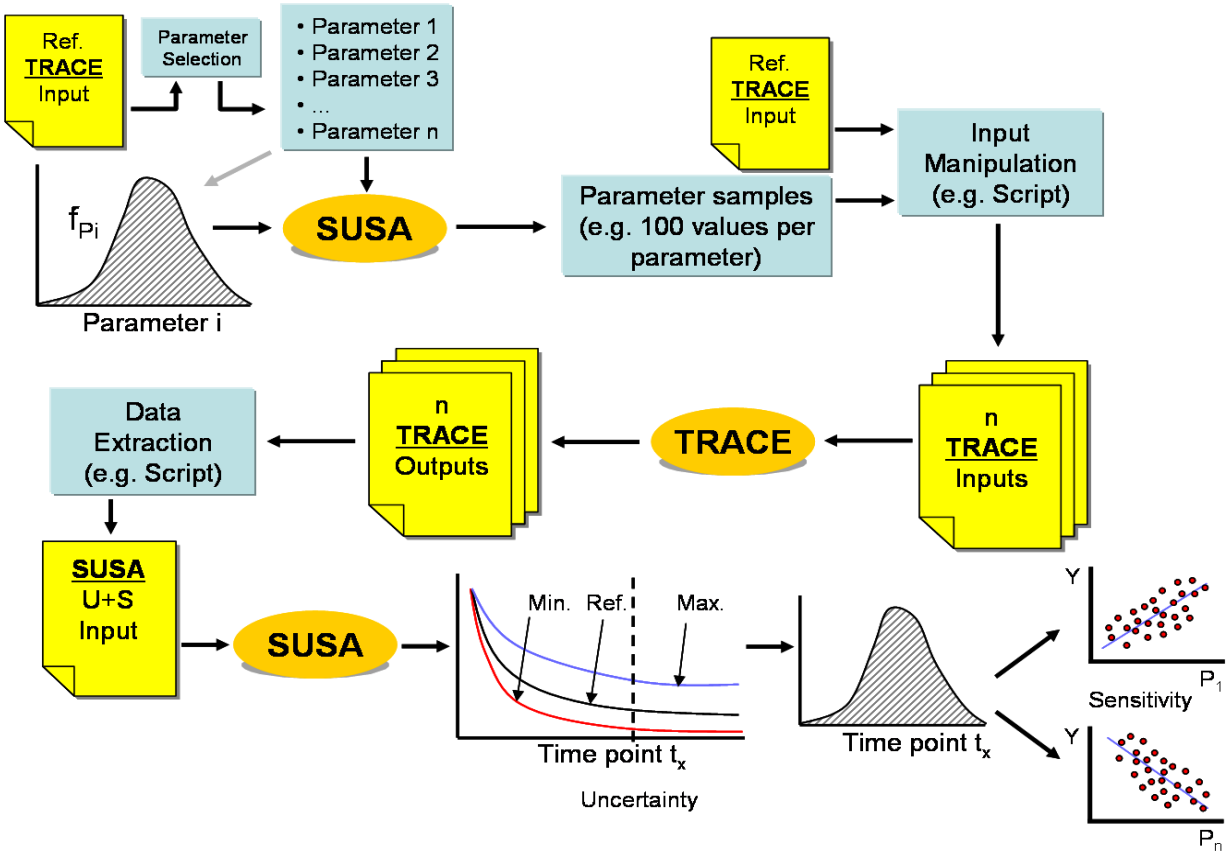

Figure 31 Flow Chart of the TRACE-SUSA Interface [26]

on best practice guidelines and experience has to be considered to define the uncertainty range of the parameters.

The next information which is required is the distribution of the uncertainty parameter between the uncertainty ranges. Usually, that information is the most difficult to obtain. Again, measurements or manufacturer can provide the distribution. In the case the distribution is unknown it is advisable to use a uniform distribution. The uniform distribution has the advantage of treating the uncertain parameter in an unbiased way since every value, no matter whether it is an extreme case (minimum or maximum) or it is the reference case, has the same frequency of occurrences (conservative value).

The three, aforementioned information, 1) uncertain parameter, 2) uncertainty range, and 3) uncertainty distribution will be entered into SUSA. In addition, the statistical fidelity needs to defined in SUSA in order to calculate the number of runs and hence the number of values per uncertain parameter (please refer to section 4.2). SUSA than generates a file which contains the information of the uncertain parameter, e.g. reference value, distribution type and the values for each uncertain parameter. That file is the base for the next step. In case of 95 % confidence level and 95 % probability content, 93 (two-sided) values per uncertain parameter will be generated. That means that 93 TRACE inputs must be generated and subsequently executed. Afterwards, selected output parameters will be extracted from the 93 TRACE output files and stored into a file which will be used to perform the actual uncertainty and sensitivity study with SUSA.

In the uncertainty evaluation, statistical parameters will be calculated for each output parameter, namely mean, median, maximum, minimum and standard deviation. These values should be compared to the result of the reference input and to the measurements of the experiment or the plant. Besides that information, the underlying distribution type of the output parameter can be evaluated. During the statistical evaluation, sensitivity coefficients will be calculated and the most important parameters can be identified.

In the following subsections, each step will be explained in detail how to get from the reference input to information regarding the uncertainty of output parameters and the sensitivity to input parameter changes.

5.2.2 How to Run SUSA: The Sampling

A detailed description of the capabilities of SUSA can be found in sub-section 4.2. Here, the path to generate the sampling for the single-phase pressure drop will be shown. SUSA will be launched and a new application will be opened. The uncertain parameters along with their range and distribution will be entered. As reported in sub section 6.2, all uncertain parameter ranges except for the inlet temperature are reported as percental variations. Therefore, an uncertainty factor was introduced which will be multiplied by the uncertain parameter in order to get the values for the uncertainty study. In case the variation is ± 1.0 % an uncertain parameter with a reference value of 1.0, a minimum of 0.99 and a maximum of 1.01 is generated. Hence, the uncertain parameter is multiplied by values between 0.99 and 1.01 which is identical to a percental variation of 1.0 %. For the inlet temperature an uncertain factor with a reference value of 0.0 is generated. That uncertain factor can range from -1.5 K to 1.5 K as reported in the benchmark specification. The uncertain factor will be added to the uncertain parameter to get the values for the study. A summary of the information, described in sub section 6.2, is given in
Figure 32. That data sheet contains information with respect to the single-phase pressure drop analysis. For the other analyses (two-phase pressure drop, void fraction, etc.) a 10th parameter, the power will be introduced.

After all information has been entered into SUSA, the sampling can be performed. For the present investigation the simple random sampling was applied.

After the SUSA sampling, a file called medusa.prn is generated containing the uncertainty information of the selected input and source code variables/parameters. A copy of the medusa.prn file which is generated for the single-phase pressure drop analysis is given in the Appendix A.

With the creation of the medusa.prn file the first step is finished and the information processing via scripts has to be performed.

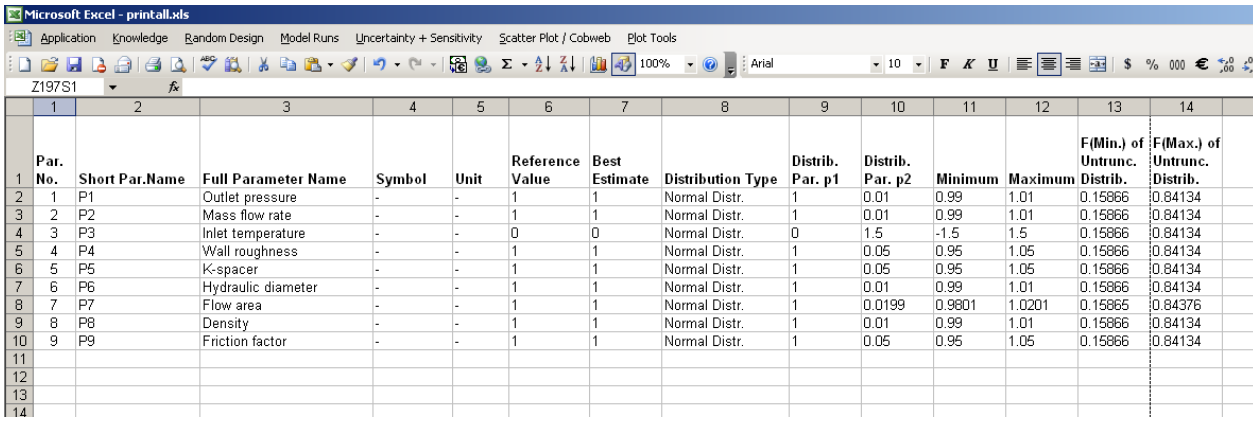

Microsoft Excel - printall.xls

Application Knowledge Random Design Model Runs Uncertainty + Sensitivity Scatter Plot / Cobweb Plot Tools

Z197S1

	1	2	3	4	5	6	7	8	9	10	11	12	13	14
1	Par. No.	Short Par.Name	Full Parameter Name	Symbol	Unit	Reference Value	Best Estimate	Distribution Type	Distrib. Par. p1	Distrib. Par. p2	Minimum	Maximum	F(Min.) of Untrunc. Distrib.	F(Max.) of Untrunc. Distrib.
2	1	P1	Outlet pressure	-	-	1	1	Normal Distr.	1	0.01	0.99	1.01	0.15866	0.84134
3	2	P2	Mass flow rate	-	-	1	1	Normal Distr.	1	0.01	0.99	1.01	0.15866	0.84134
4	3	P3	Inlet temperature	-	-	0	0	Normal Distr.	0	1.5	-1.5	1.5	0.15866	0.84134
5	4	P4	Wall roughness	-	-	1	1	Normal Distr.	1	0.05	0.95	1.05	0.15866	0.84134
6	5	P5	K-spacer	-	-	1	1	Normal Distr.	1	0.05	0.95	1.05	0.15866	0.84134
7	6	P6	Hydraulic diameter	-	-	1	1	Normal Distr.	1	0.01	0.99	1.01	0.15866	0.84134
8	7	P7	Flow area	-	-	1	1	Normal Distr.	1	0.0199	0.9801	1.0201	0.15865	0.84376
9	8	P8	Density	-	-	1	1	Normal Distr.	1	0.01	0.99	1.01	0.15866	0.84134
10	9	P9	Friction factor	-	-	1	1	Normal Distr.	1	0.05	0.95	1.05	0.15866	0.84134
11														
12														
13														
14														

Figure 32 SUSA Main Data Sheet for the Single-Phase Pressure Drop Analysis

5.2.3 How to Generate n TRACE Input Files

5.2.3.1 Auxiliary input files

The file medusa.prn must now be converted into a file called Sample.dat. In general, arbitrary names can be given to the files but for the sake of clearness default names will be introduced. The format of the Sample.dat file must be of the following.

```
n  m
A11        A21   A31   …    An1
A12        A22   A32   …    An2
A1m        A2m   A3m   …    Anm
```

where: n is the number of uncertain parameters
m is the number of values per uncertain parameter

An example of Sample.dat is given in the Appendix D. A second file needs to be generated in order to connect the information of the Sample.dat file with the reference input. That file is called UncMod.dat. An example and a description of that file is given below.

```
9
S Single Variables
0
T Trip Variables
0
B Block Variables
0
C Components
28
2 fill  100  flowin  1 3 1
1 fill  100  pin     1 1 1
3 fill  100  tlin    1 5 3
3 fill  100  tvin    1 5 3
```

```
4 chan  200  epsw    1 5 1
3 chan  200  toutl   1 5 3
3 chan  200  toutv   1 1 3
7 chan  200  vol     1 2 1          .
7 chan  200  fa      1 2 1
5 chan  200  kfac    1 4 1
5 chan  200  kfac    2 3 1
5 chan  200  kfac    3 3 1
5 chan  200  kfac    4 2 1
5 chan  200  kfac    5 1 1
5 chan  200  kfac    6 1 1
5 chan  200  kfac    6 4 1
6 chan  200  hd      1 2 1
3 chan  200  tl      1 2 3
3 chan  200  tv      1 2 3
1 chan  200  p       1 2 1
3 chan  200  tw      1 2 3
3 chan  200  rftn    1 2 3
3 chan  200  rftn    2 2 3
3 chan  200  rftn    3 2 3
3 chan  200  rftn    4 2 3
3 chan  200  matwr   2 2 3
3 break 300  tin     1 4 3
1 break 300  pin     1 5 1
M Model Variables
2
1 1
9 1
2 1
8 1
```

The number at the top of the file is the number of uncertain parameters. It must be the same number as in the Sample.dat file (n). That number is followed by information regarding how much signal, trip, block and component variables will be changed. These numbers or their sum must not be identical to the number of uncertain parameters. It is the number of locations where changes will take place. In the present case only component variables will be changed and changes will be performed at 28 positions in the TRACE input.

Then, 28 entries follow to describe which value will be replaced with which value from the Sample.dat file. The first number corresponds to the columns in sample.dat, in that case column no. 2. The second entry on that line is the component name and the third is the component number, meaning that FILL component 100 is subject of changes. The next word defines the parameter in the component which will be changed which is flowin (the inlet mass flow rate). The last three numbers define the position of the parameter in the component array. The first digit specifies the line of the variable. In case of pipe, chan, or htstr components several lines with same parameters are present (as a result of multiple cells). In case of FILL and BREAK components it happens that time dependent mass flow or pressure tables are defined. In the present case the flowin parameter appears only one time, therefore, the digit is 1. The second digit specifies the location in the line. The value for flowin appears in the third position, see below. The last digit is the flag which defines how the parameter will be changed. The user can chose between four ways of changing a variable

1: In order to replace the value with the value of the columns in Sample.dat a 0 must be entered, If 0 Then Variable_new = uncertain value.

2: To multiply the value with the value of the Sample.dat columns a 1 must be entered, If 1 Then Variable_new = Variable_old x uncertain value.

3: A fractional variation can be done to change the variable, indicated by a 2, If 2 Then Variable_new = Variable_old x (1.0 + uncertain value).

4: The uncertain value can be add or subtracted from the variable by placing a 3, If 3 Then Variable_new = Variable_old + uncertain value

As mentioned above all parameters except the temperature are multiplied by an uncertainty factor which is in the reference case 1.0. In the present case the highlighted value of the FILL component will be changed by multiplying it with the uncertain value.

```
*******   type           num        userid                component name
fill                     100             0                         Inlet
*         jun1          ifty          ioff
            10             2             0
*       twtold          rfmx        concin          felv
             0.0        1.0E20           0.0           0.0
*         dxin          volin         alpin          vlin          tlin
          0.1545   1.462034E-3           0.0           0.0    307.550000
*          pin          pain        flowin          vvin          tvin
      2.0000E+05           0.0      2.750000           0.0     307.550000
```

From the TRACE.inp one gets 2.750000 and from Sample.dat one gets 9.9578E-01 and from UncMod.dat one gets 1 which means multiplication.

2.750000 x 0.99578 = 2.738395

2.738395 is the new value which will be written in the new TRACE input. The complete input for the single-phase pressure drop analysis (reference input for test scenario 1) is given in Appendix A as example.

The last part of the of the UncMod.dat files is dedicated to the uncertain parameters in the source code. In the present case two parameters of the source code, the coolant density and the friction factor, will be considered in the uncertainty and sensitivity study. The first number is the number of locations in the TRACE source code where changes will take place (again, that is not the number of parameters which will be changed). For each value which will be changed two lines with two numbers must be entered. The first number in the first line is the identifier in the TRACE source code. The second number is the flag to determine how the parameter will be changed in TRACE. Unfortunately, these flags are different to the ones used to change the TRACE input file. For the source code, the following definitions are valid.

If 1 Then Variable_new = uncertain value	|replace
If 2 Then Variable_new = Variable_old x (1.0 + uncertain value)	|fractional variation
If 3 Then Variable_new = Variable_old + uncertain value	|summation
If 4 Then Variable_new = Variable_old x uncertain value	|multiplication

The first number on the second line defines the column number in the Sample.dat file and the last number is identical to the second number on the first line.

5.2.3.2 How to change the TRACE input file

In this step, the reference TRACE input Trace.inp will be altered and 93 new inputs called Trace_1.inp – Trace_93.inp will be created. Thanks to R. Macian, Professor at the Technical University of Munich, a FORTRAN program is available to do the altering of the TRACE input file.

The FORTRAN program, TRACEInpProc, contains six modules:

IntrTypeM.f90	That file contains the information about the general structure of the UncMod.dat file. The maximum number of single, trip, block, etc variables are defined here.
ProcessTraceFileM.f90	Reads the uncertainty data stored in the UncMod.dat file
ReadArgM.f90	An auxiliary module for data processing
ReadFilesM.f90	This module reads the TRACE input and the sample.dat file
StringProcessM.f90	An auxiliary module for data processing
TraceInpProcM.f90	The master module which calls all other moduls, sub routines and functions to generate the new TRACE inputs.

Besides the new TRACE inputs an additional file called TRACE_Unc_Models.dat will be created. The information regarding the TRACE source code changes are stored in that file. The meaning of that file will be explained in the following subsection.

The arguments for the command lines to execute TRACEInpProc.exe are the following:

-n #	<# is the sample number to get processes>
-i	<UncMod.dat>
-t	<Trace.inp>
-s	<Sample.dat>
-m	<TRACE_Unc_Models.dat>

5.2.3.3 How to change the TRACE source code parameters

To change parameters in the TRACE source code, two additional modules must be introduced to the TRACE workspace (with Compaq Visual Fortran) and some minor changes must be done in some existing TRACE source files.

Include the modules **ModUncInfoM.f90** and **ModUncVarM.f90** in the source folder of the TRACE code.

Add them in the TRACE workspace by Projects → Add to Project → Files

Change the module **trac.f90** by introducing

```
USE ModUncInfo
```

at the top of the file and

```
IF (uncInf) THEN
CALL ReadUncInfo
ENDIF
```

Right after the line containing CALL ProcessArgs

Change the module CmdLineArgsM.f90 by introducing

```
USE ModUncVar
```

at the top of the file and

```
CASE ('—unc')
UncInF = .TRUE.
```

Below the line containing runStats = .TRUE.

Safe the changes and build **trace.exe**

The module **ModUncVarM.f90** contains information on how much parameters can be changed and the module **ModUncInfoM.f90** is reading the uncertainty information stored in the TRACE_Unc_Models.dat file. This file contains the information of the UncMod.dat file along with the values stored in the Sample.dat file.

An example for TRACE_Unc_Models.dat is given below.

```
  2
*
  1  1
  1   0.9618600
*
  2  1
  1   0.9969400
```

TRACE_Unc_Models.dat is generated automatically and the user has to do nothing. In case the uncertainty and sensitivity analysis is limited to the TRACE input file an empty TRACE_Unc_Models.dat file will be generated and the TRACE executable will not consider the changes in the code.

With the changes and actions described in the previous paragraph the TRACE source code is ready to read uncertainty information. But in order to perform uncertainty investigations source code parameters need to be selected and changed as well. An example of the manipulation of a source code parameter is given below. In the present case the friction factor is selected and the altered TRACE routine is as follows. Yellow highlighted variables or comments have been added to do the uncertainty analysis.

```
REAL(sdk) FUNCTION getfChurchill(re, epswOverhd)
!
!Uncertainty.Beginning
      USE ModUncInfo
!Uncertainty.End
!
      REAL(sdk) :: a, b, re, epswOverhd, X1
!
!Uncertainty.Beginning
      INTEGER(sik) :: nuncMod = 1_sik
!Uncertainty.End
!
      X1 = 1.0_sdk
!
```

```
!Uncertainty.Beginning
      IF(UncInf)THEN
            X1 = MAX(ModUncval (nUncMod,1,X1),0.0_sdk)
      END IF
!Uncertainty.End
!
      re = MAX(10.d0, re)
      a = (2.457_sdk*LOG(1._sdk/((7._sdk/re)**0.9_sdk+0.27-
      sdk*epswOverhad)))**16_sik
      b = (37530._sdk/re)**16.0_sdk
      GetfChurchill = (2.0_sdk*((8.0d0/re)**12_sik+1.d0/(a+b)*1.5_sdk)
      **(1.0_sdk/12.0_sdk))*X1
      RETURN

END FUNCTION GetfChurchill
```

5.2.3.4 How to execute all of it

The execution is done with batch files containing all the steps explained in the previous sub-sections. The lines of the batch file performing the analysis for the single-phase pressure drop is given as example below.

In order to guarantee a proper execution and performance all commands must be in one line or line breaks have to be introduced since it is done in two loops. The outer loop is generating the "i" different reference files (depending on the different experimental scenarios which will be investigated). The second, the inner loop generates and performs "j" inputs per "i" reference cases.

Step 1: a FOR loop to generate i inputs based on one basic input, in the following called RAW.inp, is initialized. For the single-phase pressure drop analysis 36 cases will be investigated. The variable is indicated by %%i and the dimensions are given in the parenthesis; (1 = Start point, 1 = Increment, 36 = End point) meaning that the FOR loop starts at 1 and counts i+1 all the way up to 36. The "do" indicates the actual command to perform. In the present case the program **TRACEInpProc.exe** is called with the arguments –t –s –i and –n (U:\WORK\NUPEC\ must be replaced according to the location of the executable). The files Cases.dat and CasesMod.dat correspond to the files Sample.dat and UncMod.dat, respectively described in sub-section 5.2.3.2, and are given at the end of this sub section.

```
:FOR /L %%i IN (1,1,36) do "U:\WORK\NUPEC\TRACEInpProc.exe" -t RAW.inp -s
Cases.dat -i CasesMod.dat -n %%i
```

Step 2: Since the following commands are about to be executed within the FOR loop one new reference file is generated. The name of the file is RAW_MOD.inp which will be renamed to P7000%%i.inp (which is P70001.inp if i = 1). That new file is execute with TRACE. In the present case the command line argument –p is used which means that the suffix of the files (.inp) must not be given with the file name.

```
& REN RAW_MOD.inp P7000%%i.inp & "U:\WORK\NUPEC\trace.exe" -p P7000%%i
```

Step 3: The inner loop, which handles the generation and execution of the actual uncertainty study will be started. The general concept is the same as in step 1. This time 93 files will be generated in total for all 36 selected scenarios.

```
& FOR /L %%j IN (1,1,93) do "U:\WORK\NUPEC\TRACEInpProc.exe" -t P7000%%i.inp
-s Sample.dat -i UncMod.dat -m TRACE_Unc_Models.dat -n %%j
```

Step 4: The new generated file P7000%%i_MOD.inp is renamed to P7000%%i_%%j.inp (for i = 1 and j = 1: P70001_MOD.inp will be renamed to P70001_1.inp) and afterwards executed with TRACE. This time the command argument –unc must be added in order to activate the usage of the TRACE uncertainty modules and routines (see sub-section 5.2.3.3).

```
& REN P7000%%1_MOD.inp P7000%%i_%%j.inp & "U:\WORK\NUPEC\trace.exe" –unc -p
P7000%%i_%%j
```

The file Cases.dat is given below. There are three parameters (first number on first line) which will be changed according to the 36 different experimental set-ups (second number on the first line). These parameters are the pressure (first column) the Inlet temperature (second column) and the mass flow rate (third column).

```
3 36
0.2000E6  307.55  2.7500
0.2000E6  311.65  4.0278
0.2000E6  312.95  5.5278
0.2000E6  311.55  6.9167
0.2000E6  309.05  8.2778
0.2000E6  309.35  9.6667
0.2000E6  309.35  11.0278
0.2000E6  311.25  12.4444
0.2000E6  312.35  15.1667
0.2000E6  314.55  16.6111
0.2000E6  315.55  17.8333
0.2000E6  317.55  19.2222
1.0000E6  449.65  2.7500
0.9900E6  449.65  4.1389
0.9900E6  449.45  5.6389
0.9800E6  449.35  6.8889
0.9800E6  449.55  8.3056
0.9900E6  449.35  9.6389
0.9900E6  449.15  11.0556
0.9900E6  448.75  12.5833
1.0000E6  449.45  15.2222
0.9800E6  448.45  16.6111
0.9800E6  448.15  18.0000
0.9800E6  448.25  19.3889
7.1700E6  558.75  2.7500
7.1500E6  558.65  4.2778
7.1500E6  558.05  5.6389
7.1600E6  558.25  6.9167
7.1600E6  558.25  8.2778
7.1600E6  558.85  9.6389
7.1600E6  558.75  11.0278
7.1600E6  558.45  12.3889
7.1500E6  557.85  15.2778
7.1500E6  557.95  16.5833
7.1600E6  557.75  18.0000
7.1500E6  557.95  19.4167
```

File CasesMod.dat starts also with a three as the indicator of the number of parameters which will be changed. Since these parameters appear at several positions in the TRACE input file, more than thee fields will be manipulated. For instance the pressure appears in the FILL, the BREAK and in the CHAN component. Also, the temperature is changed in FILL, BREAK and CHAN component. In total, 17 values are changed to generate an input for a new experimental scenario.

```
3
S Single Variables
0
T Trip Variables
0
B Block Variables
0
C Components
17
1  fill   100   pin      1  1  0
2  fill   100   tlin     1  5  0
2  fill   100   tvin     1  5  0
3  fill   100   flowin   1  3  0
2  chan   200   toutl    1  5  0
2  chan   200   toutv    1  1  0
2  chan   200   tl       1  2  0
2  chan   200   tv       1  2  0
1  chan   200   p        1  2  0
2  chan   200   tw       1  2  0
2  chan   200   rftn     1  2  0
2  chan   200   rftn     2  2  0
2  chan   200   rftn     3  2  0
2  chan   200   rftn     4  2  0
2  chan   200   matwr    2  2  0
2  break  300   tin      1  4  0
1  break  300   pin      1  5  0
M Model Variables
```

5.2.3.5 How to extract information out of n TRACE inputs

The extraction of the relevant information is done with FORTRAN programs but can be also done with other programs like PERL or PHYTON. The information has to be stored in a file which can be read by SUSA. The formats for scalar and index dependent analysis are given below:

R11 R12 … R1m
R21 R22 … R2m
⋮ ⋮ ⋮
Rn1 Rn2 … Rnm

where n is the total number of model runs
m is the total number of model results per run
Rij is the value of model result no. j, j = 1… m, in run no. i, i=1… n

```
L1
T11     R11-1  R11-2   … R11-m
T12     R12-1  R12-2   … R12-m
  ⋮       ⋮      ⋮        ⋮
T1L1    R1L1-1 R1L1-2 ... R1L1-m
L2
T21     R21-1  R21-2   … R21-m
T22     R22-1  R22-2   … R22-m
  ⋮       ⋮      ⋮        ⋮
T2L1    R2L1-1 R2L1-2 ... R2L1-m
  ⋮
Ln
Tn1     Rn1-1  Rn1-2   … Rn1-m
Tn2     Rn2-1  Rn2-2   … Rn2-m
  ⋮       ⋮      ⋮        ⋮
TnL1    RnL1-1 RnL1-2 ... RnL1-m
```

where Li is the number of time steps in run no. i, i =1 … n
n is the total number of model runs
m is the total number of model results per run
Tik is the time value of time step no. k, k = 1 … Li in run no. i, i = 1 … n
Rik-j is the value of the model result no. j, j = 1 … m at time step no. k, k = 1 … Li in run no. i, i = 1 … n

For the single-phase pressure drop analysis the scalar format is required since only the pressure drop at steady state condition is needed. That means that n is 93 and m is 36. Due to that size (36 columns with 93 rows) a presentation is waived. For the void fraction in axial direction or the void fraction as a function of time during pump and turbine trip, the index dependent format will be used. Since TRACE does not provide the pressure drop as a general output variable a control block is defined in the TRACE input. That control block calculates the difference between the first (inlet) and last (outlet) cell of the CHAN component and subtracts the geodetic term ($\varrho \cdot g \cdot h$). In the TRACE.inp file (Appendix A this control block has the id -300 (highlighted in yellow) and can be found right above the FILL component. Appendix B shows a piece of the corresponding output, TRACE.out. The last line shows a -300, which is the control block id to calculate the pressure drop and 1.119079E+03 which is the calculated pressure drop in Pa. In order to evaluate the results of all 93 uncertainty cases per each experimental scenario this last number will be read out of the TRACE.out file and will be stored in a new file according to the specification given above. The FORTRAN code performing the extraction is given in Appendix E.

5.2.4 How to Run SUSA: The Analysis

That new file, called scalar.lst, must be copied into the corresponding SUSA directory. Based on the general SUSA window via the menu Uncertainty+Sensitivity one can chose between scalar and index dependent analysis and between uncertainty and sensitivity analysis. In the present

case the first option, scalar uncertainty analysis, is chosen. After selecting the results to be analyzed (36) and activating different statistical options (comparison with normal or uniform distribution, tolerance limits, etc.) a file is generated named EQUUS.prn. That file contains the statistical information like the minimum, the maximum, the mean, the standard deviation and the quantiles of each selected consequence. Consequence is identical to result which is in fact identical to the 36 different pressure drop sets. In addition, several graphs are generated showing the normalized distribution of the results together with fitted distribution types (e.g., normal, triangular). That procedure finishes the uncertainty analysis.

The next step is the evaluation of the sensitivities. Therefore, the second option in the Uncertainty+Sensitivity menu is selected, scalar sensitivity analysis. Again, the result(s) to be analyzed must be selected and the sensitivity measure (Pearson, Spearman, etc.) must be chosen. Furthermore, the input parameters can be selected to be displayed. In case more than 10 parameters are selected, it is recommended not to display of all of them in one graph. The new generated file, SAMOS.prn, contains the sensitivity coefficients and the ranking of each selected parameter calculated for the ordinary, the partial correlation and the standardized regression option of the selected sensitivity measure. The coefficient of determination as a figure of merit for the quality of the analysis is given as well. Together with the SAMOS.prn file plots are generated showing the sensitivity coefficients in a graphical way.

5.3 Uncertainty and Sensitivity Study with TRACE-DAKOTA

In order to perform uncertainty analysis with TRACE code, the ISE laboratories has implemented a new tool in the latest SNAP version (V2.0). This tool is based on the use of the uncertainty code DAKOTA which is described above. In this section, the main steps the user should follow to perform this kind of analysis will be described since a particular SNAP-DAKOTA user guide line is presently not available. The general implementation of DAKOTA is given in Figure 33. The report compiled by DAKOTA with respect to a single-phase flow pressure drop analysis is given in Appendix H

5.3.1 Assignment of Uncertain Parameters

Once the TRACE model is created or imported, the reference input will be executed in order to obtain the reference case. After the uncertainty analysis is performed, the reference case must be located between the minimum and maximum value. After the reference case has been obtained, the following steps must be performed.

Create a new **Job Stream** and choose **Dakota Uncertainty** and **Single Step TRACE stream** (Figure 34). To avoid confusion, the new created **Single_Step_2** should be renamed to **Uncertainty analysis**.

In order to plot the variable which is going to be analyzed (e.g. peak cladding temperature) the step described above would be sufficient. For a complete uncertainty analysis, however, additional steps are required, too.

Click on **Stream steps** inside of **Single_step_2** (or the renamed Uncertainty analysis) and select new, then click on **Extract Data**. Click again in **Stream steps** and select **DAKOTA** as new.

This step is needed in order to extract data from the output files generated by TRACE and to send the information to DAKOTA (it is helpful to rename the tasks t**imestepsize** step and step_4 as properly i.e. **aptplot**, **extracdata** and **Dakota**, Figure 36. Later, in the job status window it will be easier to distinguish between the different streams and cases,

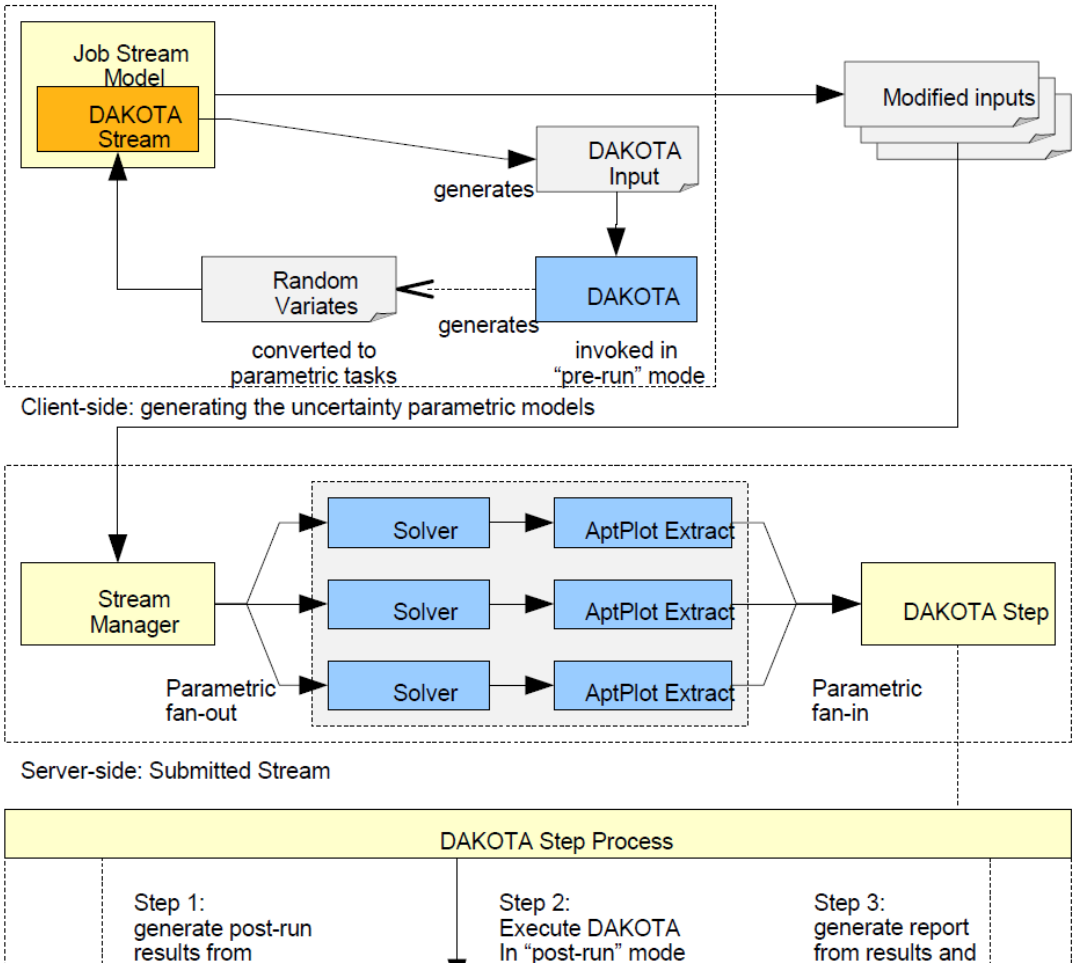

Figure 33 DAKOTA Reference Implementation Process Diagram[1]

1 Presented during the 2011 TRACE User Workshop. Potomac, Maryland, USA, March 2011.

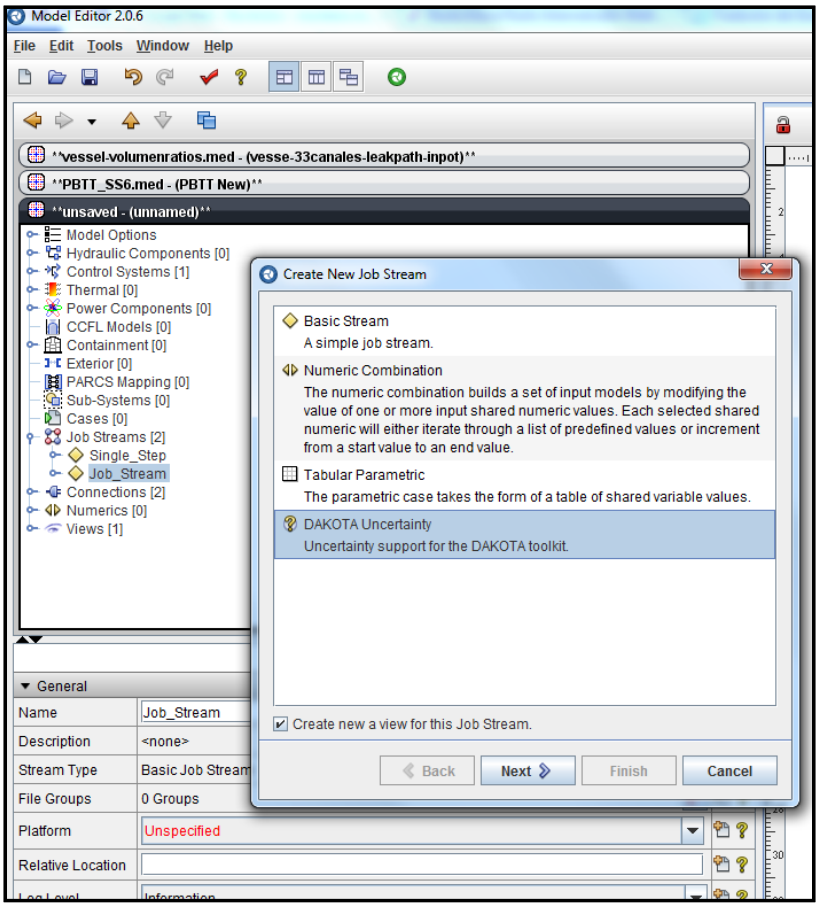

Figure 34 Adding Uncertainty Stream to Existing TRACE Job Stream

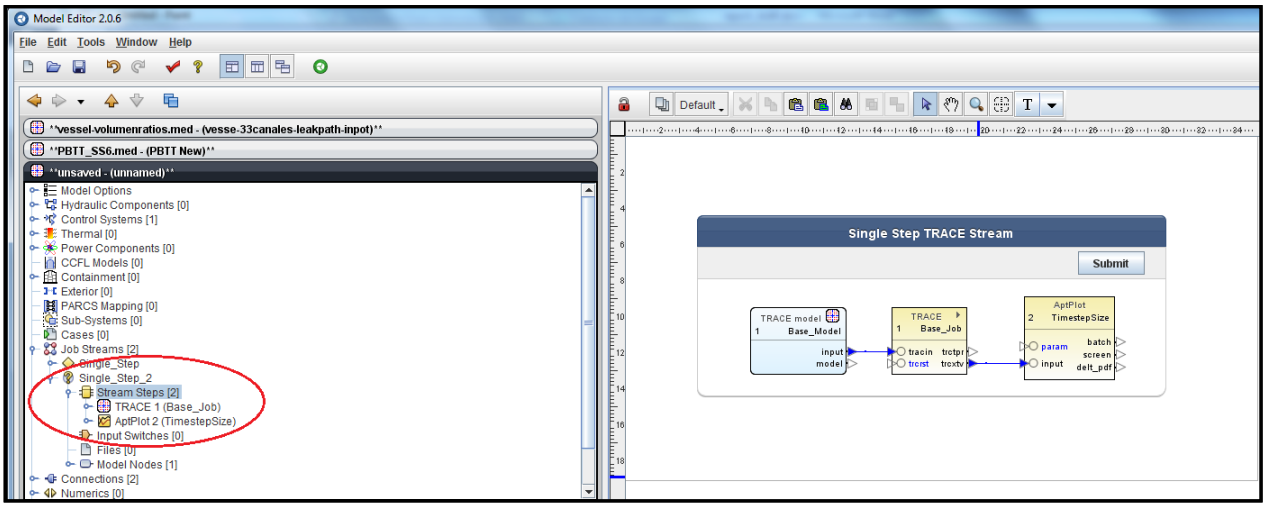

Figure 35 Single Step TRACE Stream

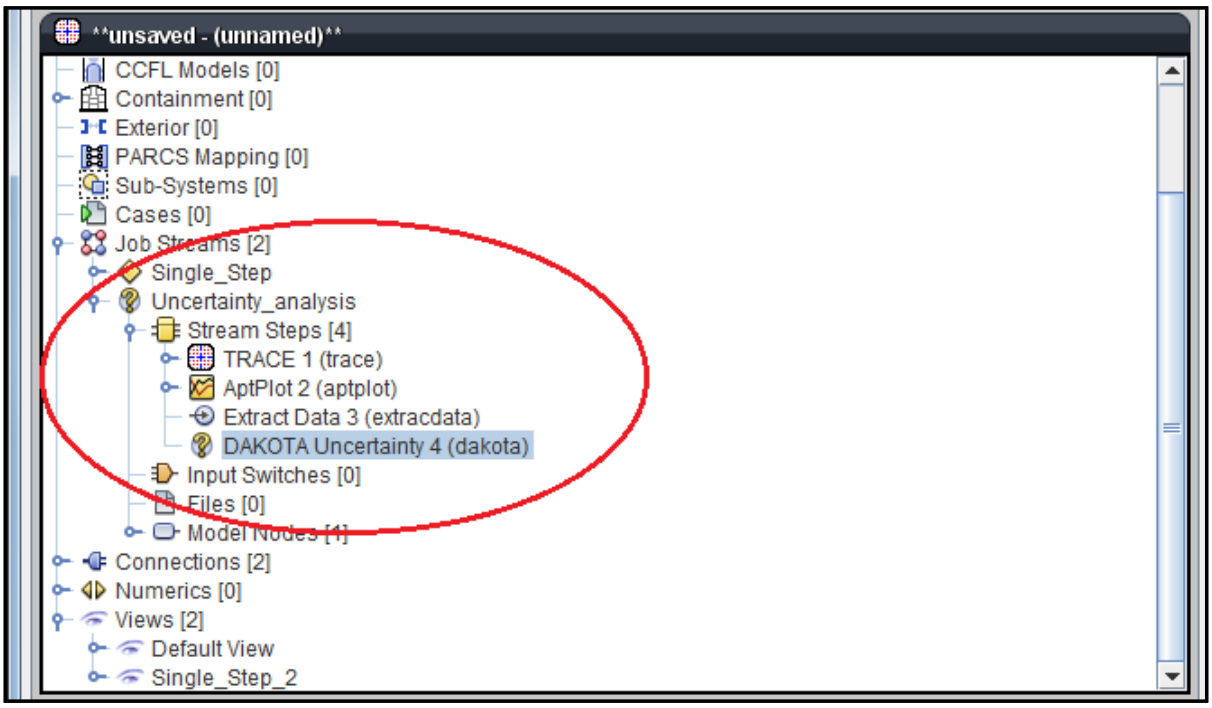

Figure 36 Job Stream Window with Added Uncertainty Step

After the uncertainty stream step is added to the job stream menu the different parameters will be assigned. To enter the parameters the **Numerics** bullet in the SNAP selection window must be selected and by a right click on **Reals** new parameters can be entered. Figure 37 shows two parameters under the **Reals** item, the mass flow rate and the pressure.

Figure 37 Unfolded Numerics Item in SNAP with Two New Parameters

In the first real, mass flow rate, the physical unit will be defined by **Available units→ mass flow (kg/s)** with a value of 2.5. For the second real **NO units** is selected with a given value of 1.0. Now, the real values will be assigned to a component. For the mass flow rate, go to:

Hydraulic Components → Fills → Initial coolant Mass Flow and select **select a shared real** (the two arrows heads pointing in opposite directions). The corresponding value must be selected.

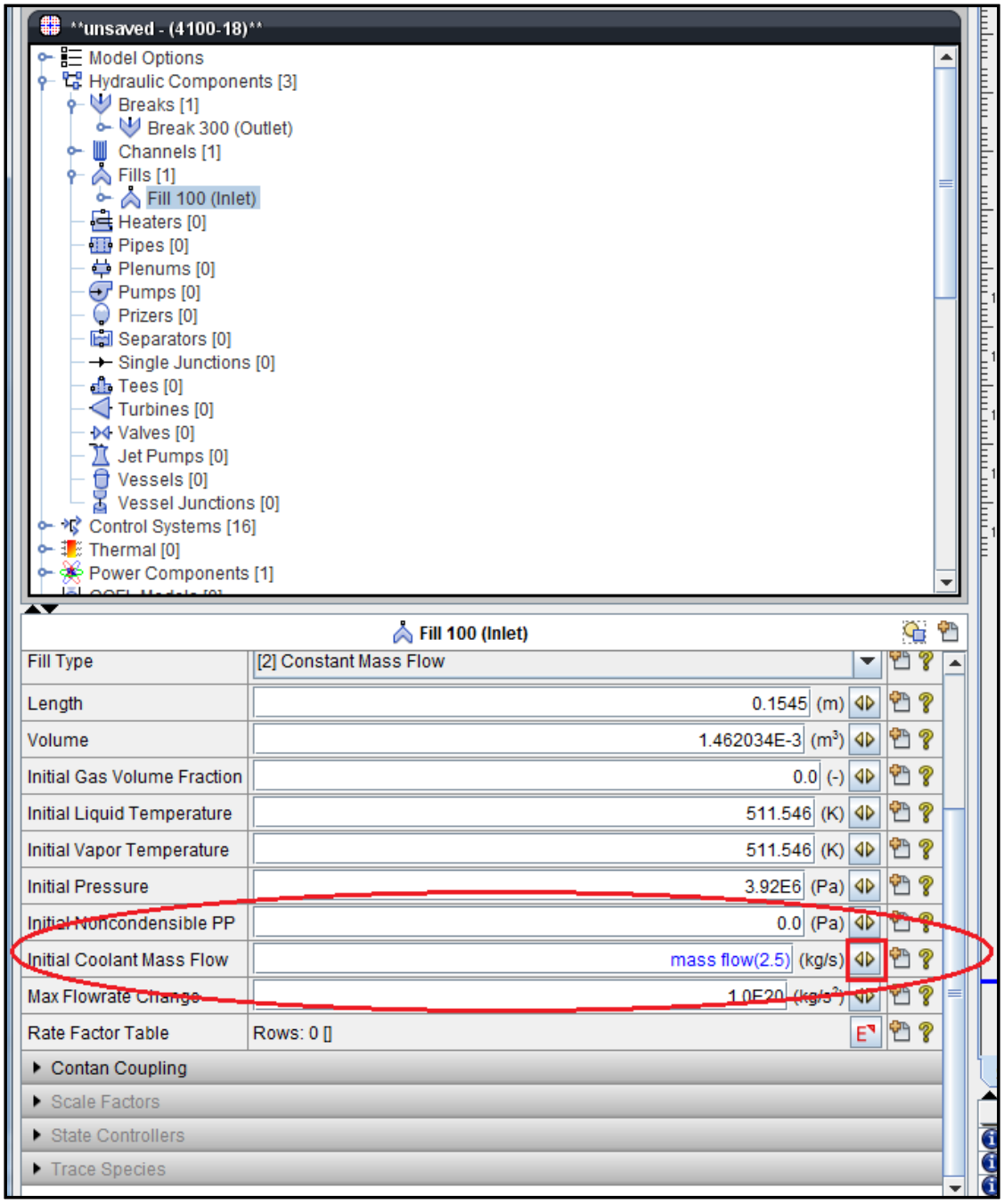

Figure 38 Fill with Initial Coolant Mass Flow Rate Assigned as an Uncertain Parameter

The **NO units** factor is useful when it is necessary to assign a PDF to a set of values (i.e. pressure table of a BREAK component). In this case, the best option is to create a control block in which the inlet table will be multiply for a factor. This factor will be the uncertain value of the pressure. The mean is equal to 1.0, meaning that during normal operation (uncertainty analysis not used) the pressure table will not be changed. A scheme of such a control block is displayed in Figure 39.

The Real value (No Units) is assigned to a constant. The multiply control block is the pressure table of the BREAK component. This option can be used for different tables in a same component (e.g., FILL components general tables for temperature, mass flow). It must be taken into account that for a successful uncertainty analysis one value must be created for each variable in order to assign a different PDF to each variable.

5.3.2 PDF and Monte Carlo Sampling

This sub-section deals with the assignment of the PDF to each variable. By clicking on **Job Streams → Uncertainty → Parametric Properties → Variables → Select new variable reference**, the window depicted in Figure 40 will open and the two previously defined variables, mass flow rate and pressure, should appear. By selecting **Mass flow → Next → Scalar** and **Pressure → Next → Factor** a distribution will be assigned which needs to be filled with information, see Figure 41. Under the **Distributions** register the distribution type can be chosen and known parameters can be entered. The information for mass flow and pressure are given in Table 8 and Figure 42.

Table 8 PDF Characteristics for Mass Flow and Pressure

Parameter	Mass flow	Pressure
Distribution type	Normal	Normal
μ (Mean)	2.5	1.0
σ (STDV = Standard deviation)	0.025	0.01
Min	2.475	0.99
Max	2.525	1.01

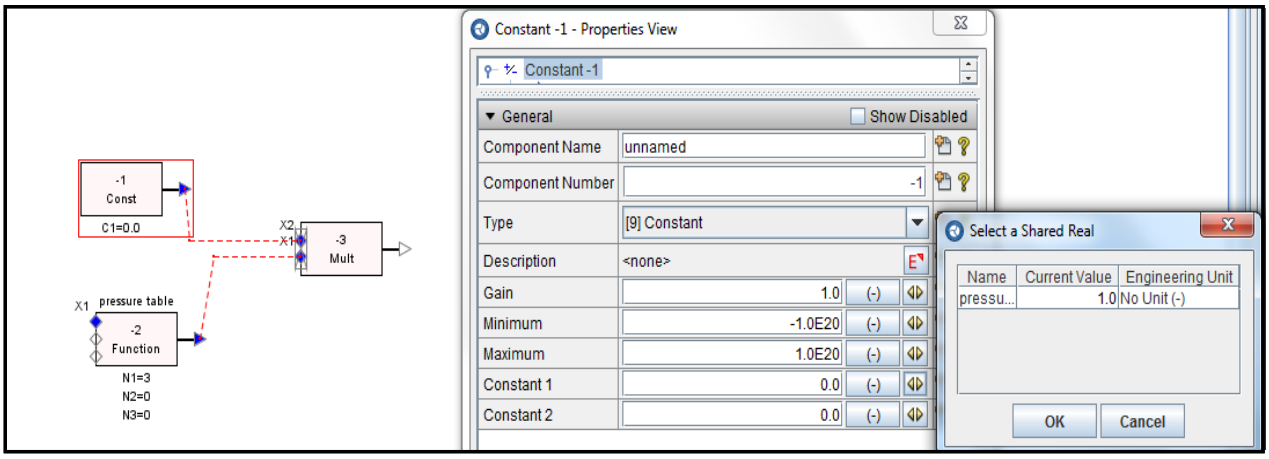

Figure 39 Control Block for the System Pressure with Assigned Shared Real (uncertain) Value

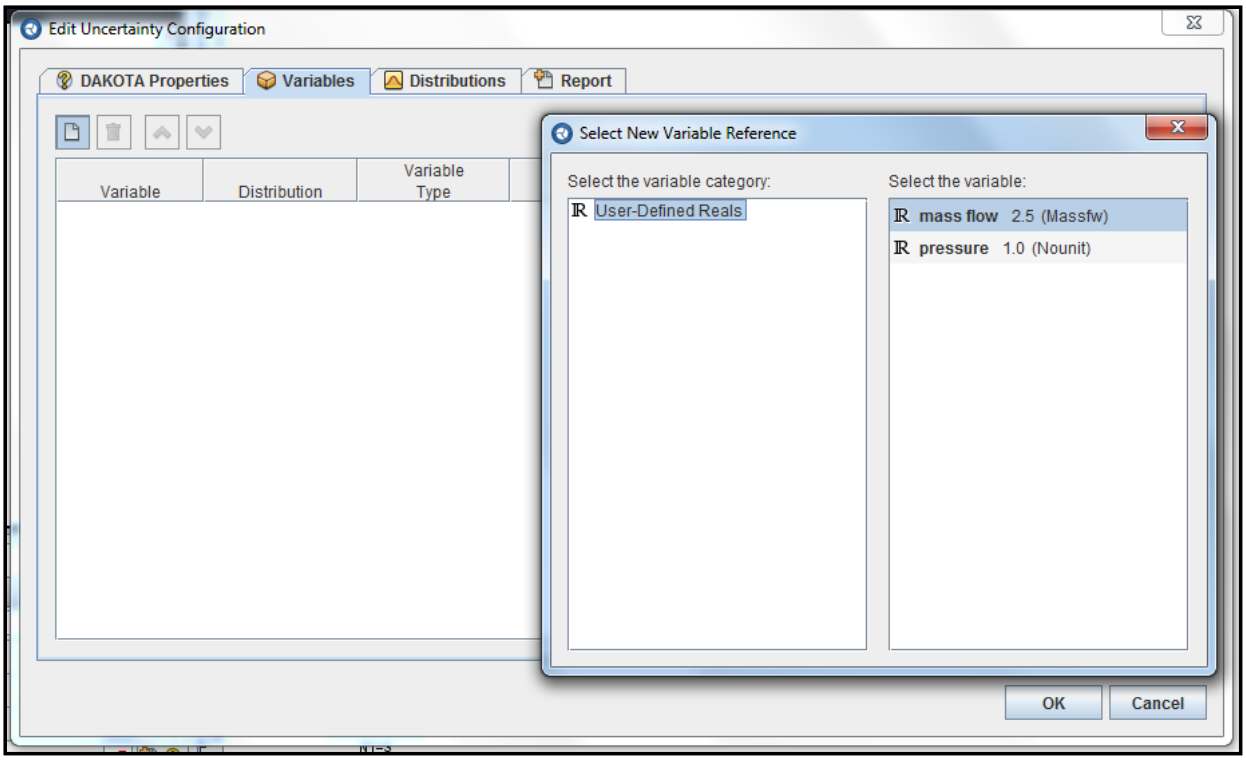

Figure 40 New Variable Reference to Assign PDF's

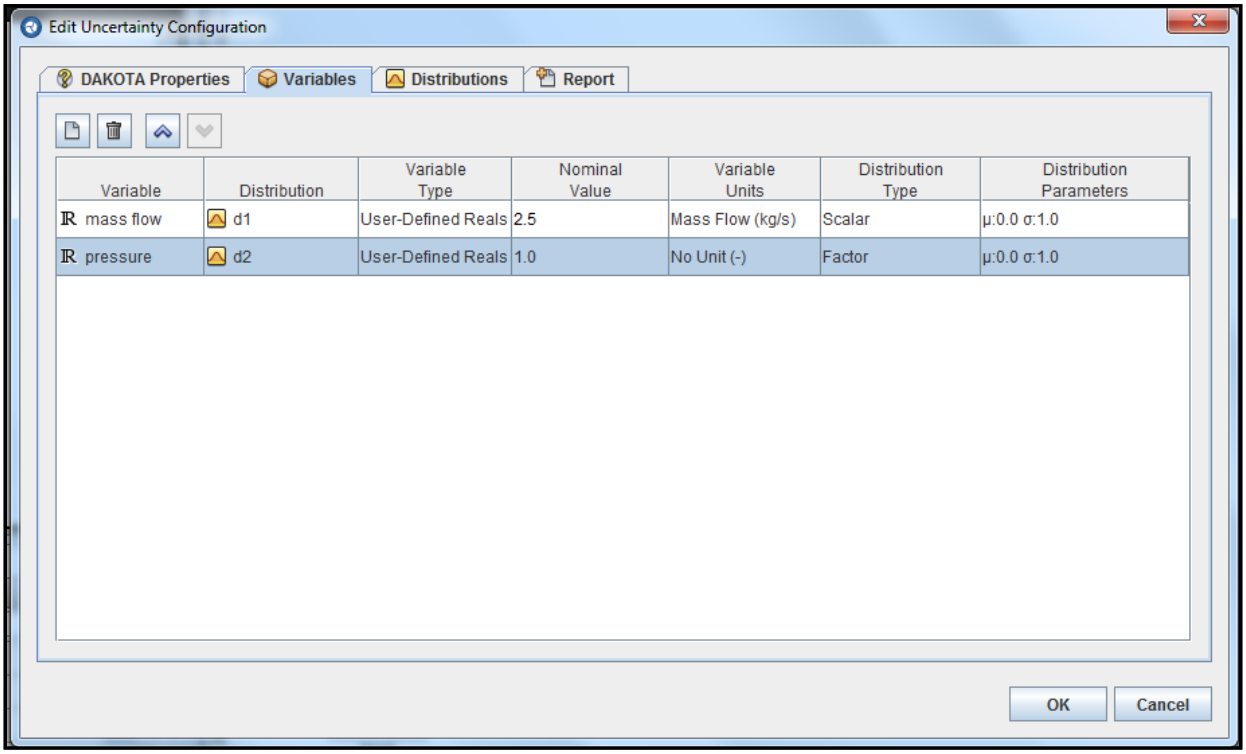

Figure 41 Assigned Distribution Type for Mass Flow Rate and Pressure

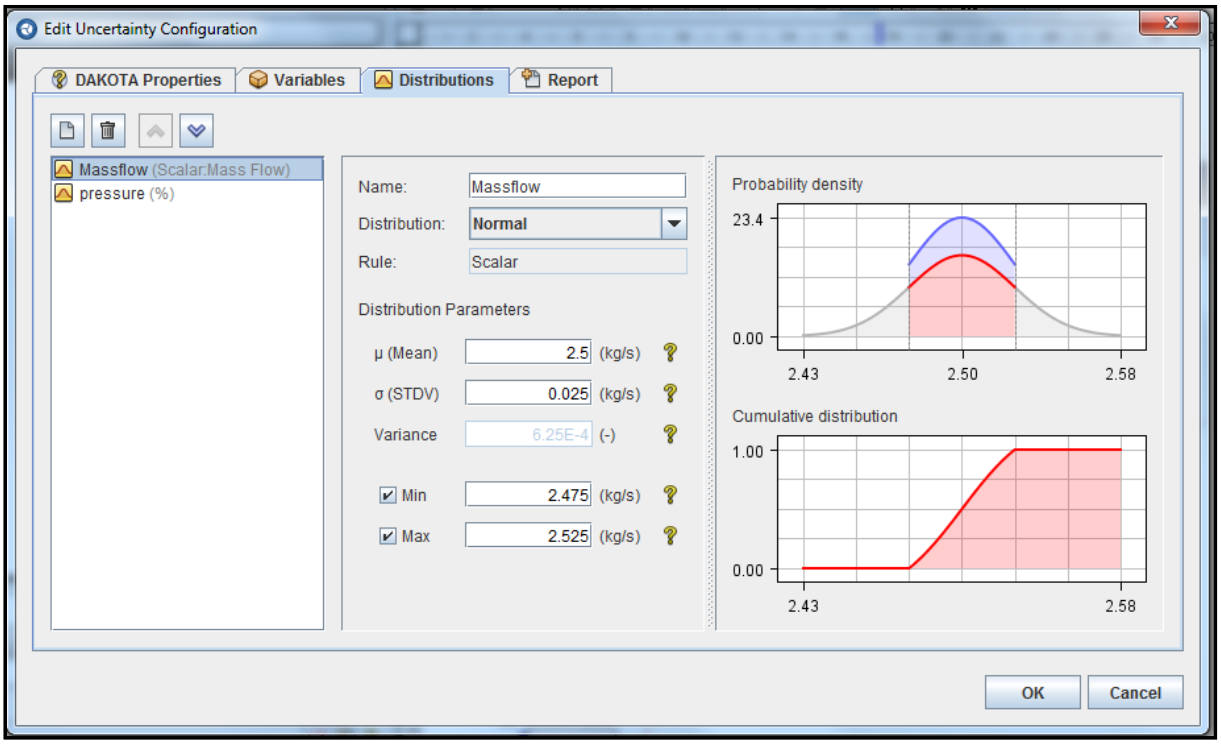

Figure 42 Parameters of the PDF's

In the **Report** window (Figure 43) all the available options for the report compiled by SNAP after the TRACE and DAKOTA calculations, can be selected such as formats, distributions, MC samples etc. For the final step the **DAKOTA Properties** register must be selected. In this window the sampling method will be selected. For a complete DAKOTA analysis at least one figure of merit must be entered (e.g. PCT or maximum void). In the new **ASV1** the lower or/and upper limit can be specified. Then, choosing the level of probability and confidence (typically 95/95 for safety analysis) the number of samples will be calculated with the formula of Wilk (for 95/95 and order 0 the result will be 59 samples = 1-sided). The options for the sampling method are Monte Carlo and Latin Hypercube.

5.3.3 Data Extraction

Once the PDFs are ready, all the applications must be connected as depicted in Figure 44. In **Extract Data** the variable which is going to be analyzed must be entered. Right click on **Extract Data** then **Properties → AptPlot Script** and the desired commandos can be entered into the AptPlot script such as shown in Figure 45. This action will extract all the values for all the cases from TRACE output files and they will be sent to DAKOTA. A last step for the setup is to click on TRACE model and then on **Parametric → True**. Now the job stream must look like in Figure 46. The difference to Figure 44 is that the icon for the TRACE input changed in a way that it is indicating several inputs.

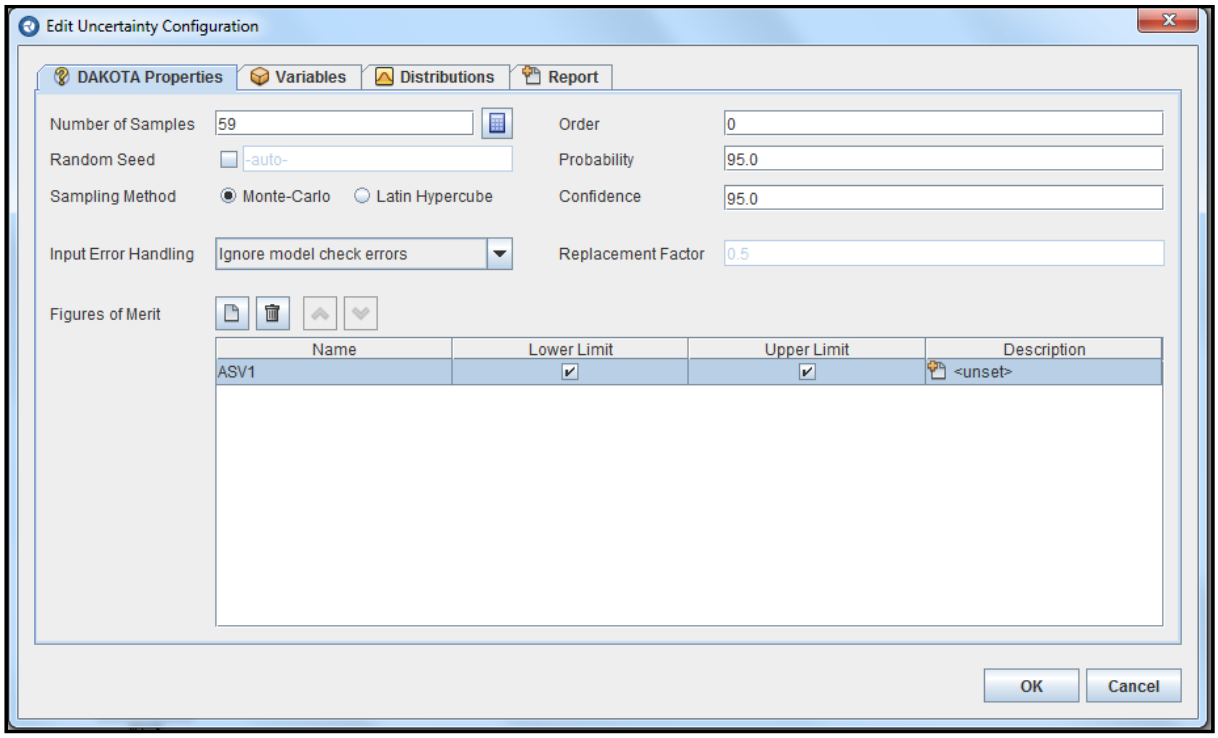

Figure 43 Definition of the Sampling Method and Size

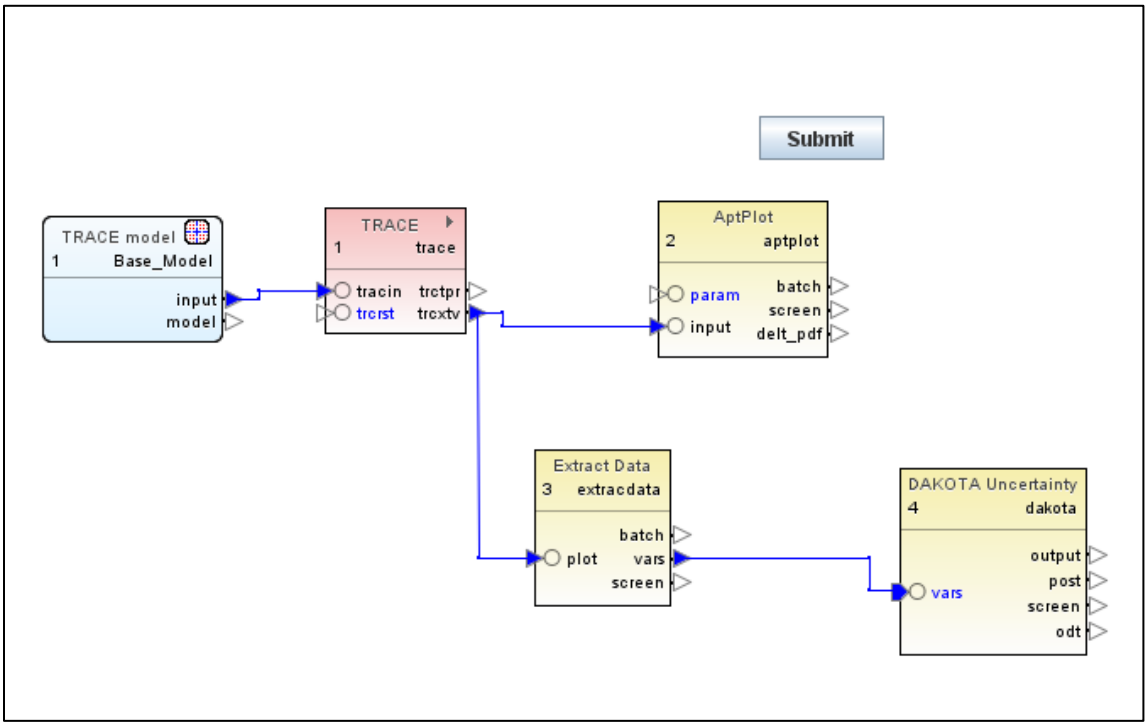

Figure 44 Job Stream with DAKOTA Uncertainty and a Single TRACE Input File

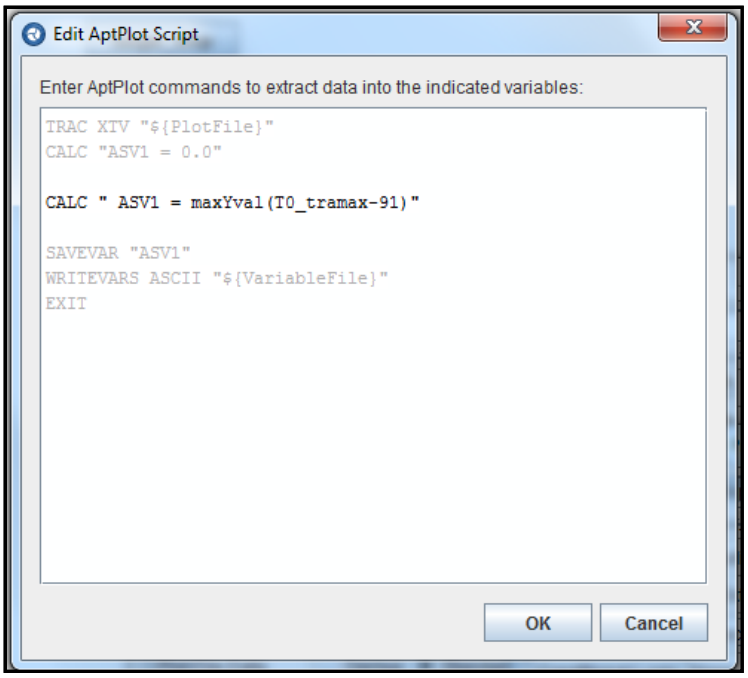

Figure 45 AptPlot Data Extraction Scripting Window

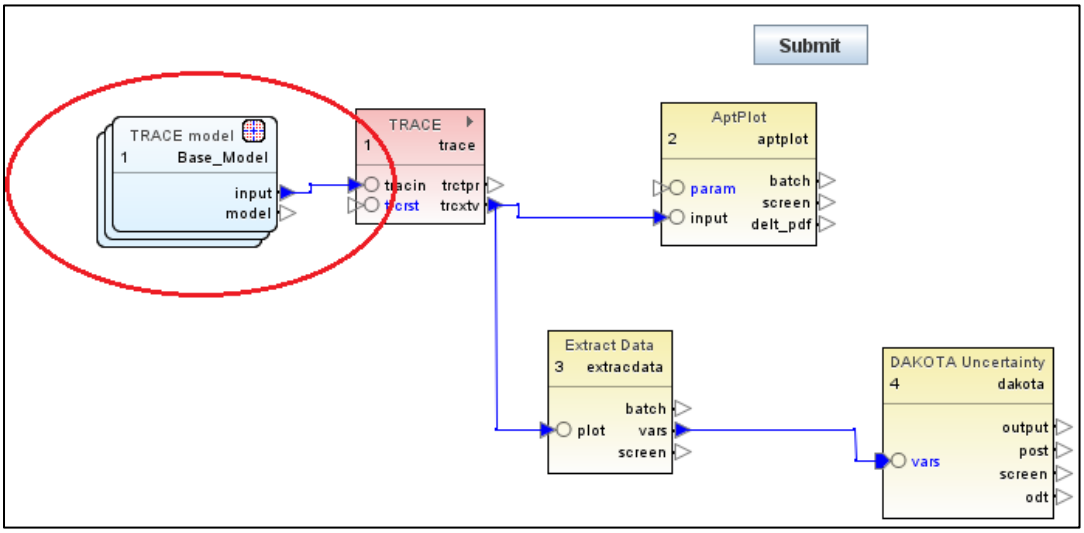

Figure 46 Job Stream with Multiple TRACE Input Files

Before the uncertainty calculation can be started the whole SNAP model should be checked for errors and saved. If errors are evident the execution can be launched by either clicking on **Tools → Submit stream to local** or by clicking on the **Submit** button displayed in the job stream window.

The given example is only one of many possibilities of doing uncertainty analysis by means of DAKOTA-SNAP. In this example, a transient case was considered and the first 150 seconds were pre-transient (steady state conditions). If two different inputs are available, steady state and

transient (restart), the model should look like Figure 47. If the uncertainty is considered in both, initial conditions and transient conditions, e.g., initial pressure and temperature uncertainty for the steady state and mass flow safety injection uncertainty for the transient, the two models must be set as parametric. In the **AptPlot Step** the variables can be chosen in order to show the desired variable for all cases (e.g. 93 cases for void fraction at certain axial location), see Figure 48.

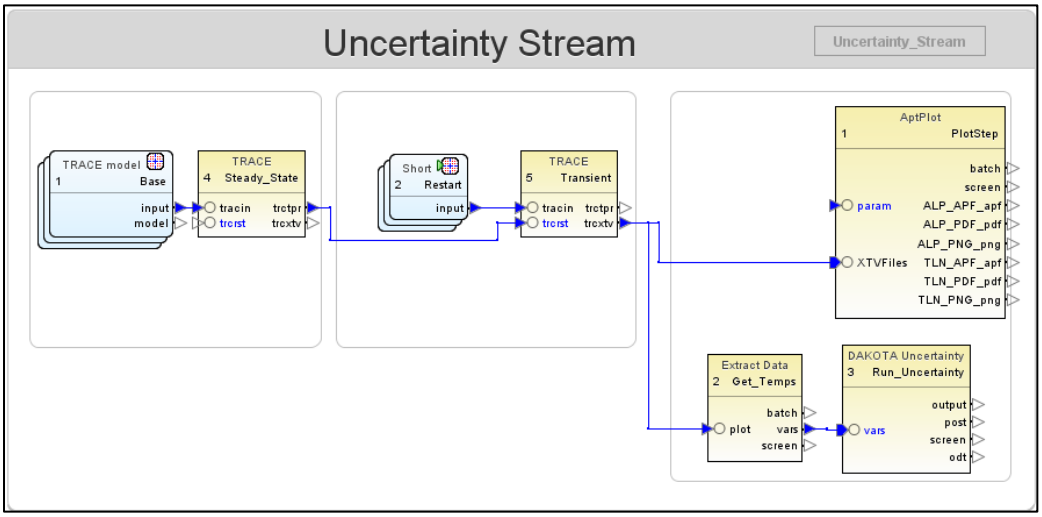

Figure 47 Job Stream Window with Steady State and Transient Uncertainty Models

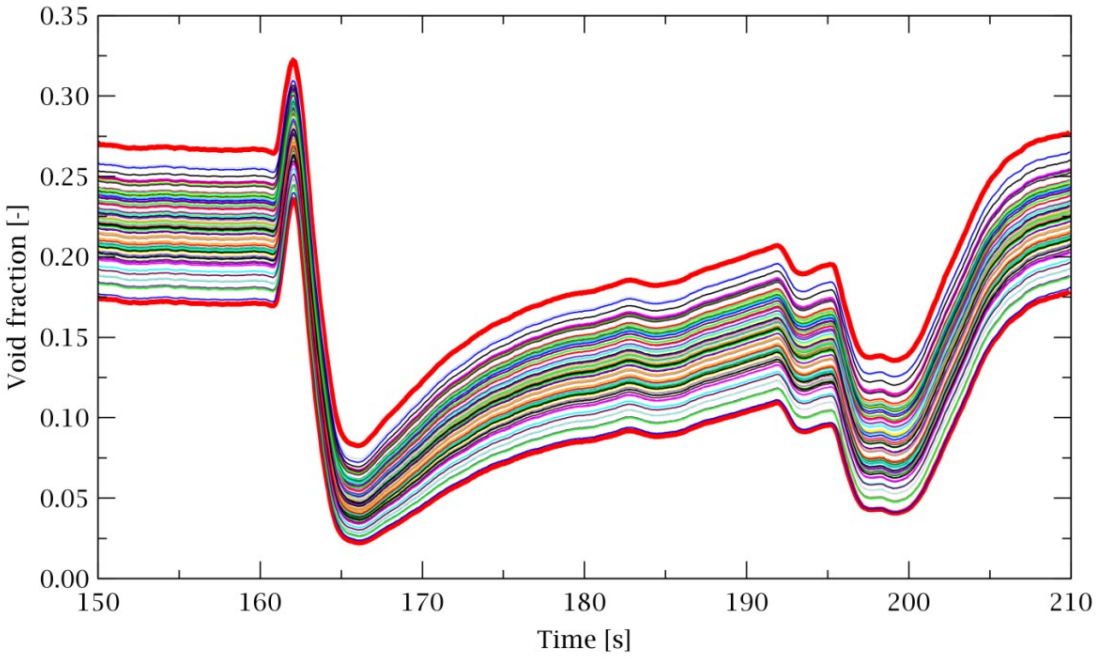

Figure 48 Example of an Uncertainty Analysis of a Specific Variable

6 RESULTS OF THE UNCERTAINTY AND SENSITIVITY ANALYSES

6.1 Modeling

Figure 49 shows the TRACE representation of the assembly types 4 and C2A. The axial nodalization is shown on the right side. In total, 25 axial levels are modeled using the CHAN component (no. 200) whereas each cell has a length of 15.45 cm. The mass flow rate boundary conditions are stored in the FILL component, bottom right side (no. 100) while the pressure boundary condition is defined in the BREAK component (no. 300). The pins with the different power are modeled according to the distribution given in Figure 9 (see sub section 3.2). Five different pins are considered. Pins one till four represent the actual fuel pins while rod type five is dedicated to the water rod (1 = 1.30, 2 = 1.15; 3 = 0.89; 4 = 0.45 and 5 = water rod). Four water rods are present in the model since the real water rod is taking the place of four regular rods.

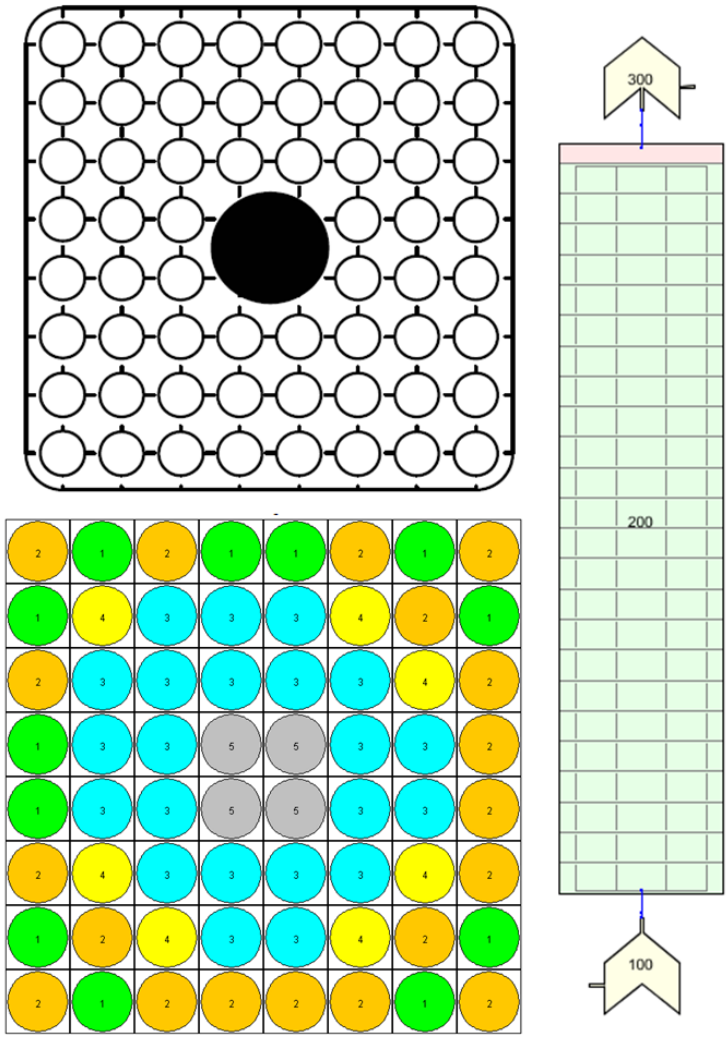

Figure 49 TRACE Model of the BFBT Assembly

6.2 Uncertain Parameters

For the present investigations the output parameters of interest are the pressure drop (single and two-phase), the void fraction (steady state and transient) and the critical power. Most of the uncertain parameters which are selected are identical for all three applications. The selected parameters are listed in Table 9 and
Table 10 for TRACE-SUSA and TRACE-DAKOTA, respectively, along with information about the uncertainty range. All uncertainty parameters have in common that the probability density function will follow a normal distribution except for the inlet temperature which is flat (uniform). The range of the uncertainties is taken from the NUPEC specification [27]. Besides the inlet temperature all uncertainty ranges are given as percental variation. For the temperature absolute values are reported. The inlet temperature varies by ± 1.5 K meaning that the mean value is 0.0 K. In order to include the temperature in the transient analysis with DAKOTA, a multiplication factor was used instead. That multiplication factor is 0.997 – 1.003 (meaning that a temperature of 500 K will be multiplied with a factor which varies between 0.997 and 1.003) and is almost identical to ± 1.5 K. However, the rather small difference will have several consequences in the analysis later on.

In addition to the reported uncertainties, physical models of the TRACE code are also affected by uncertainties. Therefore, the friction factor and the density of the water have been selected. These parameters can only be incorporated during the TRACE-SUSA analysis since for the TRACE-DAKOTA analysis, SNAP has no access to the source code and therefore only input parameters can be included.

Table 9 Uncertain Parameters, Range and Distribution for TRACE-SUSA

No.	Parameter	Range	Distribution
1	Outlet pressure	± 1.0 %	Normal
2	Mass flow rate	± 1.0 %	Normal
3	Inlet temperature	± 1.5 K	Uniform
4	Wall roughness	± 5.0 %	Normal
5	K-spacer	± 5.0 %	Normal
6	Hydraulic diameter	± 1.0 %	Normal
7	Flow area	± 1.0 %	Normal
8	Density	± 1.0 %	Normal
9	Friction Factor	± 5.0 %	Normal
10	Power	± 1.5 %	Normal

Table 10 Uncertain Parameters, Range and Distribution for TRACE-DAKOTA

No.	Parameter	Range	Distribution
1	Outlet pressure	± 1.0 %	Normal
2	Mass flow rate	± 1.0 %	Normal
3	Inlet temperature	± 1.5 K (± 0.3 %)	Uniform
4	Wall roughness	± 5.0 %	Normal
5	K-spacer	± 5.0 %	Normal
6	Power	± 1.5 %	Normal

6.3 Pressure Drop Analyses

The results presented in this sub section are for the pressure drop across the whole test section only.

6.3.1 Single Phase Flow Pressure Drop

The pressure drop is calculated between the first and the last cell of the TRACE model based on the following correlation.

$$\Delta p = (p_{inlet} - p_{outlet}) - \rho_{outlet} \cdot g \cdot \Delta h \quad (60)$$

Figure 50 and Table 11 show the input and boundary conditions of each of the 36 experimental scenarios. These 36 scenarios can be divided into three groups, low, medium and high pressure/inlet temperature. The mass flow rate in each of these groups is linearly increased in 12 steps. The pressure covers 0.2, 1.0 and 7.2 MPa, the temperature 310, 450 and 560 K while the mass flow rate ranges from 10 to 70 t/h.

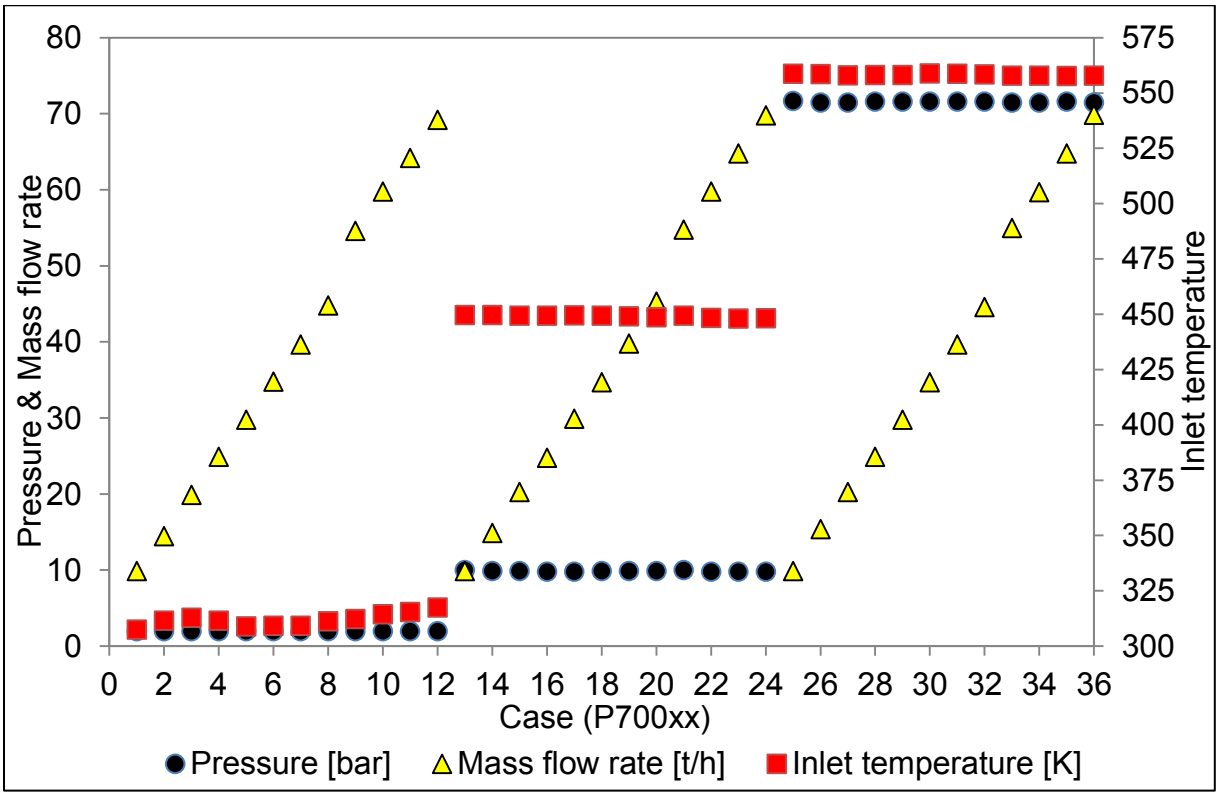

Figure 50 Input and Boundary Conditions for the Single-Phase Flow Pressure Drop Cases

Table 11 Input and Boundary Conditions for the Single-Phase Flow Pressure Drop Cases

Case	Outlet pressure [bar]	Mass flow rate [t/h]	Inlet temperature [K]
P70001	2.00	9.90	307.55
P70002	2.00	14.50	311.65
P70003	2.00	19.90	312.95
P70004	2.00	24.90	311.55
P70005	2.00	29.80	309.05
P70006	2.00	34.80	309.35
P70007	2.00	39.70	309.35
P70008	2.00	44.80	311.25
P70009	2.00	54.60	312.35
P70010	2.00	59.80	314.55
P70011	2.00	64.20	315.55
P70012	2.00	69.20	317.55
P70013	10.00	9.90	449.65
P70014	9.90	14.90	449.65
P70015	9.90	20.30	449.45
P70016	9.80	24.80	449.35
P70017	9.80	29.90	449.55
P70018	9.90	34.70	449.35
P70019	9.90	39.80	449.15
P70020	9.90	45.30	448.75
P70021	10.00	54.80	449.45
P70022	9.80	59.80	448.45
P70023	9.80	64.80	448.15
P70024	9.80	69.80	448.25
P70025	71.70	9.90	558.75
P70026	71.50	15.40	558.65
P70027	71.50	20.30	558.05
P70028	71.60	24.90	558.25
P70029	71.60	29.80	558.25
P70030	71.60	34.70	558.85
P70031	71.60	39.70	558.75
P70032	71.60	44.60	558.45
P70033	71.50	55.00	557.85
P70034	71.50	59.70	557.95
P70035	71.60	64.80	557.75
P70036	71.50	69.90	557.95

The single-phase pressure drop measurements at different elevations and the percental deviation of the predictions are given in Table 12 and Table 13, respectively. The data are limited to the cases P70027 till P70036.

Table 12 Local Single-Phase Flow Pressure Drop Measurements

Case	dPT1	dPT2	dPT3	dPT4	dPT5 [kPa]	dPT6	dPT7	dPT8	dPT9
P70027	0.30	0.35	0.39	0.45	0.47	0.46	1.33	0.52	3.12
P70028	0.46	0.51	0.58	0.65	0.64	0.68	1.98	0.75	4.59
P70029	0.64	0.72	0.81	0.91	0.93	0.94	2.79	1.03	6.46
P70030	0.79	0.95	1.05	1.19	1.26	1.25	3.73	1.36	8.57
P70031	1.11	1.25	1.41	1.58	1.60	1.63	4.87	1.77	11.23
P70032	1.37	1.54	1.73	1.93	1.95	1.99	5.96	2.17	13.76
P70033	2.06	2.30	2.55	2.87	2.91	2.96	8.85	3.22	20.43
P70034	2.41	2.69	2.99	3.35	3.39	3.46	10.36	3.76	23.87
P70035	2.81	3.14	3.46	3.90	3.95	4.03	12.05	4.37	27.77
P70036	3.25	3.63	3.99	4.50	4.55	4.65	13.89	5.04	32.03

Table 13 Percental Error of the Predicted Local Single-Phase Flow Compared to the Measurements

Case	dPT1	dPT2	dPT3	dPT4	dPT5 [kPa]	dPT6	dPT7	dPT8	dPT9
P70027	-19.99	0.67	-15.15	-2.06	-6.23	-4.19	-0.34	-3.04	7.35
P70028	-21.46	2.59	-14.78	0.89	2.53	-3.51	-0.62	-0.24	5.45
P70029	-19.56	5.49	-15.54	2.79	0.19	-1.20	-0.16	2.38	4.34
P70030	-12.42	7.25	-11.48	4.80	-0.73	0.20	0.60	3.04	4.73
P70031	-18.77	6.00	-14.88	2.92	1.39	-0.06	0.28	2.71	3.08
P70032	-17.58	8.39	-13.43	5.58	4.71	2.27	2.50	5.34	4.93
P70033	-17.48	9.46	-11.95	6.85	5.23	3.43	3.84	6.45	5.52
P70034	-17.25	9.73	-11.89	7.27	5.95	3.83	4.03	6.78	5.83
P70035	-16.46	10.63	-10.56	8.12	6.84	4.77	5.07	7.76	6.55
P70036	-16.08	11.29	-10.09	8.74	7.62	5.37	5.76	8.62	7.06

These percental deviations are plotted in Figure 51 and one can see that the largest differences appear at the top positions. The comparison of the calculated and measured total single-phase pressure drop is given in Figure 52 for all 36 reference cases. The additional lines to indicate the ± 10 % bands show that the predictions are in good agreement with the experiment. In order to see the deviation of each run, Figure 53 is given. The relative error with respect to the experiment ranges from 2 to 36 %. Three sections are visible corresponding to the three different input and boundary condition sets.

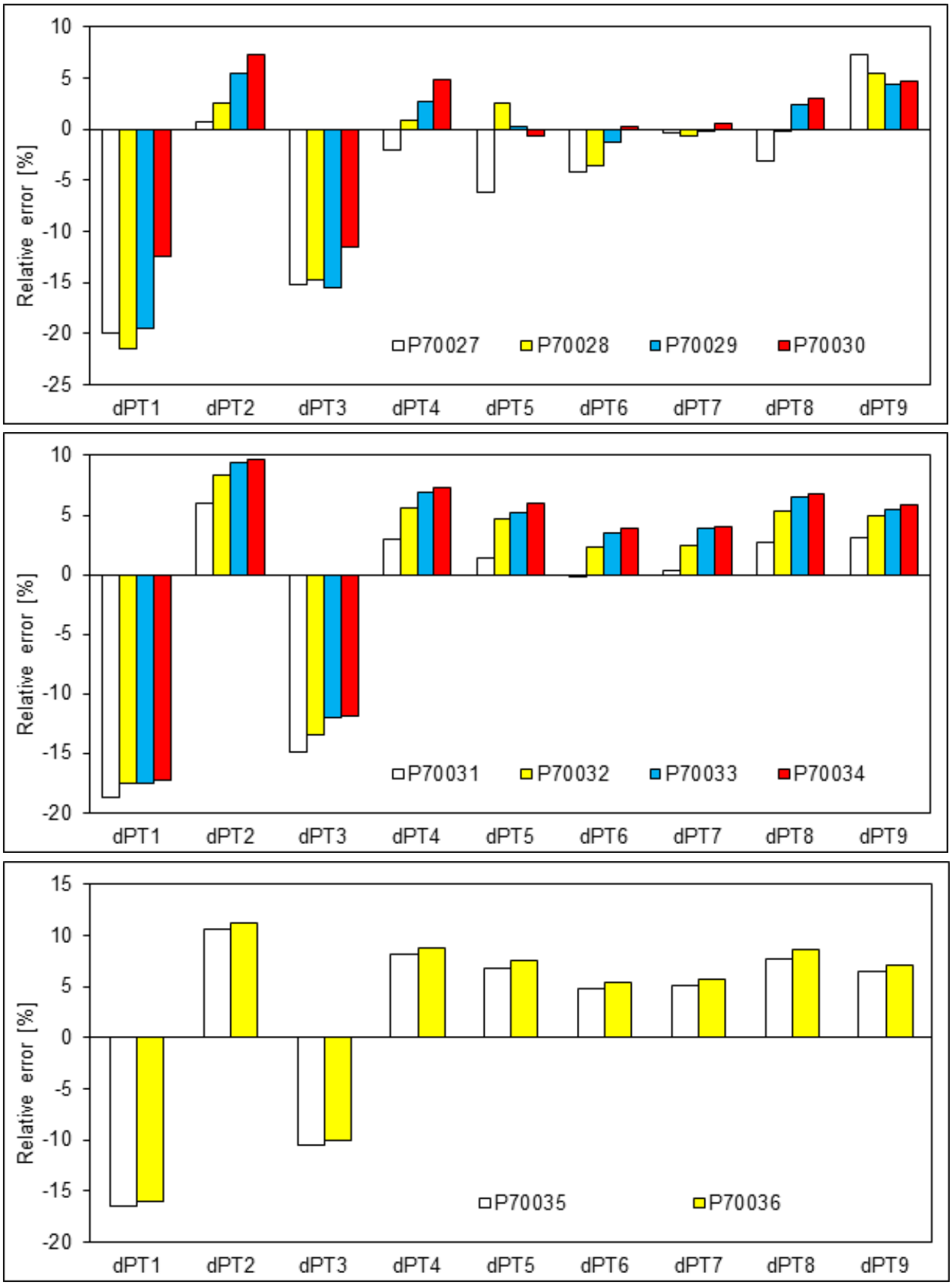

Figure 51 Relative Error of the Local Single-Phase Flow Pressure Drop for Selected Cases

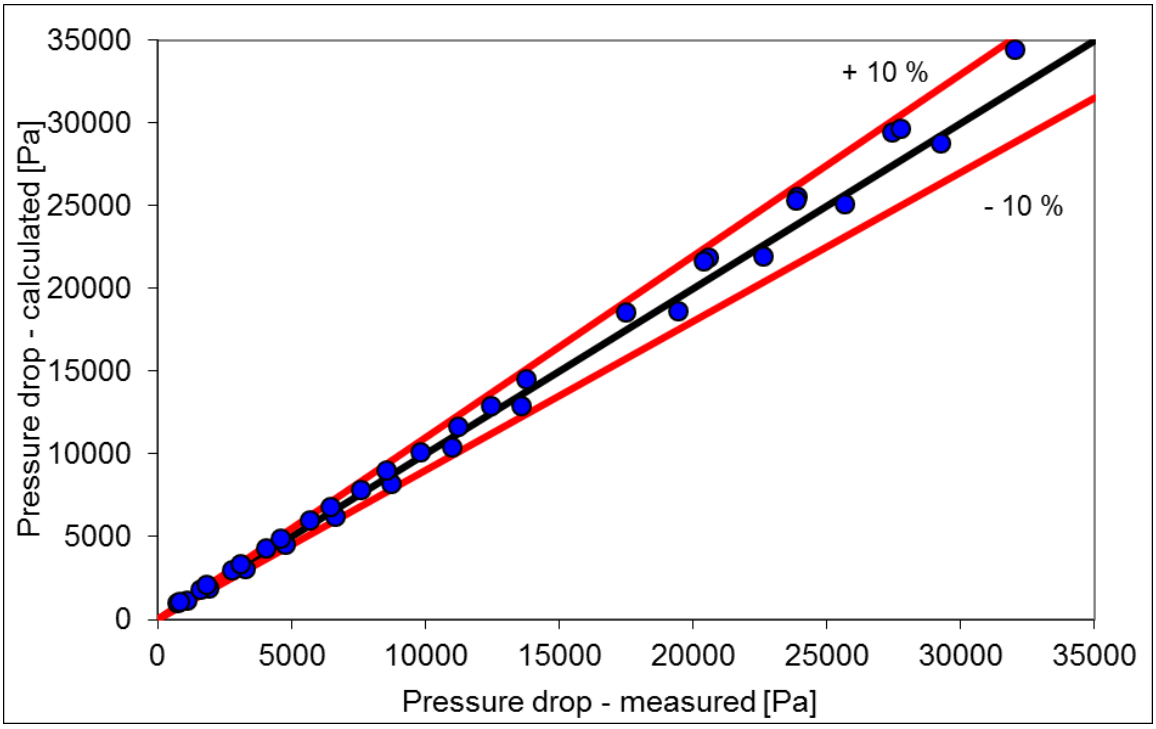

Figure 52 Calculated versus Measured Pressure Drop for the Single-Phase Flow Reference Cases

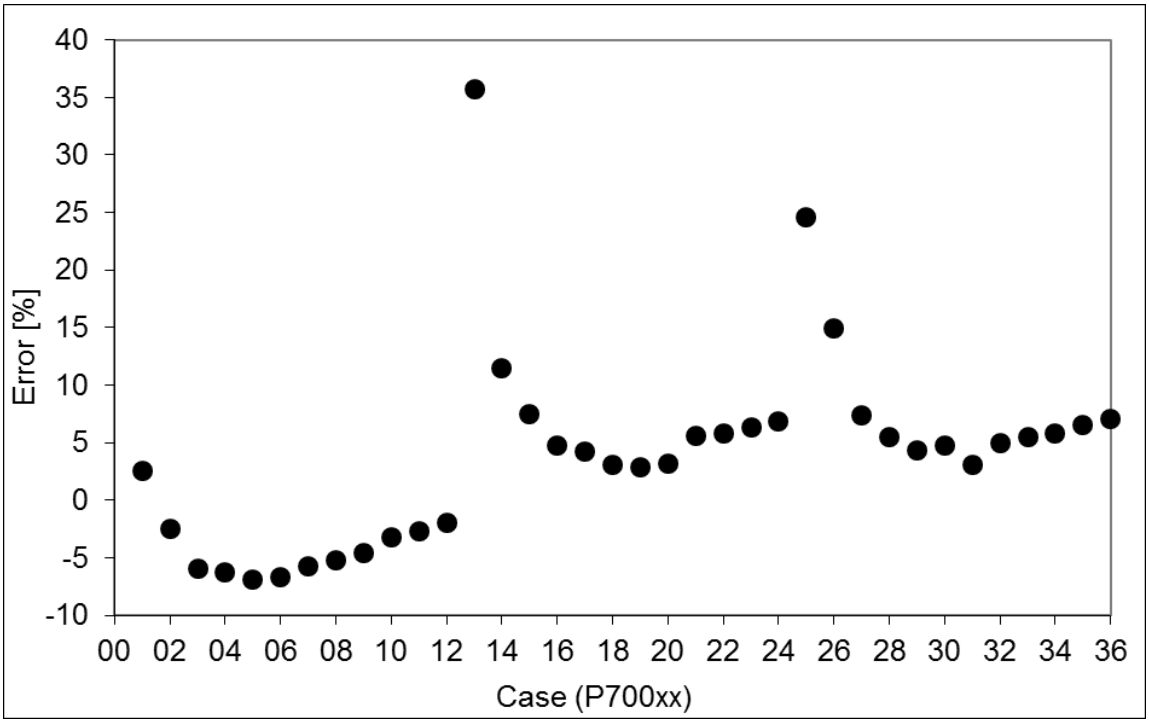

Figure 53 Percental Error of the Reference Values Compared to the Experimental Data for Single-Phase Flow Cases

In that figure, it is visible that TRACE tends to over predict the single-phase pressure drop no matter the pressure drop is high or low, especially at medium and higher pressures and inlet temperatures. That figure also reveals that some of the predictions are far off the measured values. Case 13 (35.7 %) and case 25 (24.6 %) show a big deviation. Investigating Figure 55 and Table 14 shows that the pressure drop is really small. The experimental value for case 13 is 740 Pa while the calculated one is 1000 Pa which means that the deviation is only 260 Pa. Due to the low pressure drop an absolute deviation of only 260 Pa results is a relative large error. In addition, the lower the pressure drop the more difficult it gets to measure it. The average error over all 36 cases is 6.83 %. If the cases with an experimental pressure drop of less than 1000 Pa are excluded, the average error is reduced to 5.46 %. The error as a function of pressure drop is given in Figure 54.

Figure 55 shows the absolute pressure drop for each case together with the minimum and maximum value of the uncertainty analysis compared to the experimental value. Due to the mentioned handling inconveniences only six out of 36 cases are calculated with TRACE-DAKOTA In general, the three sections characterized by the input and boundary conditions are also visible here. A clear parabolic trend is visible due to the quadratic influence of the mass flow rate (more precisely the velocity) on the pressure drop. The uncertainty band based on TRACE-DAKOTA is narrower than the one of TRACE-SUSA since less parameter is involved. The mean values, however, are almost identical. In Figure 56, the relative pressure drop is given in order to highlight the deviations of the mean values and the uncertainty band from the experimental data.

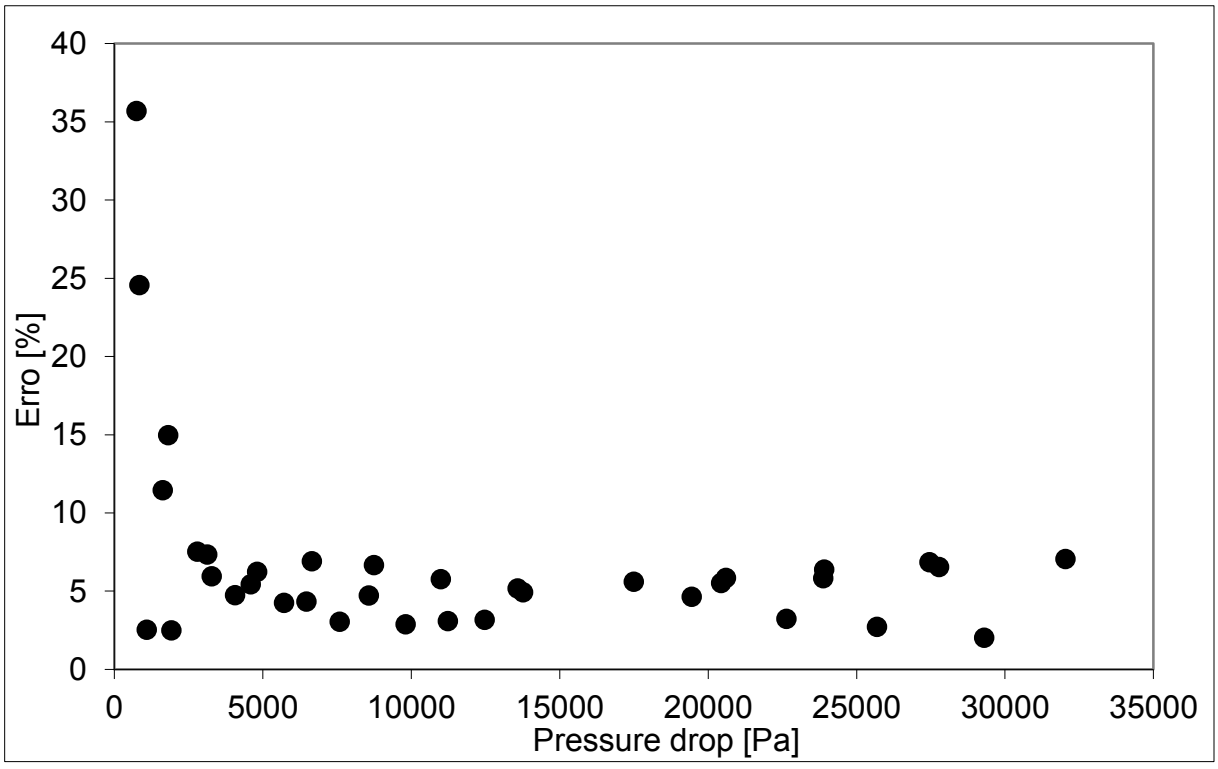

Figure 54 Error as Function of the Single-Phase Flow Pressure Drop

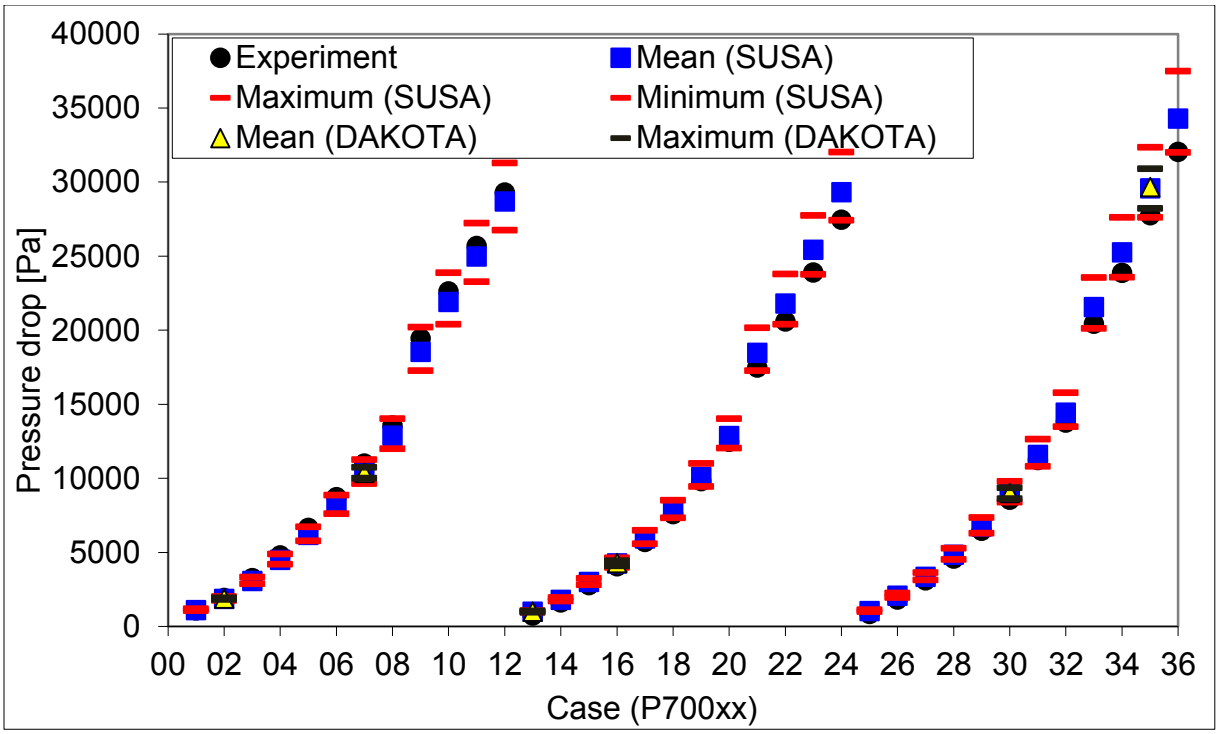

Figure 55 Comparison of the Experimental and Predicted Pressure Drops for the Single-Phase Flow Cases in Absolute Values

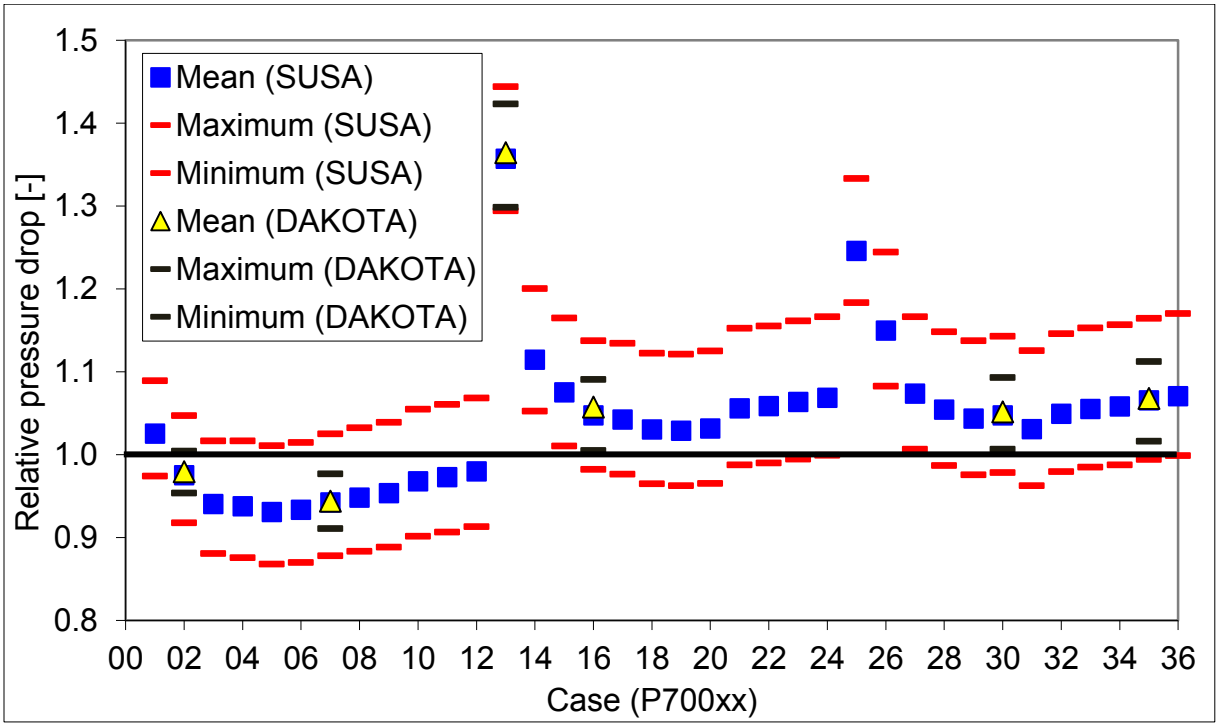

Figure 56 Comparison of the Experimental and Predicted Pressure Drops for the Single-Phase Flow Cases in Relative Values

Only in 6 out of 36 cases the maximum and minimum does not envelop the experimental data. These cases are: Case 13; 14; 15; 25; 26 and 27. The characteristic of these cases are the low pressure drop, the low mass flow rate and medium/high system pressure and inlet temperatures.

The results for the: mean, minimum, maximum, standard deviation and error, for each scenario, are summarized in Table 14 and Table 15 for the TRACE-SUSA calculations and the TRACE-DAKOTA predictions, respectively. The almost perfect agreement for the mean values and the smaller uncertainty band, best seen by the standard deviation, is verifiable.

Table 14 Results of the Uncertainty Analysis for the Single-Phase Flow Pressure Drops with TRACE-SUSA

Case	Ex [Pa]	Mean [Pa]	Max [Pa]	Min [Pa]	SD [Pa]	Error [%]
P70001	1090	1118	1187	1062	29	2.53
P70002	1920	1872	2010	1762	57	-2.49
P70003	3270	3075	3323	2879	101	-5.95
P70004	4800	4501	4878	4203	155	-6.23
P70005	6650	6190	6720	5772	218	-6.92
P70006	8740	8158	8868	7602	291	-6.65
P70007	10990	10356	11266	9647	372	-5.77
P70008	13580	12877	14017	11994	466	-5.18
P70009	19440	18539	20196	17267	675	-4.63
P70010	22630	21901	23866	20402	799	-3.22
P70011	25680	24985	27233	23277	914	-2.71
P70012	29290	28700	31289	26743	1051	-2.01
P70013	740	1004	1068	958	25	35.70
P70014	1620	1806	1944	1705	54	11.46
P70015	2790	3000	3250	2819	98	7.52
P70016	4060	4252	4618	3988	144	4.73
P70017	5710	5953	6476	5575	206	4.25
P70018	7590	7821	8518	7321	275	3.05
P70019	9810	10092	10999	9442	358	2.87
P70020	12470	12865	14030	12033	460	3.17
P70021	17490	18469	20154	17271	666	5.60
P70022	20600	21803	23797	20387	789	5.84
P70023	23900	25423	27752	23771	922	6.37
P70024	27450	29328	32019	27422	1066	6.84
P70025	840	1046	1120	994	28	24.57
P70026	1810	2081	2252	1959	66	14.98
P70027	3120	3349	3639	3140	112	7.35
P70028	4590	4840	5269	4530	167	5.45
P70029	6460	6740	7348	6301	236	4.34
P70030	8570	8975	9793	8385	318	4.73
P70031	11230	11576	12637	10809	413	3.08

Case	Ex [Pa]	Mean [Pa]	Max [Pa]	Min [Pa]	SD [Pa]	Error [%]
P70032	13760	14438	15768	13478	518	4.93
P70033	20430	21557	23554	20116	778	5.52
P70034	23870	25261	27605	23569	914	5.83
P70035	27770	29588	32337	27604	1072	6.55
P70036	32030	34291	37481	31989	1245	7.06

Table 15 Results of the Uncertainty Analysis for the Single-Phase Flow Pressure Drops with TRACE-DAKOTA

Case	Ex [Pa]	Mean [Pa]	Max [Pa]	Min [Pa]	SD [Pa]	Error [%]
P70002	1920	1881	1928	1831	24	-2.05
P70007	10990	10371	10732	10009	181	-5.63
P70013	740	1010	1053	961	22	36.43
P70016	4060	4293	4427	4079	97	5.74
P70030	8570	9011	9366	8625	159	5.15
P70035	27770	29657	30887	28221	605	6.80

After showing the impact of the input parameters in the previous graphs, the corresponding sensitivity coefficients are plotted in Figure 57 (TRACE-SUSA) and Figure 58 (TRACE-DAKOTA). It is clearly visible that parameters like the hydraulic diameter, the spacer form loss coefficient and the friction factor are the most influential parameters. The hydraulic diameter, as the dominating one has negative values for the sensitivity coefficient which indicates that an increase of the hydraulic diameter would provoke a reduction of the pressure drop and vice versa. The K factor for the spacer grid and the friction factor have positive values indicating a direct proportional relationship. As expected, the outlet pressure and the inlet temperature variations have no influence on the result since the pressure drop has only a weak dependence on them due to the pressure and temperature dependent properties. But also parameters like the density and the mass flow rate show a negligible impact even though the pressure drop is directly dependent on them. That can be explained with the presence of the other parameters where their variations have bigger influence.

Regarding the TRACE-DAKOTA investigation, the most important parameter is the form loss coefficient of the spacer grid and the mass flow rate. The values for them are higher than they are for the TRACE-SUSA analysis. That is due to the presence of the hydraulic diameter and the friction factor in the TRACE-SUSA analysis which lowers the values of K-spacer and mass flow rate compared to them during TRACE-DAKOTA investigation. Outlet pressure, wall roughness and inlet temperature show a similar behavior indicating that their variation will have no or only little effect on the pressure drop.

The ranking of the uncertain parameters with respect to their significance on the pressure drop is given in Figure 59 and Figure 60 for TRACE-SUSA and TRACE-DAKOTA, respectively. As indicated by the sensitivity coefficients, hydraulic diameter is ranked 1st, and friction factor and K factor for the spacer are ranked 2nd and 3rd (with changing positions after case 7).

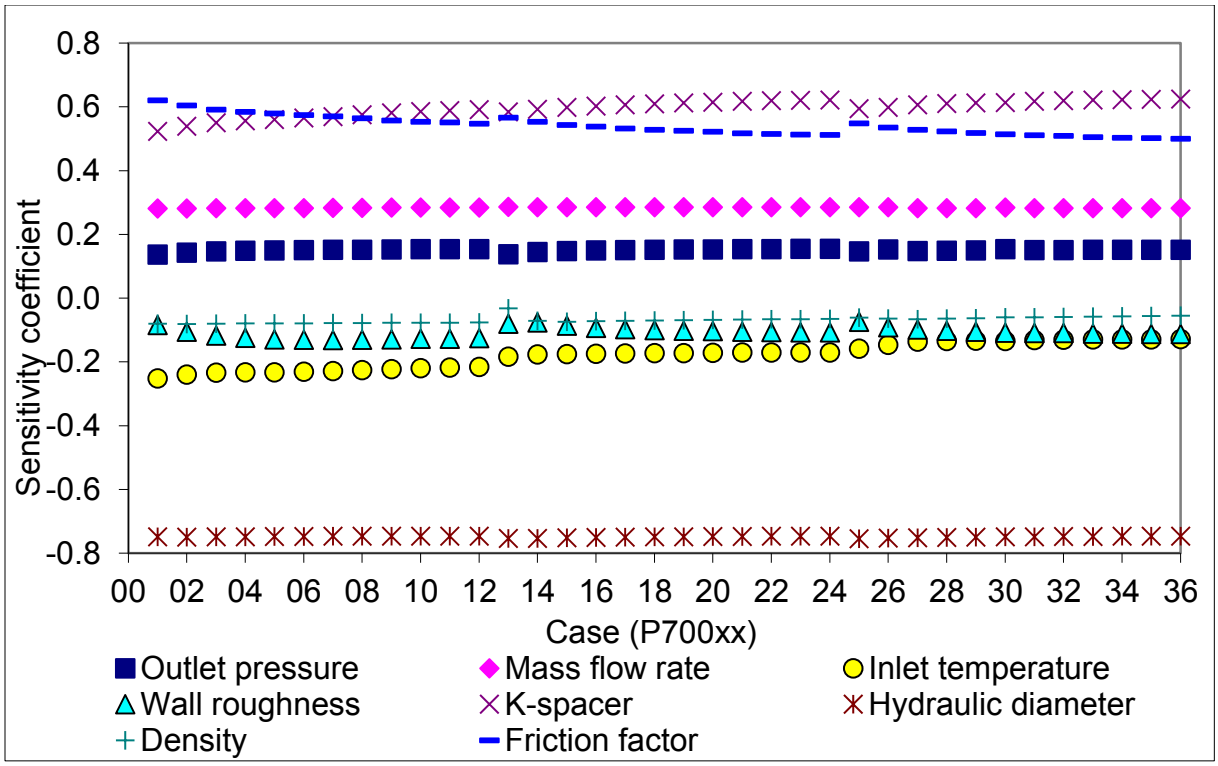

Figure 57 Sensitivity Coefficients for the Single-Phase Flow Pressure Drop Analysis with TRACE-SUSA

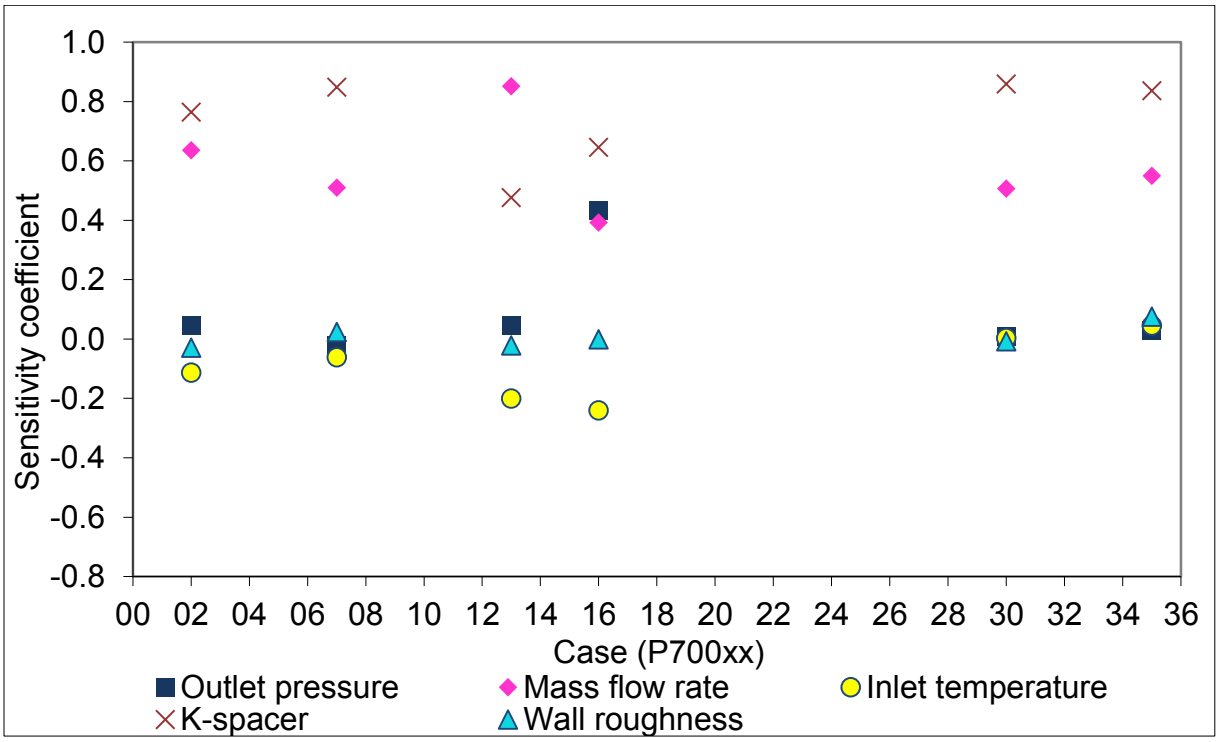

Figure 58 Sensitivity Coefficients for the Single-Phase Flow Pressure Drop Analysis with TRACE-DAKOTA

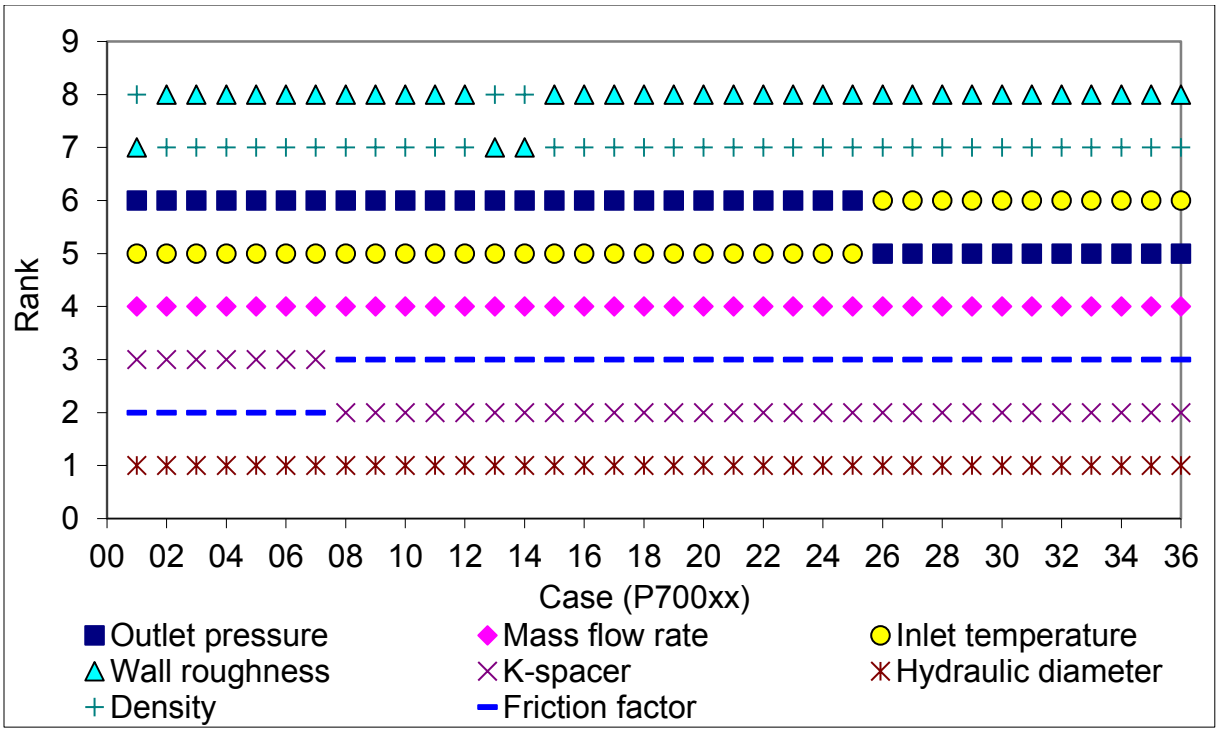

Figure 59 Ranking of the Uncertain Parameters for the Single-Phase Flow Pressure Drop Analysis with TRACE-SUSA

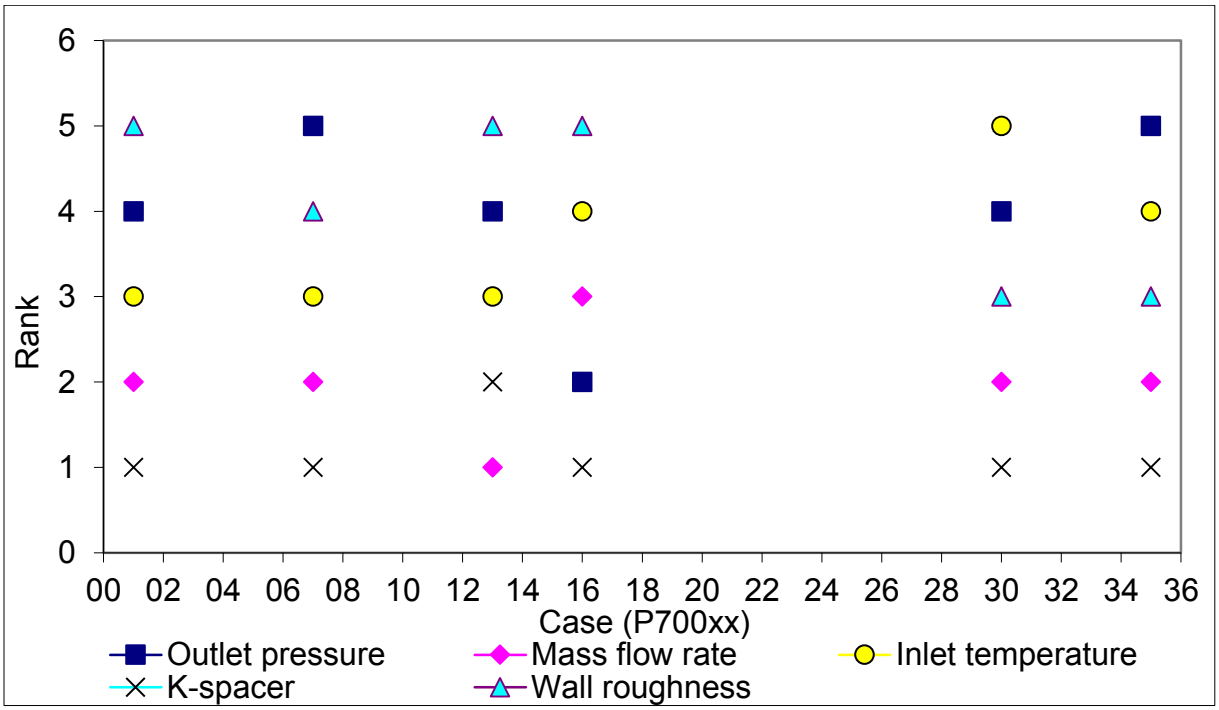

Figure 60 Ranking of the Uncertain Parameters for the Single-Phase Flow Pressure Drop Analysis with TRACE-DAKOTA

With TRACE and DAKOTA the parameter ranked no. one is the form loss coefficient for the spacer. The second rank is, during the most cases, the mass flow rate. In case 13 the spacer form loss coefficient and the mass flow rate change positions. In case 16 the outlet pressure gained importance and is positioned between form factor and mass flow rate.

The sensitivity coefficients based on Pearson's momentum correlation coefficient are listed in Table 16 and Table 17 for TRACE-SUSA and TRACE-DAKOTA, respectively.

Table 16 Pearson's Momentum Correlation Coefficients for the Single-Phase Flow Pressure Drop Cases with TRACE-SUSA

	Outlet pressure	Mass flow rate	Inlet temperature	Wall roughness	K-spacer	Hydraulic diameter	Density	Friction factor
P70001	0.1370	0.2810	-0.2517	-0.0839	0.5233	-0.7488	-0.0800	0.6207
P70002	0.1431	0.2812	-0.2396	-0.1055	0.5388	-0.7492	-0.0815	0.6041
P70003	0.1464	0.2818	-0.2337	-0.1175	0.5501	-0.7489	-0.0801	0.5916
P70004	0.1484	0.2819	-0.2323	-0.1243	0.5564	-0.7483	-0.0796	0.5845
P70005	0.1498	0.2821	-0.2327	-0.1295	0.5603	-0.7476	-0.0793	0.5798
P70006	0.1508	0.2825	-0.2305	-0.1306	0.5656	-0.7473	-0.0789	0.5744
P70007	0.1516	0.2828	-0.2289	-0.1313	0.5699	-0.7471	-0.0786	0.5700
P70008	0.1522	0.2833	-0.2255	-0.1299	0.5750	-0.7471	-0.0782	0.5648
P70009	0.1531	0.2838	-0.2223	-0.1294	0.5817	-0.7468	-0.0775	0.5578
P70010	0.1535	0.2841	-0.2193	-0.1277	0.5857	-0.7468	-0.0770	0.5537
P70011	0.1538	0.2843	-0.2178	-0.1270	0.5883	-0.7467	-0.0767	0.5510
P70012	0.1541	0.2846	-0.2154	-0.1257	0.5915	-0.7466	-0.0762	0.5477
P70013	0.1376	0.2867	-0.1837	-0.0805	0.5845	-0.7542	-0.0318	0.5661
P70014	0.1449	0.2852	-0.1770	-0.0760	0.5921	-0.7533	-0.0707	0.5530
P70015	0.1480	0.2850	-0.1752	-0.0863	0.5987	-0.7515	-0.0738	0.5437
P70016	0.1495	0.2849	-0.1741	-0.0928	0.6028	-0.7507	-0.0724	0.5378
P70017	0.1508	0.2849	-0.1730	-0.0973	0.6066	-0.7498	-0.0712	0.5326
P70018	0.1517	0.2850	-0.1726	-0.0999	0.6096	-0.7491	-0.0702	0.5286
P70019	0.1524	0.2851	-0.1720	-0.1019	0.6122	-0.7485	-0.0693	0.5250
P70020	0.1531	0.2852	-0.1715	-0.1036	0.6145	-0.7480	-0.0684	0.5218
P70021	0.1539	0.2854	-0.1706	-0.1056	0.6178	-0.7473	-0.0669	0.5172
P70022	0.1543	0.2854	-0.1706	-0.1063	0.6192	-0.7470	-0.0663	0.5153
P70023	0.1546	0.2855	-0.1704	-0.1070	0.6204	-0.7467	-0.0657	0.5135
P70024	0.1548	0.2856	-0.1701	-0.1076	0.6215	-0.7464	-0.0651	0.5119
P70025	0.1463	0.2853	-0.1588	-0.0743	0.5945	-0.7547	-0.0609	0.5484
P70026	0.1525	0.2849	-0.1464	-0.0907	0.5989	-0.7530	-0.0636	0.5356
P70027	0.1477	0.2821	-0.1368	-0.0980	0.6066	-0.7512	-0.0660	0.5281
P70028	0.1489	0.2819	-0.1348	-0.1027	0.6100	-0.7503	-0.0642	0.5228
P70029	0.1497	0.2818	-0.1332	-0.1055	0.6130	-0.7495	-0.0627	0.5183
P70030	0.1536	0.2838	-0.1348	-0.1084	0.6138	-0.7492	-0.0597	0.5145
P70031	0.1510	0.2821	-0.1312	-0.1088	0.6173	-0.7485	-0.0599	0.5115
P70032	0.1509	0.2820	-0.1304	-0.1096	0.6192	-0.7481	-0.0592	0.5090
P70033	0.1516	0.2822	-0.1298	-0.1110	0.6220	-0.7473	-0.0575	0.5048

	Outlet pressure	Mass flow rate	Inlet temperature	Wall roughness	K-spacer	Hydraulic diameter	Density	Friction factor
P70034	0.1518	0.2823	-0.1294	-0.1115	0.6230	-0.7471	-0.0568	0.5032
P70035	0.1520	0.2824	-0.1292	-0.1119	0.6240	-0.7468	-0.0561	0.5017
P70036	0.1522	0.2824	-0.1288	-0.1123	0.6249	-0.7466	-0.0554	0.5003

Table 17 Pearson's Momentum Correlation Coefficients for the Single-Phase Flow Pressure Drop Cases with TRACE-DAKOTA

	Outlet pressure	Mass flow rate	Inlet temperature	Wall roughness	K-spacer	Hydraulic diameter	Density	Friction factor
P70002	0.0297	0.5496	0.0449	0.0758	0.8363	not included		
P70007	0.0072	0.5064	0.0028	-0.0075	0.8587			
P70013	0.0451	0.6360	-0.1133	-0.0294	0.7640			
P70016	0.0438	0.8513	-0.2003	-0.0215	0.4764			
P70030	-0.0215	0.5095	-0.0621	0.0238	0.8485			
P70035	0.4335	0.3926	-0.2404	-0.0007	0.6451			

6.3.2 Two-Phase Flow Pressure Difference

For the two phase flow the pressure drop is rather a pressure difference since only the difference of the absolute pressures between inlet and outlet is considered, according to

$$\Delta p = p_{inlet} - p_{outlet} \tag{61}$$

The boundary and input conditions for the two-phase flow analysis of the pressure drop is shown in Figure 61 and Table 18 for the 33 cases. Besides pressure and mass flow rate, the inlet sub-cooling and the power are subject of variations throughout the experimental scenarios. It can be seen that the pressure is now in typical BWR regions, varying between 72 and 86 bar. The inlet sub-cooling is always around 50 kJ/kg. The power and the mass flow rate show several levels of variation making the overall distribution of the input and boundary conditions more diverse than for the single-phase flow cases.

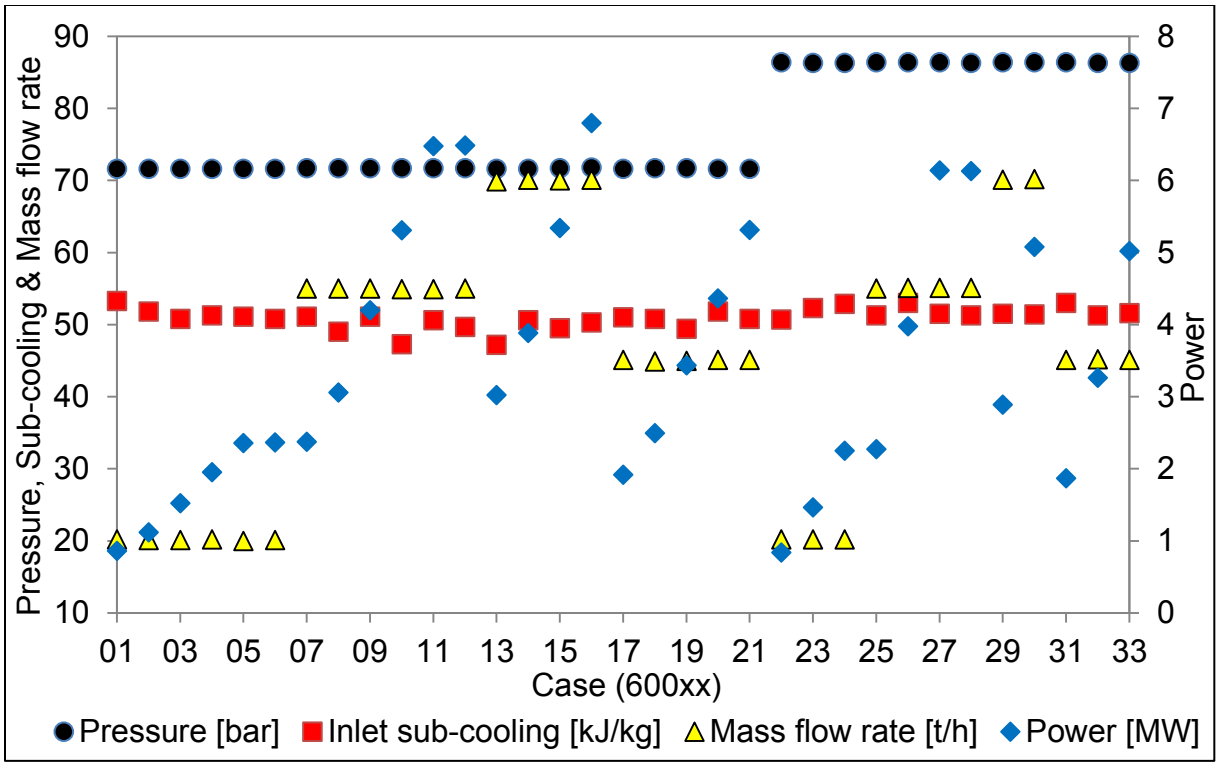

Figure 61 Input and Boundary for the Two-Phase Flow Pressure Drop Cases

Table 18 Input and Boundary Conditions for the Two-Phase Flow Pressure Drop Cases

Case	Outlet pressure [bar]	Mass flow rate [t/h]	Inlet sub-cooling [kJ/kg]	Power [MW]
P60001	71.6	20.2	53.3	0.863
P60002	71.6	20.1	51.8	1.117
P60003	71.6	20.1	50.8	1.521
P60004	71.6	20.2	51.3	1.951
P60005	71.6	20.0	51.1	2.357
P60006	71.6	20.1	50.8	2.366
P60007	71.7	55.0	51.1	2.375
P60008	71.7	55.0	49.0	3.057
P60009	71.7	55.0	51.1	4.197
P60010	71.7	54.9	47.3	5.311
P60011	71.7	54.9	50.6	6.478
P60012	71.7	55.0	49.7	6.483
P60013	71.6	69.9	47.2	3.022
P60014	71.6	70.1	50.6	3.884
P60015	71.7	70.0	49.5	5.340
P60016	71.8	70.1	50.3	6.795
P60017	71.6	45.1	51.0	1.919
P60018	71.7	44.9	50.8	2.495
P60019	71.7	45.0	49.4	3.437
P60020	71.6	45.1	51.8	4.363
P60021	71.6	45.1	50.8	5.312

Case	Outlet pressure [bar]	Mass flow rate [t/h]	Inlet sub-cooling [kJ/kg]	Power [MW]
P60022	86.4	20.2	50.7	0.837
P60023	86.3	20.2	52.3	1.464
P60024	86.3	20.2	52.9	2.252
P60025	86.4	55.0	51.3	2.271
P60026	86.4	55.1	53.0	3.975
P60027	86.4	55.1	51.5	6.137
P60028	86.3	55.1	51.3	6.132
P60029	86.4	70.1	51.5	2.888
P60030	86.4	70.2	51.4	5.076
P60031	86.4	45.1	53.0	1.869
P60032	86.3	45.2	51.3	3.262
P60033	86.3	45.1	51.6	5.021

The local two-phase flow pressure drop measurements according to the locations of Figure 12 are summarized in Table 19. The percental deviations of the predictions are given in Table 20.

Table 19 Local Two-Phase Flow Pressure Drop Measurements

Case	dPT1	dPT2	dPT3	dPT4	dPT5 [kPa]	dPT6	dPT7	dPT8	dPT9
P60001	1.15	1.96	2.53	3.48	3.66	3.93	12.27	5.50	27.40
P60003	1.54	2.22	2.81	3.61	3.63	3.69	11.72	5.50	27.22
P60005	2.10	2.81	3.43	4.26	4.11	3.97	11.84	5.47	29.16
P60007	5.59	6.70	8.11	9.55	9.06	8.40	22.84	8.25	57.89
P60009	9.24	10.91	12.39	14.26	13.54	11.83	29.30	8.48	78.59
P60011	13.56	16.05	17.81	20.04	19.39	16.73	39.14	8.93	106.72
P60013	8.92	10.24	12.15	13.58	12.98	11.65	30.31	10.07	79.71
P60015	14.93	17.00	19.33	20.96	20.33	17.40	41.22	10.48	113.97
P60017	3.93	4.91	6.08	7.23	7.03	6.73	18.92	7.24	46.54
P60019	6.43	7.73	8.94	10.54	9.98	8.90	22.97	7.44	60.11
P60021	9.30	11.24	12.51	14.42	13.98	12.17	29.32	7.72	78.76
P60022	1.11	1.94	2.49	3.44	3.48	3.88	11.99	5.36	26.83
P60023	1.39	2.08	2.62	3.44	3.49	3.63	11.54	5.36	26.38
P60024	1.82	2.49	3.03	3.88	3.55	3.75	11.47	5.33	27.55
P60025	4.96	6.08	7.29	8.74	8.15	7.96	22.05	8.17	54.66
P60026	7.75	9.23	10.47	12.61	11.43	10.50	26.89	8.36	70.06
P60027	11.18	13.30	14.69	17.40	16.10	14.40	34.79	8.79	92.41
P60029	7.60	8.96	10.54	12.32	11.43	10.70	28.79	10.08	73.55
P60030	12.39	14.28	16.19	18.14	17.16	15.33	37.62	10.40	100.77
P60031	3.49	4.50	5.50	6.78	6.36	6.42	18.29	7.09	44.32
P60032	5.42	6.62	7.63	9.34	8.47	8.02	21.35	7.28	54.32
P60033	7.61	9.31	10.28	12.62	11.50	10.49	26.21	7.54	68.44

Table 20 Percental Error of the Predicted Local Two-Phase Flow Compared to the Measurements

Case	dPT1	dPT2	dPT3	dPT4	dPT5 [%]	dPT6	dPT7	dPT8	dPT9
P60001	9.41	-10.24	4.07	-10.17	-10.19	-8.78	-4.75	-10.06	-3.74
P60003	-13.15	-16.55	-5.07	-14.26	-15.36	-14.67	-10.97	-11.09	-8.77
P60005	-23.19	-21.42	-8.49	-16.47	-17.89	-19.15	-16.25	-13.05	-12.49
P60007	-21.25	-7.11	-0.57	-3.42	-4.33	-6.07	-3.97	-6.50	-0.68
P60009	-28.04	-16.32	-0.75	-4.31	-9.06	-10.91	-9.89	-8.93	-4.35
P60011	-29.24	-18.46	-0.26	-1.63	-10.13	-14.11	-14.25	-11.72	-5.86
P60013	-24.26	-7.00	-0.05	1.37	-2.19	-4.15	-2.61	-4.20	1.07
P60015	-29.74	-15.44	-0.41	1.27	-6.88	-9.00	-8.20	-7.14	-2.33
P60017	-18.77	-8.16	-1.89	-4.97	-6.18	-7.26	-4.75	-7.84	-2.10
P60019	-27.59	-17.05	-2.77	-7.97	-11.06	-12.55	-11.00	-10.60	-6.24
P60021	-28.82	-19.77	-1.42	-5.12	-12.87	-16.11	-15.58	-12.96	-7.86
P60022	13.84	-9.08	6.15	-8.74	-5.56	-8.55	-4.55	-10.61	-3.06
P60023	-7.20	-13.81	-1.06	-12.00	-12.87	-12.73	-9.52	-11.13	-7.04
P60024	-17.77	-17.26	-3.53	-14.01	-9.21	-16.28	-13.77	-12.44	-10.16
P60025	-16.55	-2.92	2.95	-0.62	1.25	-4.11	-2.19	-6.17	1.40
P60026	-23.58	-10.69	3.29	-3.62	-2.96	-7.60	-6.91	-7.97	-1.23
P60027	-24.74	-13.16	4.99	-1.15	-4.81	-10.74	-11.22	-10.95	-2.40
P60029	-18.29	-1.31	4.30	2.57	3.21	-1.83	-0.28	-3.78	3.79
P60030	-24.87	-9.73	3.88	3.35	-1.62	-6.05	-5.68	-6.10	0.62
P60031	-13.13	-4.06	2.43	-3.21	-0.19	-5.37	-3.09	-6.97	-0.24
P60032	-22.55	-11.71	1.67	-6.29	-4.29	-9.27	-8.13	-9.41	-3.19
P60033	-23.77	-14.52	4.18	-5.23	-6.53	-12.34	-12.35	-12.03	-4.28

Apparently, not for all 33 cases values have been reported. A graphical interpretation of the percental deviation of the predictions is given in the following figures. It is visible that the error is large for dPT1 and dPT2 which measured the pressure drop over the two highest spacers. These are the positions with the highest void fractions and even small variations of it will result in rather large differences of the pressure drop. Further down the bundle the error is relatively small.

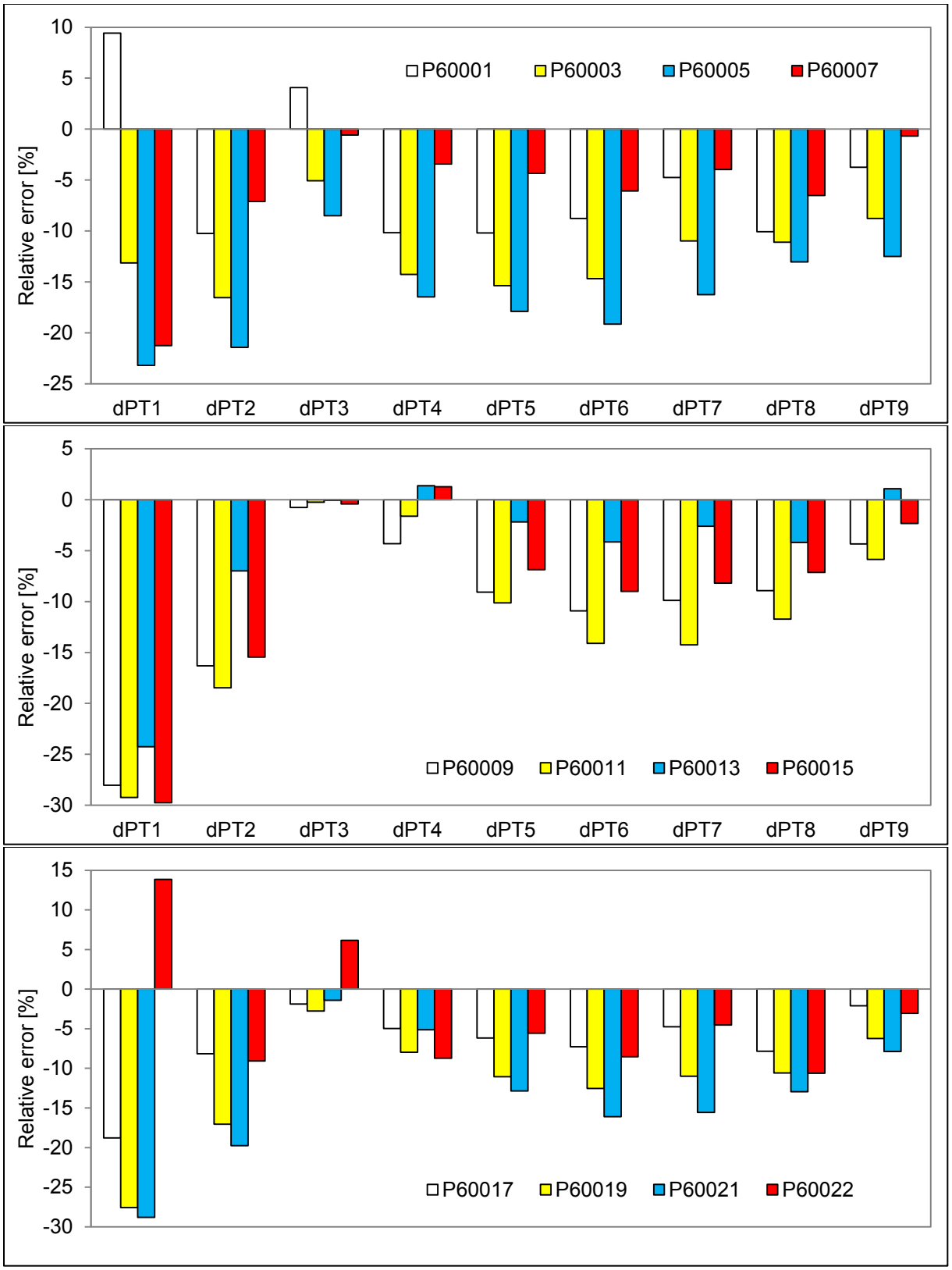

Figure 62 Relative Error of the Local Two-Phase Flow Pressure Drop for Selected Cases (1)

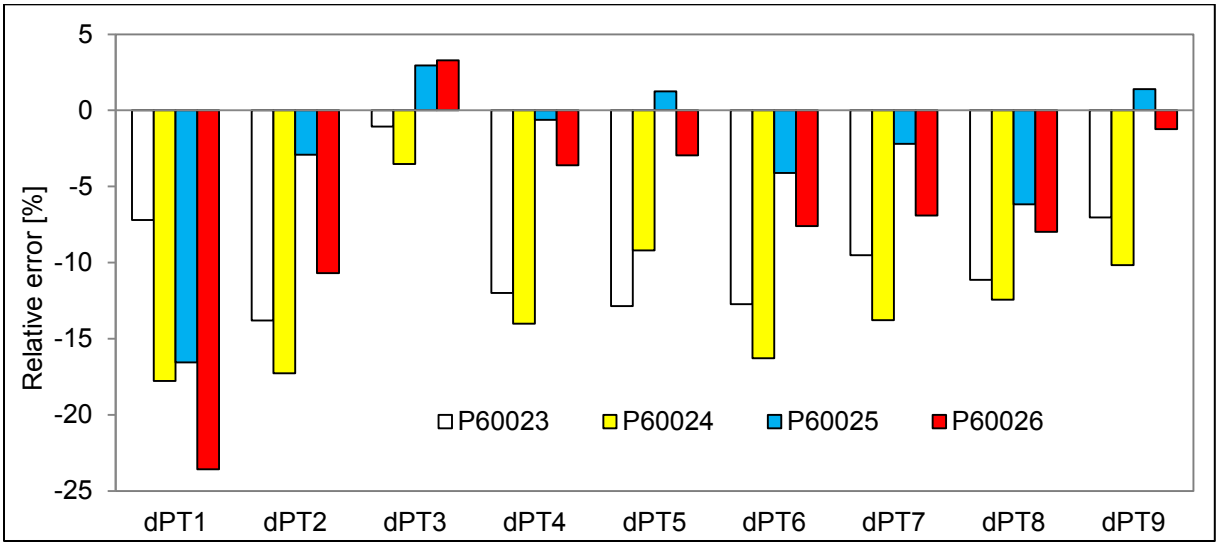

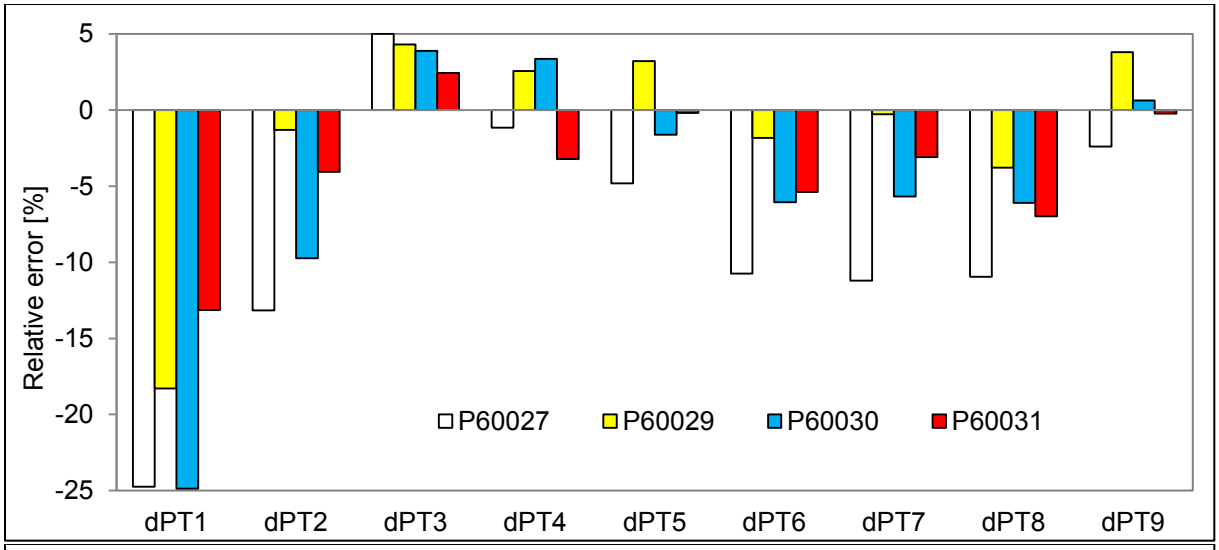

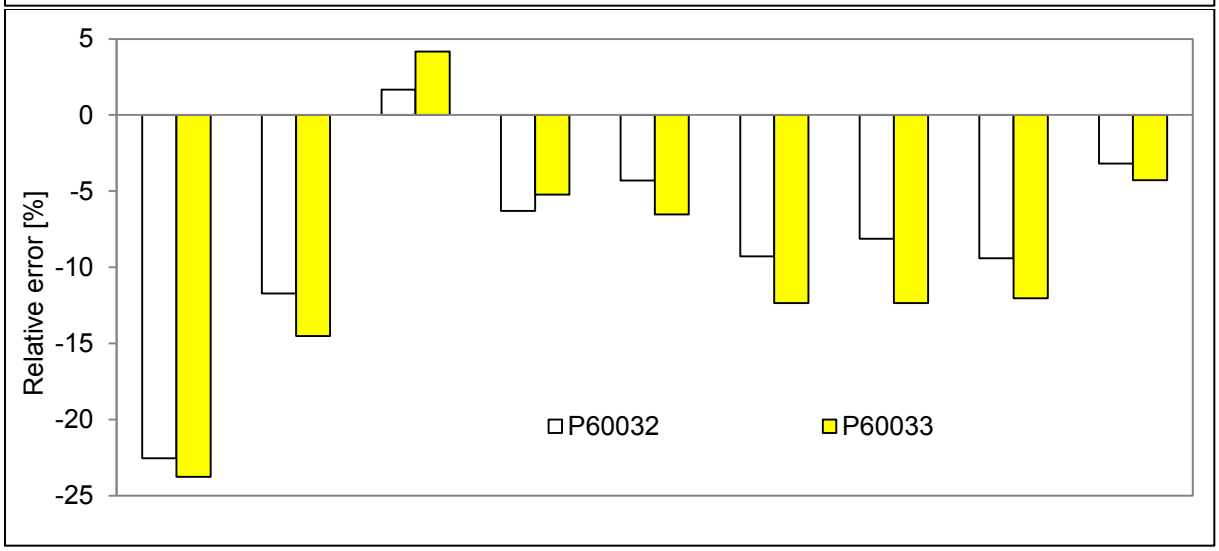

Figure 63 Relative Error of the Local Two-Phase Flow Pressure Drop for Selected Cases (2)

The calculated total reference pressure difference (dPT9) compared to the measured ones for the 33 cases is depicted in Figure 64. That graph shows on the one side a good agreement between the calculated and the measured data and on the other side that the predictions are mostly underestimating the experiment. This can be even better seen in Figure 65 where the percental error of the calculations based on the experimental is shown. In fact, only for four cases the prediction gives higher values than the experiment. The error as a function of the pressure difference is shown in Figure 66. As for the single-phase flow cases, the error is higher at lower pressure differences. But in the two-phase flow cases that difference is not that pronounced.

Figure 67 shows the results of the uncertainty study. The average error is 4.66 %.The mean values of TRACE-SUSA and TRACE-DAKOTA are depicted as squares with minimal and maximal values indicated by horizontal lines. The experimental values are shown as circles. Due to the wide pressure drop range of the experimental cases, a graph with relative pressure drops helps for the understanding.

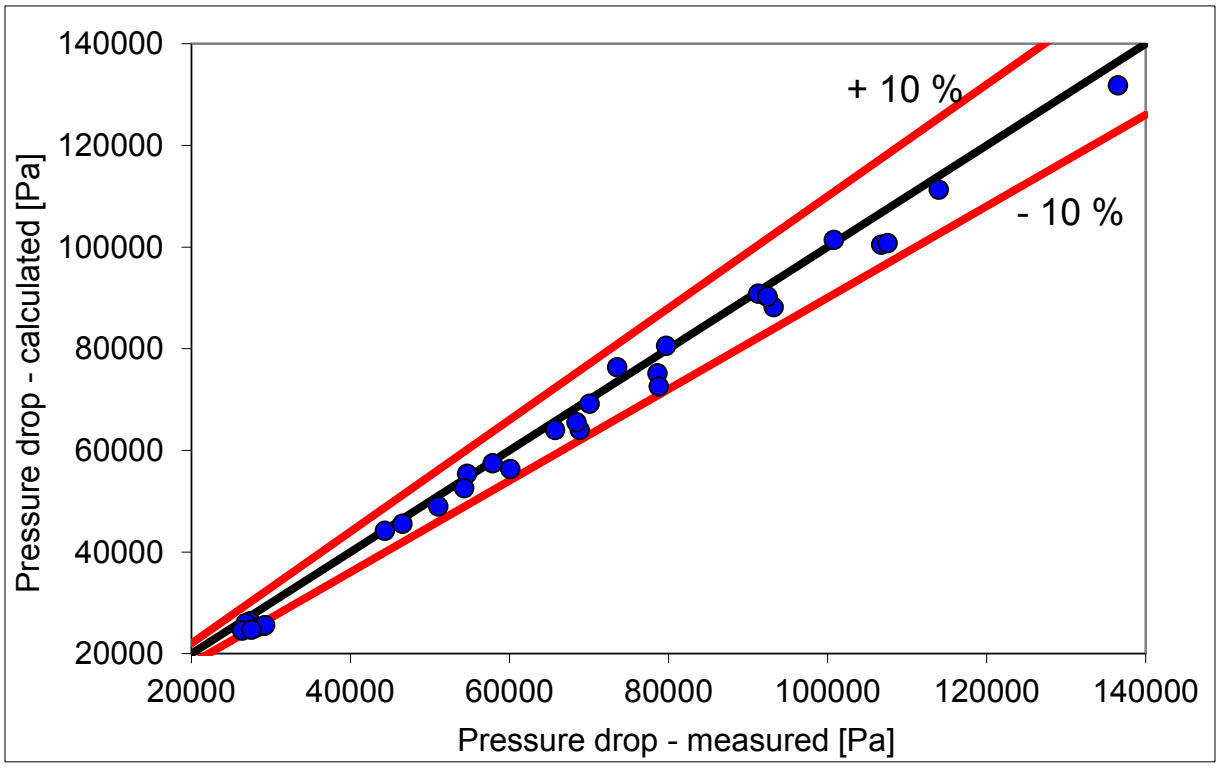

Figure 64 Calculated versus Measured Pressure Drop for the Two-Phase Flow Reference Cases

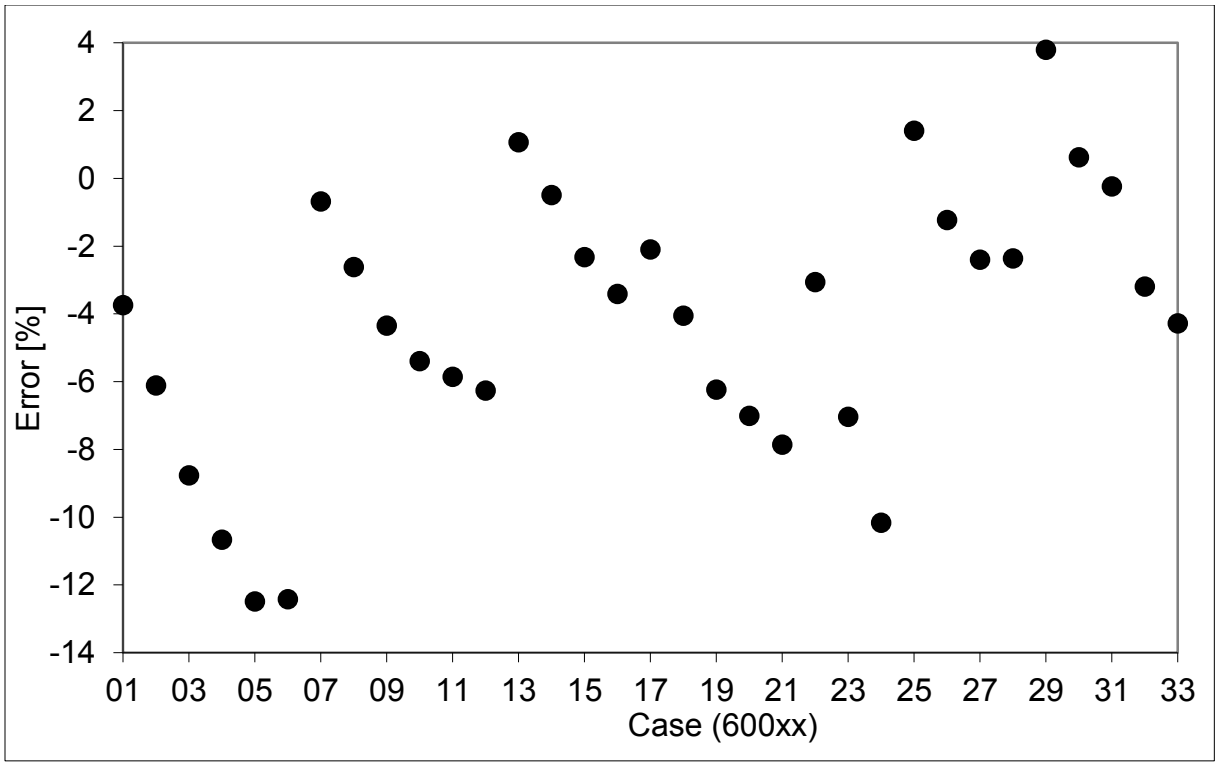

Figure 65 Percental Error of the Reference Values Compared to the Experimental Data for the Two-Phase Flow Cases

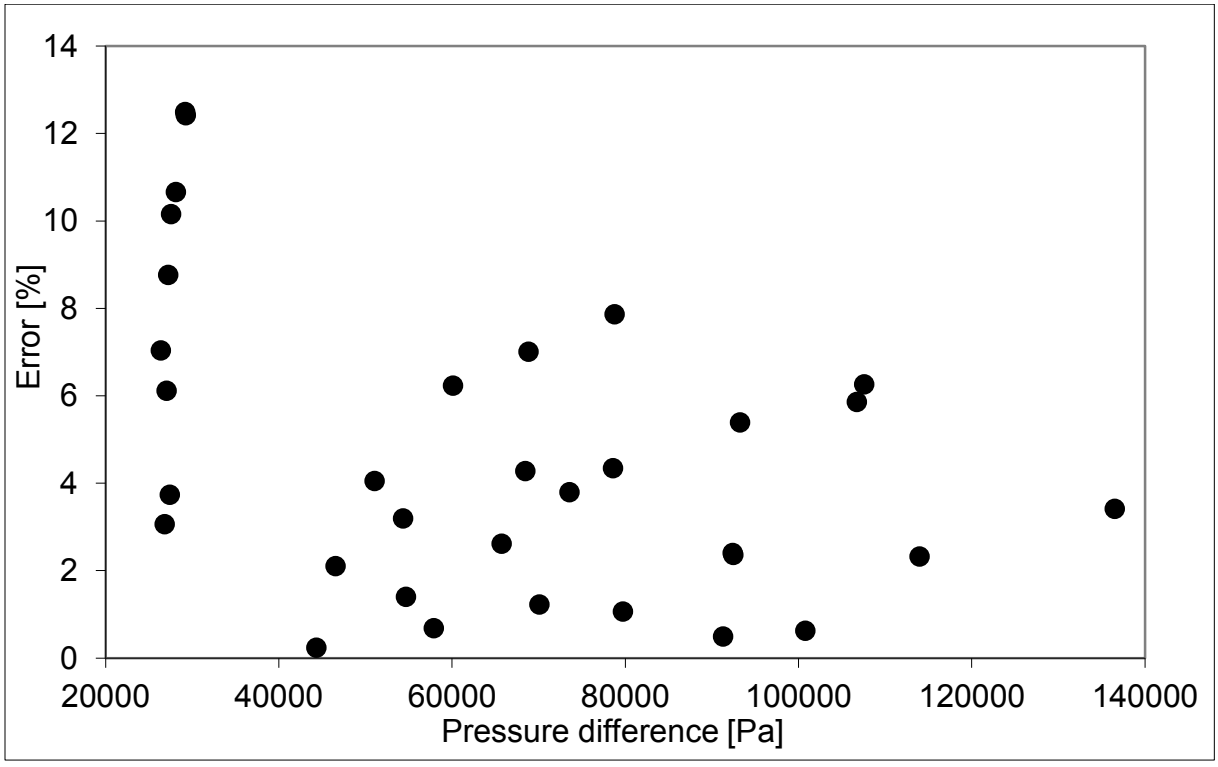

Figure 66 Error as Function of the Two-Phase Flow Pressure Difference

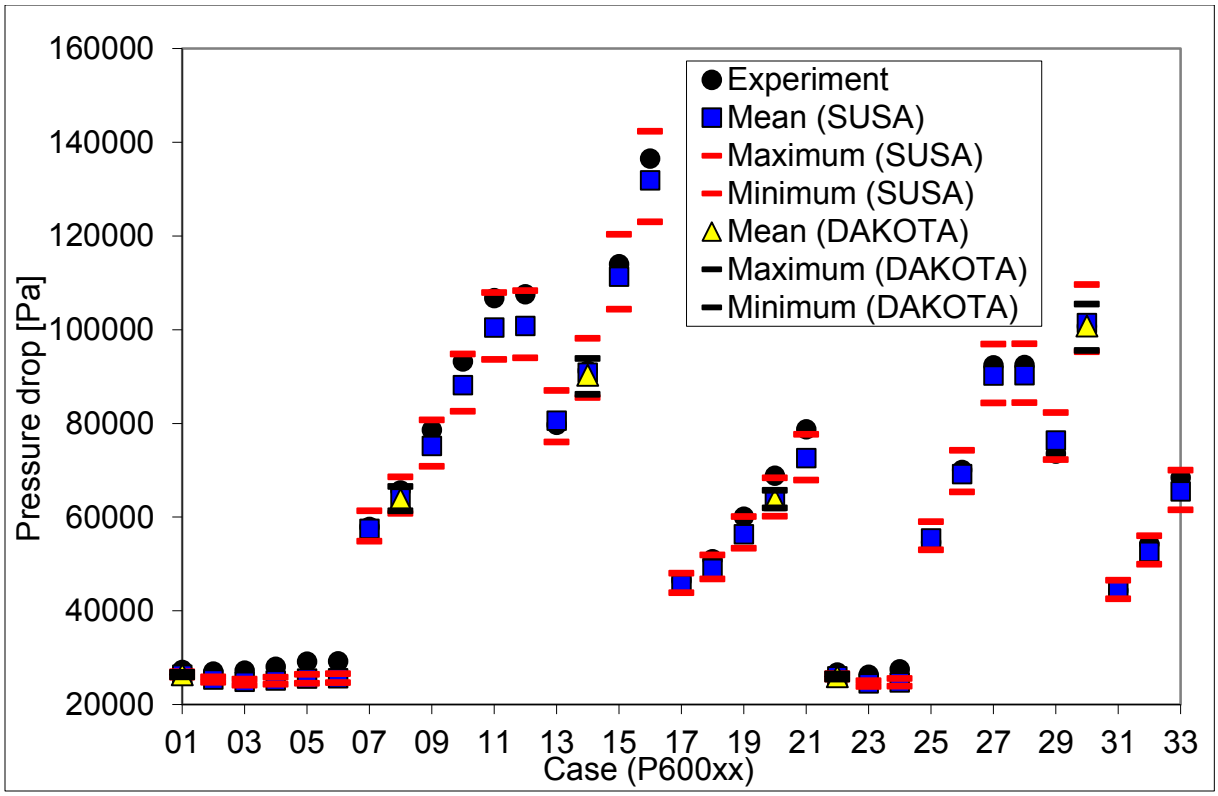

Figure 67 Comparison of the Experimental and Predicted Pressure Drops for the Two-Phase Flow Cases in Absolute Values

Figure 68 shows again that most of the predicted values are below the experimental values (indicated by the vertical line intersecting with y = 1.0). Furthermore, it is visible that the uncertainty band of the TRACE-DAKOTA analysis is narrower than for the TRACE-SUSA calculations as expected since less uncertainty parameters are taken into account in the first case. In addition, the lower band/value being almost similar, the upper values show larger differences between TRACE-SUSA and TRACE-DAKOTA. The results for the two phase flow pressure drop cases are summarized in Table 21 and Table 22 for TRACE-SUSA and TRACE-DAKOTA, respectively.

As mentioned above the average error is 4.66 % which is lower than for the single-phase case. Considering the complexity of two phase flow and the connected challenge in measuring pressures, the opposite would be expected. A reason for the lower average error in two phase flow can be the definition of the pressure drop. In single-phase flow the pressure drop is defined as the difference of the absolute pressures minus the difference of the geodetic pressure term, which involves the density. Therefore, considering the pure formalism and definition of the pressure drop it is more complex in single-phase flow than in two phase flow where only the difference of the absolute pressures is considered. In addition, the single-phase pressure drop is between 1000 and 30000 Pa. Especially at low pressure drop values the error is large which is connected to, on the one hand, the insensitivity of measurement devises at very low quantities and on the other hand the pronounced impact of a mismatch between measurement position and position of calculation. Due to the rather coarse nodalization in TRACE the pressure drop can only be calculated in approx. 15 cm increments.

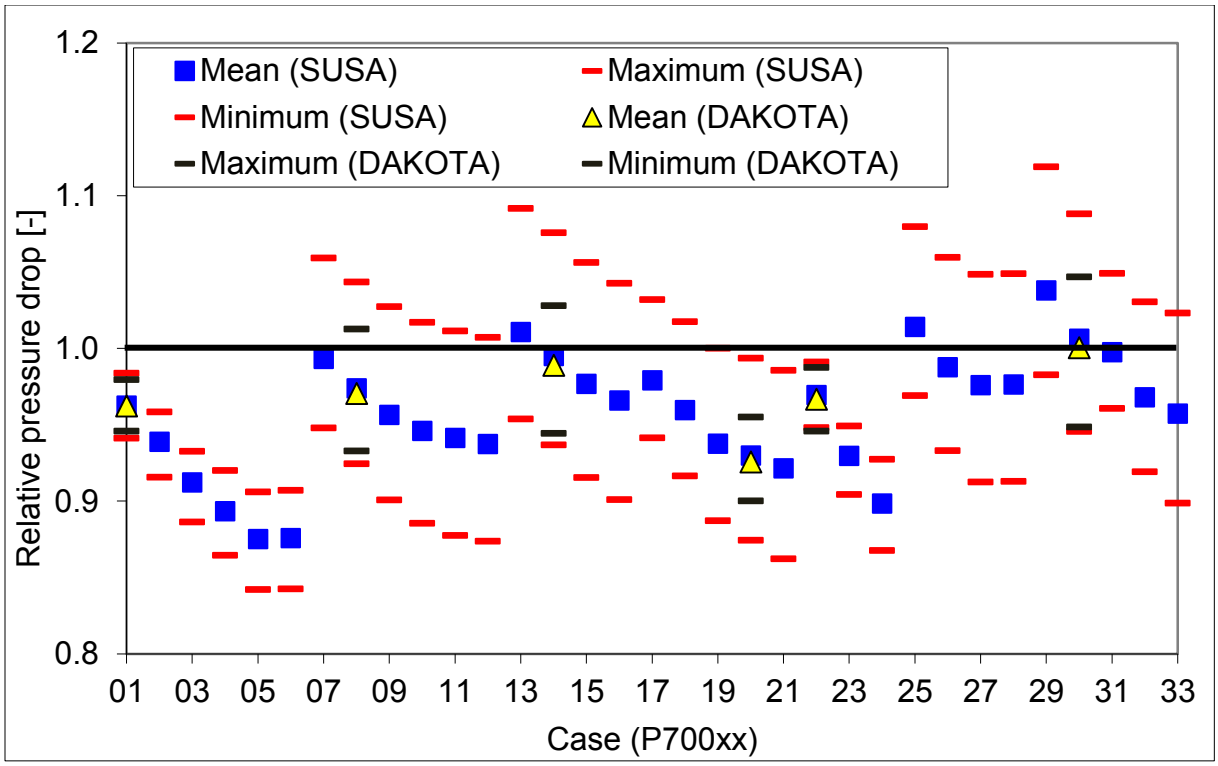

Figure 68 Comparison of the Experimental and Predicted Pressure Drops for the Two-Phase Flow Cases in Relative Values

Table 21 Results of the Uncertainty Analysis for the Two-Phase flow Pressure Drops with TRACE-SUSA

Case	Ex [Pa]	Mean [Pa]	Max [Pa]	Min [Pa]	SD [Pa]	Error [%]
P60001	27400	26376	26955	25788	264	-3.74
P60002	27020	25368	25892	24741	254	-6.12
P60003	27220	24833	25385	24122	283	-8.77
P60004	28100	25104	25852	24293	340	-10.66
P60005	29160	25518	26419	24551	398	-12.49
P60006	29260	25626	26538	24648	402	-12.42
P60007	57890	57494	61313	54877	1413	-0.68
P60008	65720	64000	68566	60755	1732	-2.62
P60009	78590	75174	80735	70791	2195	-4.35
P60010	93230	88199	94808	82549	2680	-5.40
P60011	106720	100465	107939	93651	3084	-5.86
P60012	107560	100824	108334	93981	3097	-6.26
P60013	79710	80561	87004	76017	2404	1.07
P60014	91270	90818	98174	85491	2817	-0.50
P60015	113970	111316	120364	104329	3596	-2.33
P60016	136510	131850	142309	122993	4271	-3.41
P60017	46540	45562	48022	43815	908	-2.10
P60018	51050	48982	51934	46781	1116	-4.05
P60019	60110	56361	60109	53328	1471	-6.24
P60020	68830	64003	68386	60185	1777	-7.01

Case	Ex [Pa]	Mean [Pa]	Max [Pa]	Min [Pa]	SD [Pa]	Error [%]
P60021	78760	72566	77622	67899	2092	-7.86
P60022	26830	26008	26587	25435	262	-3.06
P60023	26380	24523	25037	23853	265	-7.04
P60024	27550	24751	25548	23905	354	-10.16
P60025	54660	55427	59016	52968	1311	1.40
P60026	70060	69198	74237	65362	1952	-1.23
P60027	92410	90190	96885	84328	2734	-2.40
P60028	92460	90276	96984	84407	2738	-2.36
P60029	73550	76341	82295	72269	2187	3.79
P60030	100770	101399	109640	95273	3216	0.62
P60031	44320	44214	46496	42579	840	-0.24
P60032	54320	52585	55971	49930	1306	-3.19
P60033	68440	65509	70025	61503	1838	-4.28

Table 22 Results of the Uncertainty Analysis for the Two-Phase Flow Pressure Drops with TRACE-DAKOTA

Case	Ex [Pa]	Mean [Pa]	Max [Pa]	Min [Pa]	SD [Pa]	Error [%]
P60001	27400	26369	26840	25915	196	-3.76
P60008	65720	63774	66553	61297	1098	-2.96
P60014	91270	90257	93822	86191	1835	-1.11
P60020	68830	63712	65725	61955	960	-7.44
P60022	26830	25934	26492	25377	236	-3.34
P60030	100770	100810	105480	95578	2086	0.04

The sensitivity coefficients are plotted in Figure 69 (TRACE-SUSA) and Figure 70 (TRACE-DAKOTA). In general, for the SUSA cases, the sensitivity coefficients for the different parameters are almost at similar values for all 33 cases. The fluctuations between the cases are related to the varying input and boundary conditions. The only exception is the inlet temperature which has (relative high) negative values for cases 1 - 6 and 22 - 24 but for the rest of the cases positive values of approximately 0.3 - 0.4. For the named cases, the plot of the boundary conditions shows that they are characterized by a low mass flow rate and low power. Therefore, the impact of their variation is losing against the impact of the inlet sub cooling (inlet temperature) which is almost constant for all cases. The highest values are calculated again for the hydraulic diameter and the friction factor, followed by the inlet temperature and the K-factor for the spacer grid.

The sensitivity coefficients of the TRACE-DAKOTA analysis indicate a slightly different relation between the parameters. For the inlet temperature exclusively high positive values, > 0.6, are calculated, even for case 1 for which the TRACE-SUSA analysis predicted a value of – 0.64. That means that for the TRACE-SUSA analysis the pressure drop would increase with decreasing inlet temperature. For TRACE-DAKOTA the influence of the inlet temperature would be in the opposite direction; increasing inlet temperature yield higher pressure drop. One explanation could be the absence of the friction factor and the hydraulic diameter in the TRACE-DAKOTA analysis, which amplifies the influence of the inlet temperature compared to the TRACE-SUSA analysis. The ranks of the uncertain parameters are plotted in Figure 71 and Figure 72 for TRACE-SUSA and TRACE-DAKOTA, respectively.

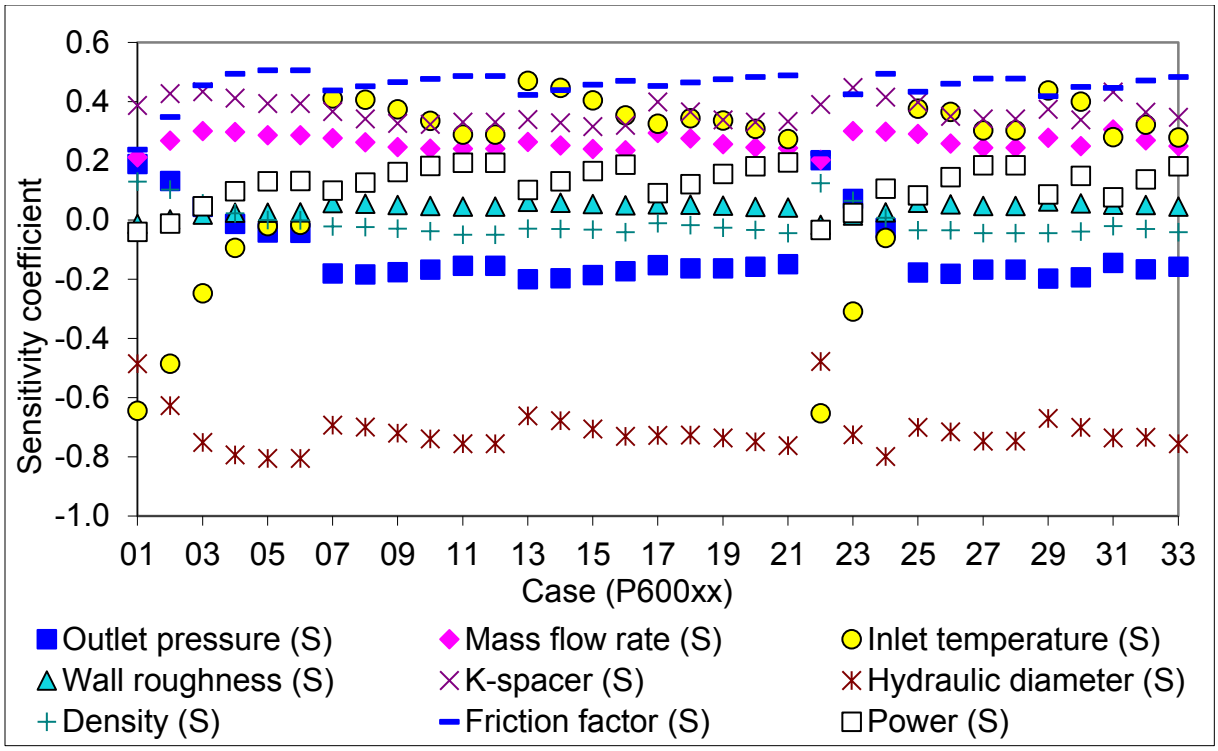

Figure 69 Sensitivity Coefficients for the Two-Phase Flow Pressure Drop Analysis with TRACE-SUSA

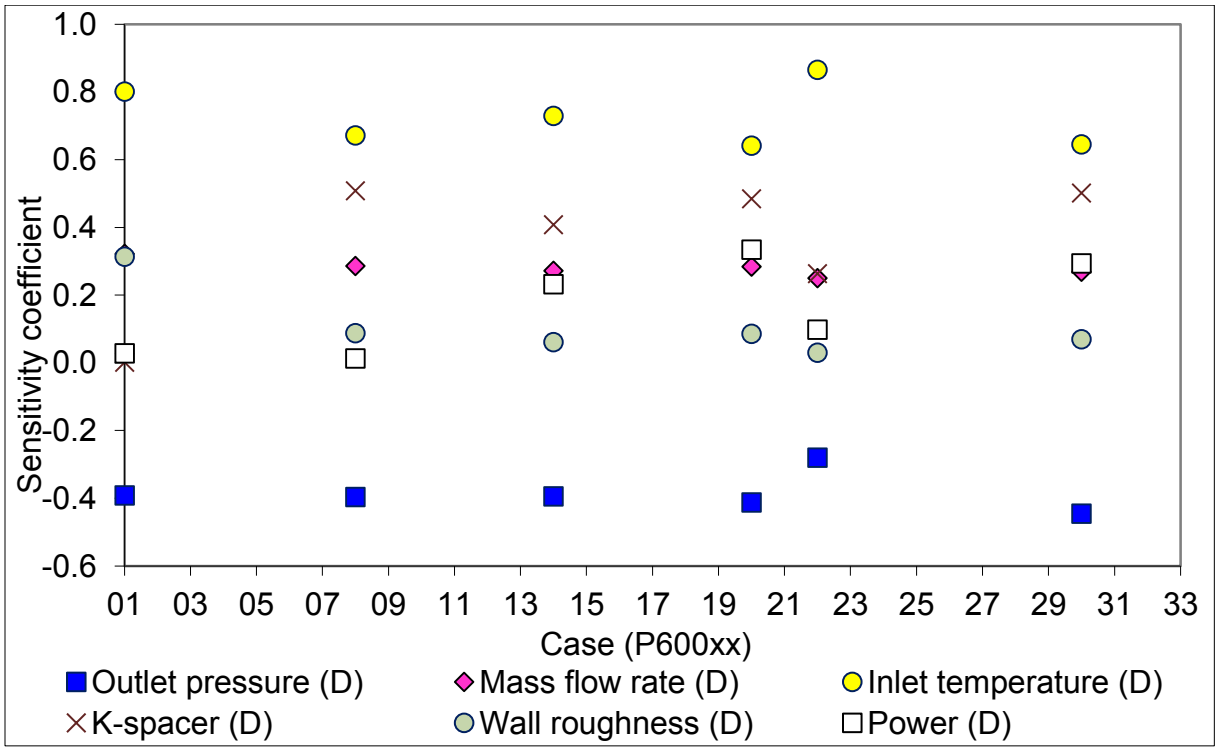

Figure 70 Sensitivity Coefficients for the Two-Phase Flow Pressure Drop Analysis with TRACE-DAKOTA

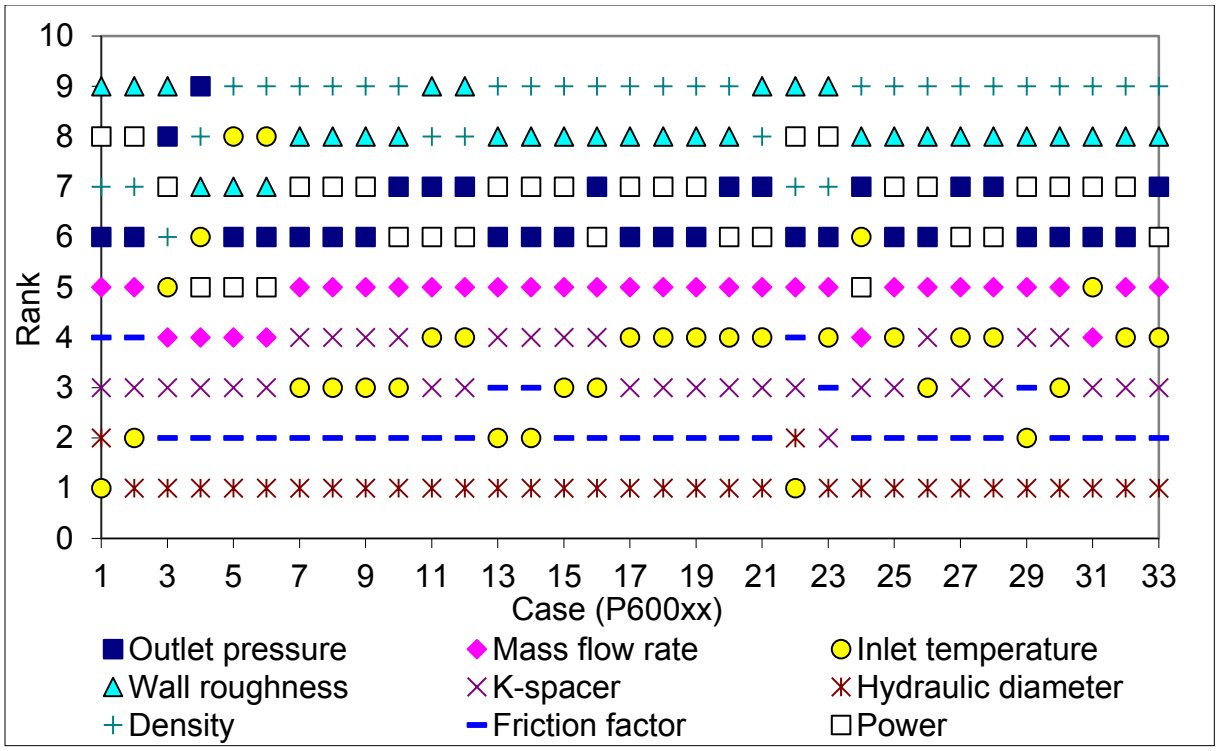

Figure 71 Ranking of the Uncertain Parameters for the Two-Phase Flow Pressure Drop Analysis with TRACE-SUSA

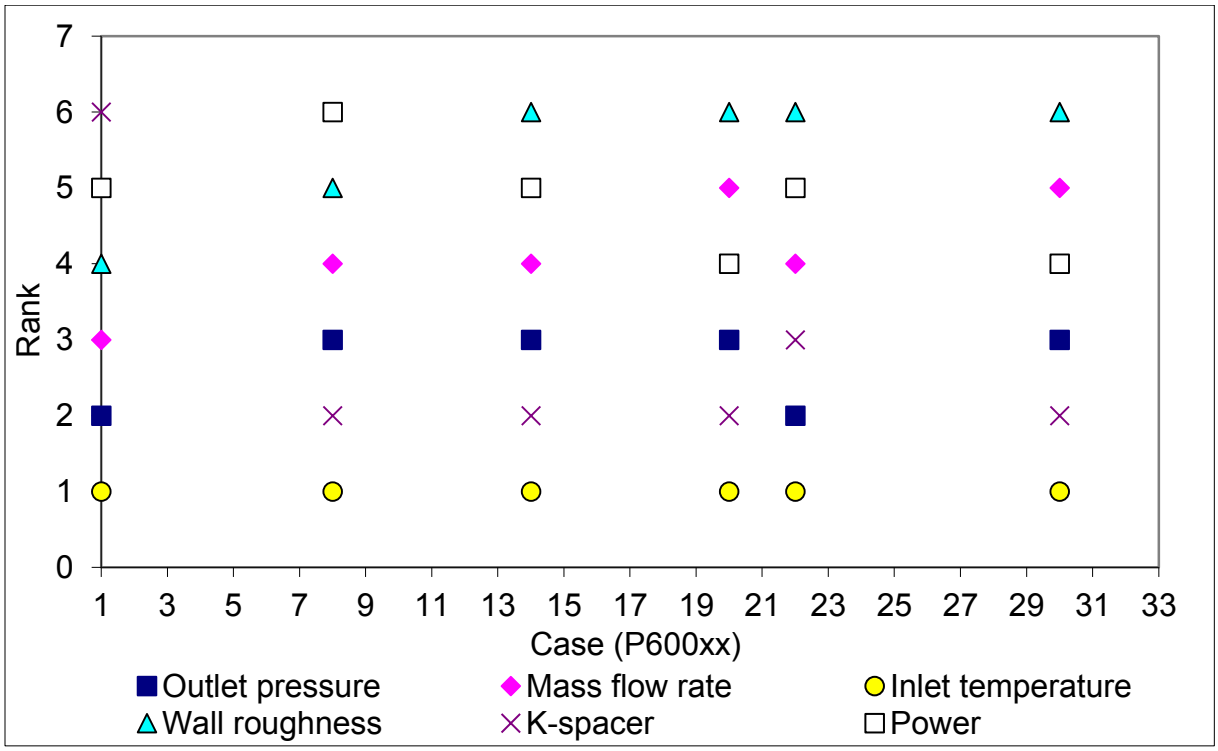

Figure 72 Ranking of the Uncertain Parameters for the Two-Phase Flow Pressure Drop Analysis with TRACE-DAKOTA

Table 23 Pearson's Momentum Correlation Coefficients for the Two-Phase Flow Pressure Drop Cases with TRACE-SUSA

	Outlet pressure	Mass flow rate	Inlet temperature	Wall roughness	K-spacer	Hydraulic diameter	Density	Friction factor	Power
P60001	0.189	0.212	-0.645	-0.013	0.387	-0.486	0.129	0.237	-0.040
P60002	0.131	0.268	-0.485	0.002	0.427	-0.627	0.102	0.348	-0.012
P60003	0.044	0.300	-0.248	0.019	0.434	-0.751	0.057	0.455	0.047
P60004	-0.013	0.297	-0.094	0.025	0.412	-0.794	0.022	0.494	0.098
P60005	-0.042	0.286	-0.020	0.025	0.393	-0.806	-0.000	0.505	0.131
P60006	-0.044	0.286	-0.017	0.025	0.393	-0.806	-0.002	0.506	0.132
P60007	-0.181	0.277	0.411	0.057	0.366	-0.693	-0.022	0.438	0.099
P60008	-0.184	0.263	0.406	0.055	0.342	-0.700	-0.024	0.452	0.126
P60009	-0.177	0.247	0.374	0.051	0.327	-0.720	-0.030	0.466	0.162
P60010	-0.167	0.241	0.335	0.048	0.323	-0.739	-0.038	0.477	0.183
P60011	-0.155	0.241	0.289	0.045	0.331	-0.756	-0.050	0.486	0.194
P60012	-0.155	0.241	0.289	0.045	0.331	-0.756	-0.050	0.486	0.194
P60013	-0.200	0.263	0.470	0.061	0.339	-0.662	-0.029	0.423	0.102
P60014	-0.197	0.252	0.447	0.058	0.328	-0.678	-0.030	0.439	0.131
P60015	-0.186	0.240	0.404	0.054	0.316	-0.706	-0.033	0.457	0.165
P60016	-0.173	0.235	0.353	0.050	0.312	-0.731	-0.041	0.470	0.187
P60017	-0.153	0.294	0.325	0.052	0.398	-0.728	-0.011	0.453	0.090
P60018	-0.163	0.276	0.344	0.051	0.365	-0.727	-0.017	0.465	0.121
P60019	-0.164	0.256	0.336	0.048	0.338	-0.737	-0.026	0.476	0.156
P60020	-0.158	0.245	0.308	0.044	0.331	-0.750	-0.034	0.483	0.181
P60021	-0.149	0.243	0.273	0.042	0.333	-0.763	-0.045	0.489	0.194
P60022	0.202	0.203	-0.653	-0.017	0.390	-0.479	0.124	0.225	-0.033
P60023	0.071	0.300	-0.309	0.015	0.447	-0.726	0.064	0.424	0.024
P60024	-0.027	0.298	-0.061	0.026	0.415	-0.799	0.008	0.494	0.105
P60025	-0.177	0.291	0.376	0.058	0.398	-0.701	-0.034	0.433	0.083
P60026	-0.182	0.259	0.365	0.053	0.351	-0.716	-0.035	0.460	0.144
P60027	-0.167	0.244	0.302	0.048	0.342	-0.747	-0.045	0.478	0.185
P60028	-0.167	0.245	0.302	0.048	0.342	-0.747	-0.045	0.478	0.184
P60029	-0.198	0.278	0.438	0.062	0.374	-0.670	-0.044	0.418	0.087
P60030	-0.193	0.250	0.400	0.056	0.338	-0.701	-0.039	0.450	0.149
P60031	-0.145	0.306	0.279	0.052	0.432	-0.736	-0.021	0.447	0.077
P60032	-0.167	0.269	0.322	0.051	0.365	-0.734	-0.030	0.471	0.138
P60033	-0.159	0.250	0.279	0.045	0.347	-0.756	-0.041	0.483	0.181

Table 24 Pearson's Momentum Correlation Coefficients for the Two-Phase Flow Pressure Drop Cases with TRACE-DAKOTA

	Outlet pressure	Mass flow rate	Inlet temperature	Wall roughness	K-spacer	Hydraulic diameter	Density	Friction factor	Power
P60001	-0.391	0.322	0.802	0.314	0.002	not included			0.029
P60008	-0.396	0.287	0.672	0.087	0.509				0.013
P60014	-0.394	0.272	0.730	0.061	0.408				0.232
P60020	-0.413	0.284	0.641	0.086	0.485				0.334
P60022	-0.280	0.250	0.865	0.030	0.263				0.098
P60030	-0.445	0.269	0.646	0.070	0.502				0.294

6.4 Void Fraction Analyses

The third parameter which is subject of the presented investigation is the void fraction measurements. As mentioned in sub section 3.5 the void fraction has been measured at four different positions. At the first three positions (Z1 = 0.682 m; Z2 = 1.706 m; Z3 = 2.730 m) X-ray densitometers where used while at the fourth and highest position (Z4 = 3.758 m) an X-ray CT scanner was used.

In an investigation performed by Glück [28], the reliability of the X-ray densitometer void fraction measurements have been discussed. Due to the used measurement technique, only a limited volume/layer of the bundle cross section was scanned. That yield to an under prediction of the void fraction during bubbly flow since the void is concentrated near the wall. With slug flow, the void is gathered in the center of the sub channel and the measurement gives higher values than expected. Glück proposed correlations to correct the void fraction measurements' depending which assembly type is used. Since only assembly type four/C2A is used only the respective correlation will be depicted (void fraction in %).

$$\alpha_{\text{corrected}} = \frac{\alpha_{\text{measured}}}{-0.001 \cdot \alpha_{\text{measured}} + 1.167} \tag{62}$$

Due to the different measurement procedure with the CT scanner, a correction was not necessary. The scanners employ 512 detectors with the scanner rotation around the tube. Compared to the rather simple design of the X-ray densitometers, a high spatial resolution was achieved with a pixel size of 0.3 x 0.3 mm.

The input and boundary combination of 86 considered cases are depicted in Figure 73. In addition, Table 25 shows the input and boundary conditions for each case.

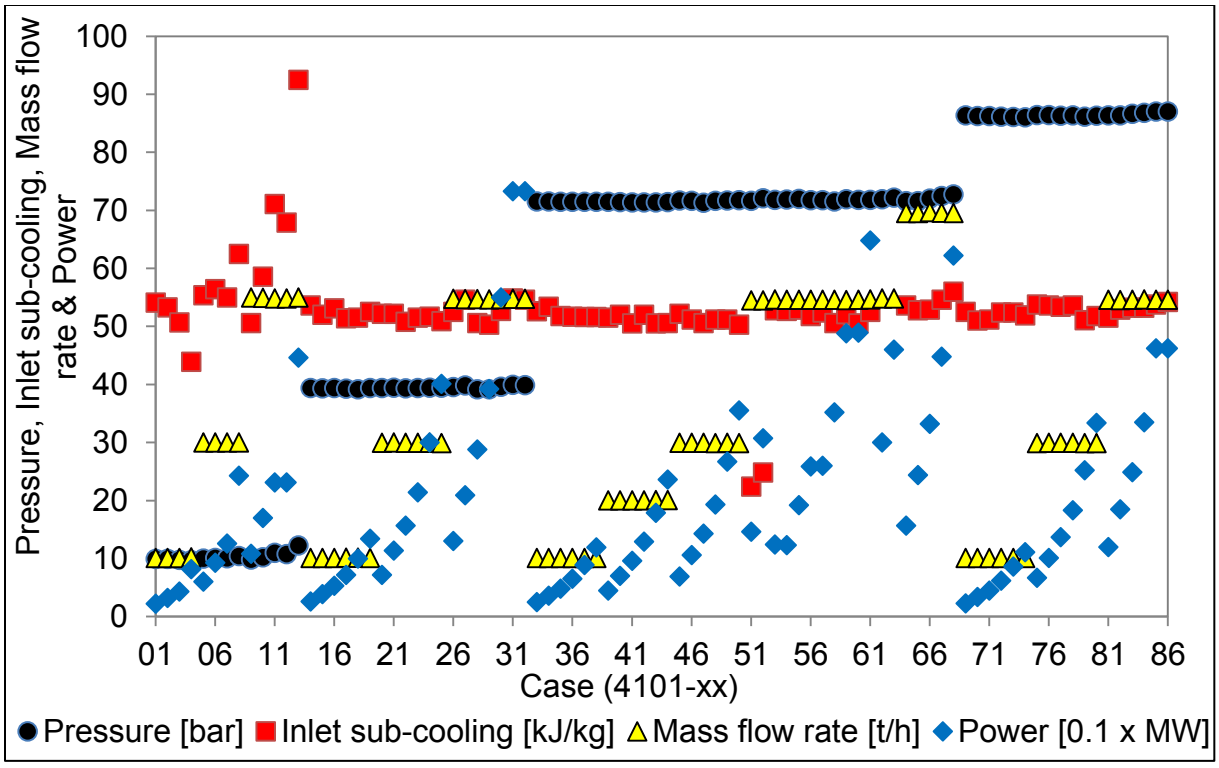

Figure 73 Input and Boundary Conditions for the Steady State Void Fraction Measurements

Table 25 Input and Boundary Conditions for the Steady State Void Fraction Measurements

Case	Outlet pressure [bar]	Inlet sub-cooling [kJ/kg]	Mass flow rate [t/h]	Power [0.1 x MW]
4101-01	9.95	54.1	10.12	2.20
4101-02	9.94	53.3	10.12	3.20
4101-03	9.78	50.7	10.12	4.30
4101-04	9.73	43.9	10.20	8.20
4101-05	10.02	55.4	30.00	6.00
4101-06	10.08	56.4	30.01	9.30
4101-07	10.06	55.0	30.00	12.60
4101-08	10.42	62.5	30.02	24.30
4101-09	9.84	50.6	54.99	10.80
4101-10	10.21	58.6	54.95	17.00
4101-11	10.96	71.1	54.85	23.10
4101-12	10.79	67.9	54.80	23.10
4101-13	12.24	92.5	55.01	44.60
4101-14	39.37	53.6	10.11	2.60
4101-15	39.32	52.0	10.10	3.90
4101-16	39.36	53.1	10.13	5.30
4101-17	39.25	51.4	10.14	7.20
4101-18	39.19	51.5	10.14	10.00
4101-19	39.36	52.5	10.12	13.40

Case	Outlet pressure [bar]	Inlet sub-cooling [kJ/kg]	Mass flow rate [t/h]	Power [0.1 x MW]
4101-20	39.40	52.2	29.98	7.20
4101-21	39.42	52.2	29.99	11.40
4101-22	39.31	50.8	29.97	15.70
4101-23	39.37	51.5	29.97	21.40
4101-24	39.43	51.7	29.93	30.00
4101-25	39.43	50.9	29.92	40.10
4101-26	39.55	52.5	54.78	13.00
4101-27	39.82	54.6	54.73	20.90
4101-28	39.18	50.6	54.71	28.80
4101-29	39.17	50.3	54.68	39.20
4101-30	39.61	52.7	54.71	55.00
4101-31	39.91	54.8	54.75	73.30
4101-32	39.88	54.6	54.77	73.30
4101-33	71.52	52.6	10.12	2.50
4101-34	71.55	53.4	10.12	3.60
4101-35	71.50	51.8	10.12	4.80
4101-36	71.45	51.7	10.10	6.50
4101-37	71.46	51.6	10.12	8.90
4101-38	71.50	51.6	10.12	11.90
4101-39	71.47	51.5	20.05	4.50
4101-40	71.44	52.0	20.03	7.00
4101-41	71.34	50.5	20.03	9.60
4101-42	71.38	52.0	20.03	12.90
4101-43	71.38	50.5	20.06	17.90
4101-44	71.41	50.6	20.09	23.60
4101-45	71.67	52.2	29.94	6.90
4101-46	71.63	51.2	29.93	10.60
4101-47	71.32	50.6	29.94	14.30
4101-48	71.65	51.2	29.91	19.30
4101-49	71.68	51.2	29.94	26.70
4101-50	71.76	50.3	29.91	35.50
4101-51	71.62	22.4	54.52	14.60
4101-52	72.09	24.8	54.52	30.70
4101-53	71.81	52.8	54.65	12.40
4101-54	71.86	52.7	54.63	12.30
4101-55	71.95	52.9	54.59	19.20
4101-56	71.75	51.8	54.62	25.90
4101-57	71.74	52.4	54.58	26.00
4101-58	71.52	50.6	54.58	35.20
4101-59	71.90	52.1	54.57	48.80
4101-60	71.78	50.5	54.62	48.90
4101-61	71.80	52.5	54.65	64.80
4101-62	71.90	127.0	54.84	30.00
4101-63	72.17	128.0	54.80	46.00
4101-64	71.59	53.6	69.53	15.70
4101-65	71.60	52.8	69.53	24.40
4101-66	72.02	52.9	69.69	33.20
4101-67	72.48	54.6	69.58	44.80

Case	Outlet pressure [bar]	Inlet sub-cooling [kJ/kg]	Mass flow rate [t/h]	Power [0.1 x MW]
4101-68	72.75	56.0	69.56	62.20
4101-69	86.38	52.5	10.08	2.30
4101-70	86.28	51.0	10.08	3.40
4101-71	86.28	51.2	10.09	4.50
4101-72	86.17	52.4	10.08	6.20
4101-73	86.11	52.4	10.10	8.60
4101-74	86.06	51.9	10.10	11.10
4101-75	86.41	53.8	29.88	6.70
4101-76	86.44	53.6	29.93	10.10
4101-77	86.33	53.4	29.93	13.70
4101-78	86.38	53.6	29.93	18.30
4101-79	86.14	51.1	29.89	25.20
4101-80	86.31	51.8	29.88	33.40
4101-81	86.36	51.5	54.60	12.00
4101-82	86.35	52.9	54.54	18.50
4101-83	86.66	53.2	54.62	24.90
4101-84	86.80	53.2	54.66	33.50
4101-85	87.00	53.8	54.61	46.20
4101-86	87.05	54.2	54.59	46.20

As Figure 73 indicates, a scheme can be identified for the parameter combinations. The inlet sub-cooling is around 50 kJ/kg in the most cases. Only a few cases show an inlet sub-cooling of more than 100 kJ/kg. The pressure is divided into four sections, section 1 around 10 bar; section 2 around 40 bar; section 3 around 71 bar and section 4 around 86 bar. The mass flow rate is between 10 and 70 kg/s while the power ranges, without showing a pattern or routine, between 0.2 and 7.4 MW.

The calculated void fractions at the exit for each of the 86 cases are compared to the experimental values in Figure 74. It can be seen that the agreement is very good no matter it is in the low or high void fraction range. The relative error is plotted in Figure 75 for each case. A tendency to over predict the measured data can be seen with an average error of 3.72 %. Also, the errors based on the reference calculations, see Figure 76 are lower at higher void fractions. As for the previous cases, the uncertainty and sensitivity analysis was performed with TRACE and SUSA for all cases while for TRACE and DAKOTA only six of them were performed. The results in terms of absolute values are shown in Figure 77. One clear tendency can be deduced from that graph; the higher the void fraction the lower the uncertainty. At lower void fractions the results are spread over a wider range than at higher void fractions. That might be related to the flow regime which is present at the different void fractions. At lower void fractions the regime is bubbly slug flow while at higher void fractions annular mist flow is present. The differences in calculating the interfacial friction and their sensitivity to the parameters which are varied are most likely the reason for the observed behavior.

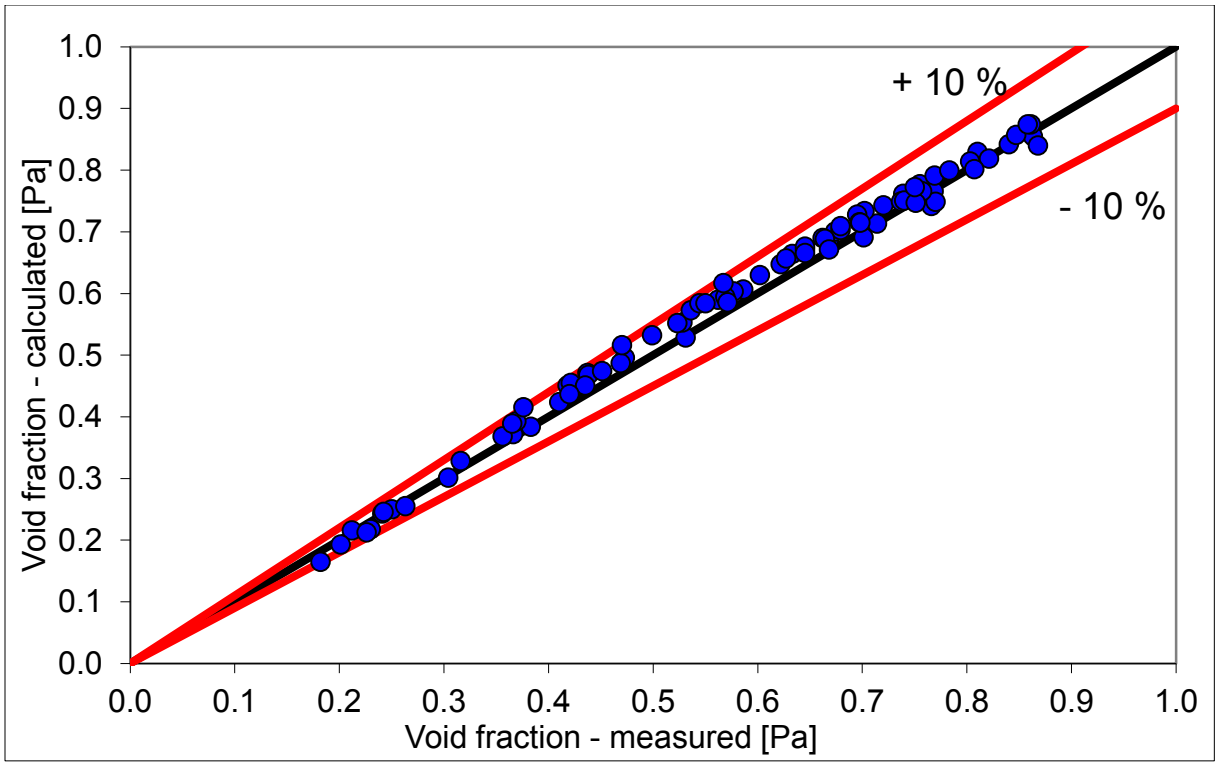

Figure 74 Calculated versus Measured Outlet Void Fractions

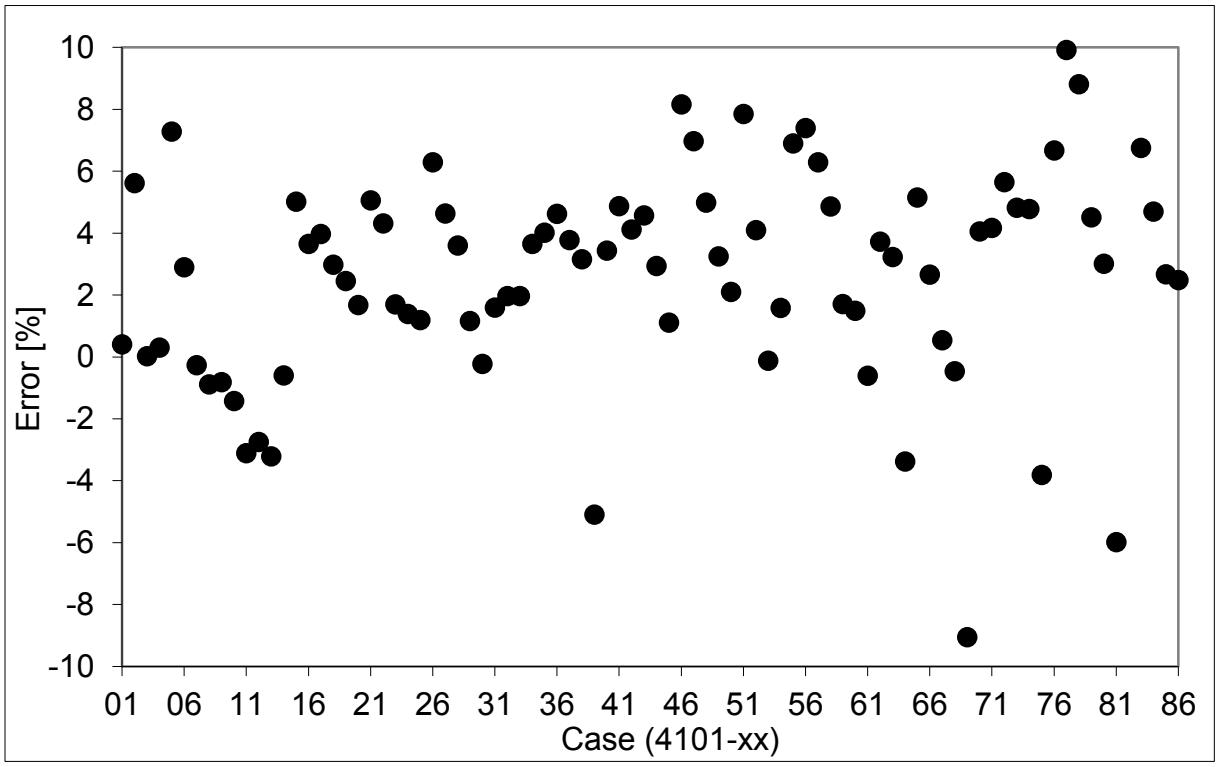

Figure 75 Percental Error of the Reference Values Compared to the Experimental Data for the Outlet Void Fraction

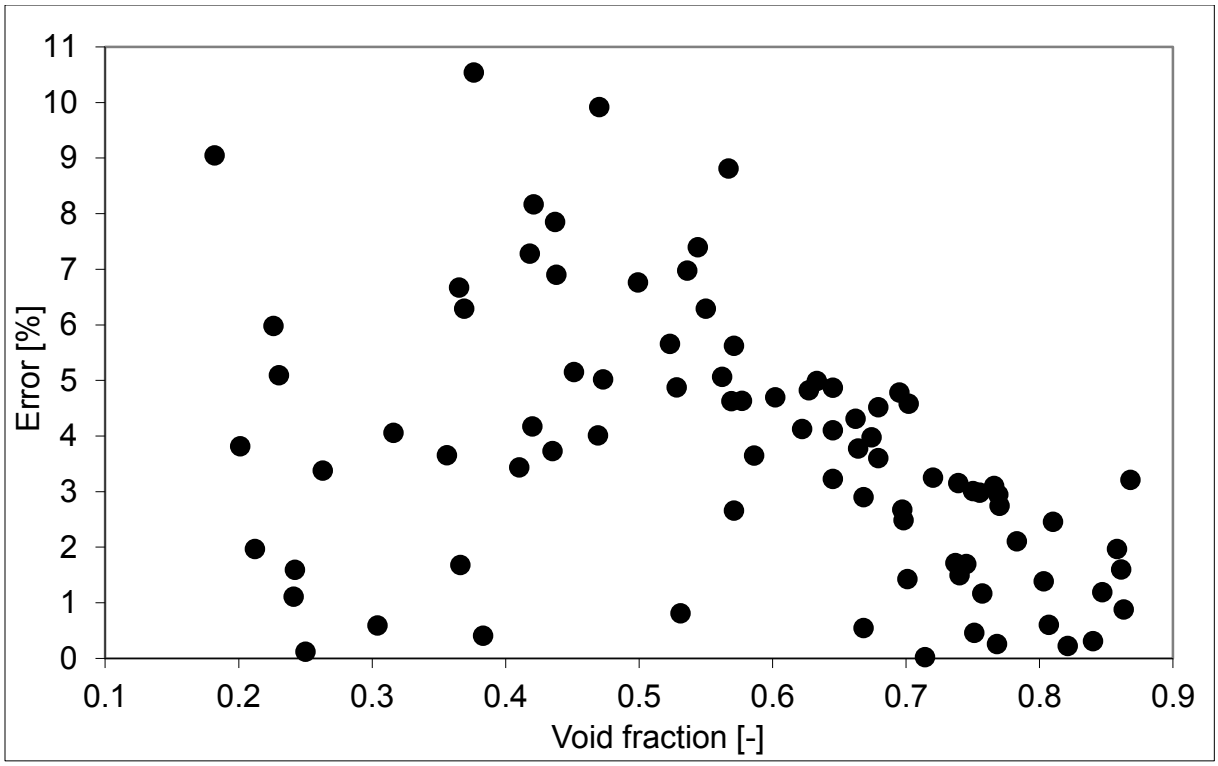

Figure 76 Error as a Function of the Void Fraction

Due to the complexity of the models for wall and interfacial drag it is challenging to determine which input and boundary parameter is influencing parameters related to the two different flow regimes a priori. A plausible explanation could be that at low void fractions the system is more sensitive to variations than at higher void fractions. A more quantitative explanation of the behavior can be given after the sensitivity analysis.

The relative void fractions along with the uncertainty band for TRACE-SUSA and TRACE-DAKOTA is given in Figure 78. The tendency to over predict the outlet void fraction can be seen here very clearly. One can also see that the uncertainty band is wider for the TRACE-DAKOTA cases. This is rather unexpected since less parameters are used in the uncertainty analysis.

The results of the uncertainty analysis by means of mean, maximal and minimal value together with the standard deviation and the relative error are also given in Table 26 and in Table 27 for TRACE-SUSA and TRACE-DAKOTA, respectively.

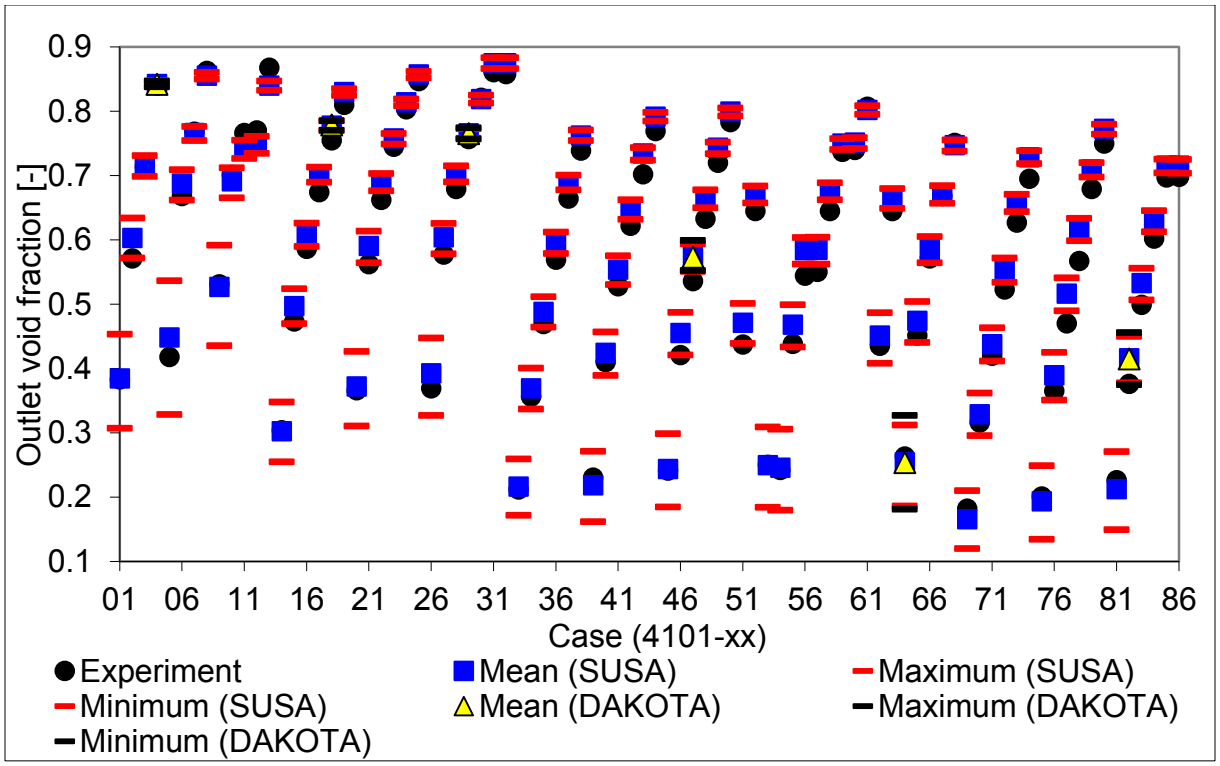

Figure 77 Comparison of the Experimental and Outlet Void Fractions in Absolute Values

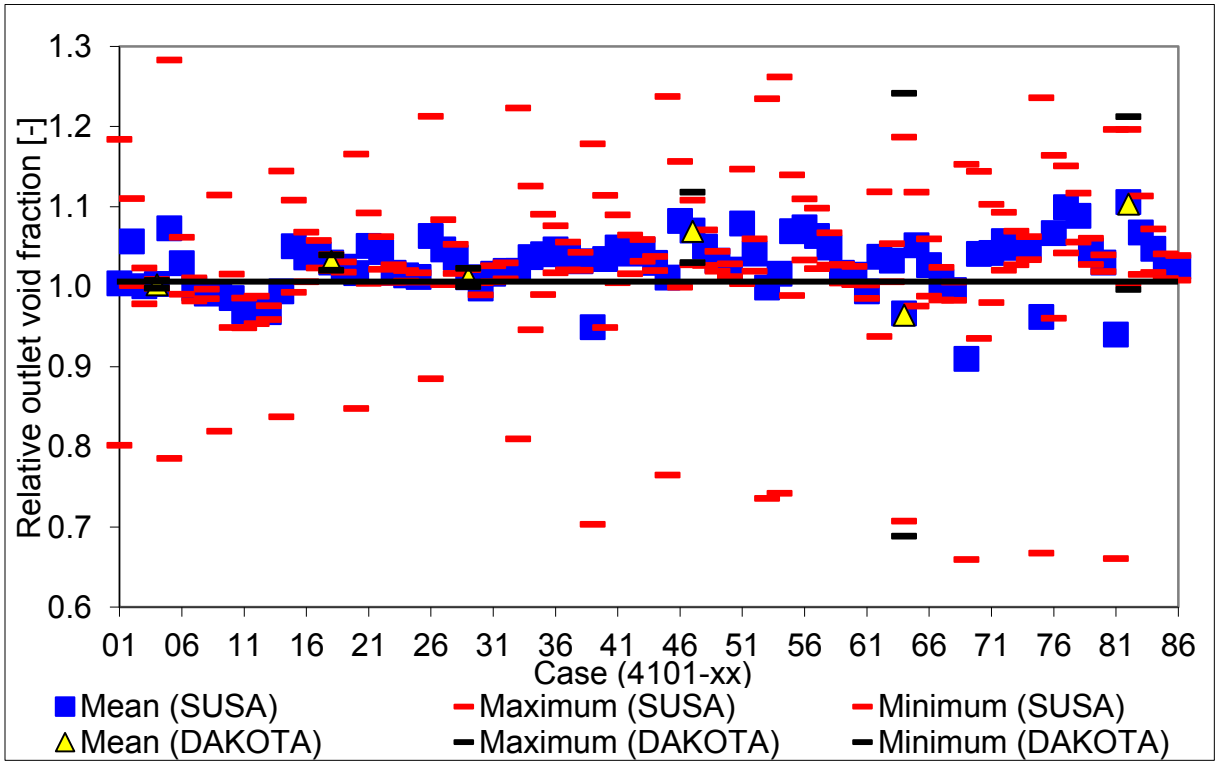

Figure 78 Comparison of the Experimental and Predicted Outlet Void Fractions in Relative Values

Table 26 Results of the Uncertainty Analysis for the Outlet Void Fraction with TRACE-SUSA

Case	Ex [-]	Mean [-]	Max [-]	Min [-]	SD [-]	Error [%]
4101-01	0.383	0.385	0.453	0.307	0.036	0.41
4101-02	0.571	0.603	0.634	0.572	0.015	5.62
4101-03	0.714	0.714	0.731	0.699	0.007	0.02
4101-04	0.840	0.843	0.847	0.838	0.002	0.31
4101-05	0.418	0.448	0.536	0.328	0.052	7.28
4101-06	0.668	0.687	0.709	0.662	0.011	2.90
4101-07	0.768	0.766	0.776	0.754	0.005	-0.26
4101-08	0.863	0.855	0.860	0.850	0.002	-0.88
4101-09	0.531	0.527	0.592	0.435	0.039	-0.81
4101-10	0.701	0.691	0.712	0.665	0.011	-1.43
4101-11	0.766	0.742	0.755	0.727	0.007	-3.10
4101-12	0.770	0.749	0.761	0.734	0.006	-2.75
4101-13	0.868	0.840	0.847	0.832	0.003	-3.21
4101-14	0.304	0.302	0.348	0.255	0.023	-0.59
4101-15	0.473	0.497	0.524	0.470	0.013	5.02
4101-16	0.586	0.607	0.626	0.590	0.008	3.65
4101-17	0.674	0.701	0.713	0.690	0.005	3.97
4101-18	0.755	0.778	0.785	0.770	0.003	2.98
4101-19	0.810	0.830	0.835	0.824	0.002	2.46
4101-20	0.366	0.372	0.427	0.310	0.029	1.68
4101-21	0.562	0.591	0.614	0.564	0.011	5.06
4101-22	0.662	0.691	0.703	0.676	0.006	4.31
4101-23	0.745	0.758	0.765	0.749	0.004	1.70
4101-24	0.803	0.814	0.819	0.808	0.002	1.39
4101-25	0.847	0.857	0.862	0.852	0.002	1.19
4101-26	0.369	0.392	0.447	0.327	0.030	6.29
4101-27	0.577	0.604	0.625	0.578	0.011	4.63
4101-28	0.679	0.704	0.715	0.690	0.006	3.61
4101-29	0.757	0.766	0.773	0.758	0.004	1.17
4101-30	0.821	0.819	0.825	0.813	0.003	-0.22
4101-31	0.861	0.875	0.883	0.866	0.004	1.60
4101-32	0.858	0.875	0.883	0.866	0.004	1.97
4101-33	0.212	0.216	0.259	0.172	0.022	1.97
4101-34	0.356	0.369	0.401	0.337	0.015	3.66
4101-35	0.469	0.488	0.511	0.464	0.011	4.01
4101-36	0.569	0.595	0.612	0.579	0.007	4.63
4101-37	0.664	0.689	0.701	0.678	0.005	3.78
4101-38	0.739	0.762	0.771	0.754	0.003	3.16
4101-39	0.230	0.218	0.271	0.162	0.028	-5.10
4101-40	0.410	0.424	0.457	0.389	0.016	3.43
4101-41	0.528	0.554	0.575	0.531	0.010	4.87
4101-42	0.622	0.648	0.662	0.632	0.007	4.12
4101-43	0.702	0.734	0.743	0.724	0.004	4.58
4101-44	0.769	0.792	0.798	0.784	0.003	2.95
4101-45	0.241	0.244	0.298	0.184	0.029	1.11
4101-46	0.421	0.455	0.487	0.421	0.016	8.17
4101-47	0.536	0.573	0.594	0.551	0.010	6.97

Case	Ex [-]	Mean [-]	Max [-]	Min [-]	SD [-]	Error [%]
4101-48	0.633	0.665	0.678	0.650	0.006	4.99
4101-49	0.720	0.743	0.752	0.734	0.004	3.25
4101-50	0.783	0.800	0.805	0.793	0.003	2.11
4101-51	0.437	0.471	0.501	0.439	0.016	7.85
4101-52	0.645	0.671	0.684	0.658	0.006	4.10
4101-53	0.250	0.250	0.309	0.184	0.033	-0.12
4101-54	0.242	0.246	0.305	0.180	0.033	1.59
4101-55	0.438	0.468	0.499	0.433	0.016	6.90
4101-56	0.544	0.584	0.604	0.562	0.010	7.40
4101-57	0.550	0.585	0.604	0.562	0.01	6.29
4101-58	0.645	0.676	0.688	0.662	0.006	4.87
4101-59	0.737	0.750	0.757	0.740	0.004	1.71
4101-60	0.740	0.751	0.759	0.742	0.004	1.49
4101-61	0.807	0.802	0.809	0.795	0.003	-0.61
4101-62	0.435	0.451	0.487	0.408	0.017	3.73
4101-63	0.645	0.666	0.679	0.649	0.006	3.23
4101-64	0.263	0.254	0.312	0.186	0.033	-3.38
4101-65	0.451	0.474	0.504	0.440	0.016	5.15
4101-66	0.571	0.586	0.605	0.564	0.010	2.66
4101-67	0.668	0.672	0.684	0.657	0.006	0.55
4101-68	0.751	0.748	0.755	0.738	0.004	-0.46
4101-69	0.182	0.166	0.210	0.120	0.024	-9.05
4101-70	0.316	0.329	0.362	0.296	0.016	4.06
4101-71	0.420	0.438	0.463	0.412	0.012	4.17
4101-72	0.523	0.553	0.571	0.534	0.008	5.66
4101-73	0.627	0.657	0.670	0.644	0.006	4.82
4101-74	0.695	0.728	0.738	0.718	0.004	4.78
4101-75	0.201	0.193	0.248	0.134	0.030	-3.81
4101-76	0.365	0.389	0.425	0.351	0.018	6.67
4101-77	0.470	0.517	0.541	0.490	0.012	9.92
4101-78	0.567	0.617	0.633	0.599	0.008	8.81
4101-79	0.679	0.710	0.720	0.698	0.005	4.52
4101-80	0.750	0.773	0.780	0.764	0.003	3.01
4101-81	0.226	0.213	0.270	0.150	0.032	-5.98
4101-82	0.376	0.416	0.450	0.377	0.018	10.54
4101-83	0.499	0.533	0.556	0.507	0.012	6.76
4101-84	0.602	0.630	0.645	0.613	0.007	4.70
4101-85	0.697	0.716	0.725	0.704	0.005	2.67
4101-86	0.698	0.715	0.725	0.704	0.005	2.48

Table 27 Results of the Uncertainty Analysis for the Outlet Void Fraction with TRACE DAKOTA

Case	Ex [-]	Mean [-]	Max [-]	Min [-]	SD [-]	Error [%]
4101-04	0.840	0.842	0.846	0.838	0.002	0.25
4101-18	0.755	0.779	0.785	0.770	0.003	3.14
4101-29	0.757	0.765	0.774	0.757	0.004	1.11
4101-47	0.536	0.573	0.599	0.552	0.010	6.91
4101-64	0.263	0.254	0.327	0.181	0.033	-3.56
4101-82	0.376	0.415	0.456	0.375	0.020	10.31

The sensitivity coefficients according to Pearson's momentum correlation coefficient are plotted in Figure 79 for TRACE-SUSA and in Figure 80 for TRACE-DAKOTA. For the TRACE-SUSA plot, a repeating pattern can be seen which is related to combination of the input and boundary condition parameters. It is clearly visible, also for the TRACE-DAKOTA, that the inlet temperature, which represents the inlet sub-cooling, is the input parameter of highest importance. Besides the inlet temperature, the power is also of importance but sensitivity coefficients range from almost zero to values up to 0.6. At low void fractions the values for the mass flow rate are close to zero while for high void fractions the values are close to -0.4, meaning that an increase of the mass flow rate always results in a decrease of the void fraction. Parameters like the friction factor, hydraulic diameter or K factor have almost no impact on the outlet void fraction.

In order to evaluate the reason why at low void fractions the uncertainty band is wider than at higher values, the sensitivity coefficients for the inlet temperature and the power are plotted as a function of the void fraction, see Figure 81. It can be seen that at low void fractions the sensitivity coefficient for the inlet temperature is very high, around 0.9 while the power coefficient is very low. With increasing void fraction the sensitivity coefficient for the inlet temperature decrease to values of around 0.5 at a void fraction of > 0.8. The coefficient for the power is increasing linearly with increasing void fractions, going from < 0.1 at a void fraction of 0.15 to values of around 0.6 at void fractions of around 0.9. Since the variation is almost constant, ± 1.5 K for the inlet temperature and ± 1 % for the power, the change of the absolute values is getting more pronounced with higher temperatures and powers. With increasing assembly power the outlet void fraction is increased. That means that a variation of 1% of an already high assembly power will result in much more additional energy which is released in the systems as 1 % at a low assembly power.

At low void fractions, the variation of the inlet sub-cooling (inlet temperature) has more influence on the resulting void fraction compared to higher void fractions because the inlet sub-cooling is the only parameter which affects the results according to the sensitivity study.

The ranks of the input and boundary condition parameters are given in Figure 82 and Figure 83 for TRACE-SUSA and TRACE-DAKOTA, respectively.

For the sake of completeness the individual sensitivity coefficients for each parameter are listed in Table 28.

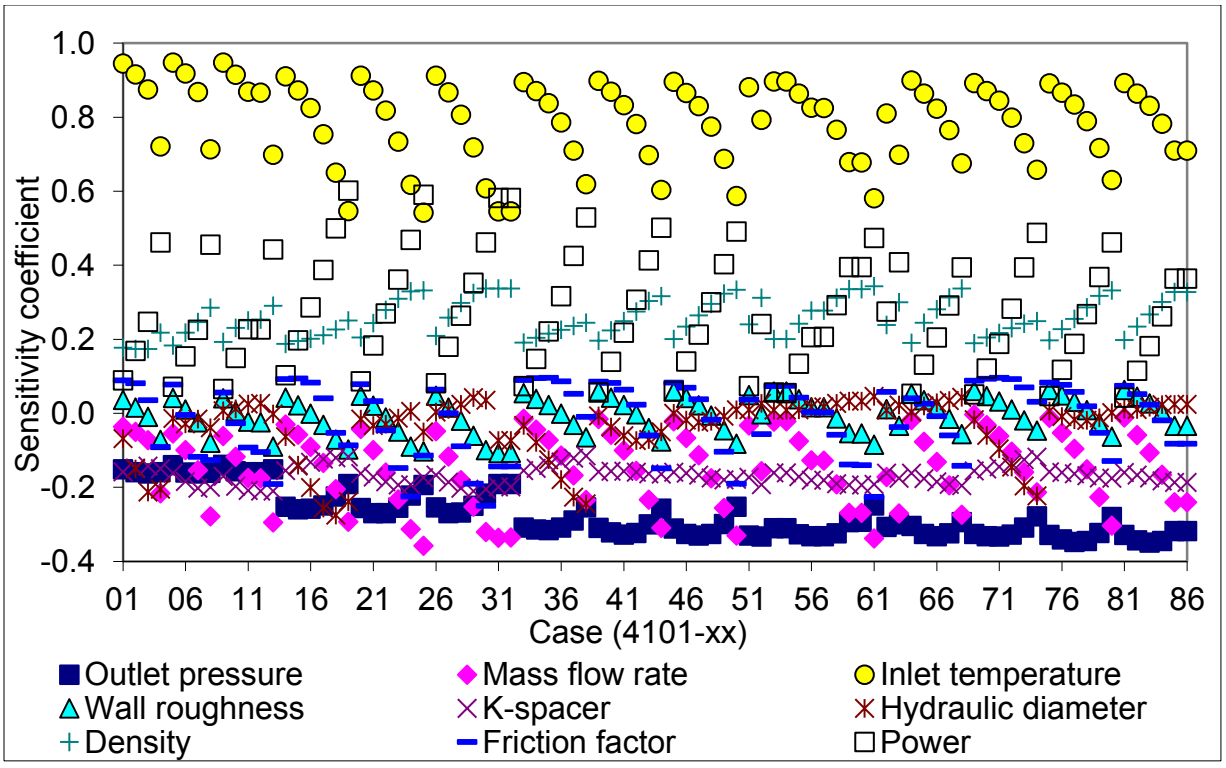

Figure 79 Sensitivity Coefficients for the Outlet Void Fraction Analysis with TRACE-SUSA

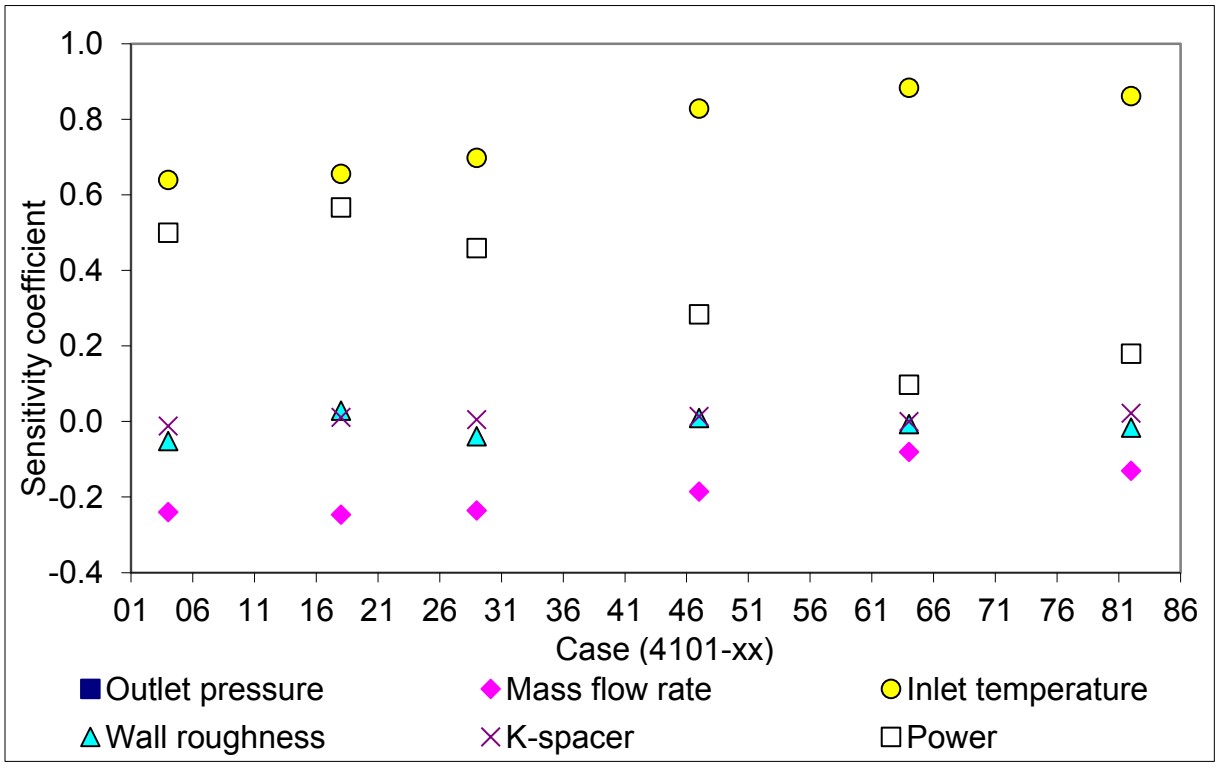

Figure 80 Sensitivity Coefficients for the Outlet Void Fraction Analysis with TRACE-DAKOTA

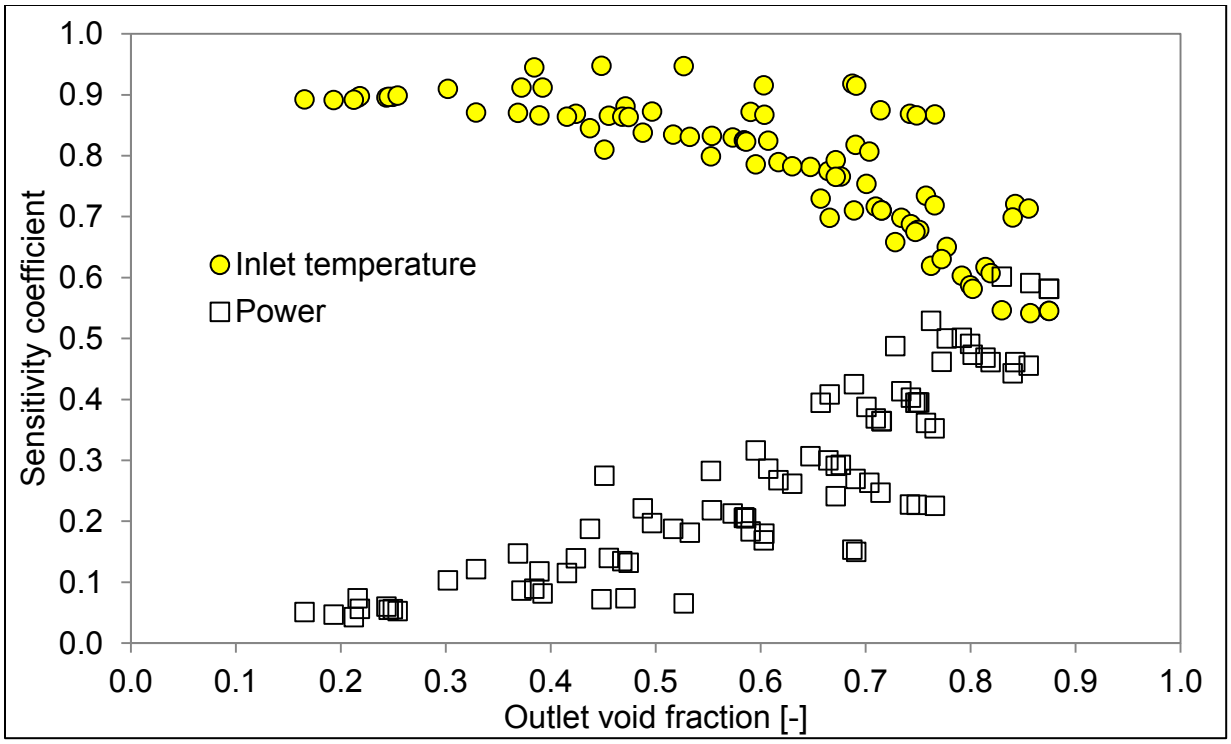

Figure 81 Sensitivity Coefficients for Inlet Temperature and Power versus the Outlet Void Fraction

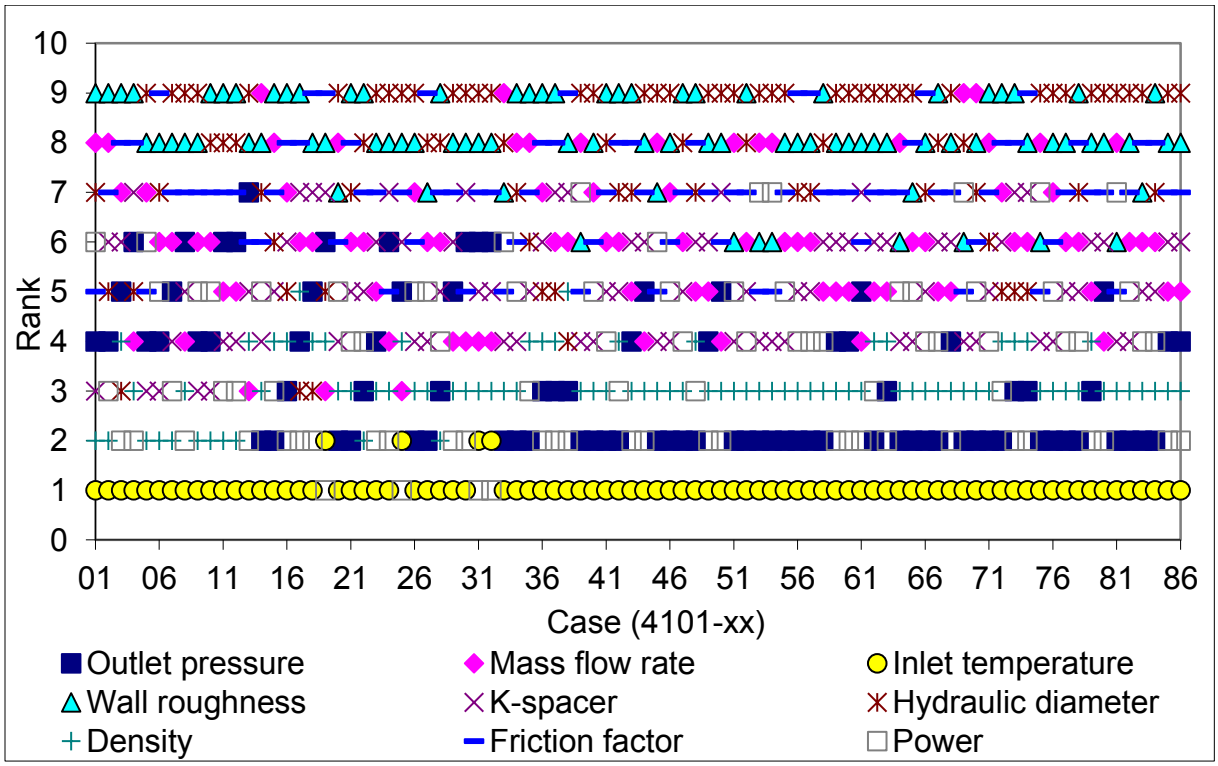

Figure 82 Ranking of the Uncertain Parameters for the Outlet Void Fraction with TRACE-SUSA

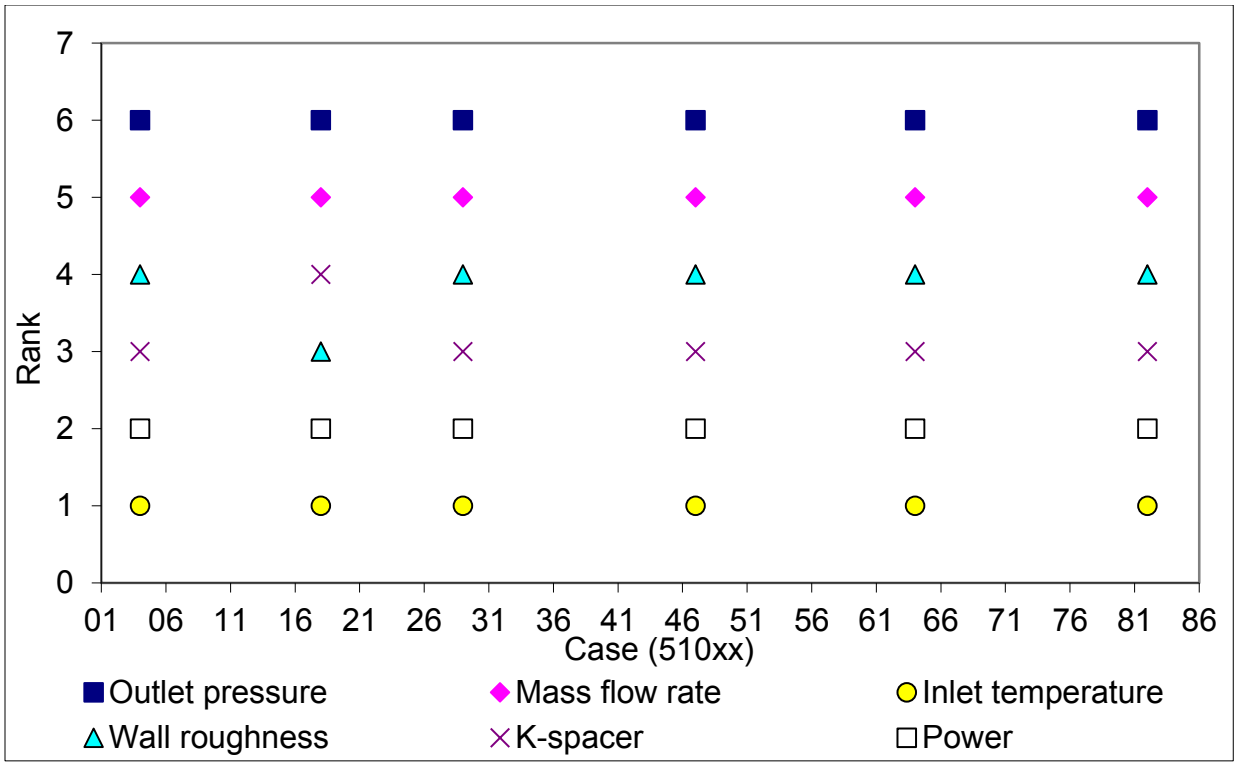

Figure 83 Ranking of the Uncertain Parameters for the Outlet Void Fraction with TRACE-DAKOTA

Table 28 Pearson's Momentum Correlation Coefficients for the Outlet Void Fraction Cases with TRACE-SUSA

	Outlet pressure	Mass flow rate	Inlet temperature	Wall roughness	K-spacer	Hydraulic diameter	Density	Friction factor	Power
4101-01	-0.151	-0.036	0.945	0.036	-0.158	-0.068	0.177	0.089	0.089
4101-02	-0.159	-0.050	0.916	0.016	-0.148	-0.150	0.174	0.081	0.169
4101-03	-0.163	-0.073	0.875	-0.010	-0.142	-0.213	0.174	0.036	0.247
4101-04	-0.159	-0.216	0.721	-0.072	-0.150	-0.205	0.218	-0.090	0.461
4101-05	-0.140	-0.054	0.947	0.042	-0.162	-0.013	0.183	0.078	0.072
4101-06	-0.160	-0.099	0.918	0.010	-0.184	-0.028	0.218	-0.004	0.154
4101-07	-0.163	-0.154	0.868	-0.025	-0.203	-0.015	0.246	-0.118	0.226
4101-08	-0.161	-0.278	0.714	-0.080	-0.200	-0.039	0.285	-0.126	0.455
4101-09	-0.139	-0.061	0.947	0.041	-0.171	0.007	0.193	0.056	0.065
4101-10	-0.157	-0.117	0.915	0.006	-0.197	0.012	0.231	-0.027	0.150
4101-11	-0.159	-0.174	0.869	-0.023	-0.208	0.025	0.251	-0.092	0.227
4101-12	-0.159	-0.175	0.866	-0.024	-0.210	0.027	0.254	-0.105	0.227
4101-13	-0.151	-0.294	0.698	-0.090	-0.210	-0.002	0.291	-0.191	0.443
4101-14	-0.253	-0.031	0.910	0.043	-0.155	-0.064	0.188	0.092	0.103
4101-15	-0.259	-0.058	0.872	0.022	-0.143	-0.140	0.196	0.095	0.197

	Outlet pressure	Mass flow rate	Inlet temperature	Wall roughness	K-spacer	Hydraulic diameter	Density	Friction factor	Power
4101-16	-0.258	-0.091	0.825	-0.001	-0.132	-0.200	0.202	0.083	0.286
4101-17	-0.249	-0.134	0.754	-0.031	-0.124	-0.256	0.211	0.041	0.388
4101-18	-0.225	-0.205	0.651	-0.071	-0.120	-0.275	0.226	-0.053	0.500
4101-19	-0.191	-0.293	0.546	-0.098	-0.118	-0.238	0.251	-0.087	0.602
4101-20	-0.255	-0.042	0.912	0.048	-0.162	-0.016	0.205	0.079	0.086
4101-21	-0.269	-0.099	0.872	0.021	-0.172	-0.033	0.244	0.033	0.183
4101-22	-0.270	-0.160	0.818	-0.011	-0.185	-0.029	0.280	-0.046	0.269
4101-23	-0.255	-0.233	0.734	-0.050	-0.194	-0.013	0.309	-0.148	0.362
4101-24	-0.222	-0.313	0.617	-0.090	-0.193	0.005	0.330	-0.224	0.469
4101-25	-0.193	-0.358	0.542	-0.103	-0.174	-0.050	0.332	-0.114	0.591
4101-26	-0.254	-0.049	0.912	0.047	-0.167	0.004	0.209	0.064	0.082
4101-27	-0.269	-0.117	0.867	0.016	-0.186	0.010	0.259	0.000	0.180
4101-28	-0.268	-0.181	0.807	-0.020	-0.202	0.024	0.299	-0.089	0.263
4101-29	-0.250	-0.252	0.718	-0.060	-0.210	0.043	0.325	-0.190	0.352
4101-30	-0.217	-0.321	0.608	-0.099	-0.205	0.035	0.337	-0.250	0.462
4101-31	-0.191	-0.336	0.545	-0.107	-0.198	-0.074	0.337	-0.144	0.582
4101-32	-0.191	-0.336	0.546	-0.107	-0.199	-0.074	0.338	-0.144	0.582
4101-33	-0.309	-0.015	0.895	0.054	-0.155	-0.033	0.192	0.090	0.074
4101-34	-0.314	-0.044	0.870	0.039	-0.148	-0.078	0.204	0.095	0.147
4101-35	-0.315	-0.073	0.838	0.023	-0.141	-0.125	0.215	0.096	0.221
4101-36	-0.309	-0.114	0.786	-0.001	-0.131	-0.179	0.226	0.086	0.316
4101-37	-0.290	-0.168	0.710	-0.031	-0.121	-0.227	0.236	0.053	0.425
4101-38	-0.254	-0.235	0.619	-0.065	-0.115	-0.245	0.244	-0.009	0.529
4101-39	-0.310	-0.016	0.898	0.059	-0.158	-0.007	0.197	0.085	0.056
4101-40	-0.322	-0.058	0.869	0.042	-0.157	-0.038	0.224	0.083	0.140
4101-41	-0.327	-0.100	0.833	0.023	-0.157	-0.061	0.249	0.064	0.218
4101-42	-0.323	-0.156	0.782	-0.002	-0.159	-0.073	0.275	0.023	0.307
4101-43	-0.300	-0.233	0.698	-0.039	-0.164	-0.070	0.304	-0.060	0.414
4101-44	-0.257	-0.309	0.603	-0.076	-0.164	-0.050	0.317	-0.149	0.501
4101-45	-0.312	-0.021	0.896	0.059	-0.159	0.000	0.201	0.083	0.060
4101-46	-0.326	-0.067	0.865	0.041	-0.162	-0.018	0.234	0.069	0.140
4101-47	-0.331	-0.114	0.830	0.021	-0.167	-0.024	0.264	0.038	0.213
4101-48	-0.326	-0.175	0.775	-0.006	-0.175	-0.021	0.296	-0.017	0.300
4101-49	-0.299	-0.256	0.688	-0.046	-0.180	-0.008	0.324	-0.104	0.403
4101-50	-0.253	-0.330	0.587	-0.083	-0.178	0.010	0.334	-0.190	0.491
4101-51	-0.330	-0.033	0.881	0.049	-0.173	0.010	0.240	0.037	0.074
4101-52	-0.333	-0.157	0.793	-0.003	-0.193	0.027	0.312	-0.056	0.241
4101-53	-0.311	-0.023	0.897	0.059	-0.161	0.009	0.201	0.074	0.056
4101-54	-0.311	-0.022	0.897	0.059	-0.161	0.009	0.200	0.074	0.055
4101-55	-0.327	-0.075	0.864	0.038	-0.171	0.010	0.242	0.043	0.134
4101-56	-0.332	-0.127	0.825	0.017	-0.181	0.017	0.278	0.003	0.205
4101-57	-0.332	-0.128	0.825	0.017	-0.181	0.017	0.278	0.003	0.207
4101-58	-0.325	-0.192	0.766	-0.014	-0.190	0.027	0.312	-0.058	0.293
4101-59	-0.294	-0.269	0.678	-0.054	-0.193	0.033	0.335	-0.138	0.395

	Outlet pressure	Mass flow rate	Inlet temperature	Wall roughness	K-spacer	Hydraulic diameter	Density	Friction factor	Power
4101-60	-0.293	-0.269	0.678	-0.054	-0.193	0.033	0.336	-0.140	0.395
4101-61	-0.249	-0.338	0.581	-0.084	-0.192	0.046	0.344	-0.225	0.474
4101-62	-0.307	-0.172	0.810	0.011	-0.162	0.008	0.239	0.058	0.275
4101-63	-0.300	-0.271	0.698	-0.034	-0.175	0.023	0.300	-0.037	0.408
4101-64	-0.304	-0.018	0.899	0.053	-0.162	0.004	0.190	0.041	0.053
4101-65	-0.326	-0.077	0.864	0.035	-0.176	0.020	0.245	0.026	0.132
4101-66	-0.332	-0.132	0.823	0.014	-0.185	0.029	0.281	-0.008	0.205
4101-67	-0.324	-0.195	0.766	-0.014	-0.192	0.035	0.313	-0.059	0.291
4101-68	-0.294	-0.274	0.675	-0.056	-0.195	0.044	0.337	-0.142	0.394
4101-69	-0.326	-0.004	0.893	0.061	-0.155	-0.018	0.189	0.088	0.051
4101-70	-0.332	-0.032	0.871	0.047	-0.150	-0.060	0.205	0.094	0.121
4101-71	-0.333	-0.061	0.845	0.032	-0.145	-0.096	0.217	0.096	0.188
4101-72	-0.328	-0.104	0.799	0.010	-0.136	-0.146	0.230	0.092	0.283
4101-73	-0.308	-0.159	0.729	-0.019	-0.126	-0.196	0.242	0.070	0.394
4101-74	-0.278	-0.214	0.658	-0.047	-0.118	-0.223	0.249	0.031	0.488
4101-75	-0.328	-0.012	0.891	0.063	-0.158	0.006	0.197	0.083	0.047
4101-76	-0.341	-0.053	0.866	0.049	-0.160	-0.009	0.227	0.077	0.118
4101-77	-0.347	-0.096	0.835	0.032	-0.163	-0.017	0.256	0.058	0.188
4101-78	-0.345	-0.151	0.790	0.009	-0.168	-0.019	0.286	0.019	0.268
4101-79	-0.323	-0.227	0.717	-0.026	-0.175	-0.012	0.318	-0.053	0.369
4101-80	-0.280	-0.303	0.630	-0.063	-0.176	0.002	0.332	-0.129	0.462
4101-81	-0.328	-0.011	0.892	0.063	-0.160	0.011	0.198	0.075	0.042
4101-82	-0.343	-0.059	0.864	0.045	-0.167	0.011	0.234	0.052	0.115
4101-83	-0.349	-0.107	0.831	0.027	-0.175	0.016	0.267	0.024	0.181
4101-84	-0.345	-0.166	0.783	0.002	-0.182	0.023	0.301	-0.019	0.262
4101-85	-0.318	-0.240	0.710	-0.034	-0.187	0.025	0.328	-0.082	0.364
4101-86	-0.318	-0.241	0.710	-0.034	-0.186	0.024	0.328	-0.082	0.364

Table 29 Pearson's Momentum Correlation Coefficients for Outlet Void Fraction Cases with TRACE-DAKOTA

	Outlet pressure	Mass flow rate	Inlet temperature	Wall roughness	K-spacer	Hydraulic diameter	Density	Friction factor	Power
4101-04	-0.474	-0.239	0.640	-0.052	-0.012				0.500
4101-18	-0.415	-0.246	0.656	0.029	0.012				0.567
4101-29	-0.476	-0.236	0.698	-0.039	0.005		not included		0.459
4101-47	-0.425	-0.185	0.828	0.010	0.014				0.284
4101-64	-0.450	-0.080	0.884	-0.006	0.001				0.098
4101-82	-0.502	-0.130	0.862	-0.016	0.022				0.180

Since the void fraction has been measured at four axial elevations the predictions along the BWR fuel assembly mock-up can be compared to them, Figure 84 to Figure 94. In addition to the corrected results, the original measured data points are plotted. It can be seen that the correction is more pronounced at higher void fractions. The agreement of the experimental values and the calculated ones is very good in the most cases. In these graphs it is also visible that the uncertainty range (indicated by the two red lines) is wider at low void fractions and getting smaller at higher elevations with higher void fractions.

For two selected cases, case 4101-04 and 4101-18, the results of TRACE-SUSA are compared to the ones of TRACE-DAKOTA in Figure 95 and Figure 96. In both cases the results of TRACE-SUSA and TRACE-DAKOTA overlap each other. Even though in the TRACE-DAKOTA investigation less parameters are used the results are identical. The reason for that is that the parameters which are considered in the TRACE-SUSA study but not in the TRACE-DAKOTA study are of no importance for the void fraction.

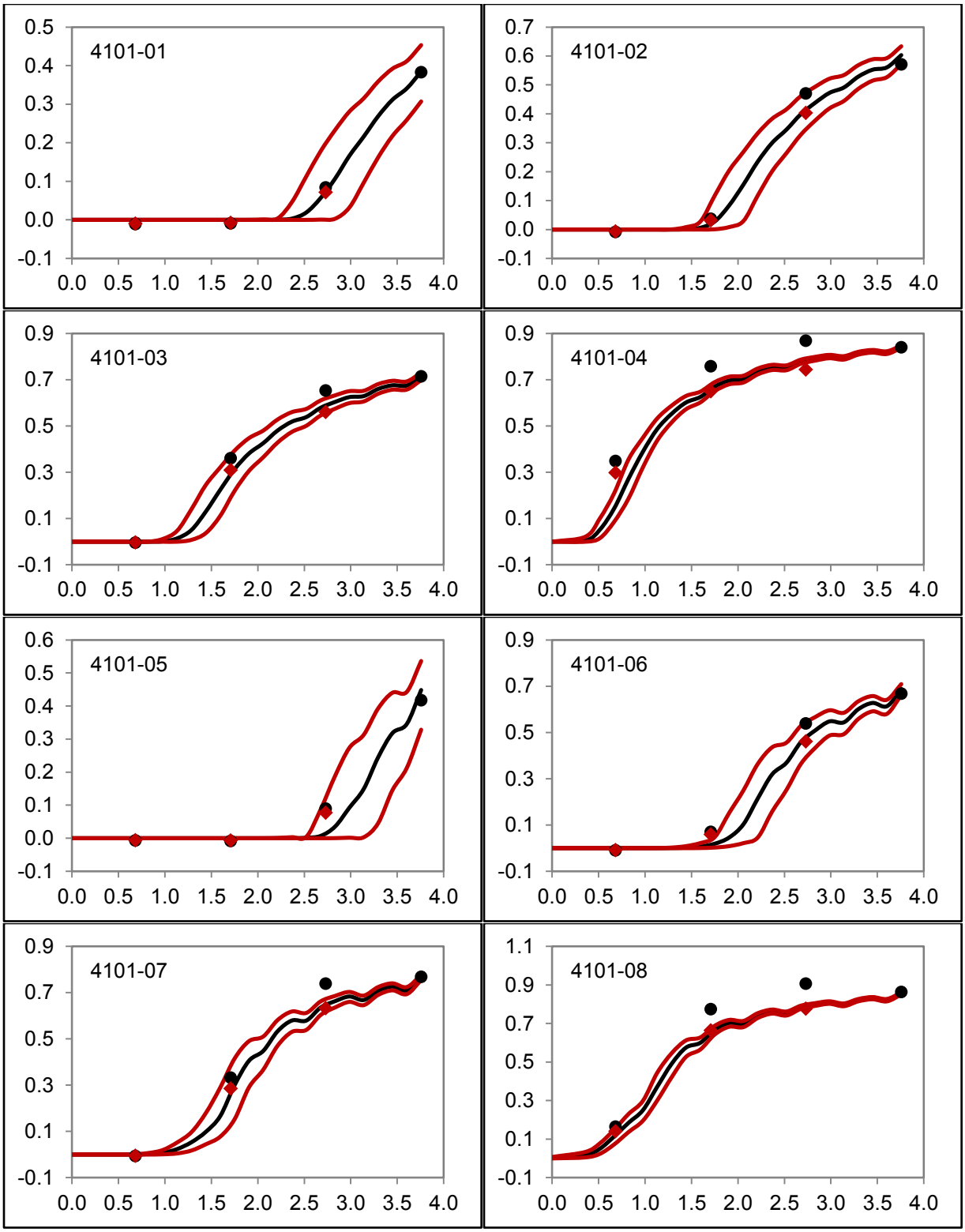

Figure 84 Axial Void Fraction for Cases 4101-01 - 4101-08 (x-axes = Axial Location [m]; y-axes = Void Fraction; Black Circles = Original Experimental Data; Red Diamonds = Corrected Experimental Data; Red Line = Uncertainty Range; Black Line = Mean Value of the Calculations)

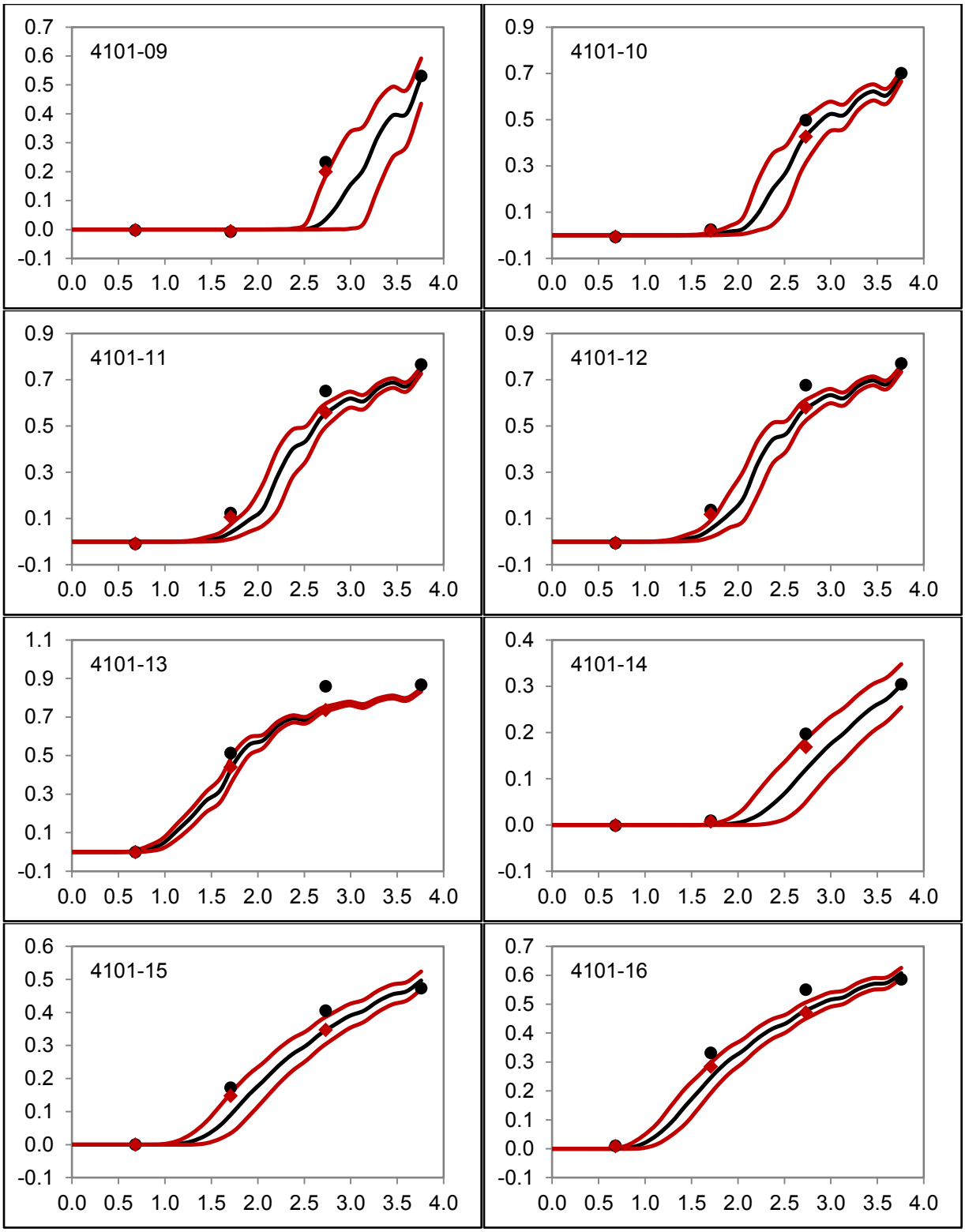

Figure 85 Axial Void Fraction for Cases 4101-09 - 4101-16 (x-axes = Axial Location [m]; y-axes = Void Fraction; Black Circles = Original Experimental Data; Red Diamonds = Corrected Experimental Data; Red Line = Uncertainty Range; Black Line = Mean Value of the Calculations)

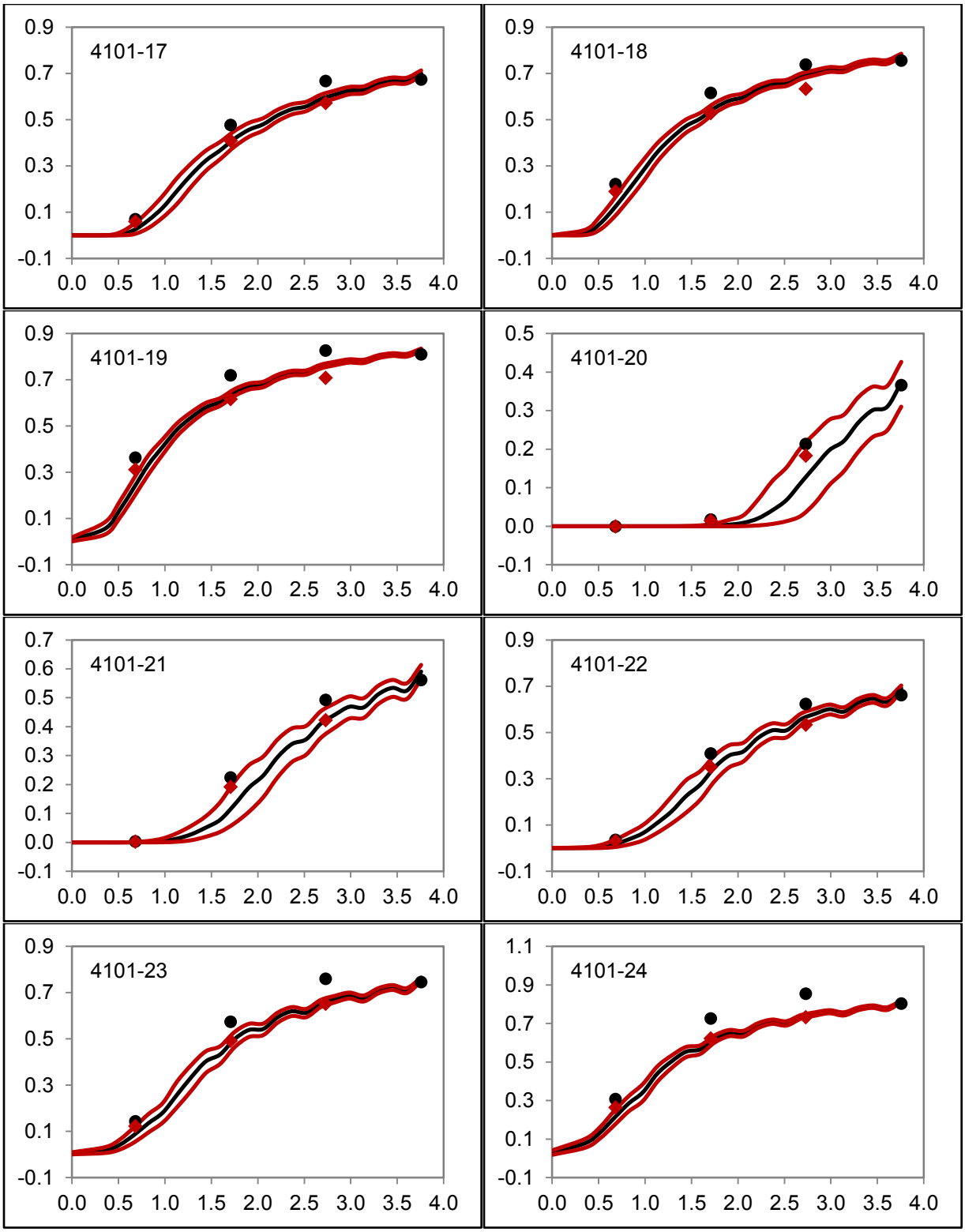

Figure 86 Axial Void Fraction for Cases 4101-17 - 4101-24 (x-axes = Axial Location [m]; y-axes = Void Fraction; Black Circles = Original Experimental Data; Red Diamonds = Corrected Experimental Data; Red Line = Uncertainty Range; Black Line = Mean Value of the Calculations)

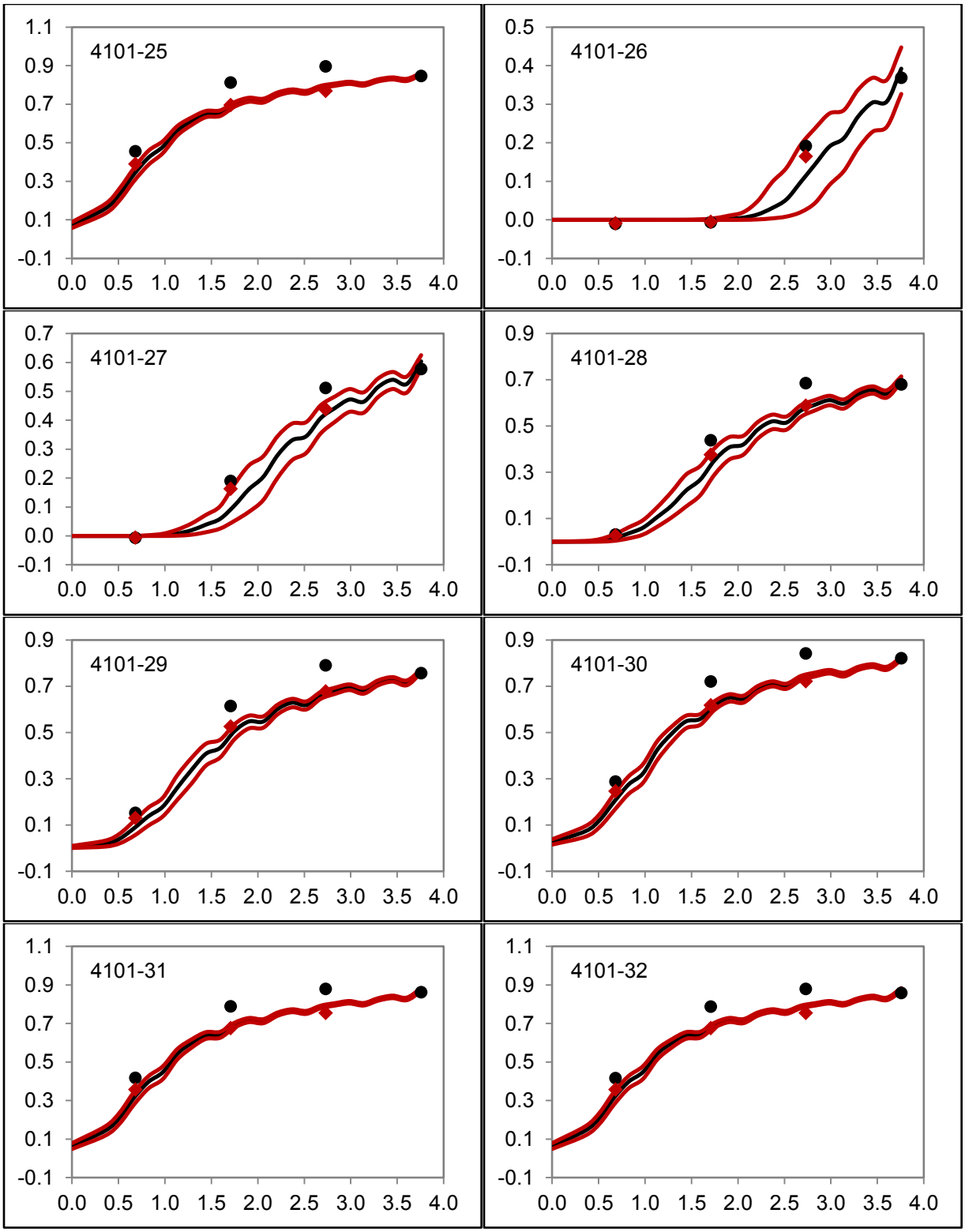

Figure 87 Axial Void Fraction for Cases 4101-25 - 4101-32 (x-axes = Axial Location [m]; y-axes = Void Fraction; Black Circles = Original Experimental Data; Red Diamonds = Corrected Experimental Data; Red Line = Uncertainty Range; Black Line = Mean Value of the Calculations)

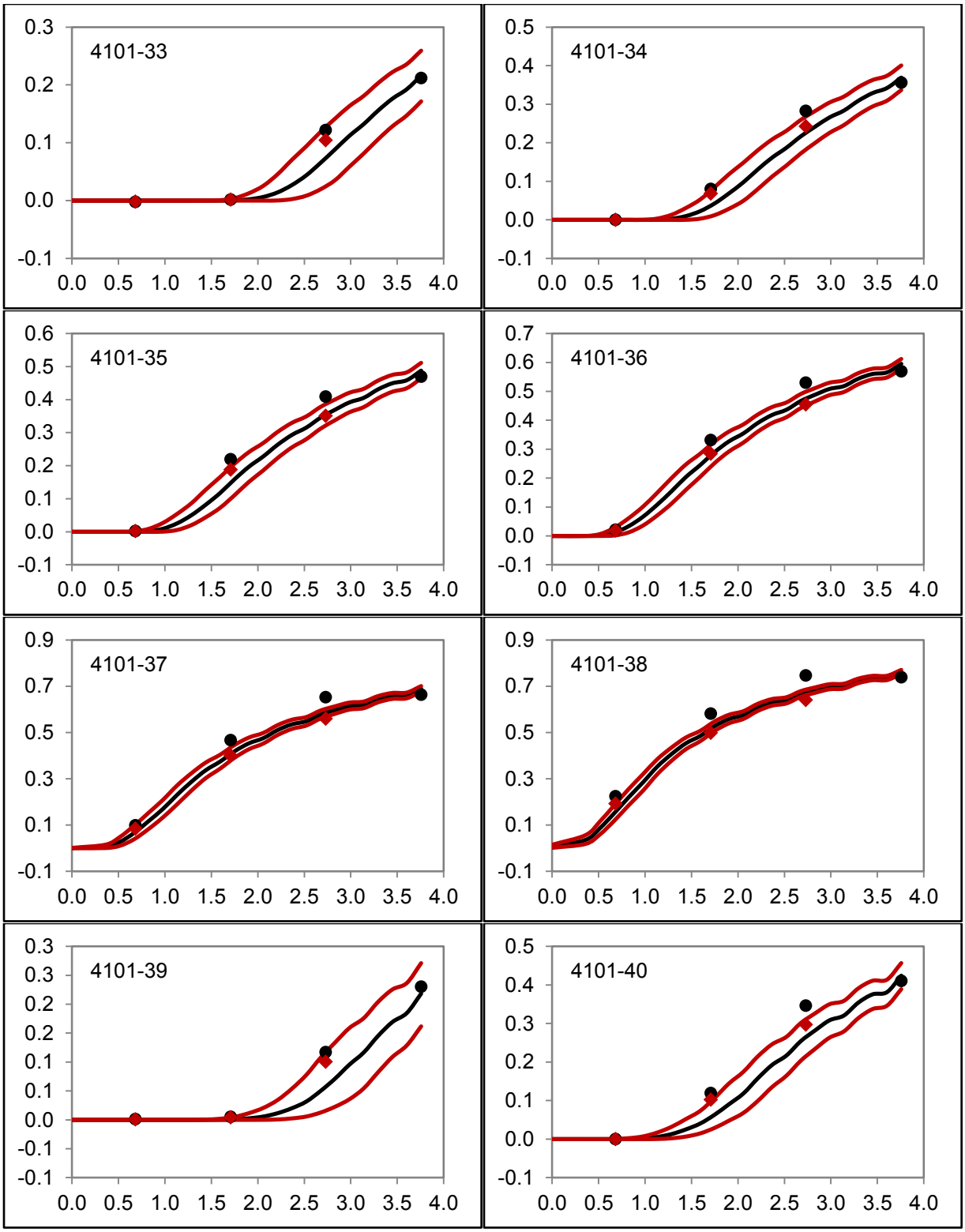

Figure 88 Axial Void Fraction for Cases 4101-33 - 4101-40 (x-axes = Axial Location [m]; y-axes = Void Fraction; Black Circles = Original Experimental Data; Red Diamonds = Corrected Experimental Data; Red Line = Uncertainty Range; Black Line = Mean Value of the Calculations)

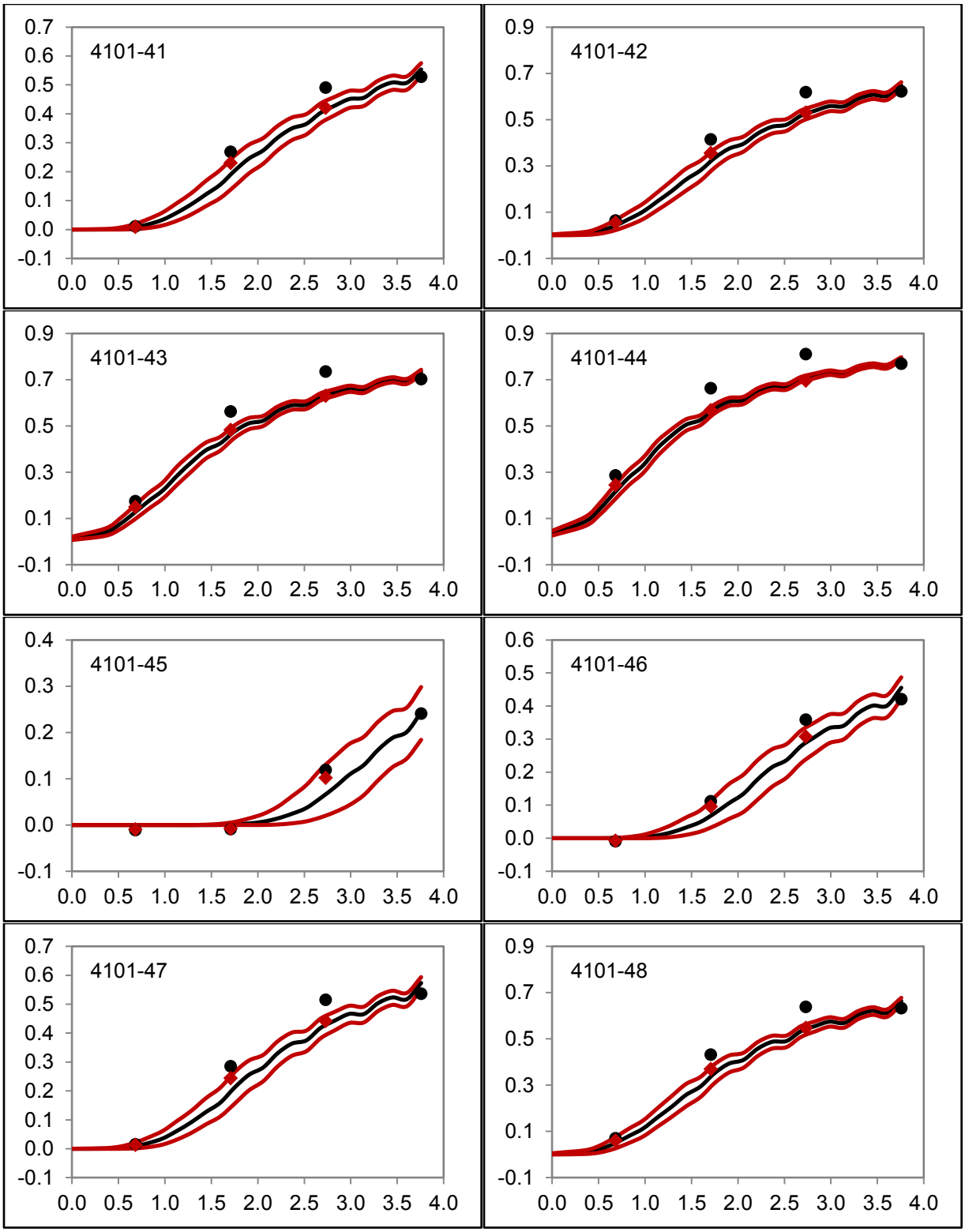

Figure 89 Axial Void Fraction for Cases 4101-41 - 4101-48 (x-axes = Axial Location [m]; y-axes = Void Fraction; Black Circles = Original Experimental Data; Red Diamonds = Corrected Experimental Data; Red Line = Uncertainty Range; Black Line = Mean Value of the Calculations)

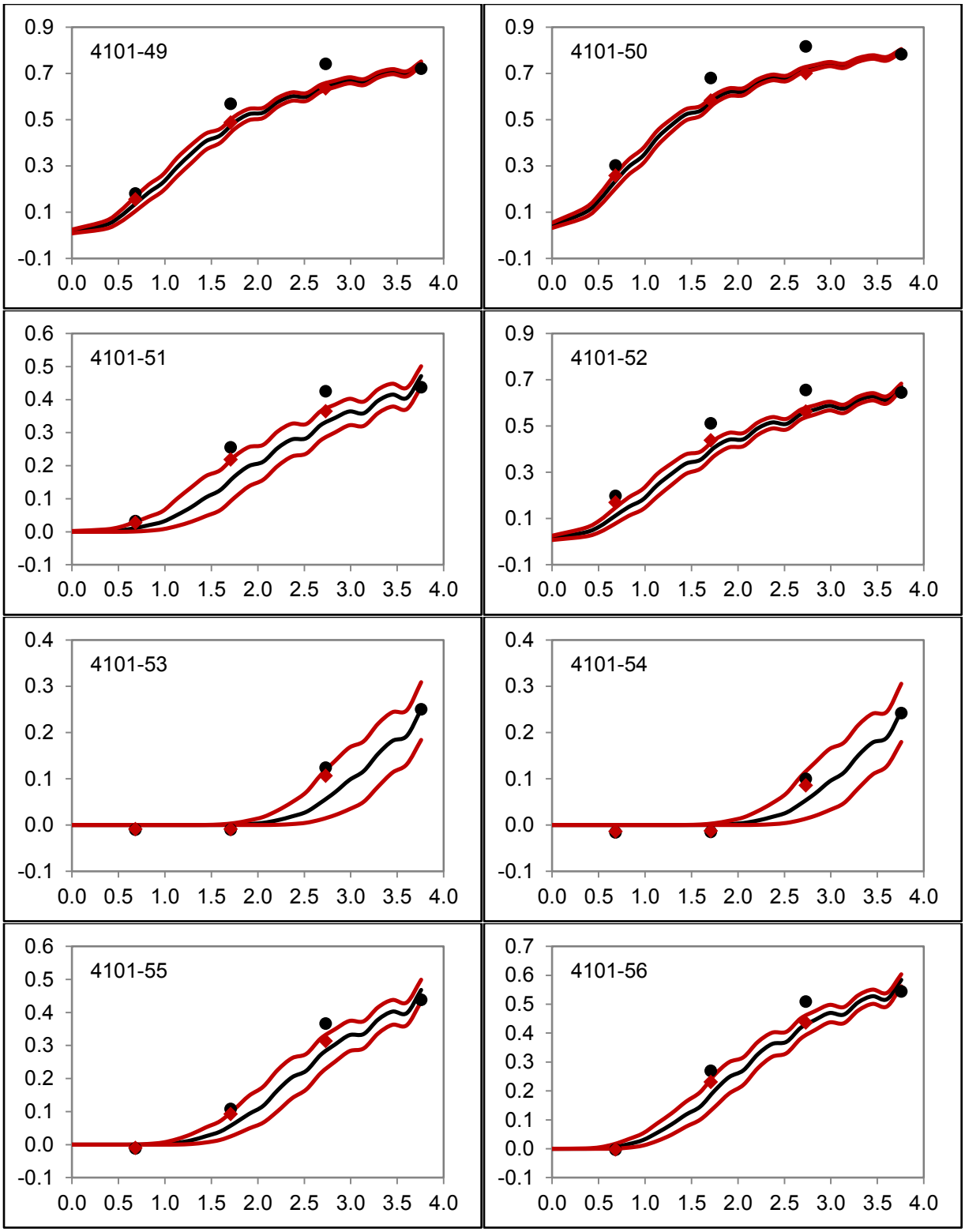

Figure 90 Axial Void Fraction for Cases 4101-49 - 4101-56 (x-axes = Axial Location [m]; y-axes = Void Fraction; Black Circles = Original Experimental Data; Red Diamonds = Corrected Experimental Data; Red Line = Uncertainty Range; Black Line = Mean Value of the Calculations)

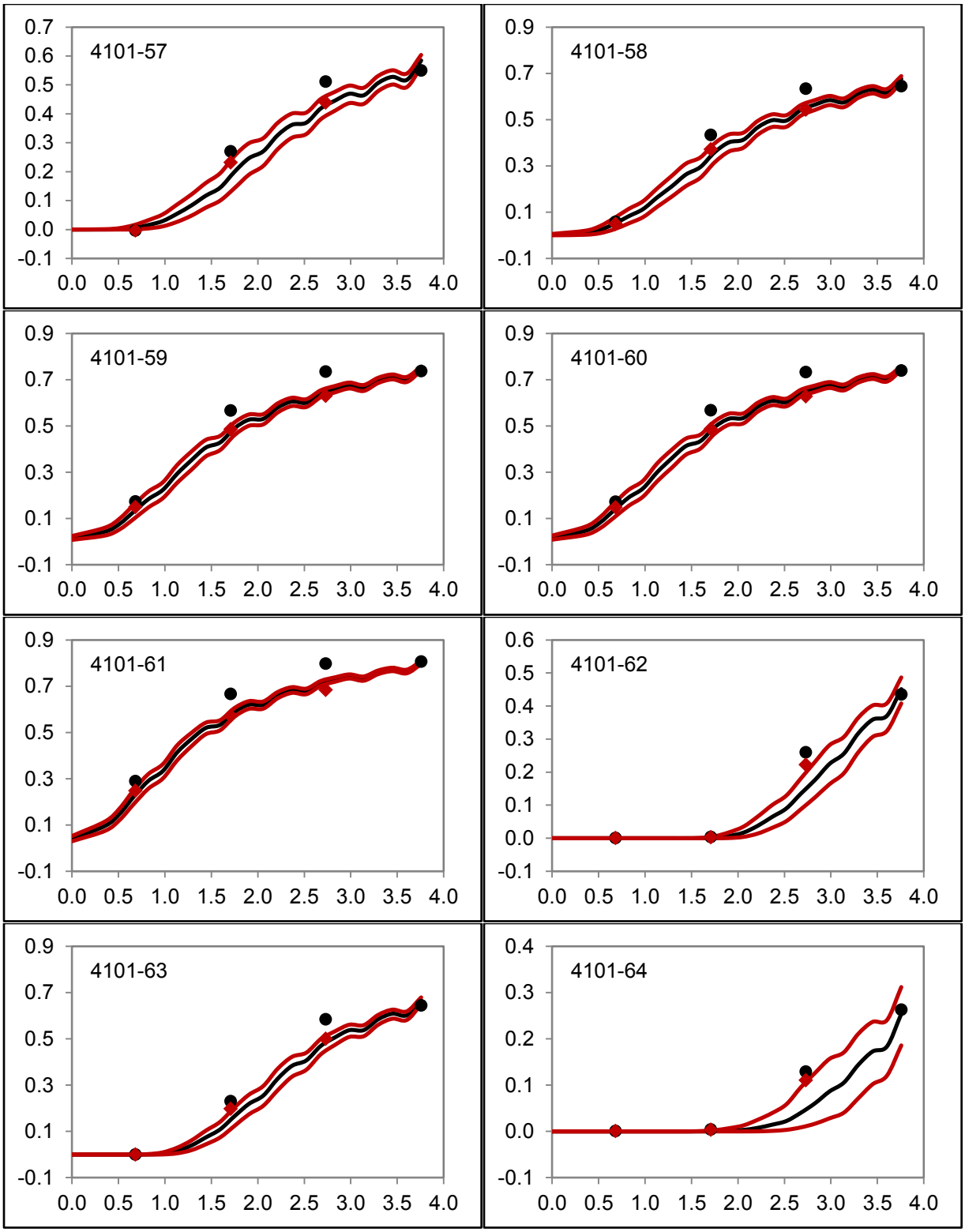

Figure 91 Axial Void Fraction for Cases 4101-57 - 4101-64 (x-axes = Axial Location [m]; y-axes = Void Fraction; Black Circles = Original Experimental Data; Red Diamonds = Corrected Experimental Data; Red Line = Uncertainty Range; Black Line = Mean Value of the Calculations)

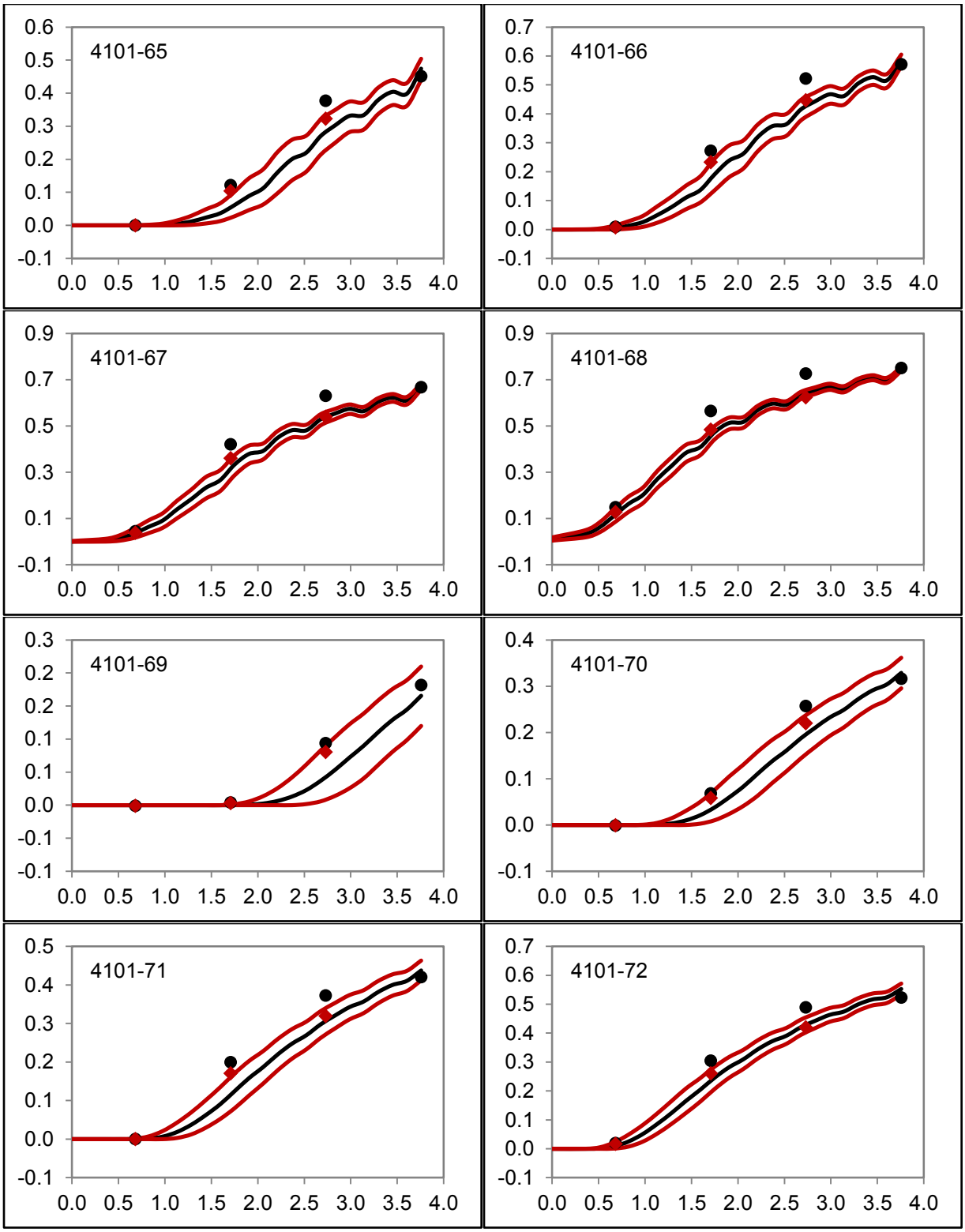

Figure 92 Axial Void Fraction for Cases 4101-65 - 4101-72 (x-axes = Axial Location [m]; y-axes = Void Fraction; Black Circles = Original Experimental Data; Red Diamonds = Corrected Experimental Data; Red Line = Uncertainty Range; Black Line = Mean Value of the Calculations)

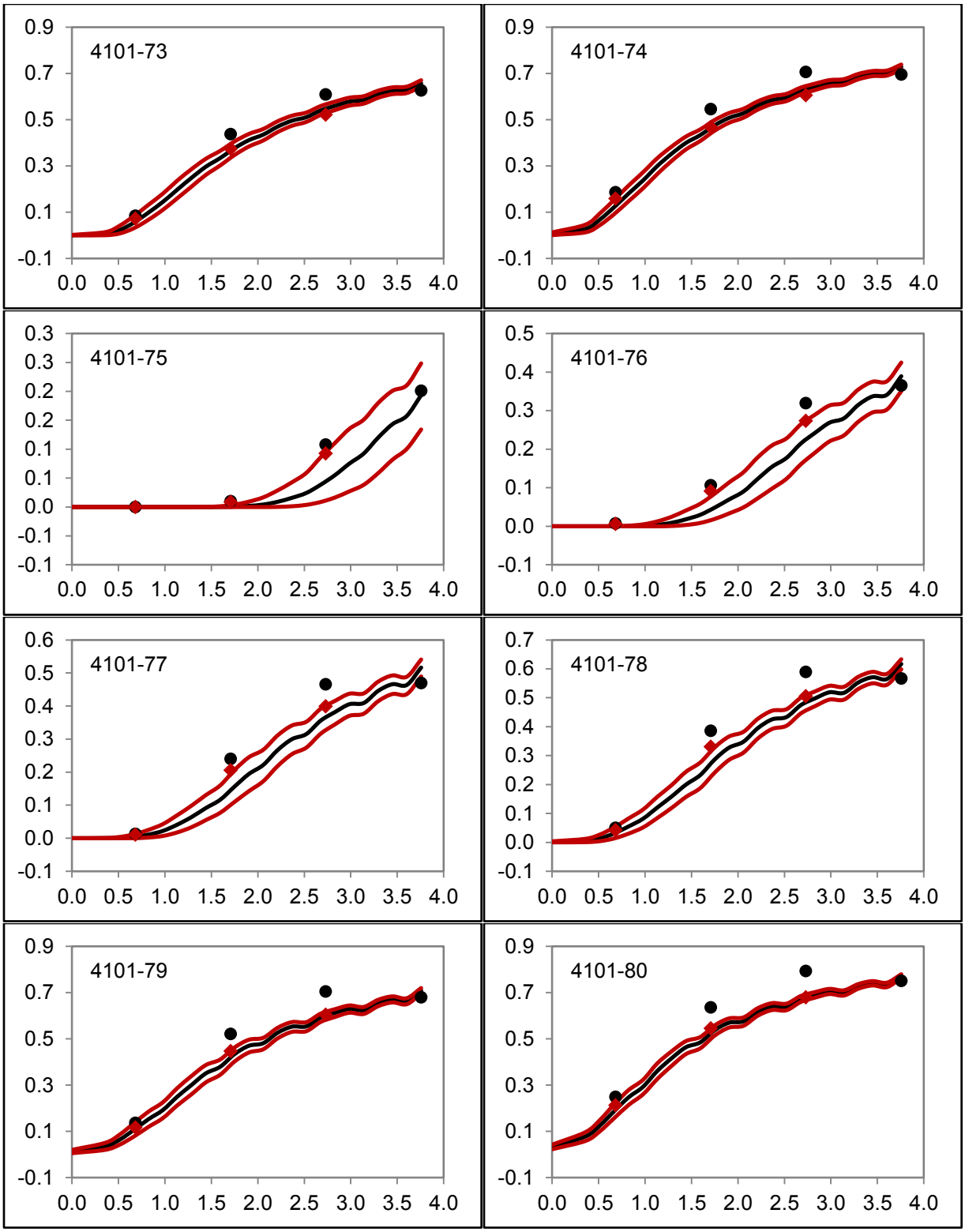

Figure 93 Axial Void Fraction for Cases 4101-73 - 4101-80 (x-axes = Axial Location [m]; y-axes = Void Fraction; Black Circles = Original Experimental Data; Red Diamonds = Corrected Experimental Data; Red Line = Uncertainty Range; Black Line = Mean Value of the Calculations)

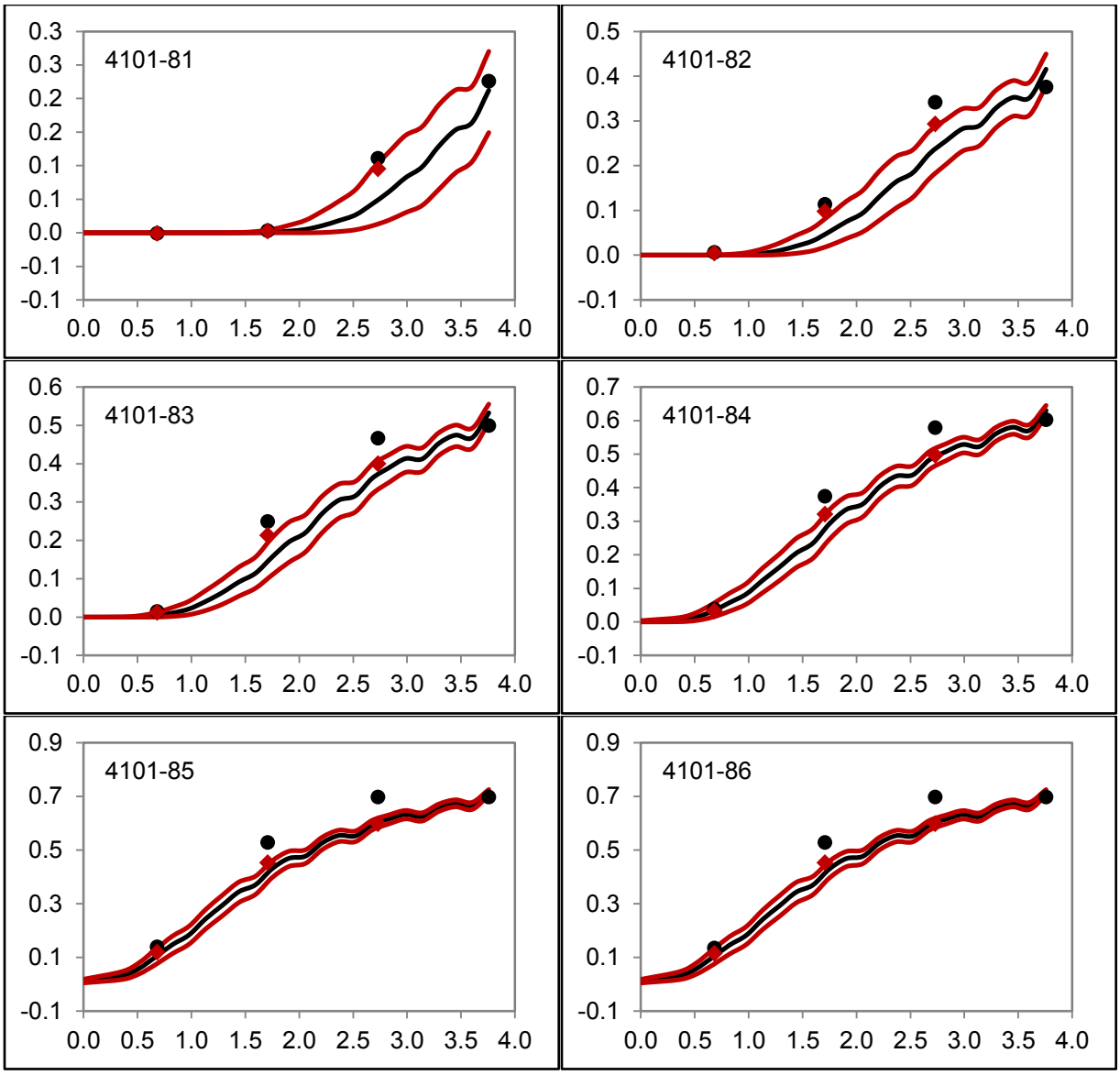

Figure 94 Axial Void Fraction for Cases 4101-81 - 4101-86 (x-axes = Axial Location [m]; y-axes = Void Fraction; Black Circles = Original Experimental Data; Red Diamonds = Corrected Experimental Data; Red Line = Uncertainty Range; Black Line = Mean Value of the Calculations)

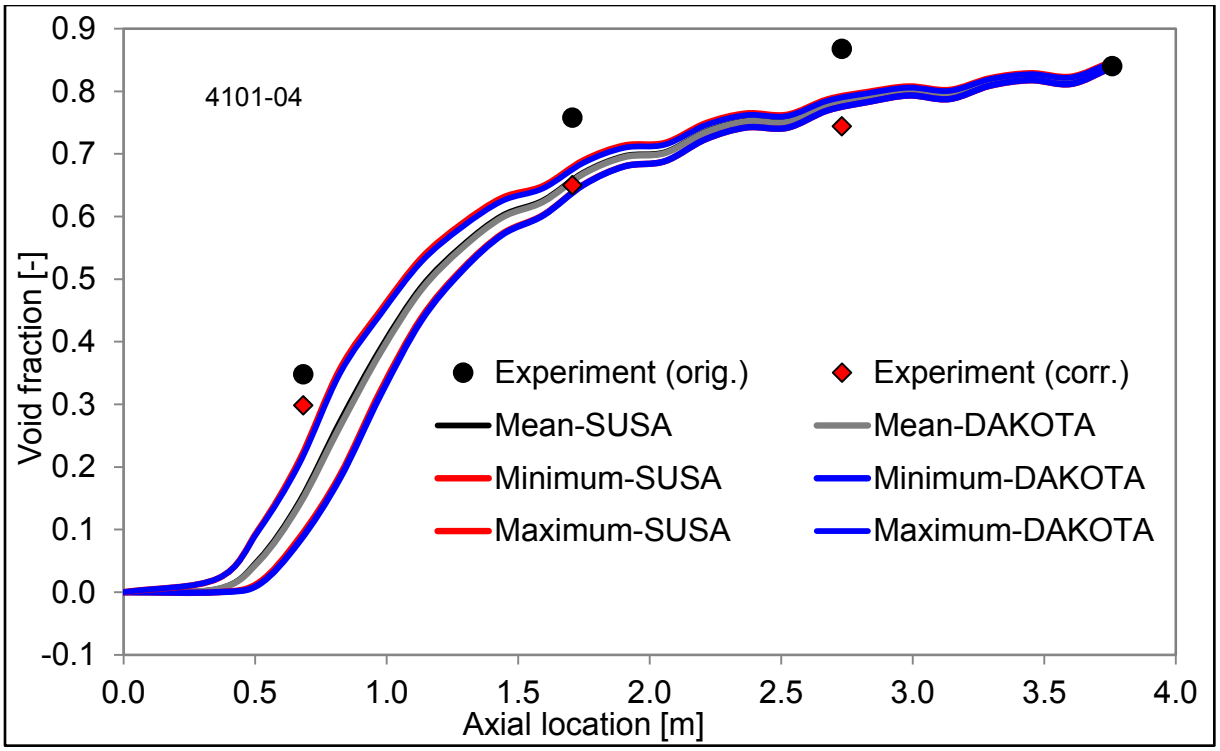

Figure 95 Comparison of the Axial Void Fraction Predicted with TRACE-SUSA and TRACE-DAKOTA for Case 4101-04

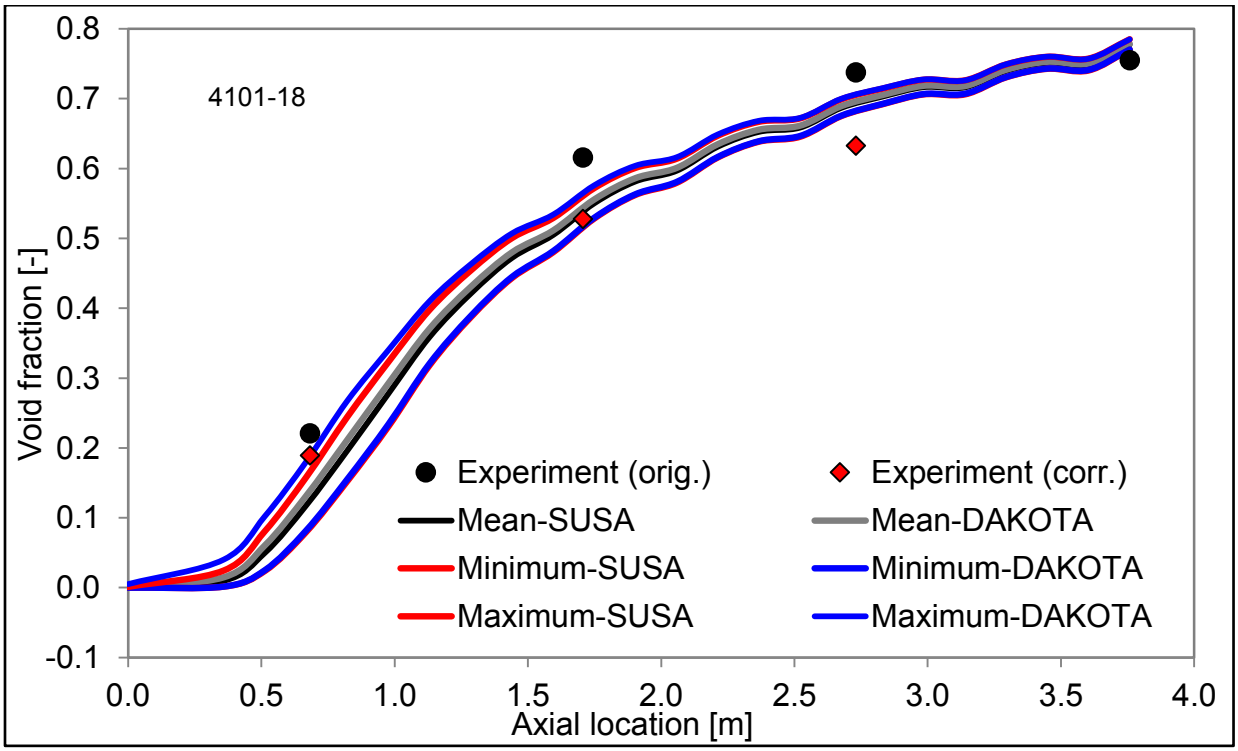

Figure 96 Comparison of the Axial Void Fraction Predicted with TRACE-SUSA and TRACE-DAKOTA for Case 4101-18

6.5 Critical Power Analyses

The critical power is not directly calculated in TRACE. What TRACE calculates is the critical power ratio based on a predefined input power. Therefore, the experimental results of the critical power serve as input values for the TRACE calculations. The obtained critical power ratio is than multiplied by the initial power input, where the result is the critical power based on TRACE simulations.

The combination of pressure, inlet sub-cooling and mass flow rate is given in Figure 97 and Table 30. As one can see, the spread of the inlet sub-cooling does not follow a pattern and is rather chaotically distributed between values of 20 and 140 kJ/kg. The mass flow rate shows also a wide spread ranging from 10 to 65 kg/s. The pressure, on the contrary, ranges between three distinct areas. Pressures of around 55, 72 and 86 bar were realized. In total, 79 combinations of pressure, inlet sub-cooling and mass flow rate were investigated.

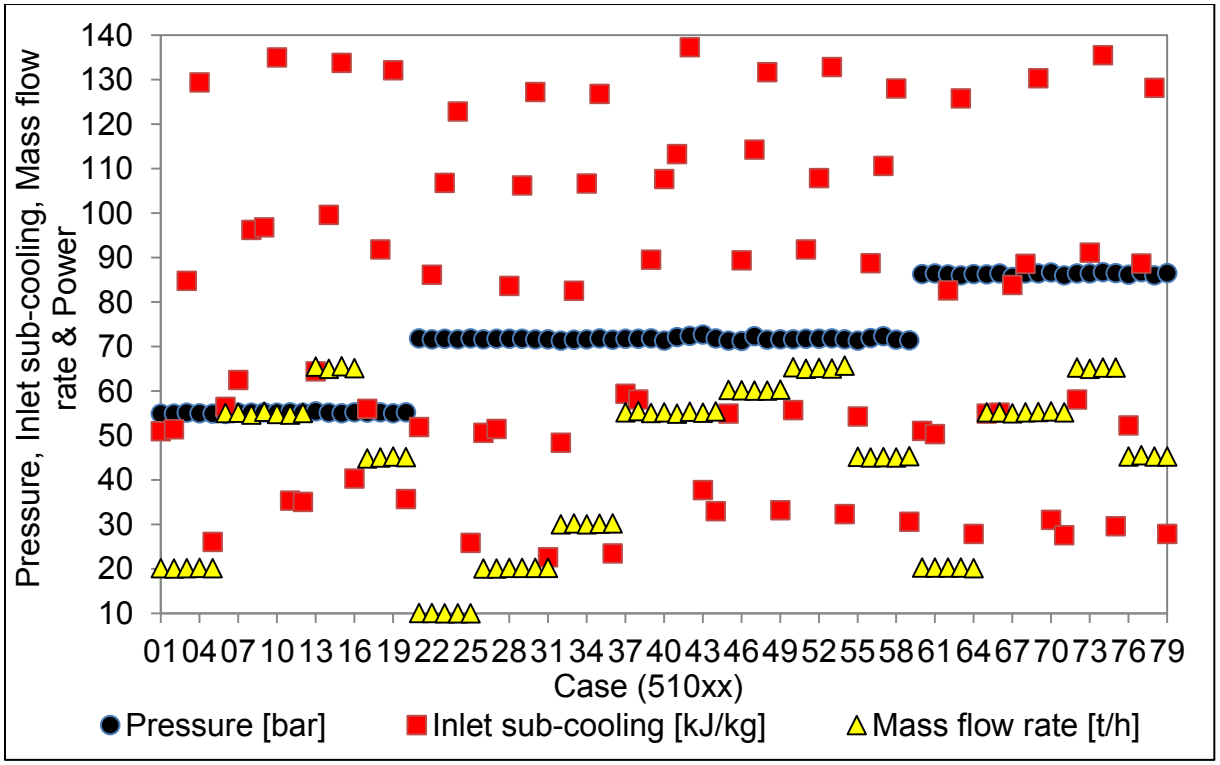

Figure 97 Input and Boundary Conditions for the Critical Power Cases

Table 30 Input and Boundary Conditions for the Critical Power Cases

Case	Outlet pressure [bar]	Inlet sub-cooling [kJ/kg]	Mass flow rate [t/h]
51001	54.90	50.95	20.16
51002	54.90	51.35	20.10
51003	55.10	84.79	20.12
51004	55.00	129.38	20.19
51005	54.90	26.04	20.14
51006	54.80	56.41	55.06
51007	55.10	62.48	55.11

Case	Outlet pressure [bar]	Inlet sub-cooling [kJ/kg]	Mass flow rate [t/h]
51008	55.10	96.16	54.70
51009	55.20	96.79	55.34
51010	55.10	134.97	54.81
51011	55.20	35.33	54.70
51012	55.10	35.02	55.05
51013	55.40	64.36	65.48
51014	55.10	99.60	64.97
51015	55.00	133.75	65.52
51016	55.20	40.30	65.12
51017	55.10	55.98	44.85
51018	55.20	91.83	45.03
51019	55.00	132.07	45.28
51020	55.20	35.66	45.13
51021	71.80	51.85	10.07
51022	71.60	86.12	10.07
51023	71.70	106.75	10.00
51024	71.60	122.79	10.00
51025	71.80	25.82	10.01
51026	71.60	50.55	20.09
51027	71.70	51.44	20.07
51028	71.70	83.57	20.19
51029	71.70	106.22	20.24
51030	71.60	127.20	20.21
51031	71.60	22.61	20.21
51032	71.30	48.35	30.02
51033	71.50	82.55	30.23
51034	71.60	106.63	30.00
51035	71.80	126.80	30.12
51036	71.50	23.42	30.23
51037	71.70	59.39	55.20
51038	71.70	58.09	55.47
51039	71.80	89.53	55.05
51040	71.30	107.61	55.20
51041	72.10	113.28	54.88
51042	72.40	137.26	55.30
51043	72.70	37.73	55.10
51044	71.80	32.94	55.42
51045	71.30	54.89	60.23
51046	71.20	89.39	60.18
51047	72.30	114.29	60.10
51048	71.50	131.68	60.07
51049	71.60	33.18	60.30
51050	71.60	55.66	65.36
51051	71.70	91.82	64.99
51052	71.70	107.82	65.19
51053	71.80	132.81	65.01
51054	71.60	32.31	65.72
51055	71.30	54.21	45.17
51056	71.90	88.72	45.01

Case	Outlet pressure [bar]	Inlet sub-cooling [kJ/kg]	Mass flow rate [t/h]
51057	72.30	110.60	45.13
51058	71.50	128.01	45.07
51059	71.40	30.59	45.35
51060	86.30	51.00	20.30
51061	86.40	50.28	20.30
51062	86.20	82.58	20.26
51063	86.00	125.79	20.31
51064	86.30	27.84	20.13
51065	86.20	54.89	55.15
51066	86.40	55.12	55.16
51067	85.60	83.85	55.00
51068	86.40	88.54	55.21
51069	86.40	130.30	55.28
51070	86.60	30.97	55.38
51071	86.00	27.55	55.15
51072	86.40	58.08	65.25
51073	86.40	91.08	64.95
51074	86.70	135.52	65.27
51075	86.50	29.55	65.22
51076	86.10	52.22	45.24
51077	86.70	88.65	45.52
51078	86.00	128.18	45.23
51079	86.50	27.81	45.24

The comparison of the experimental critical power points and the ones predicted for the reference scenarios are shown in Figure 98. The resulting critical power can be classified in three groups. The first group is between 3.0 and 3.5 MW, the second group between 5.0 and 6.5 MW, and the last group, with the biggest range, from 7.0 to 11.0 MW. For the values below 7.0 MW the TRACE predictions are always below the experimental values. For critical power values higher than 7.0 MW TRACE over- and underestimates the critical power in the same way. The error in percent is given in Figure 99. The average error considering all 79 cases is 4.70 %. The error as a function of the critical power is given in Figure 100. It is visible that at values below 7 MW the error is always higher than 6 % while at higher critical power values the error can range from almost 0 to 8 %. The calculated critical power values along with maximal and minimal values from the uncertainty study are compared to the experimental values in Figure 101 for absolute values and Figure 102 for relative values.

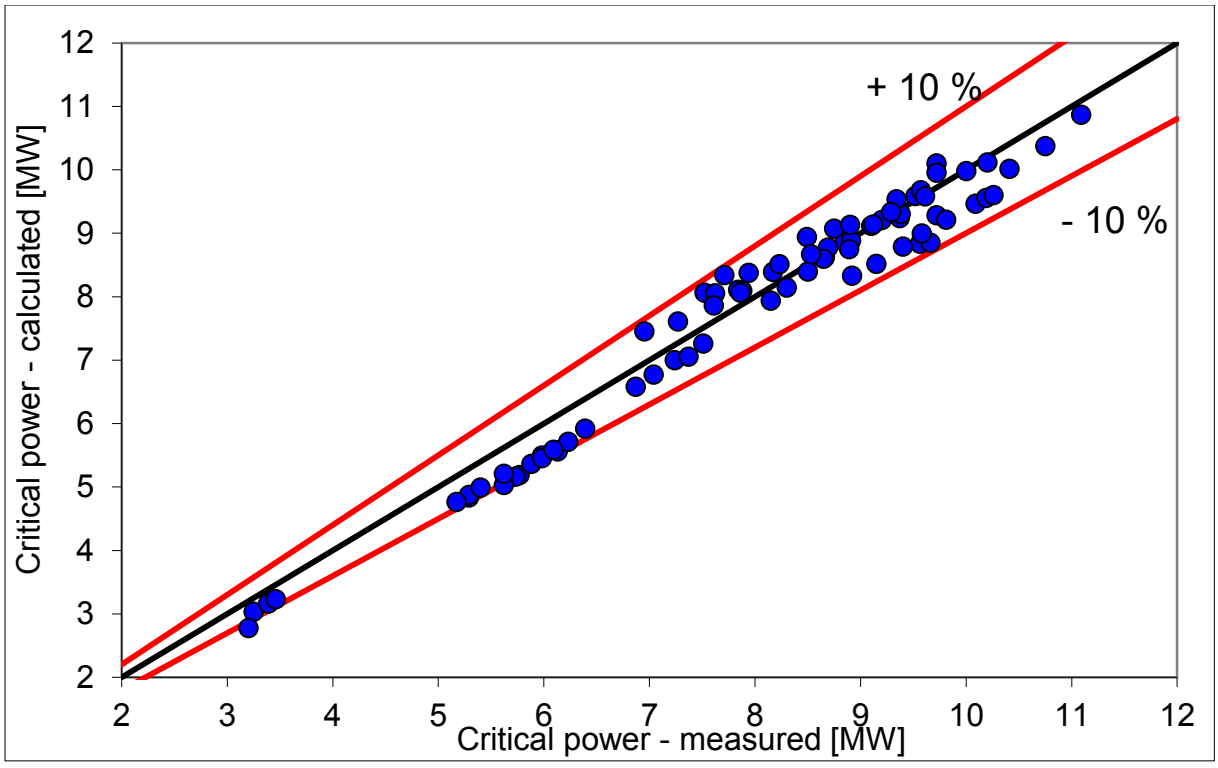

Figure 98 Calculated versus Measured Critical Power

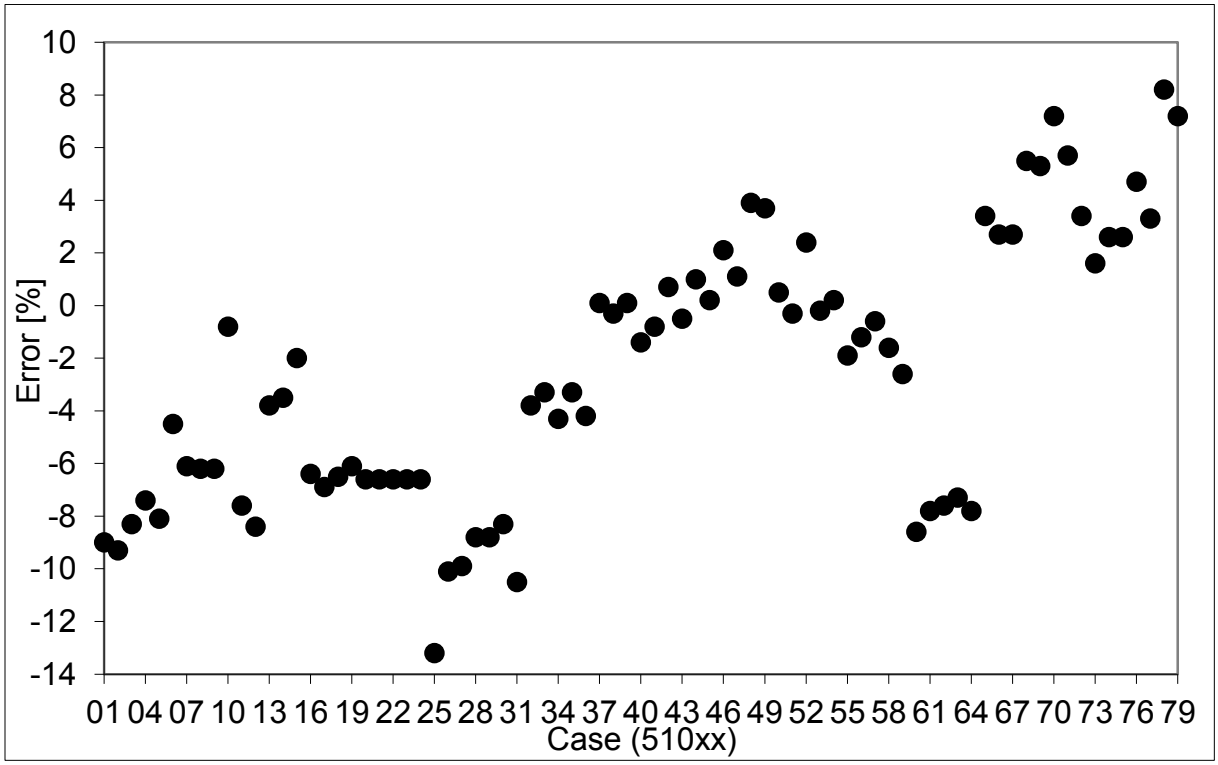

Figure 99 Percental Error of the Reference Values Compared to the Experimental Data for the Critical Power Cases

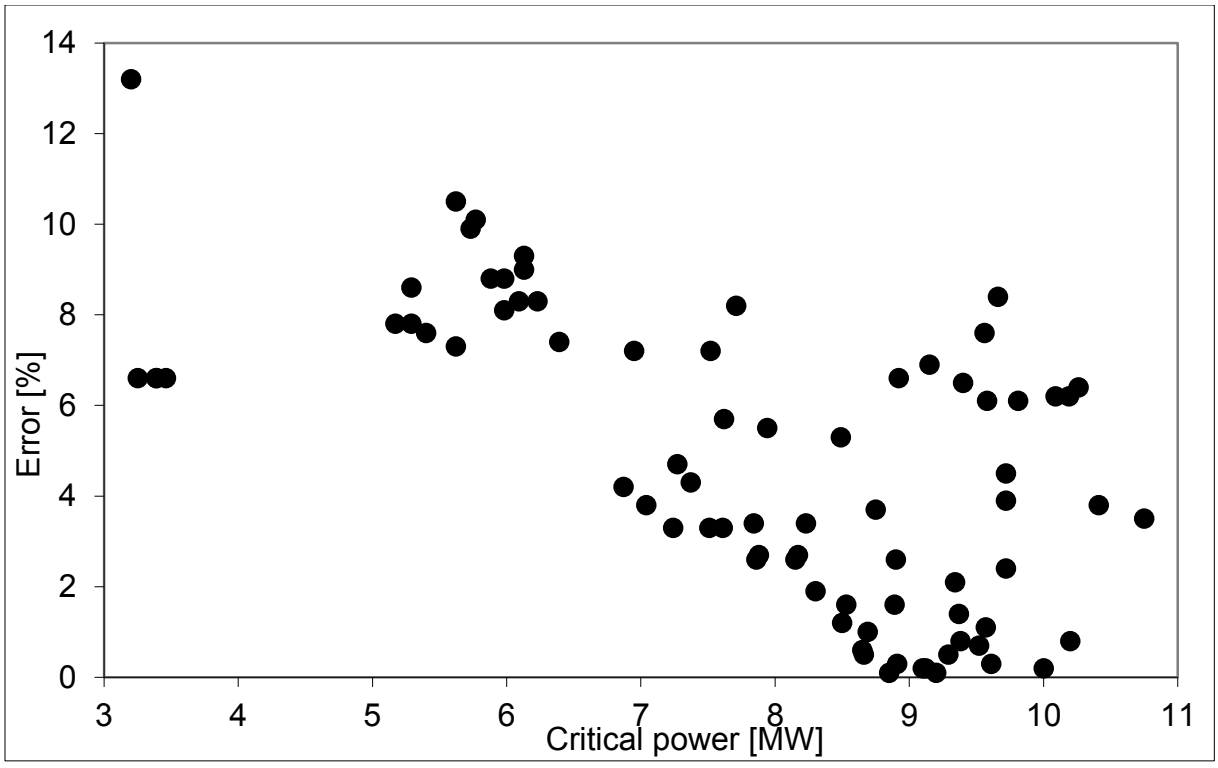

Figure 100 Error as Function of the Critical Power

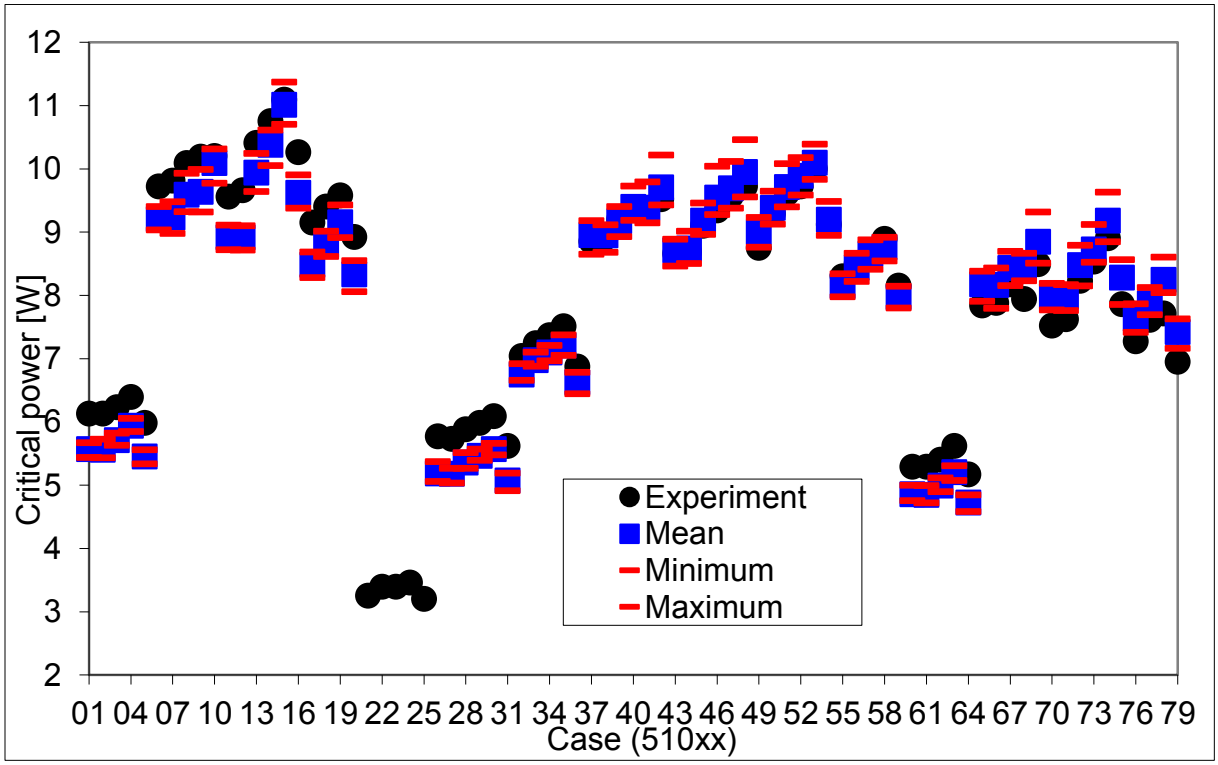

Figure 101 Comparison of the Experimental and Predicted Critical Power in Absolute Values

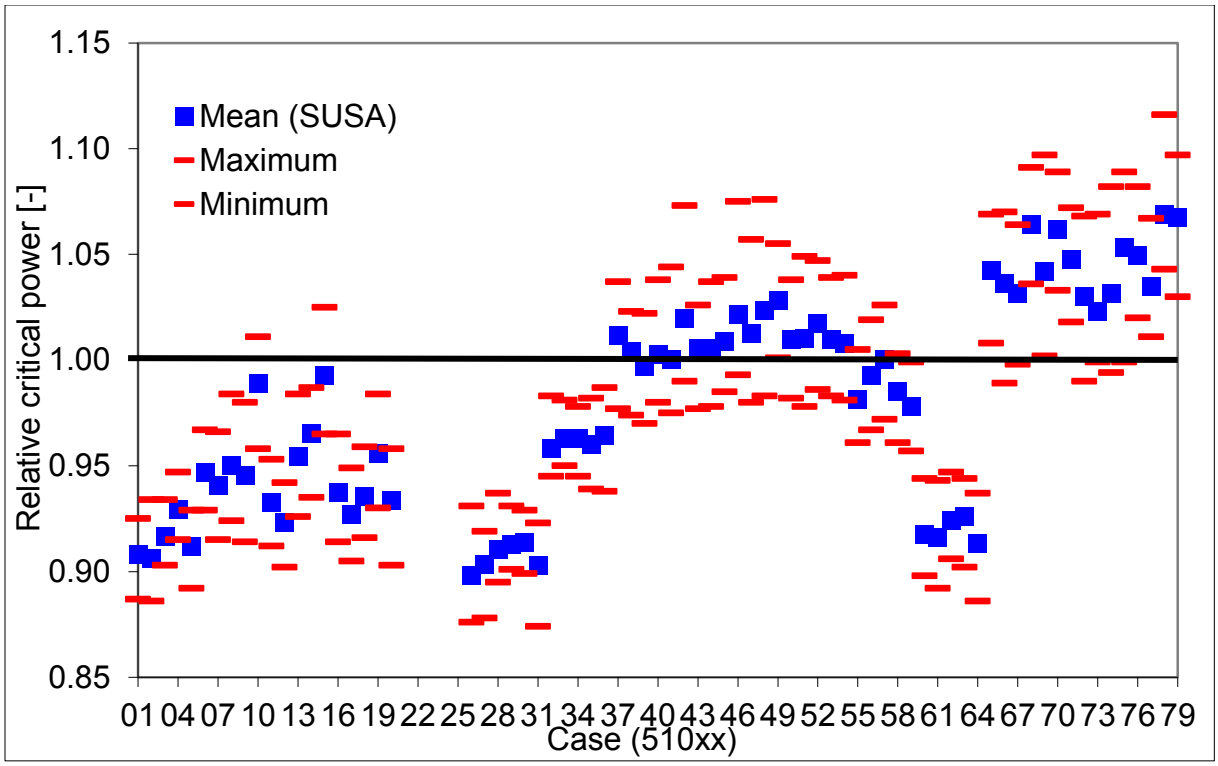

Figure 102 Comparison of the Experimental and Predicted Pressure Drops for Critical Power in Relative Values

As Figure 101 and Figure 102 indicate, no results are obtained for cases 51021 till 51025. As a matter of fact, during the execution of the 93 input decks for the uncertainty analysis not all execution delivered results. In some cases, the critical power ratio was not calculated by TRACE and hence the critical power could not be evaluated. Therefore, the affected critical power cases have been omitted from the analysis. Only the cases with an experimental value for the critical power of < 3.5 caused problems. These cases are also the ones where the lowest mass flow rate was considered.

Moreover, no results are given for TRACE-DAKOTA because the critical power ratio cannot be extracted with DAKOTA. As mentioned in sub section 5.3.3, the variable which is the subject of the investigation must be selected in DAKOTA. Unfortunately, that variable is not present and can therefore not be included in the analysis.

The results of the critical power investigation are also gathered in Table 31.

Table 31 Results of the Uncertainty Analysis for the Critical Power with TRACE-SUSA

Case	Ex [MW]	Mean [MW]	Max [MW]	Min [MW]	SD [MW]	Error [%]
51001	6.13	5.57	5.67	5.44	0.043	-9.21
51002	6.13	5.56	5.73	5.43	0.042	-9.37
51003	6.23	5.71	5.82	5.63	0.041	-8.34
51004	6.39	5.94	6.05	5.85	0.045	-7.06
51005	5.98	5.45	5.56	5.33	0.050	-8.82
51006	9.72	9.20	9.40	9.03	0.076	-5.32

Case	Ex [MW]	Mean [MW]	Max [MW]	Min [MW]	SD [MW]	Error [%]
51007	9.81	9.23	9.48	8.98	0.106	-5.93
51008	10.09	9.59	9.93	9.32	0.135	-4.97
51009	10.19	9.63	9.99	9.31	0.126	-5.46
51010	10.20	10.09	10.31	9.77	0.114	-1.09
51011	9.56	8.92	9.11	8.72	0.078	-6.74
51012	9.66	8.92	9.10	8.71	0.083	-7.69
51013	10.41	9.94	10.24	9.64	0.139	-4.55
51014	10.75	10.38	10.61	10.05	0.120	-3.47
51015	11.09	11.01	11.37	10.70	0.130	-0.74
51016	10.26	9.62	9.90	9.38	0.110	-6.27
51017	9.15	8.48	8.68	8.28	0.092	-7.30
51018	9.40	8.79	9.01	8.61	0.085	-6.45
51019	9.58	9.15	9.43	8.91	0.106	-4.44
51020	8.92	8.33	8.55	8.05	0.093	-6.61
51021	3.25					
51022	3.39					
51023	3.39					
51024	3.46					
51025	3.20					
51026	5.77	5.18	5.37	5.05	0.052	-10.18
51027	5.73	5.18	5.27	5.03	0.043	-9.65
51028	5.88	5.35	5.51	5.26	0.044	-8.95
51029	5.98	5.46	5.57	5.39	0.039	-8.71
51030	6.09	5.57	5.66	5.47	0.045	-8.61
51031	5.62	5.07	5.19	4.91	0.057	-9.73
51032	7.04	6.75	6.92	6.65	0.056	-4.16
51033	7.24	6.97	7.10	6.88	0.048	-3.69
51034	7.37	7.10	7.21	6.96	0.056	-3.70
51035	7.51	7.21	7.37	7.05	0.065	-4.02
51036	6.87	6.63	6.78	6.44	0.070	-3.56
51037	8.85	8.95	9.18	8.65	0.089	1.15
51038	8.91	8.95	9.11	8.68	0.085	0.41
51039	9.20	9.17	9.40	8.92	0.098	-0.32
51040	9.37	9.40	9.73	9.18	0.115	0.27
51041	9.38	9.38	9.79	9.15	0.133	0.02
51042	9.52	9.70	10.21	9.42	0.152	1.94
51043	8.66	8.71	8.89	8.46	0.079	0.54
51044	8.69	8.74	9.01	8.50	0.085	0.55
51045	9.10	9.18	9.45	8.96	0.095	0.85
51046	9.34	9.54	10.04	9.27	0.152	2.18
51047	9.57	9.69	10.12	9.38	0.124	1.25
51048	9.72	9.95	10.46	9.55	0.169	2.32
51049	8.75	9.00	9.23	8.76	0.095	2.81
51050	9.29	9.38	9.64	9.12	0.104	0.97
51051	9.61	9.71	10.08	9.40	0.132	1.05
51052	9.72	9.89	10.18	9.58	0.129	1.72
51053	10.00	10.10	10.39	9.83	0.129	0.97
51054	9.12	9.19	9.48	8.95	0.105	0.80
51055	8.30	8.15	8.34	7.98	0.074	-1.86

Case	Ex [MW]	Mean [MW]	Max [MW]	Min [MW]	SD [MW]	Error [%]
51056	8.50	8.44	8.66	8.22	0.085	-0.75
51057	8.65	8.65	8.87	8.41	0.110	0.04
51058	8.89	8.76	8.92	8.54	0.089	-1.47
51059	8.15	7.97	8.14	7.80	0.087	-2.21
51060	5.29	4.85	4.99	4.75	0.047	-8.25
51061	5.29	4.85	4.99	4.72	0.052	-8.40
51062	5.40	4.99	5.11	4.89	0.044	-7.58
51063	5.62	5.21	5.31	5.07	0.048	-7.38
51064	5.17	4.72	4.84	4.58	0.066	-8.66
51065	7.84	8.17	8.38	7.90	0.087	4.22
51066	7.88	8.16	8.43	7.79	0.099	3.61
51067	8.17	8.43	8.69	8.15	0.102	3.16
51068	7.94	8.45	8.66	8.23	0.102	6.40
51069	8.49	8.85	9.31	8.51	0.140	4.18
51070	7.52	7.98	8.19	7.77	0.099	6.18
51071	7.62	7.98	8.17	7.76	0.096	4.76
51072	8.23	8.48	8.79	8.15	0.126	3.02
51073	8.53	8.72	9.12	8.52	0.119	2.29
51074	8.90	9.18	9.63	8.85	0.141	3.14
51075	7.86	8.28	8.56	7.85	0.105	5.31
51076	7.27	7.63	7.87	7.42	0.084	4.94
51077	7.61	7.87	8.12	7.69	0.079	3.46
51078	7.71	8.24	8.60	8.04	0.133	6.90
51079	6.95	7.42	7.62	7.16	0.111	6.76

The sensitivity coefficients for the TRACE-SUSA analysis, except cases 51021 and 51025, are shown in Figure 103 and Table 32. The ranking is given in Figure 104. Based on the sensitivity coefficients, the inlet temperature (inlet sub-cooling) is the most important parameter. One can see that a reduction of the inlet temperature results in an increase of the critical power. This is because with a lower inlet temperature, more heat is needed to reach critical heat flux. In addition, all other parameters, besides inlet temperature, mass flow rate and hydraulic diameter, are of no or only low importance.

Besides the difficulties to calculate the critical power at certain parameter combinations, the U+S analysis provides also the coefficient of determination. For all previous investigations, that coefficient is close to unity indicating a well performed analysis. Unfortunately, that coefficient is here in the range of 0.15 to 0.8, indicating a sometimes rather poor performance, even though the qualitative and quantitative comparison of the reference results shows a good agreement, room for improvement is given.

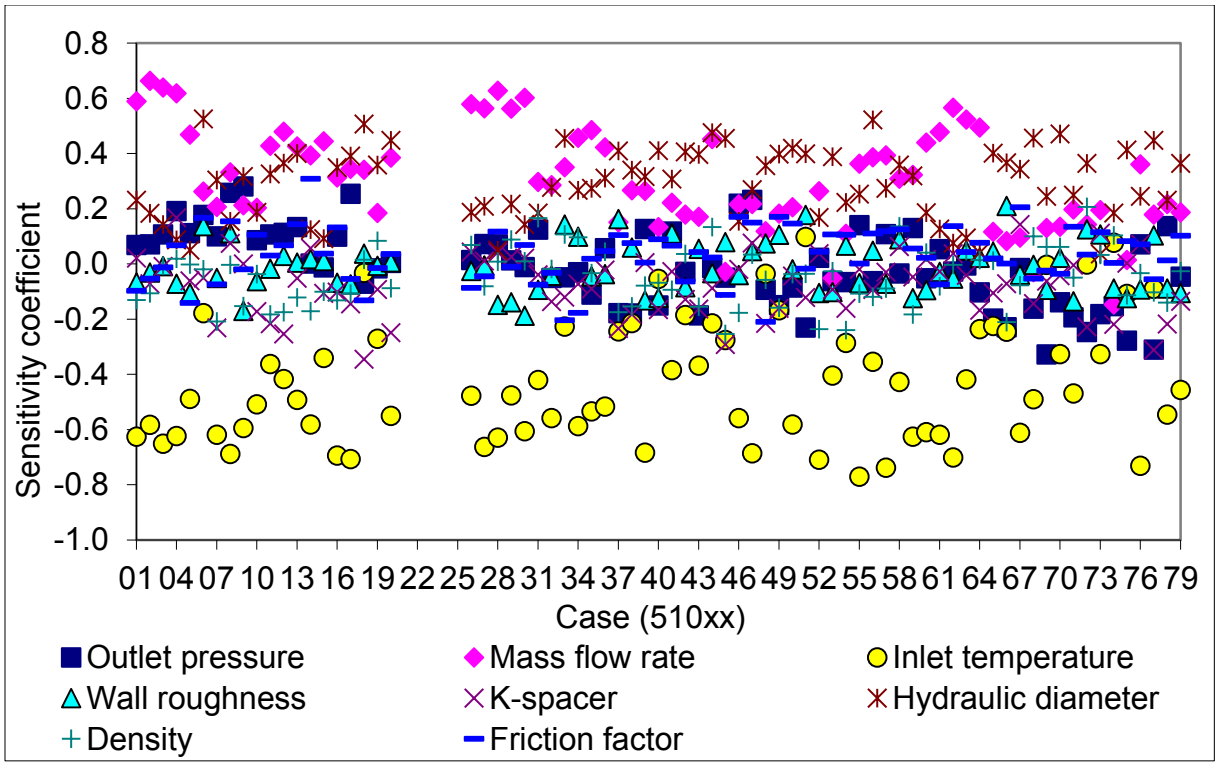

Figure 103 Sensitivity Coefficients for the Critical Power Analysis with TRACE-SUSA

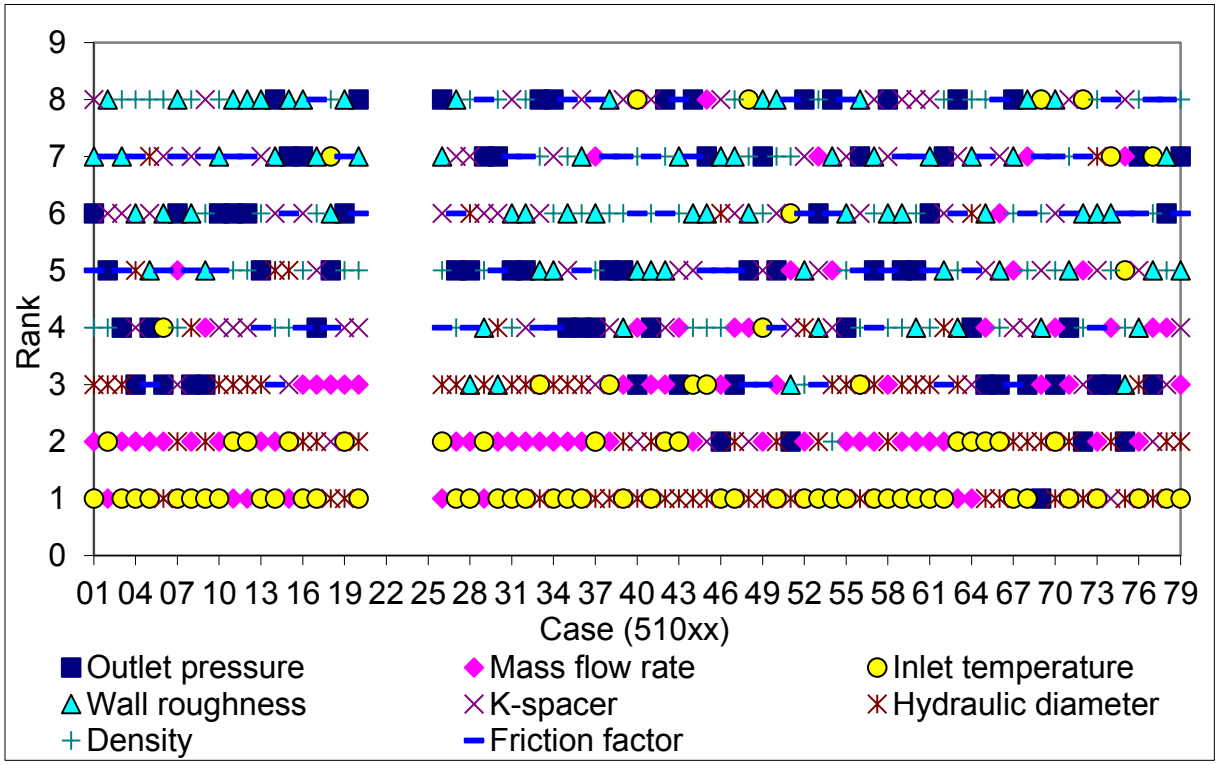

Figure 104 Ranking of the Uncertain Parameters for the Critical Power Analysis with TRACE-SUSA

Table 32 Pearson's Momentum Correlation Coefficients for the Critical Power Cases with TRACE-SUSA

	Outlet pressure	Mass flow rate	Inlet temperature	Wall roughness	K-spacer	Hydraulic diameter	Density	Friction factor
51001	0.069	0.590	-0.625	-0.067	0.021	0.231	-0.130	-0.097
51002	0.072	0.663	-0.583	-0.030	-0.071	0.184	-0.106	-0.053
51003	0.107	0.640	-0.651	-0.007	-0.009	0.143	-0.006	-0.012
51004	0.191	0.618	-0.624	-0.072	0.168	0.088	0.019	0.068
51005	0.111	0.468	-0.489	-0.105	-0.061	0.051	-0.002	-0.141
51006	0.178	0.262	-0.178	0.137	-0.050	0.525	-0.019	0.167
51007	0.101	0.207	-0.618	-0.051	-0.231	0.304	-0.208	-0.074
51008	0.258	0.332	-0.688	0.112	0.075	0.155	-0.003	0.155
51009	0.281	0.212	-0.594	-0.170	0.000	0.317	-0.153	-0.019
51010	0.086	0.203	-0.508	-0.063	-0.172	0.187	-0.037	0.106
51011	0.108	0.429	-0.362	-0.017	-0.216	0.327	-0.183	0.031
51012	0.113	0.479	-0.417	0.030	-0.254	0.365	-0.175	0.068
51013	0.134	0.426	-0.492	0.005	-0.051	0.400	-0.121	0.144
51014	0.002	0.394	-0.582	0.018	0.057	0.124	-0.171	0.308
51015	-0.013	0.444	-0.341	0.010	-0.107	0.092	-0.100	0.038
51016	0.099	0.314	-0.694	-0.068	-0.102	0.350	-0.132	0.133
51017	0.254	0.345	-0.706	-0.074	-0.145	0.391	-0.107	-0.054
51018	-0.071	0.341	-0.032	0.037	-0.345	0.507	0.015	-0.132
51019	-0.015	0.185	-0.271	-0.006	-0.092	0.359	0.084	-0.015
51020	0.004	0.385	-0.550	0.006	-0.249	0.448	-0.087	0.036
51021								
51022								
51023								
51024								
51025								
51026	0.014	0.579	-0.477	-0.025	0.043	0.187	0.069	-0.087
51027	0.072	0.563	-0.663	-0.005	0.011	0.209	-0.081	-0.045
51028	0.071	0.627	-0.629	-0.148	0.042	0.051	0.008	0.117
51029	0.014	0.563	-0.476	-0.139	0.026	0.218	0.088	-0.010
51030	-0.012	0.602	-0.606	-0.188	0.021	0.143	0.010	0.069
51031	0.124	0.298	-0.420	-0.093	-0.039	0.185	0.166	-0.075
51032	-0.050	0.285	-0.558	-0.042	-0.136	0.277	-0.018	-0.032
51033	-0.048	0.351	-0.226	0.143	-0.120	0.455	0.107	-0.204
51034	-0.030	0.457	-0.587	0.099	-0.072	0.267	0.096	-0.177
51035	-0.111	0.485	-0.534	-0.045	-0.090	0.274	-0.033	0.019
51036	0.057	0.423	-0.517	-0.036	-0.021	0.311	0.044	0.047
51037	-0.178	0.152	-0.245	0.163	-0.234	0.410	-0.175	0.105
51038	-0.179	0.268	-0.215	0.060	-0.182	0.340	-0.154	0.076
51039	0.127	0.265	-0.683	-0.132	0.005	0.317	-0.078	0.005
51040	-0.150	0.134	-0.055	-0.122	-0.166	0.411	-0.068	0.090
51041	0.118	0.222	-0.384	0.111	-0.028	0.307	-0.094	0.066
51042	-0.029	0.179	-0.185	-0.084	-0.129	0.406	0.037	-0.064

	Outlet pressure	Mass flow rate	Inlet temperature	Wall roughness	K-spacer	Hydraulic diameter	Density	Friction factor
51043	-0.187	0.171	-0.369	0.055	-0.163	0.397	-0.155	0.044
51044	-0.015	0.453	-0.216	-0.033	-0.087	0.476	0.134	0.024
51045	-0.049	-0.029	-0.276	0.080	-0.292	0.455	-0.253	-0.112
51046	0.218	0.216	-0.558	-0.040	-0.019	0.155	-0.177	0.171
51047	0.233	0.218	-0.686	0.047	0.076	0.270	0.034	0.150
51048	-0.093	0.118	-0.036	0.075	-0.215	0.356	-0.057	-0.210
51049	-0.149	0.183	-0.167	0.107	-0.160	0.399	-0.159	0.171
51050	-0.085	0.205	-0.581	-0.020	-0.044	0.419	-0.037	0.146
51051	-0.231	0.099	0.098	0.178	-0.122	0.399	-0.036	-0.017
51052	0.022	0.264	-0.709	-0.106	0.038	0.169	-0.236	0.045
51053	-0.062	-0.052	-0.404	-0.101	-0.092	0.389	-0.026	0.107
51054	-0.066	0.109	-0.286	0.066	-0.160	0.223	-0.240	0.106
51055	0.141	0.363	-0.770	-0.069	-0.020	0.253	-0.108	0.002
51056	-0.062	0.387	-0.354	0.048	-0.092	0.522	-0.119	0.111
51057	0.109	0.393	-0.738	-0.071	-0.030	0.275	-0.089	0.119
51058	-0.034	0.309	-0.427	0.090	0.063	0.359	0.136	0.126
51059	0.130	0.323	-0.626	-0.124	-0.047	0.319	-0.183	0.056
51060	-0.052	0.440	-0.610	-0.094	0.017	0.186	0.041	0.022
51061	0.054	0.478	-0.619	-0.029	-0.028	0.127	-0.080	-0.074
51062	-0.028	0.567	-0.701	-0.053	0.038	0.076	-0.003	0.138
51063	-0.005	0.523	-0.418	0.049	-0.041	0.094	0.046	0.044
51064	-0.103	0.495	-0.236	0.023	-0.167	0.041	0.014	0.077
51065	-0.197	0.116	-0.225	0.044	-0.105	0.401	0.012	0.020
51066	-0.229	0.083	-0.245	0.210	-0.071	0.367	-0.211	0.001
51067	-0.015	0.095	-0.612	-0.039	0.144	0.344	-0.077	0.205
51068	-0.162	-0.030	-0.490	-0.003	-0.143	0.455	0.100	-0.053
51069	-0.327	0.130	-0.003	-0.093	-0.062	0.245	0.062	-0.024
51070	-0.139	0.135	-0.327	0.022	-0.042	0.471	0.062	-0.036
51071	-0.194	0.197	-0.470	-0.135	-0.004	0.250	-0.050	0.135
51072	-0.247	0.143	-0.002	0.126	-0.228	0.365	0.206	0.034
51073	-0.182	0.195	-0.326	0.107	0.112	0.037	0.033	0.115
51074	-0.152	-0.147	0.077	-0.089	-0.219	0.184	0.104	0.004
51075	-0.278	0.014	-0.108	-0.123	0.002	0.413	-0.113	0.083
51076	0.071	0.361	-0.731	-0.093	0.072	0.246	-0.033	0.071
51077	-0.310	0.179	-0.090	0.104	-0.312	0.448	-0.103	-0.055
51078	0.137	0.217	-0.546	-0.089	-0.218	0.231	-0.140	0.013

6.6 Transient Analyses

For the present analysis two transients, based on phase 1, exercise 3 of the NUPEC BFBT benchmark, are selected. The first transient is a turbine trip without bypass and the second one is a re-circulation pump trip. Information regarding the time depended trends of the inlet temperature, the bundle mass flow rate, the outlet pressure and the assembly power are provided. These time trends will be used as input and boundary conditions for the uncertainty and sensitivity

study. These time-dependent trends are given in Figure 105 till Figure 108. Both transients start from steady state conditions, first 10 seconds of the plots.

At 10 seconds the turbine is isolated. The outlet pressure changes due to the fast closure of the turbine isolation valve. That causes a pressure wave which is propagating from the main steam line through the core. As a consequence, the water level collapses and a better moderation takes place since the density is higher. That improved moderation leads then an increase of the power. In order to stabilize the system and to reduce the power, the pumps are throttled. The whole procedure takes place within 35 to 40 seconds (starting at second 10). Later on, the mass flow rate is increased to nominal condition.

During the pump trip the mass flow rate is reduced resulting in a higher void fraction. With increased void fraction the moderation is deteriorated and the power is decreasing. The impact on the outlet pressure is not as pronounced as during the turbine trip. For the next 30 seconds the mass flow rate is stable at 1/3 of the nominal value. At second 40 the pump(s) are back online and the mass flow rate increases as the power does.

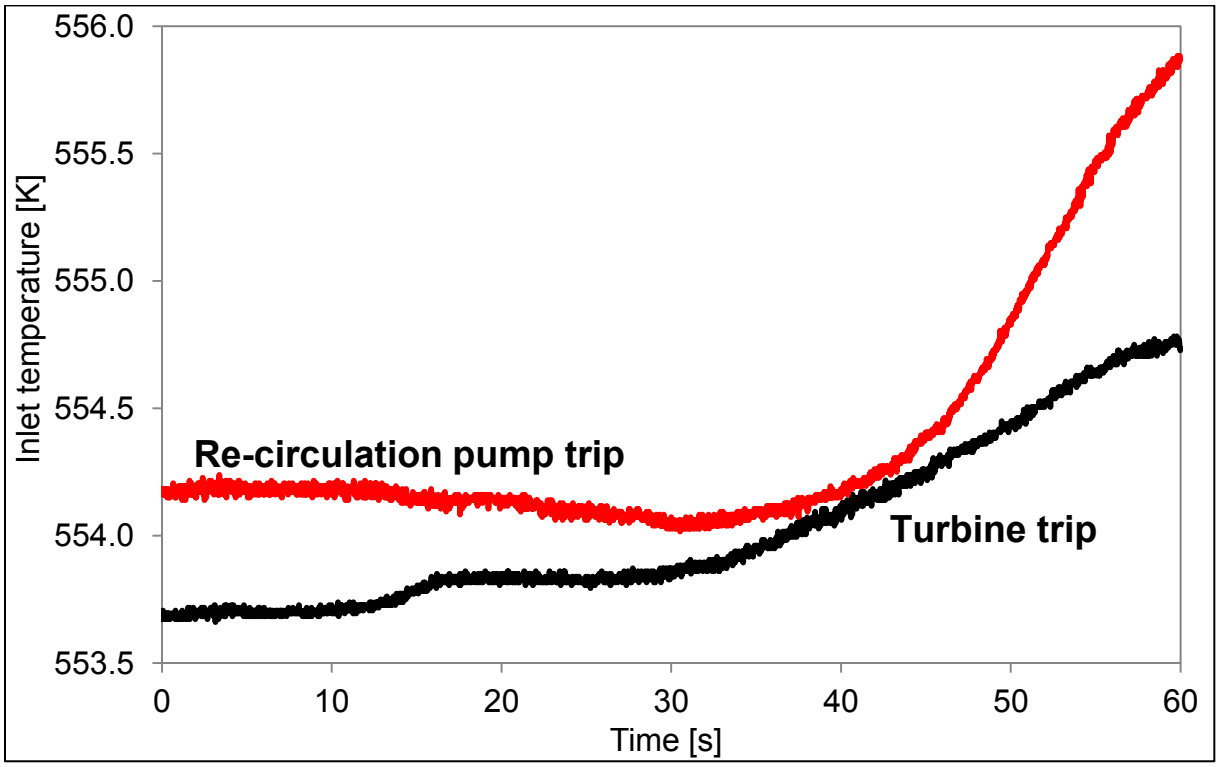

Figure 105 Inlet Temperature Evolution During the Transients

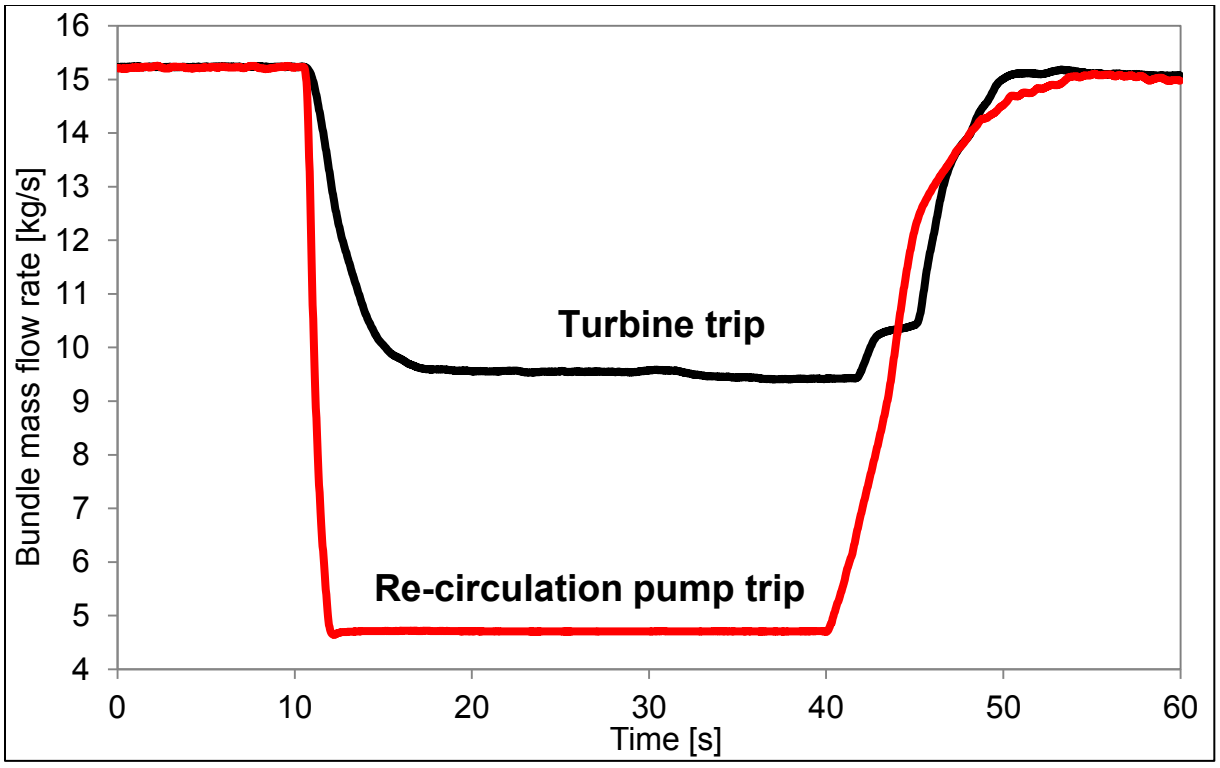

Figure 106 Bundle Mass Flow Rate Evolution During the Transients

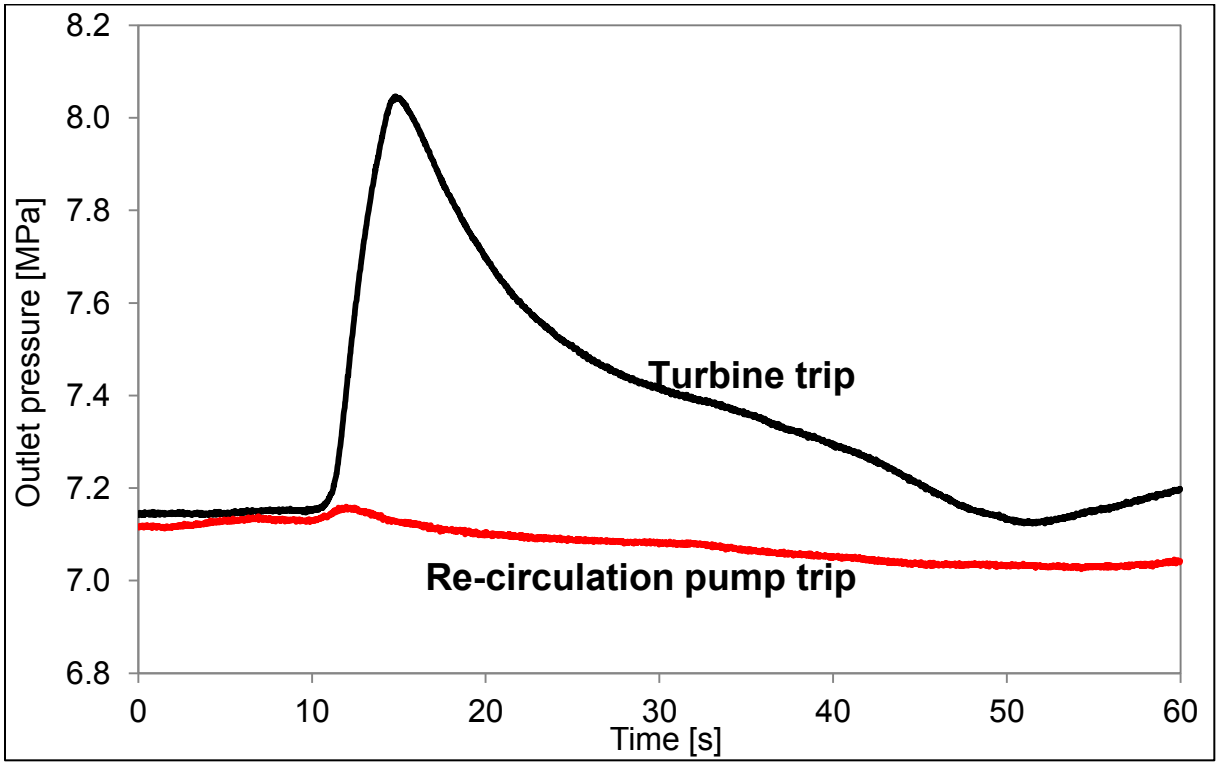

Figure 107 Outlet Pressure Evolution During the Transients

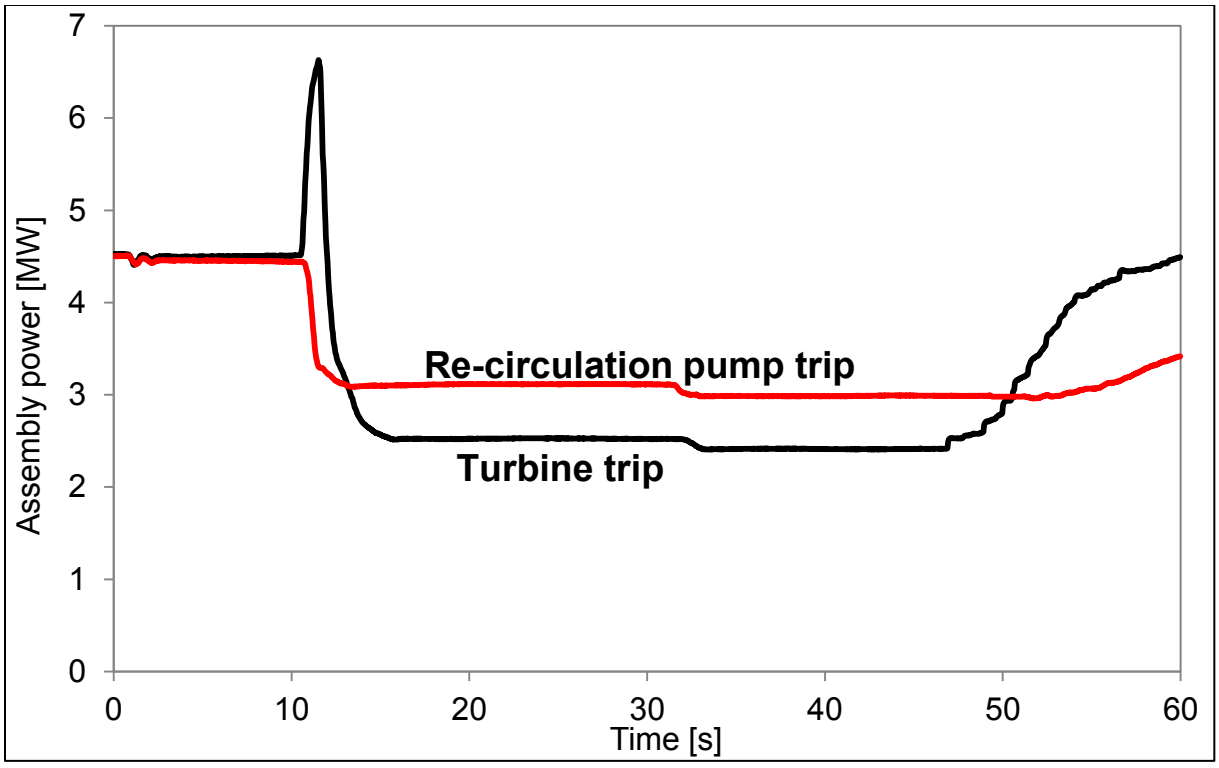

Figure 108 Assembly Power Evolution During the Transients

6.6.1 Results for the Pressure Drop

The transient pressure drop for the turbine trip and the re-circulation pump trip are plotted in Figure 109 and Figure 110, respectively. The plots contain the experimental data (yellow dots), the mean value of the uncertainty calculations for TRACE-SUSA (black line) and TRACE-DAKOTA (grey line) as well as their uncertainty band; red for TRACE-SUSA and blue for TRACE-DAKOTA.

The experimental data show a rather large spread which seems to be to high keeping in mind a reported uncertainty of the pressure of just 1 %. The reason is related to the used pressure sensors. As mentioned in sub section 3.4, the differential pressure taps have only been used for the steady state scenarios (e.g. dpt9 for the total pressure drop). During the transients, the absolute pressure sensors PTN010 and PTN007 were used. The specification does not distinguish between the different sensors when assigning a general pressure (drop) uncertainty of 1 %. But if one takes the difference of two absolute pressure sensors and the difference is rather small even a small uncertainty will yield to a large spread of the resulting pressure difference. As example, for the turbine trip the inlet pressure at second 0 is 7.241 MPa and the outlet pressure is 7.141 MPa. An uncertainty of 1 % would be 0.07 MPa or 70000 Pa. The difference between outlet and inlet is at the beginning of the transient only 100000 Pa. With that in mind, the large spread of the experimental data is comprehensible but sobering. An explanation why the absolute pressure taps instead of the differential pressure taps dpT9 was used cannot be found in the specification. An explanation could be a faster sampling time of the absolute sensors compared to the differential ones.

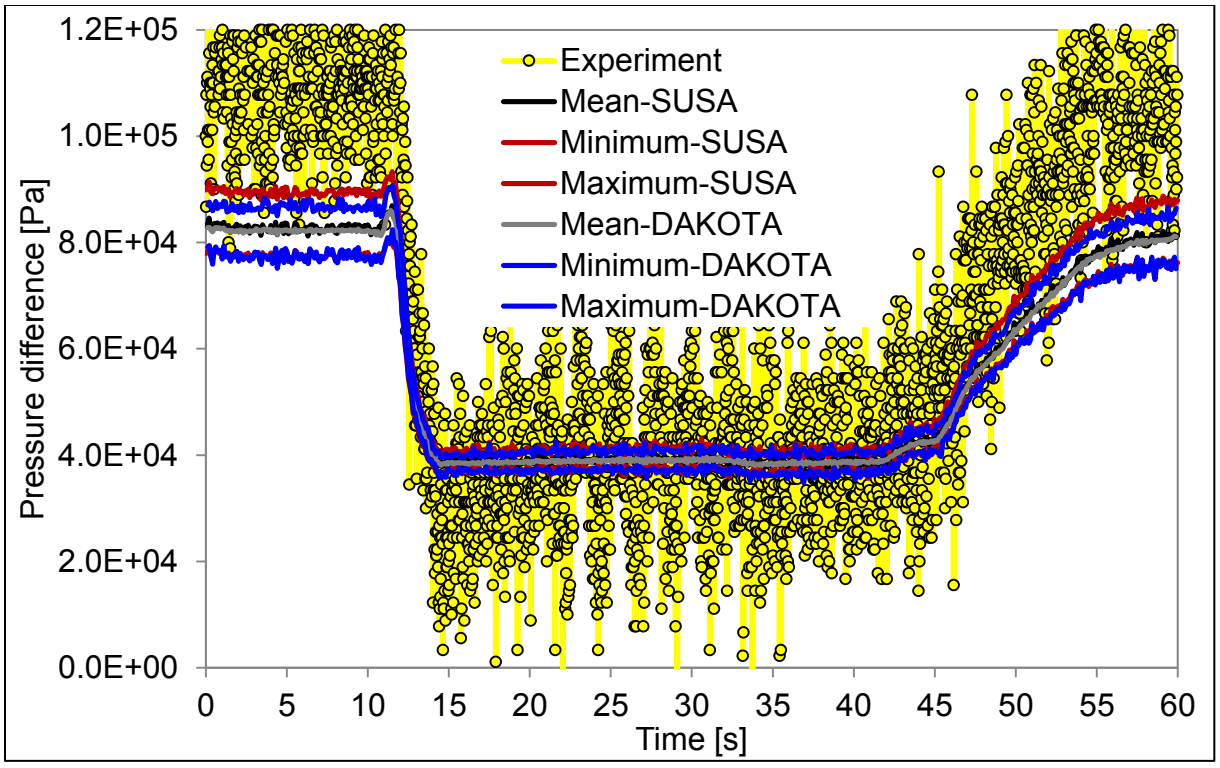

Figure 109 Pressure Drop During the Turbine Trip Transient

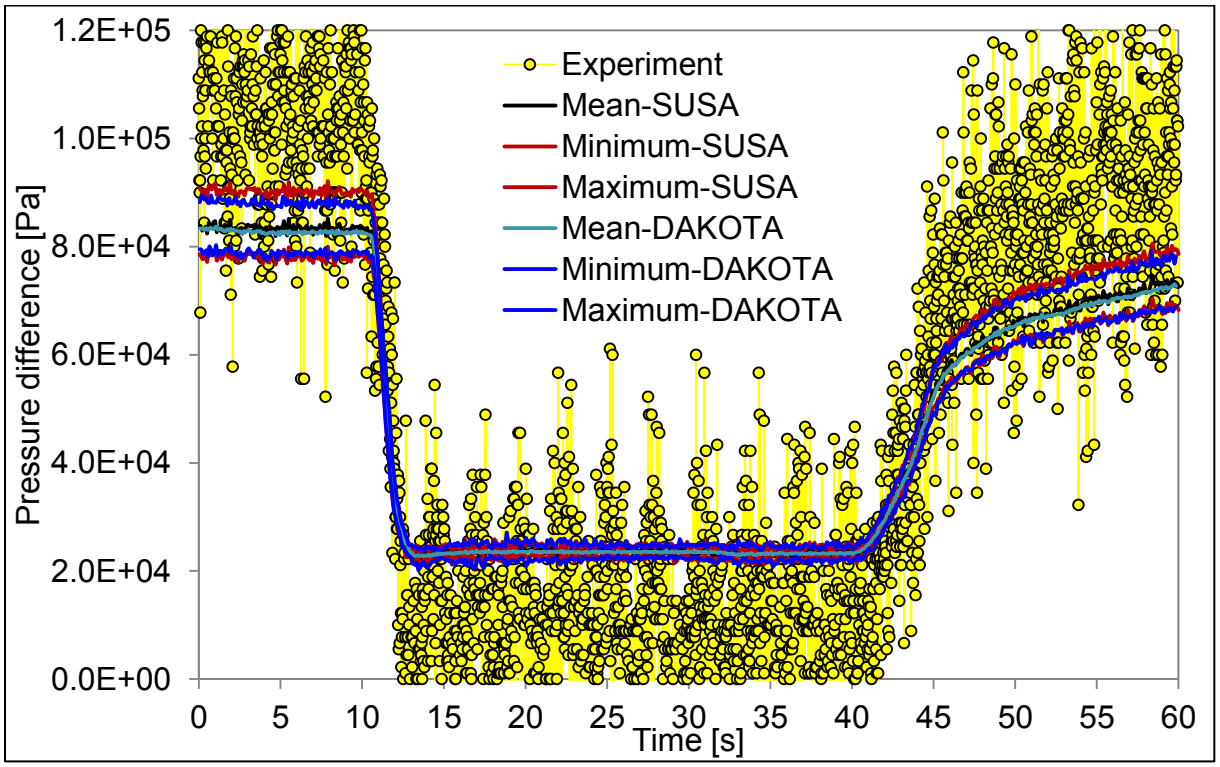

Figure 110 Pressure Drop During the Re-Circulation Pump Trip

As the initial and boundary conditions show, the variations, as a function of time, are not limited to the mass flow rate. As explained above, the initiating event (closure of the turbine valve and shut down of a re-circulation pump) will also affect the power and the pressure with different magnitudes. The change of the power will change the void fraction in the bundle and therefore the pressure drop is not only a function of the mass flow rate since density and velocity will change in axial direction.

The TRACE predictions show an underestimation during the beginning (second 0 – 10) and at the end (second 45 – 60) of the transient. As mentioned above, at the beginning of the transient the experimental pressure difference was around 1 bar. TRACE predicts a value of around 0.825 bar. Between second 10 and 40 the TRACE predictions are much closer to the average experimental value. For the turbine trip, the TRACE predictions are almost identical to the average experimental data. In both cases, a pressure drop of about 0.4 bar can be read from the plots. For the re-circulation transient, the TRACE predictions with around 0.2 bar are twice as high as the average experimental value, 0.1 bar. A check of the transient boundary conditions shows that for the turbine trip the reduction of the mass flow rate is from 100 % to around 66 %. The resulting experimental pressure drop reduction is therefore reasonable. For the re-circulation pump trip, the mass flow rate is reduced from 100 % to around 33 %. Again, the resulting reduction of the experimental pressure drop is understandable.

One result of the present uncertainty study is that during normal operation (100 % mass flow rate) the pressure drop is subject of a variation of ± 0.04 bar while for the transient part (reduced mass flow rate) the error band is ± 0.02 bar and ± 0.01 bar for the turbine trip and the re-circulation pump trip, respectively.

It is also visible that the uncertainty band is wider for DAKOTA than for SUSA even though less parameters are considered in the TRACE-DAKOTA study. That is due to the different treatment of the inlet temperature during the uncertainty study; please refer to sub section 6.2.

The results of the sensitivity analysis with SUSA for the pressure drop are given in Figure 111. As one can see, the sensitivity coefficients of inlet temperature, hydraulic diameter and form loss coefficient (the three most important ones in terms of influence of their variation) change with time. The changes are rather small but observable. The hydraulic diameter, as parameter with the highest importance, is gaining importance for the time the mass flow rate is reduced. That behavior is more pronounced during the re-circulation pump trip since the mass flow rate reduction is considerably larger.

The importance of the inlet temperature is reduced during the reduced mass flow rate period. It drops from values of 0.4 to about 0.2 for the turbine trip and 0.1 for the re-circulation pump trip. The form loss coefficient, on the contrary, is slightly gaining importance. For both transients the sensitivity coefficients are similar.

6.6.2 Results for the Void Fraction

The void fraction for the three X-ray densitometer positions, 682, 1706 and 2730 mm during the turbine trip are plotted in Figure 112, Figure 113 and Figure 114, respectively. Even though the X-ray CT scanner has been used during the transient void fraction measurements, only the first couple of seconds have been reported. Therefore, the comparisons of predictions to X-ray CT scanner results are not shown in this report.

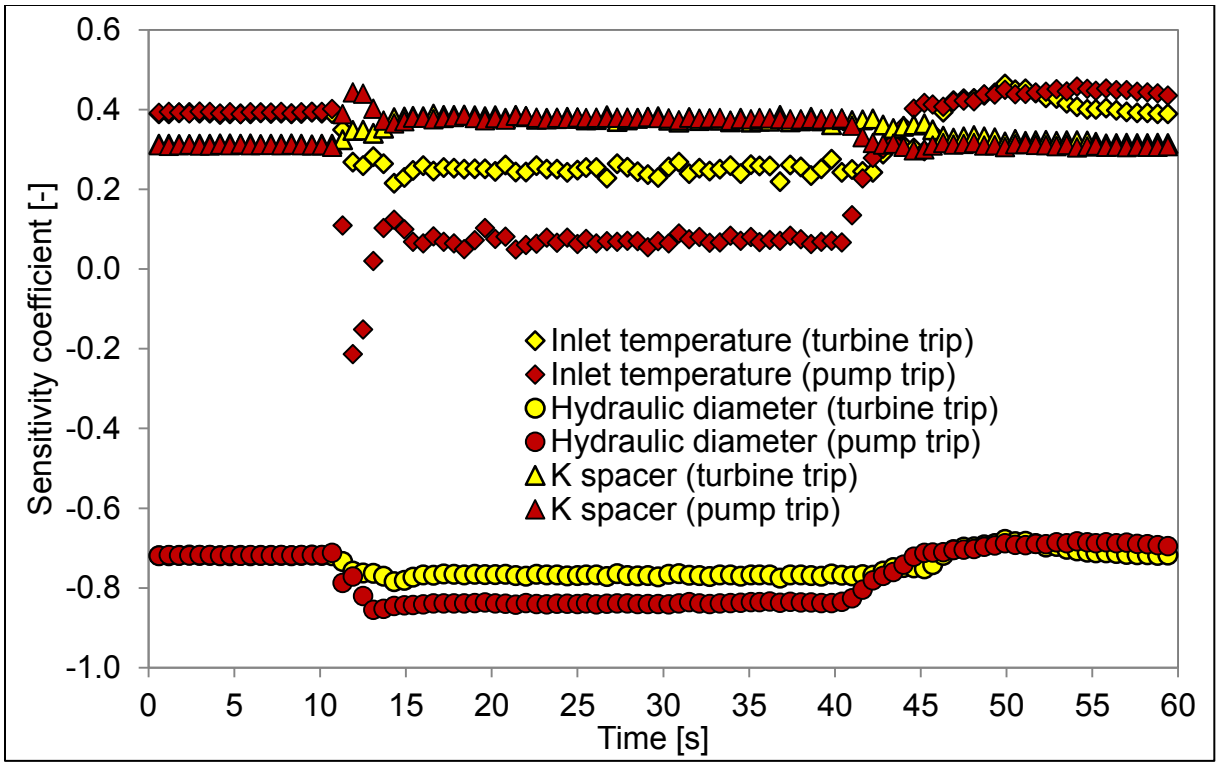

Figure 111 Sensitivity Coefficients for the Transient Pressure Drop Analysis with SUSA

Each of the mentioned plots shows the original reported measured void fraction and the corrected one in order to see the improvement and the behavior over time. The mean values for TRACE-SUSA and TRACE-DAKOTA are plotted along with their corresponding maximum and minimum values. What is plotted there are the mean, maximum and minimum values based on the 93 runs for each interval. In SUSA, the 60 seconds transient time are split into 100 equidistant intervals. For each interval the mean is calculated and the minimum and maximum are derived. In theory, each maximum and minimum can originate from different runs since it is not taking the one which has the overall minimum or maximum and a given time.

The impact of changing input and boundary conditions can clearly be seen. During the turbine trip, the power is increased for a short period of time resulting in a sharp increase of the void fraction. This is followed by a very pronounced drop of the void fraction due to the mass flow rate reduction. Afterwards, the void fraction rises continuously due to the slowly decreasing pressure, which results in a reduced saturation temperature and therefore a higher void generation. After the power, pressure and mass flow rate are reestablished to nominal condition the void fraction at the end of the transient (60 sec.) is almost identical to the one at the beginning (0 sec.).

The diagrams also show that the correction is most effective at higher void fractions. Especially at the lowest densitometer one can see a clear difference between the beginning of the transient (high void) and the void at second 15. There, the difference between original and corrected is barely visible. The qualitative comparison of the mean values of TRACE-SUSA and TRACE-DAKOTA show a good agreement for all three positions. Especially, for the second level (1706 mm), the prediction and the experimental data are almost identical. For the lower and the upper level one can see a trend to overestimate the experiment.

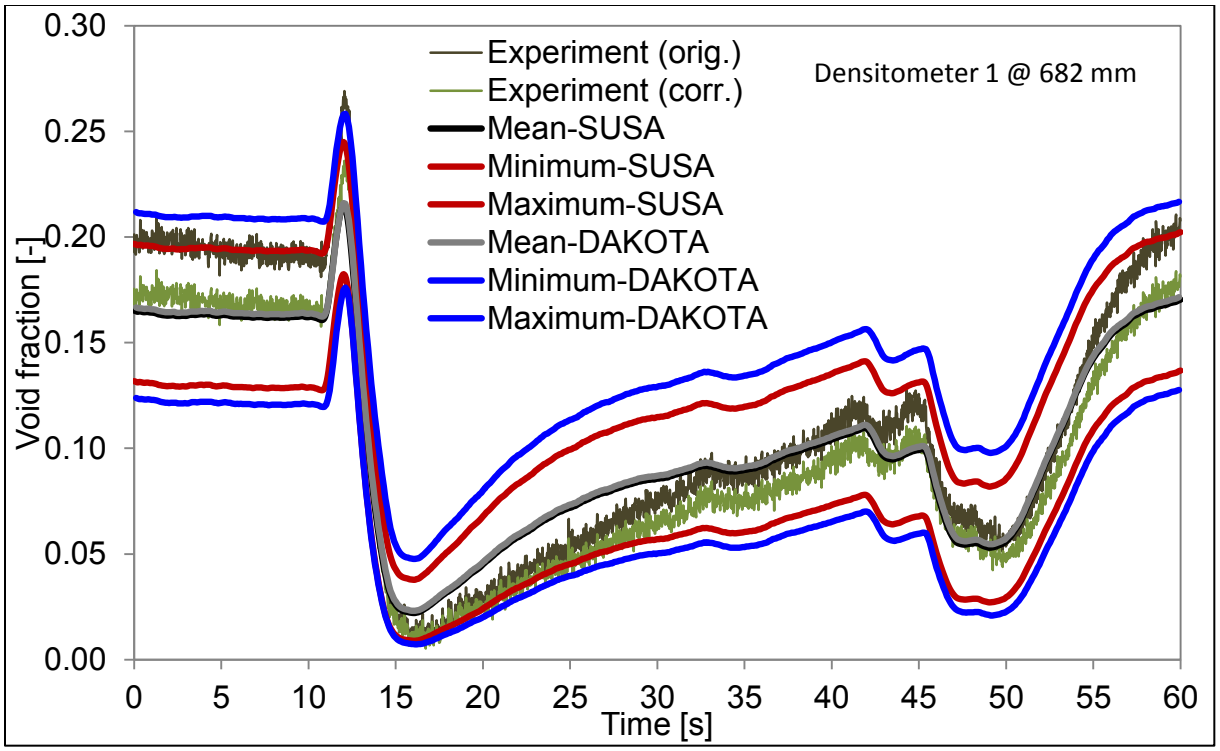

Figure 112 Void Fraction Predictions with Uncertainty Band Compared to Original and Corrected Turbine Trip Measurements for the First Densitometer at 682 mm

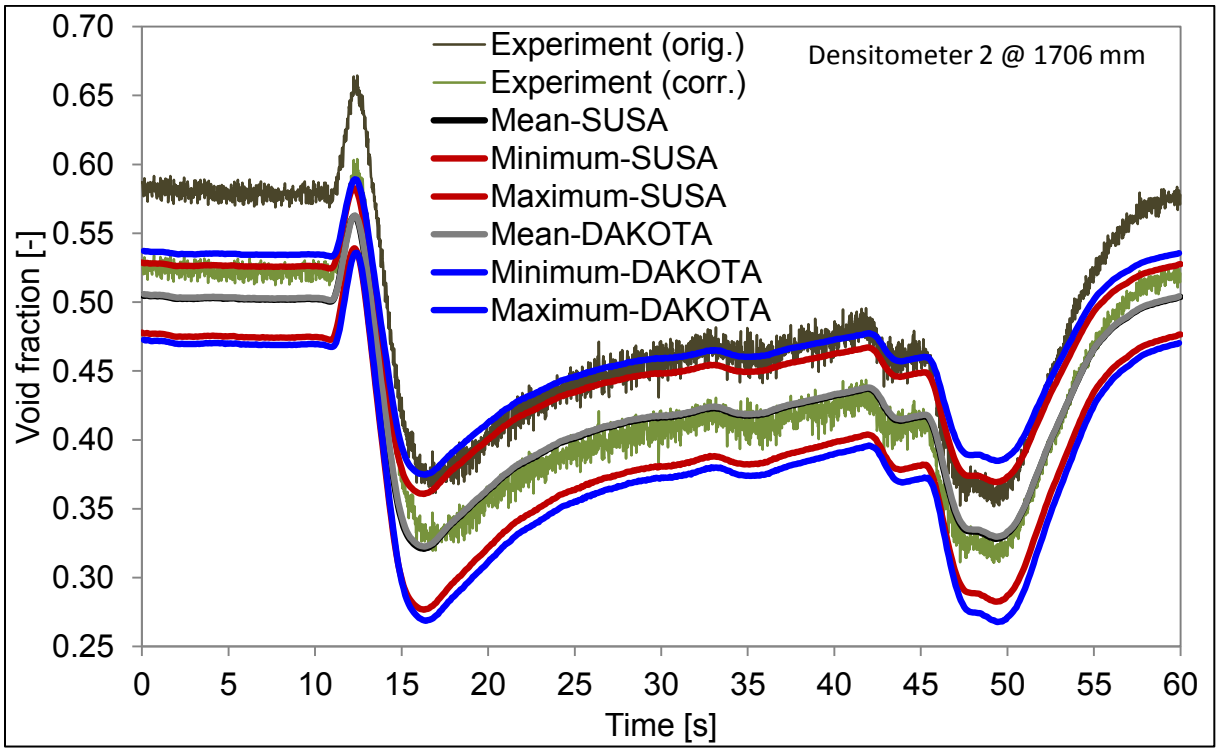

Figure 113 Void Fraction Predictions with Uncertainty Band Compared to Original and Corrected Turbine Trip Measurements for the Second Densitometer at 1706 mm

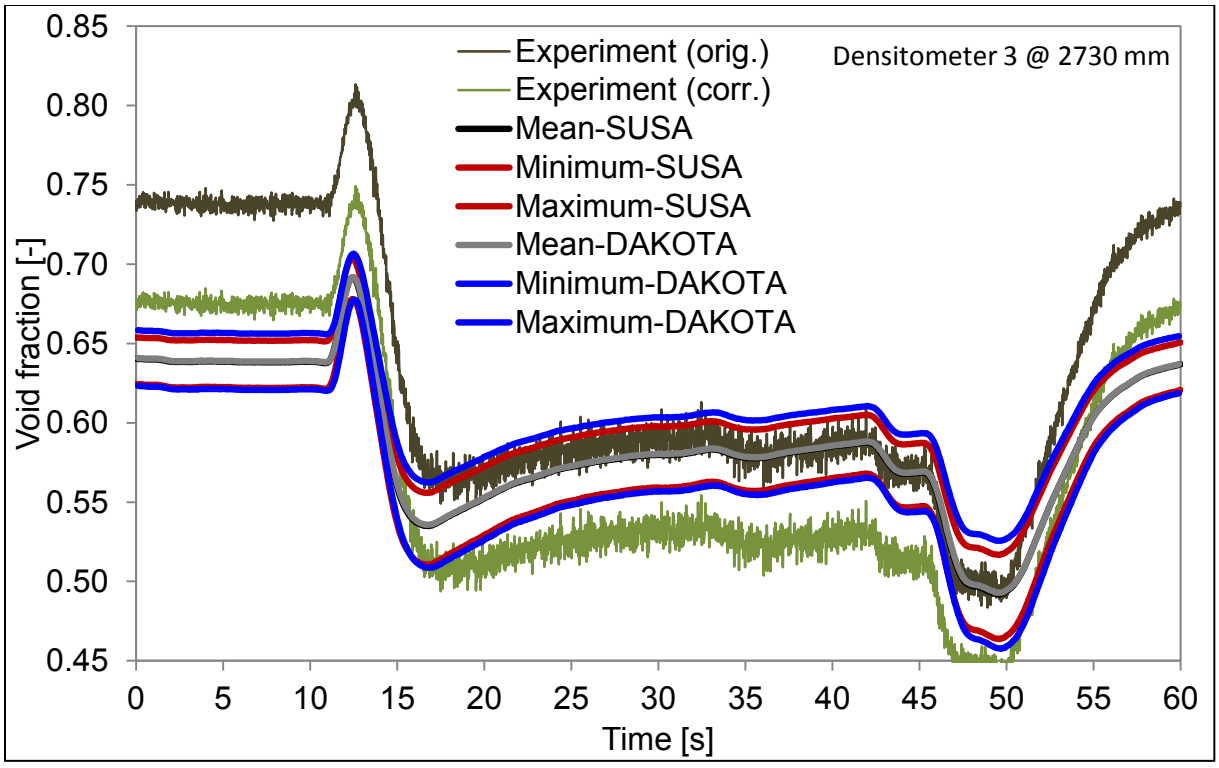

Figure 114 Void Fraction Predictions with Uncertainty Band Compared to Original and Corrected Turbine Trip Measurements for the Third Densitometer at 2730 mm

The quantitative comparison, given in Figure 115, shows the deviation of the calculated value from the corrected experimental one in percent. Even though the qualitative comparison seems to be good for the lower level a deviation of more than 100 % can be seen directly following the power peak (around second 15). Steadily, the deviation reduces with a progressing transient until second 45. A closer look to Figure 112 shows that at second 15 the experimental void fraction is around 0.01 while the prediction gives 0.02. This means a factor of 2 (100 % deviation) in relative words but the absolute deviation is marginal, and from the practical point of view it can be neglected. In general, TRACE and other system codes have problems at low void fractions where a transition from sub cooled boiling to nucleate boiling takes place.

For the other two axial positions, the deviations are within ± 10 %. In general, there is an underestimation at the beginning and at the end of the transient (0 – 10 and 55 – 60 sec.) and an overestimating during the transient (10 – 55 sec.).

One reason for the deviations, besides the applicability of the physical models used in TRACE, is the nodalization. As mentioned, the axial locations of the sensors are at 682, 1706 and 2730 mm. With the rather coarse nodalization of TRACE it is impossible to extract the void fraction at exactly 682 mm. In order to calculate them at the three given positions, a much finer nodalization would be necessary including different axial cell lengths. From practical point of view TRACE models are not intended to have cell lengths of just a few mm. In addition, the corrective measure might not represent the reality but a possible one.

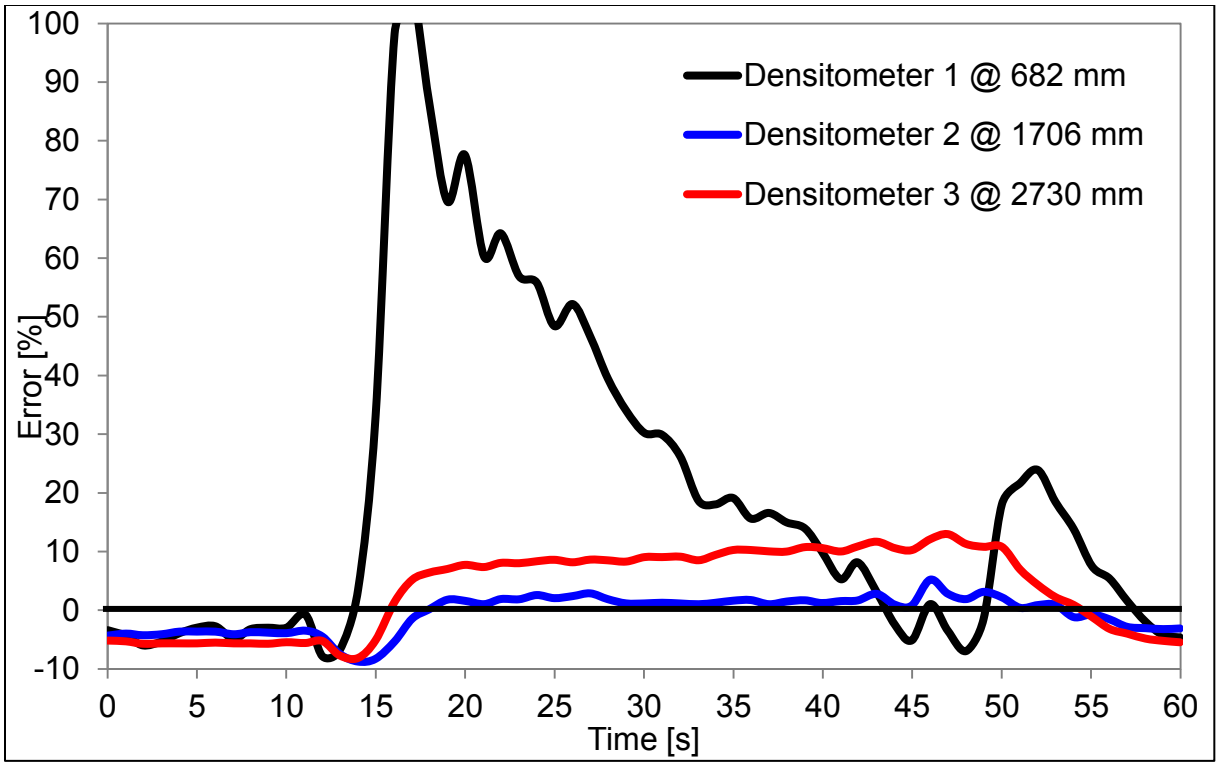

Figure 115 Deviation of the Fredictions from the Corrected Turbine Trip Measurements for all Three Densitometer Positions

The plots show also that the uncertainty band is getting smaller with increasing void fractions. That phenomenon has been seen during the steady state scenarios for the void fraction post-test simulations.

Besides that, one can see that the uncertainty band of TRACE-SUSA is enveloped by the one of TRACE-DAKOTA. That seems to be unrealistic since with TRACE-SUSA more parameters have been considered and hence the uncertainty band of TRACE-SUSA should envelop the one of TRACE-DAKOTA. As the steady state investigations of the void fraction showed, the hydraulic diameter, e.g., is not of importance for the void. Therefore, both uncertainty bands should be identical. The reason for that situation is, most likely, the treatment of the inlet temperature. In sub section 6.2, the problems have been mentioned which arose with the transient temperature treatment. Since the ± 1.5 K could not be considered a multiplier was used instead. Ranging from 0.997 to 1.003, the resulting temperatures for e.g. 554 K would be 555.62 K (554 x 1.003), which is slightly higher than the 555.5 which would be obtained with the ± 1.5 K (554 + 1.5) procedure. The steady state void fraction results showed also that the inlet temperature (inlet sub-cooling) is the parameter where a change of it has the biggest impact.

The void fraction recorded and predicted for the re-circulation pump trip are given in Figure 116, Figure 117 and Figure 118 for 682, 1706 and 2730 mm, respectively. During this transient, only power and mass flow rate change. After 10-15 seconds, the mass flow rate is reduced which automatically provokes a rise in the void fraction. That rise would be even more pronounced since the mass flow rate reduces to 33 % of the nominal values if the power is reduced. Therefore, a stable void fraction is established between second 15 and 40.

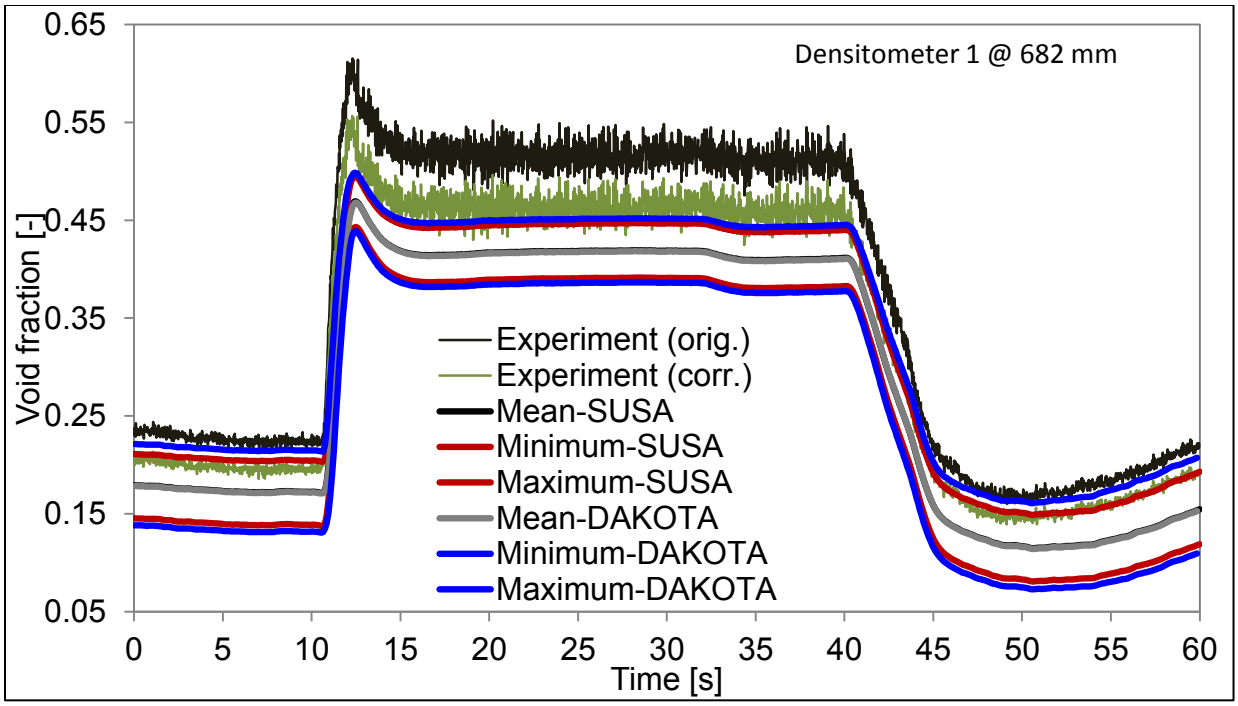

Figure 116 Void Fraction Predictions with Uncertainty Band Compared to Original and Corrected Re-Circulation Pump Trip Measurements for the First Densitometer at 682 mm

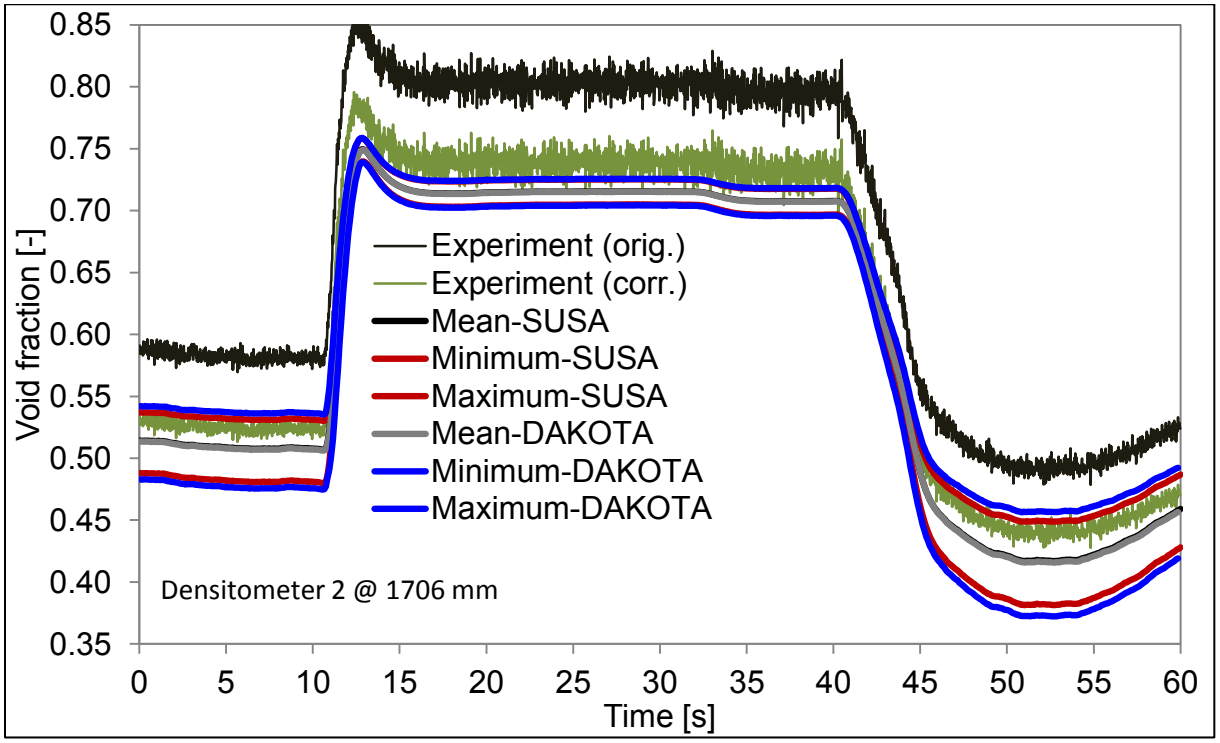

Figure 117 Void Fraction Predictions with Uncertainty Band Compared to Original and Corrected Re-Circulation Pump Trip Measurements for the Second Densitometer at 1706 mm

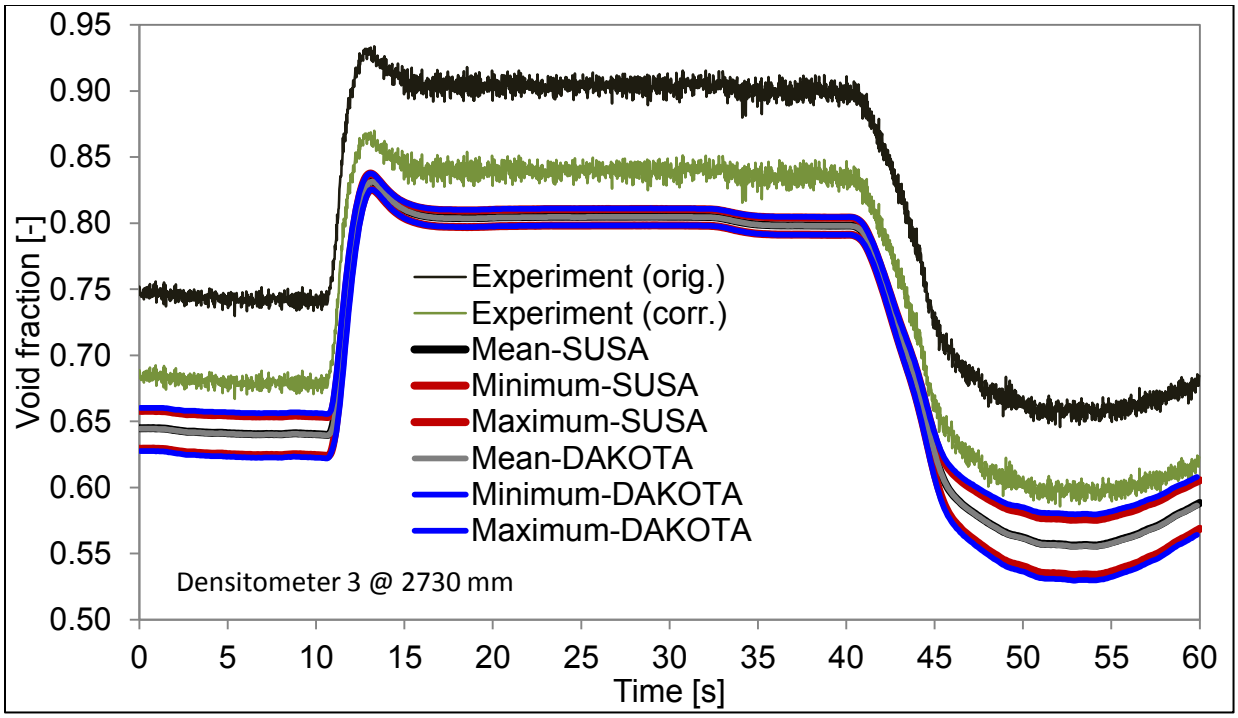

Figure 118 Void Fraction Predictions with Uncertainty Band Compared to Original and Corrected Re-Circulation Pump Trip Measurements for the Third Densitometer at 2730 mm

Afterwards, the mass flow rate and the bundle power are increased again to nominal values. Hence, the void fraction at the end of the transient is similar to the initial one.

The same general trends and behaviors as during the turbine trip can be seen here. The difference between original and corrected void fraction is more pronounced at higher void fractions, uncertainty band of TRACE-DAKOTA envelopes the one of TRACE-SUSA, the uncertainty band is getting smaller with higher void fractions. The main difference, between the actual trend, is that a general under prediction is evident in this case.

The quantitative comparison for the re-circulation pump trip is depicted in Figure 119. The highest deviations can be found for the lowest densitometer position, as for the turbine trip. That trend has been also confirmed during the steady state scenarios: the lower the void fraction, the higher the deviation to the experiment. The error is less than 15 % for the first 40 seconds and less than 25 % for the last 15 seconds. At second 11, the time of the initiation of the mass flow rate and power reduction, the error is in the range of 30 % for just a few seconds. The deviation for the highest densitometer is less than 10 % while for the one in the middle an error of 5 % or less is computed.

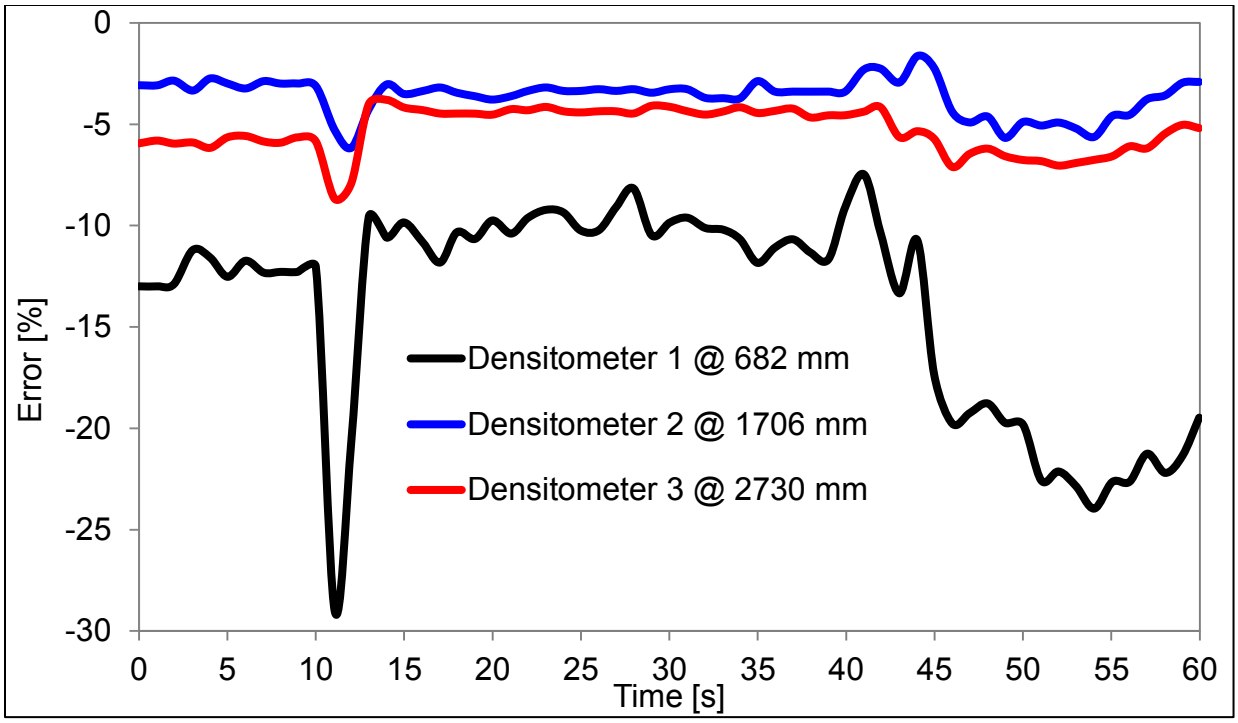

Figure 119 Deviation of the Predictions from the corrected Re-Circulation Pump Trip Measurements for all Three Densitometer Positions

As for the pressure drop, a sensitivity study has been performed with SUSA to identify the most important parameters and to evaluate their behavior as function of time (void fraction). The resulting sensitivity coefficients for inlet temperature and power are plotted in Figure 120 and Figure 121 for the turbine trip and the re-circulation pump trip, respectively.

As mentioned above, the TRACE-DAKOTA uncertainty band envelopes the one of TRACE-SUSA. Even though the differences between TRACE-SUSA and TRACE-DAKOTA with respect to the treatment of the inlet temperature are marginal, the differences in the uncertainty band are clearly visible. The inlet temperature has been identified as the parameter with the highest importance, as for the steady state void fraction investigation. The values are in the range of 0.8 – 0.9 at the beginning and at the end of the transient. They indicate a very strong relation between inlet temperature and void fraction. It can be seen that at lower void fractions (densitometer one) the sensitivity is at its maximum. In addition, the lower the void fraction, the lower the impact of the power. Values less than 0.3 are computed for the beginning and the end of the transient. This means actually a very weak or even no correlation between power and void fraction. However, this behavior changes with time. After the mass flow rate and the power has been reduced in both transients, the sensitivity coefficients for the inlet temperature are decreasing while the one for the power is increasing. During the re-circulation pump trip this behavior is more pronounced since the void fractions are larger. The changes are the most visible at densitometer 1. The sensitivity coefficients for power and inlet temperature are almost identical at that position.

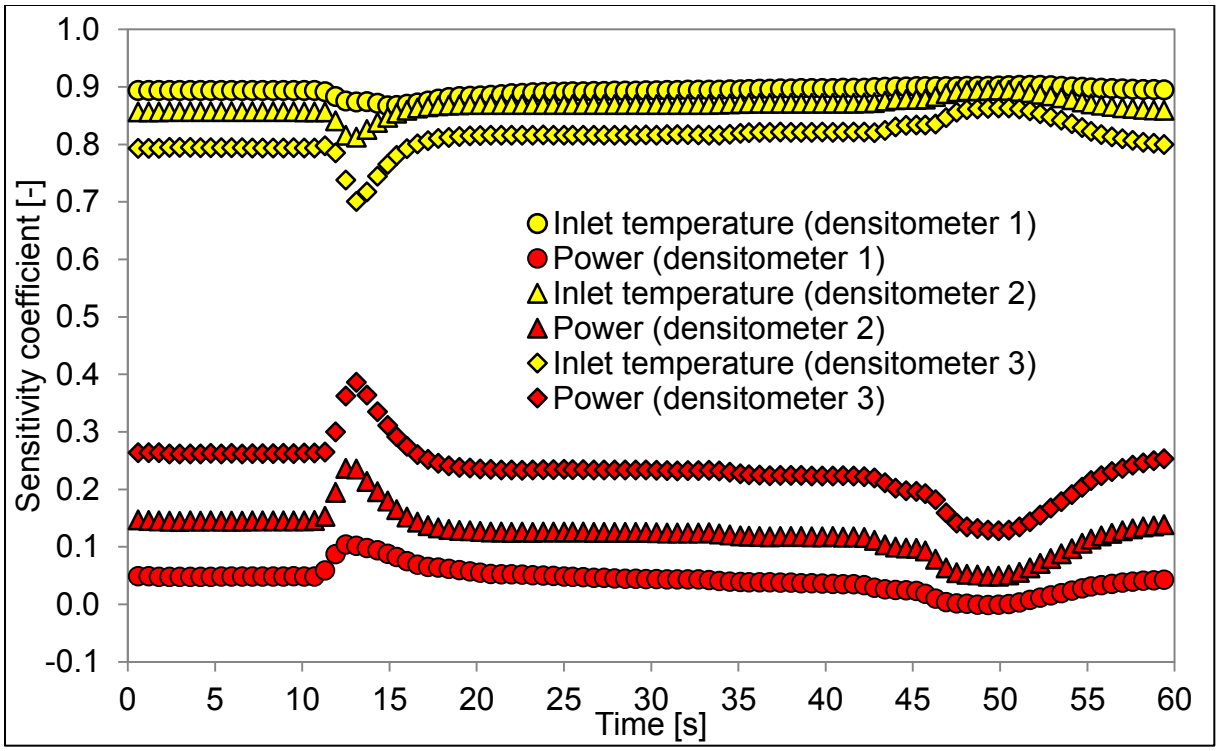

Figure 120 Sensitivity Coefficients for the Void Fraction Related to the Turbine Trip with SUSA

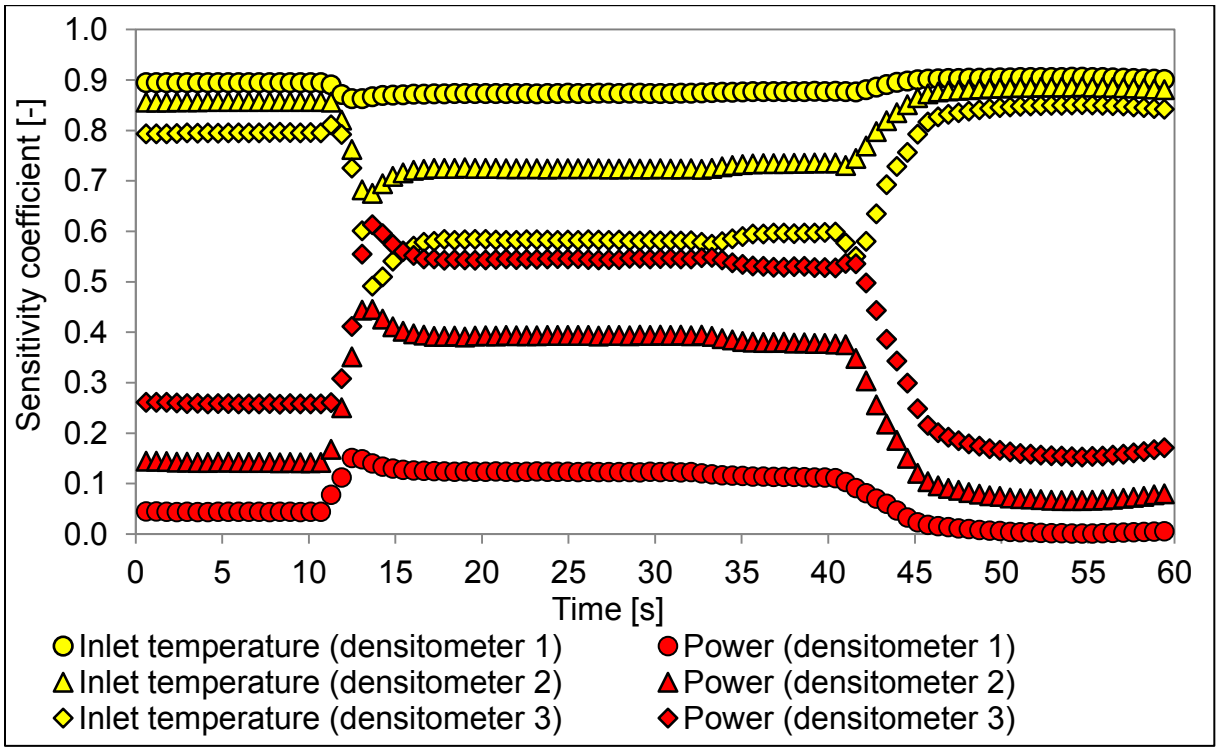

Figure 121 Sensitivity Coefficients for the Void Fraction Related to the Re-Circulation Pump Trip with SUSA

7 SUMMARY AND CONCLUSION

7.1 Summary

The present report contains a guideline for the performance of thermal hydraulic investigations with the best estimate system code TRACE in combination with U+S. For two U+S tools, SUSA and DAKOTA, the working methodology is presented in a way that the reader/user is possible to reproduce the presented results or to conduct a new investigation.

Results are shown for steady state single and two phase flow pressure drop scenarios, void fraction and critical power tests. Each test scenarioss has been investigated with TRACE. Due to the structure of the TRACE-SUSA interface it was possible that for each of these cases a U+S was be performed. Unfortunately, such a comprehensive analysis was not possible with TRACE-DAKOTA. Instead, six representative cases were selected for each variable.

The comparison of the reference values with the experiments showed a good agreement in general. Just for a limited number of scenarios an agreement was not given. The reasons for these discrepancies have been pointed out and only in the minority of these cases, shortcomings or flaws of the TRACE code are responsible. The average errors are listed in Table 33. During the uncertainty study, it was possible for most scenarios that the calculated uncertainty band is enveloping the experimental value. The sensitivity study provided a qualitative and quantitative way of evaluating how sensitive an output parameter is to an input parameter variation. These parameters are listed also in Table 33. One figure of merit to evaluate the quality of a U+S study is the coefficient of determination. In general a high number has been calculated for the pressure drop and the void fraction cases. Only for the critical power cases low numbers are computed. A possible explanation is that these simulations are characterized by a poor quality. These values are only available for SUSA but not for DAKOTA.

Transient scenarios have been investigated as well. Two representative transients were selected. The first one was a turbine trip and the second one was a re-circulation pump trip. Both transients are characterized by variation of the pressure, the mass flow rate and the bundle power over time. A quantitative comparison of the void fraction at different axial levels is given in order to show the agreement to the measurement. Additional sensitivity studies were performed to identify the variation of the sensitivity coefficients as a function of time.

Table 33 Summary of the Uncertainty and Sensitivity Investigations

	Δp (single-phase)	Δp (two phase)	void fraction	critical power
Error	6.83 %	4.66 %	4.46 %	3.72 %
		SUSA		
R1	Hyd. diameter	Hyd. diameter	Inlet temperature	Inlet temperature
R2	K-spacer	K-spacer	Power	Mass flow rate
R3	Friction factor	Friction factor	-	Hyd. diameter
R^2	>0.95	> 0.95	> 0.95	0.15 – 0.80
		DAKOTA		
R1	K-spacer	Inlet temperature	Inlet temperature	-
R2	Mass flow rate	K-spacer	Outlet pressure	-
R3	Inlet temperature	Outlet pressure	-	-
R^2	NA	NA	NA	-

7.2 Discussion

The mathematical theory behind SUSA and DAKOTA is similar, almost identical. Therefore, the results are almost identical, too. The major difference between the two programs is the way they are utilized. The exchange between TRACE and SUSA is based on self-written scripts, requiring certain programming knowledge. That allows the user to manipulate every parameter of interest. Since a SNAP plugin of DAKOTA exists, the user can utilize the graphical user interface of SNAP to assign a U+S to any TRACE calculation. This is done automatically with predefined user functions which mean that no additional tools or programming skills are required. The disadvantage of it is that the number of input and output parameters to be manipulated is limited. Hence, the U+S might not be as comprehensive as with SUSA due to missing input and output parameters in the predefined list of variables. Another major drawback of DAKOTA is that in the current SNAP-DAKOTA interface access to the TRACE source code parameters is not available. Thus, the influence of physical models on the results cannot be analyzed. With SUSA it is not a problem. If the source code is available, an additional TRACE module is needed which reads in a second input file. This second input file contains information about selected TRACE models. Inside the TRACE source code, flags are inserted at the selected models to manipulate them (usually a simple multiplier in order to change the result of the model by ± X %). This is not in particular a SUSA task. But since TRACE and SUSA are used as a standalone tool independent of the framework of SNAP the user has more freedom during the application.

As mentioned, the results of TRACE-SUSA and TRACE-DAKOTA are close together. The only difference occurred during the transient void fraction investigations. Despite the fact that TRACE-DAKOTA employs less parameters than TRACE-SUSA, the uncertainty band is enveloping the one of TRACE-SUSA. A good explanation to that is the way the transient inlet temperature is treated in DAKOTA. As the sensitivity study revealed, the inlet temperature is one major parameter for the void fraction evaluation. Even (very) small changes of the temperature will provoke very pronounced changes in the void.

As shown in sub section 6.5 some critical power cases (low mass flow rate, low critical power) could not have been simulated. It was also shown that the sensitivity study revealed a somehow poor analysis. The reason why especially these cases could not be performed is unclear and must be identified in further efforts.

Besides the physical and engineering part of the sub section, it should be mentioned that at the time of the analysis no user manual was existing for DAKOTA and SNAP-DAKOTA. That could be a possible reason why some results are not satisfying

7.3 Fields of Improvement

The investigations showed some fields where investigations should be done in order to improve the results. The first is related to TRACE. As shown in sub section 6.5 problems occured during the critical power simulations. At low mass flow rate it was not possible to extract the critical power or to be more precise the critical power ratio. TRACE simply did not print these numbers in the output file. It needs to be checked whether that problem is related to the applied correlation (validation) or to the way the correlation is called/used inside TRACE (verification).

A second field for TRACE improvements is the sub cooled boiling model. As shown during the transient void fraction investigation related to the turbine trip the predictions of TRACE differ

considerably from the experiment. The review of the implemented sub cooled boiling models will be done in the aftermath of the present investigation. The sub cooled boiling process is characterized by its complex nature due to involvement of several phenomena like evaporation and condensation. The present TRACE model is based on the work of Lahey, Zuber & Saha and originates from the 1970's (1). An improvement would require the analysis of recent experiments.

DAKOTA, to be more precise its implementation in SNAP, has also the potential for improvements, especially the access to TRACE source code parameters would be preferable. As shown in the previous sections, not all TRACE input deck parameters can be used for the U+S study. Either the parameters cannot be selected or it is too time consuming to change every parameter (e.g. each volume or flow area of the cells) by hand. Furthermore, an option to correlate two or more parameters to each other was not found. This is especially necessary if the change of one parameter requires the change of another one, such as the change of diameter, flow area and volume at the same time. Besides the missing input parameter in the DAKOTA environment, some output parameters are not listed. That is the reason why no U+S study was performed for the critical power scenarios. In addition, in the present implementation status of DAKOTA only one sensitivity measure is available, Pearson's product moment coefficient. SUSA offers four measures; Pearson's product momentum correlation coefficient, Spearman's rank correlation coefficient, Kendall's tau and Blomqvist's medial correlation coefficient. Furthermore, SUSA can compute the ordinary coefficient, the partial correlation coefficient and the standardized regression coefficient for each of the four sensitivity measures. For reasons of comparability it would be reasonable if more than one sensitivity measure is available in DAKOTA.

7.4 Conclusion

The investigation showed that TRACE is able to reproduce the experimental results with a high magnitude of agreement. The existing discrepancies between the experimental data and the predictions can be explained. By means of the U+S study, the investigation showed that even small variations of input parameters sometimes have a huge influence on selected output parameters. The general conclusion of this work and this report is that TRACE in combination with SUSA or DAKOTA is ready to be applied for further applications like large scale integral experimental facilities or even real plants.

7.5 Outlook

The next step is the application of these tools/programs to bigger problems like real plants in order to evaluate the design. Furthermore, valuable insights can be gained during the investigation of transients or accident scenarios such as LOCA's.

Besides the application of TRACE in combination with SUSA or DAKOTA, the validation of TRACE is not finished and my not be finished at all. The INR is strongly involved in two major fields of TRACE application, among others. The first application is the validation regarding LWR, especially BWR applications. The successful simulation of BFBT experiments is a prerequisite for the application to BWRs. The focus on the BWR application is the simulation of operational transients where a feedback between thermal hydraulic and neutron kinetic is present. In order to describe the phenomena taking place in a BWR it is necessary to improve the models of TRACE but also of the neutronic counterpart.

The second field of application is related to liquid metals. Thereby, the implementation of new models is necessary to describe coolants like sodium, lead and lead-bismuth eutectics. For LWRs in general and BWRs in particular routines are available to describe the heat transfer or the wall drag. These models have been validated over the last decade by many members of the CAMP project. Concerning liquid metals, the validating process has just started.

In both cases, the application of U+S is helpful to determine whether or not the design withstand the operational or transient conditions.

8 REFERENCES

[1] IAEA, "Safety margins of operating reactors," International Atomic Energy Agency, IAEA-TECDOC-1332, Vienna, 2003.

[2] IAEA, "Best estimate safety analysis for nuclear power plants: Uncertainty evaluation," International Atomic Energy Agency, No. 52, 2008.

[3] B. Neykov, F. Aydogan, L. Hochreiter, K. Ivanov, H. Utsuno, K. Fumio, E. Sartori and M. Martin, "NUPEC BWR Full-Size Fine Mesh Buncle Test (BFBT) benchmark Volume I: Specifications," OECD/NEA, 2005.

[4] W. Jäger, *Validation and Application of the System Code TRACE for Safety Related Investigations of Innovative Nuclear Energy Systems,* Technical University of Dresden, 2011.

[5] US NRC, "TRACE V5.0 Theory Manual - Field Equations, Solution Methods, and Physical Models," U.S. Nuclear Regulatory Commission, 2010.

[6] R. Nourgaliev, *Requirements, architecture, numerics and computational platform of a next generation system code,* Idaho Falls, Idaho, USA, 2009.

[7] J. Spore, J. Elson, S. Joll-Woodruff, T. Knight, J. Lin, R. Nelson, K. Pasa, R. Steinke, C. Unal, J. Mahaffay and C. Murray, "TRACM/FORTRAN 90 (Version 3.0) Theory Manual," Los Alamos National Laboratory, LA-UR-00-910, Los Alamos, 2000.

[8] D. Gorenflo, P. Sokol and S. Caplanis, "Pool boiling heat transfer from single plain tubes to various hydrocarbons," *International Journal on Refrigeration,* vol. 19, pp. 286-292, 1990.

[9] M. El-Genk, B. Su and Z. Guo, "Experimental Studies of Forced, Combined and Natural Convection of Water in Vertical Nine-Rod Bundles with a Square Lattice," *International Journal on Heat and Mass Transfer,* vol. 36, pp. 2359-2374, 1993.

[10] S. Churchill, "Friction factor equations spans all fluid-flow regime," *Chemical Engineering,* vol. 84, pp. 91-92, 1977.

[11] USNRC, "Thermal-hydraulic codes news," vol. 8, no. 1, March 1998.

[12] GRS, "SUSA V3.5 user's guide and tutorial," Gesellschaft fuer Anlagen- und Reaktorsicherheit, 2002.

[13] B. Krzykacs, E. Hofer and M. Kloos, "A software system for probabilistic uncertainty and sensitivity analysis of results from computer models," in *International Conference on Probabilistic Safety Assessment and Management*, San Diego, USA, 1994.

[14] R. Macián-Juan, *Uncertainty and sensitivity evaluation for best estimate coupled calculations,* Karlsruhe, Germany, 2011.

[15] W. Conover, Practical nonparametric statistics, John Wiley & Sons, Inc., 1999.

[16] S. Wilks, "Determination of sample sizes for setting tolerance limits," *The Annals of Mathematical Statistics,* no. 12, pp. 91-96, 1941.

[17] USNRC, "NRC Regulations Title 10, Code of Federal Regulations," US NRC, Washington, D.C., 2012.

[18] M. McKay, R. Beckman and W. Conover, "A comparison of three methods for selecting values of input variables in the analysis of output from a computer code," *Technometrics,*

no. 42, pp. 55-61, 2000.

[19] J. Helton and F. Davis, "Latin hypercube sampling and the propagation of uncertainty in analyses of complex systems," *Reliability Engineering & System Safety,* no. 81, pp. 23-69, 2003.

[20] G. Wyss and K. Jorgensen, "A user's guide to LHS: Sandia's latin hypercube sampling software," Sandia National Laboratories, 1998.

[21] P. Berthouex and L. Brown, Statistics for environmental engineers, Bacon Raton: Lewis Publisher, 2002.

[22] M. Kendall, "A new measure of rank correlation," *Biometrika,* no. 30, pp. 81-93, 1938.

[23] N. Blomqvist, "On a measure of dependence between two random variables," *The Annals of mathematical Statistics,* no. 21, pp. 593-600, 1950.

[24] B. Adams, K. Dalbey, M. Eldred, D. Gay, L. Swiler, W. Bohnhoff, J. Eddy, K. Haskell, P. Hough and S. Lefantzi, "DAKOTA, A Multilevel Parallel Object-Oriented Framework for Design Optimization, Parameter Estimation, Uncertainty Quantification, and Sensitivity Analysis Version 5.1 User's Manual," Sandia National Laboratories, Livermore, California, USA, 2011.

[25] APT1, "Symbolic Nuclear Analysis Package (SNAP) - User's Manual," Applied Programming Technology, Inc., 2011.

[26] W. Jäger, V. Sánchez and R. Macián-Juan, "On the uncertainty and sensitivity analysis of experiments with supercritical water with TRACE and SUSA," in *18th International Conference on Nuclear Enginnering (ICONE-18)*, Xi'an, China, 2010.

[27] B. Neykov, L. Hochreiter, K. Ivanov, H. Utsuno, E. Sartori and M. Martin, "NUPEC BWR Full-Size Fine-Mesh Bundle Test (BFBT Benchmark) Volume II: Uncertainty and sensitivity analyses of void distribution and critical power - specification," 2007.

[28] M. Glück, "Validation of the sub-channel code F-COBRA-TF Part II: Recalculation of void measurements," *Nuclear Engineering and Design,* no. 238, pp. 2317-2327, 2008b.

APPENDIX A TRACE.INP

```
free format
*
*************
* main data *
*************
*
*       numtcr          ieos         inopt          nmat          id2o
            1             0             1             0             0

*
*****************
* namelist data *
*****************
*
 &inopts
    dtstrt=-1.0,
    iadded=0,
    idiag=4,
    ikfac=1,
    inlab=3,
    iogrf=0,
    ioinp=0,
    iolab=0,
    ipowr=1,
    isscvt=1,
    nosets=0,
    nsdl=0,
    nsdu=0,
    usesjc=3,
    xtvres=4,
    npower=1
 &end
*
***************
* Model Flags *
***************
*
*        dstep         timet
            0           0.0
*       stdyst        transi         ncomp          njun          ipak
            1             0             4             2             1
*         epso          epss
        1.0E-4        1.0E-4
*       oitmax        sitmax        isolut        ncontr         nccfl
           25            25             0             0             0
*         ntsv          ntcb          ntcf          ntrp          ntcp
            5             6             6             0             0
*
************************
* component-number data *
************************
```

```
*
*  Component input order (IORDER)
*-- type ---- num ----- name ----------------  +    jun1   jun2   jun3
* FILL     *    100 s * Inlet                 +      10
* CHAN     *    200 s * Bundle                +      10    20
* POWER    *    201 s * Power                 +
* BREAK    *    300 e * Outlet                +      20
*
************************************************
* Starting Signal Variable Section of Model      *
************************************************
*
*         idsv          isvn          ilcn          icn1          icn2
            1             0             0             0             0
*n: pressure
*
*         idsv          isvn          ilcn          icn1          icn2
           106            21           200             1             0
*
*         idsv          isvn          ilcn          icn1          icn2
           206            75           200            25             0
*n: pressure
*
*         idsv          isvn          ilcn          icn1          icn2
           210            21           200            25             0
*n: pressure
*
*         idsv          isvn          ilcn          icn1          icn2
           211            21           300             1             0
************************************************
* Finished Signal Variable Section of Model      *
************************************************
*
*********************************************
* Starting Control System Section of Model  *
*********************************************
*
****** Control Blocks ******
*
*         idcb          icbn          icb1          icb2          icb3
          -206            59           210           211             0
*       cbgain        cbxmin        cbmax        cbcon1        cbcon2
            1.0      -1.0E20       1.0E20           0.5           0.5
*
*
*         idcb          icbn          icb1          icb2          icb3
          -207             9             0             0             0
*       cbgain        cbxmin        cbmax        cbcon1        cbcon2
            1.0      -1.0E20       1.0E20         3.708           0.0
*
*
*         idcb          icbn          icb1          icb2          icb3
          -208             9             0             0             0
*       cbgain        cbxmin        cbmax        cbcon1        cbcon2
            1.0      -1.0E20       1.0E20         9.806           0.0
```

```
*
*n: geodatic
*
*         idcb           icbn           icb1           icb2           icb3
          -209            104              3              0              0
*        cbgain         cbxmin         cbmax         cbcon1         cbcon2
            1.0       -1.0E20         1.0E20            0.0            0.0
*  ids   *          206         -207         -208e
*
*n: Outlet
*
*         idcb           icbn           icb1           icb2           icb3
          -211              3           -206           -209              0
*        cbgain         cbxmin         cbmax         cbcon1         cbcon2
            1.0       -1.0E20         1.0E20            0.0            0.0
*
*
*         idcb           icbn           icb1           icb2           icb3
          -300             54            106           -211              0
*        cbgain         cbxmin         cbmax         cbcon1         cbcon2
            1.0       -1.0E20         1.0E20            0.0            0.0
*
*******************************************
* Finished Control System Section of Model  *
*******************************************
*
*******   type            num         userid                 component name
fill                      100              0                          Inlet
*         jun1           ifty           ioff
            10              2              0
*        twtold           rfmx         concin           felv
            0.0         1.0E20            0.0            0.0
*          dxin          volin          alpin           vlin           tlin
         0.1545    1.462034E-3            0.0            0.0     307.550000
*           pin           pain         flowin           vvin           tvin
       2.0000E+05            0.0      2.750000            0.0      307.550000
*
*
*******   type            num         userid                 component name
chan                      200              0                Heizstabbuendel
*         ncell          nodes           jun1           jun2           epsw
            25              3             10             20     2.5000E-6
*        nsides
              2
* Water Rod inlet junction
*          nclk          junlk         ncmpto         nclkto         nlevto
             1            210              0              0              0
*         theta
            0.0
* Water Rod outlet junction
*          nclk          junlk         ncmpto         nclkto         nlevto
            24            220              0              0              0
*         theta
            0.0
*          ichf          iconc         iaxcnd         liqlev          nhcom
```

```
             2             0             0             0             0
*        width            th         houtl         houtv         toutl
      0.516265        3.0E-3           0.0           0.0     307.550000
*        toutv       advbwrf       quadsym      numwrods       nvfrays
      307.550000             1             2             1             0
*         ngrp        nchans        nodesr          nrow          ncrz
             5             1            22             8            24
*        icrnk         icrlh         nmwrx          nfci         nfcil
             0             0             0             0             0
*         fmon       reflood         nzmax        nzmaxw         ibeam
             0             0           100           100             0
*        dznht        dznhtw        dtxht1        dtxht2
        1.0E-3        1.0E-3           2.0          10.0
*         hgapo         pdrat          pldr         fucrac         norad
        6300.0     1.3170732           0.0           1.0             1
*        emcif1        emcif2        emcif3         noani
           0.0           0.0           0.0             0
*        emcof1        emcof2        emcof3
           0.0           0.0           0.0
* dx    *   0.1545        0.1545        0.1545        0.1545s
* dx    *   0.1545        0.1545        0.1545        0.1545s
* dx    *   0.1545        0.1545        0.1545        0.1545s
* dx    *   0.1545        0.1545        0.1545        0.1545s
* dx    *   0.1545        0.1545        0.1545        0.1545s
* dx    *   0.1545        0.1545        0.1545        0.1545s
* dx    *   0.1e
* vol   *   f 1.5112E-3 e
* fa    *   f 9.7810E-3 e
* kfac  *   0.0           0.0           0.0           1.2 s
* kfac  *   0.0           0.0           1.2           0.0 s
* kfac  *   0.0           0.0           1.2           0.0 s
* kfac  *   0.0           1.2           0.0           0.0 s
* kfac  *   1.2           0.0           0.0           0.0 s
* kfac  *   1.2           0.0           0.0           1.2 s
* kfac  *   0.0           0.0e
* grav  *  f    1.0 e
* hd    *  f    0.01295 e
* nff   *  f    1  e
* alp   *  f    0.0 e
* vl    *  f    0.0 e
* vv    *  f    0.0 e
* tl    *  f    307.55000 e
* tv    *  f    307.55000 e
* p     *  f    2.0000E+05 e
* pa    *  f    0.0 e
* qppp  *  f    0.0 e
* mat   *         12          12 e
* tw    *  f    307.55000 e
*  rdx  *        12.0        19.0        22.0         7.0         1.0e
* radrd *         0.0  4.41667E-4  8.83333E-4    1.325E-3  1.76667E-3s
* radrd *  2.20833E-3     2.65E-3  2.81667E-3  2.98333E-3     3.15E-3s
* radrd *  3.31667E-3  3.48333E-3     3.65E-3     3.85E-3     4.05E-3s
* radrd *     4.25E-3     4.45E-3     4.65E-3     4.85E-3  5.28333E-3s
* radrd *  5.71667E-3     6.15E-3e
* matrd *           4           4           4           4s
```

```
* matrd *           4           4           5           5s
* matrd *           5           5           5           5s
* matrd *           4           4           4           4s
* matrd *           4           4          12          12s
* matrd *          12e
*  nfax *  f    3 e
*  rftn *  f    307.55000 e
*  rftn *  f    307.55000 e
*  rftn *  f    307.55000 e
*  rftn *  f    307.55000 e
* rdpwr *       0.0         0.0         0.0         0.0         0.0s
* rdpwr *       0.0         1.0         1.0         1.0         1.0s
* rdpwr *       1.0         1.0         1.0         0.0         0.0s
* rdpwr *       0.0         0.0         0.0         0.0         0.0s
* rdpwr *       0.0         0.0e
* cpowr *       1.3        1.15        0.89        0.45e
* radpw *  f    1.0   e
* fpuo2 *       0.0         0.0         0.0         0.0e
*   ftd *       1.0         1.0         1.0         1.0e
*  gmix *  f    0.0e
* pgapt *       0.0         0.0         0.0         0.0e
*  burn *  f    0.0 e
*  burn *  f    0.0 e
*  burn *  f    0.0 e
*  burn *  f    0.0 e
* mrod *           2           1           2           1           1s
* mrod *           2           1           2           1           4s
* mrod *           3           3           3           4           2s
* mrod *           1           2           3           3           3s
* mrod *           3           3           4           2           1s
* mrod *           3           3           5           5           3s
* mrod *           3           2           1           3           3s
* mrod *           5           5           3           3           2s
* mrod *           2           4           3           3           3s
* mrod *           3           4           2           1           2s
* mrod *           4           3           3           4           2s
* mrod *           1           2           1           2           2s
* mrod *           2           2           1           2           6e
*    partial length rods
*           i           j        levrod
           -1
*
*     water rod locations *
*           i           j          flag          xloc          yloc
            4           4             1       0.06625      -0.06625
            4           5             1           0.0           0.0
            5           4             1           0.0           0.0
            5           5             1           0.0           0.0
-1
*     water rod data sets
*
*        igeom       wrnodes
            1             3
*      wrinlet      wroutlet           dia         sidea         sideb
            1            24         0.034           0.0           0.0
```

```
*           th       rcorner      flowarea      flwareai      flwareao
        1.0E-3           0.0   9.079203E-4   9.079203E-4   9.079203E-4
*           hd          hdri          hdro      thrmdiai      thrmdiao
         0.032         0.032         0.032         0.032         0.032
*     wrflossi      wrflosso      wrrlossi      wrrlosso
        1.0E20        1.0E20        1.0E20        1.0E20
*  matwr  *  f         12 e
*  tw     *  f   307.55000 e
*
*
*******   type           num        userid                component name
break                    300             0                        Outlet
*         jun1          ibty          isat          ioff      adjpress
            20             0             0             1             0
*         dxin         volin         alpin          tin           pin
        0.1545   1.462034E-3           0.0     307.550000     2.0000E+05
*         pain        concin          rbmx          poff          belv
           0.0           0.0        1.0E20           0.0           0.0
*
*
****************************************
*     Starting Power Components         *
****************************************
*
*******   type           num        userid                component name
power                    201             1                        Power
*       numpwr       chanpow
             1             1
*        htnum    *     200e
*       irpwty          ndgx          ndhx         nrts         nhist
             6             0             0          100             0
*       irpwtr        irpwsv        nrpwtb       nrpwsv        nrpwrf
             0             1             2            0             0
*       izpwtr        izpwsv        nzpwtb       nzpwsv        nzpwrf
             0             1             4            0             0
*       ipwrad        ipwdep      promheat     decaheat       wtbypass
             0             0           0.0          0.0           0.0
*        nzpwz         nzpwi        nfbpwt        nrpwr         nrpwi
             0             0             0            1             0
*        react         tneut        rpwoff       rrpwmx         rpwscl
           0.0           0.0           0.0       1.0E20            1.0
*       rpowri         zpwin        zpwoff       rzpwmx
           0.1           0.0      -1.0E19       1.0E20
*       extsou         pldr          pdrat       fucrac
           0.0           0.0            1.0          1.0
* zpwtb1*  0.0s
* zpwtb1*  0.46    0.58    0.69    0.79    0.88s
* zpwtb1*  0.99    1.09    1.22    1.22    1.34s
* zpwtb1*  1.34    1.40    1.40    1.34    1.34s
* zpwtb1*  1.22    1.22    1.09    0.99    0.88s
* zpwtb1*  0.79    0.69    0.58    0.46s
* zpwtb2*  1.0s
* zpwtb2*  0.46    0.58    0.69    0.79    0.88s
* zpwtb2*  0.99    1.09    1.22    1.22    1.34s
* zpwtb2*  1.34    1.40    1.40    1.34    1.34s
```

```
* zpwtb2*  1.22    1.22    1.09    0.99    0.88s
* zpwtb2*  0.79    0.69    0.58    0.46s
* zpwtb3*  2.0s
* zpwtb3*  0.46    0.58    0.69    0.79    0.88s
* zpwtb3*  0.99    1.09    1.22    1.22    1.34s
* zpwtb3*  1.34    1.40    1.40    1.34    1.34s
* zpwtb3*  1.22    1.22    1.09    0.99    0.88s
* zpwtb3*  0.79    0.69    0.58    0.46s
* zpwtb4*  1.0E6s
* zpwtb4*  0.46    0.58    0.69    0.79    0.88s
* zpwtb4*  0.99    1.09    1.22    1.22    1.34s
* zpwtb4*  1.34    1.40    1.40    1.34    1.34s
* zpwtb4*  1.22    1.22    1.09    0.99    0.88s
* zpwtb4*  0.79    0.69    0.58    0.46e
* rpwtbr*  0.0     0.1s
* rpwtbr*  100.0   0.1e
****************************************
*     Finished Power Components         *
****************************************
*
end
*
*****************
* Timestep Data *
*****************
*        dtmin         dtmax          tend         rtwfp
        1.0E-6          0.01         100.0          10.0
*        edint         gfint        dmpint        sedint
         100.0           0.1         100.0         100.0
*
*      endflag
          -1.0
```

APPENDIX B TRACE.OUT

```
================================================================================================================
 trac large edit


problem time is 0.000000E+00 s, time-step size is  3.9724E-03 s, time-step number is  455, outer-iteration number
is  1

 maximum convective power differance has been 0.0000000E+00   w    in component   200002 at time-1.0000000E+00 s
 time-step size was limited by component       0 at cell      26 to 4.5025E-01 s
 average outer-iteration count over the last  456 time steps was   3.068
 last minimum number of outer iterations was  1 at time step     454
 (limited by component     200 with fr.error of 2.7052E-07)
 last maximum number of outer iterations was 12 at time step     292
 (limited by component     200 with fr.error of 9.9715E-07)
 total number of times that each component (id#) was the last to converge since the last short edit
    4(  200001)  451(     200)    0(     100)    0(     300)
 current maximum time-step sizes and limitation counts since the last short edit
    delamx        delcmx        deldmx        delemx        delpmx        delrmx        delvmx        delxmx
  1.0000E+08 s    1.0000E+08 s    1.0000E+08 s    1.0000E+08 s    1.0000E+08 s    1.0000E+08 s    4.5025E+02 s
1.0000E+08 s
        0            50             0             0             0             0             0             0
 further limitation counts on what controls delcmx
    dtlmx         dtvmx         dprmx         dtsms         dtrmx         delt/2
     0             0            49             0             0             1

 cpu execution time of this run is 3.603623E+00 s

 total time steps since time 0.0 s is          455
 total cpu time since time 0.0 s is 3.603623E+00 s

**********************************     signal-variable     values     at     time               -0.00397     s
************************************

     id     sig.var.        id     sig.var.        id     sig.var.        id     sig.var.        id     sig.var.

      1    9.219819E-02       106    2.379322E+05       206    9.948135E+02       210    2.012821E+05       211
2.000000E+05
             time (s)           pressure (pa)          lq den (kg/m3)           pressure (pa)           pressure
(pa)

*********************************    control-block    output    values    at    time             -0.00397    s
***********************************

     id     con.blk.        id     con.blk.        id     con.blk.        id     con.blk.        id     con.blk.

   -206    2.006411E+05      -207    3.708000E+00      -208    9.806000E+00      -209    3.617206E+04      -211
2.368131E+05
                   *                     *                     *                     *                     *
   -300   1.119079E+03
          *
```

APPENDIX C MEDUSA.PRN

```
Uncertainty and Sensitivity Analysis


DATUM: 2012/02/02
TIME:  10:00

TYPE OF DESIGN: SIMPLE RANDOM

NUMBER OF PARAMETERS                  =     9
NUMBER OF FULLY DEPENDENT PARAMETERS =     1
NUMBER OF FREE PARAMETERS             =     8
SAMPLE SIZE                           =    93
INITIAL DSEED =                  123457.0

================================================================

DISTRIBUTIONS OF THE PARAMETERS
==================================

PARAMETER NO.   1 : N O R M A L  DISTRIBUTION
WITH MY=  1.0000E+00, SIGMA=  1.0000E-02
TRUNCATED AT ITS
1.59E+01 %-       AND    8.41E+01 %-QUANTILES
----------------------------------------------------------------
PARAMETER NO.   2 : N O R M A L  DISTRIBUTION
WITH MY=  1.0000E+00, SIGMA=  1.0000E-02
TRUNCATED AT ITS
1.59E+01 %-       AND    8.41E+01 %-QUANTILES
----------------------------------------------------------------
PARAMETER NO.   3 : N O R M A L  DISTRIBUTION
WITH MY=  0.0000E+00, SIGMA=  1.5000E+00
TRUNCATED AT ITS
1.59E+01 %-       AND    8.41E+01 %-QUANTILES
----------------------------------------------------------------
PARAMETER NO.   4 : N O R M A L  DISTRIBUTION
WITH MY=  1.0000E+00, SIGMA=  5.0000E-02
TRUNCATED AT ITS
1.59E+01 %-       AND    8.41E+01 %-QUANTILES
----------------------------------------------------------------
PARAMETER NO.   5 : N O R M A L  DISTRIBUTION
WITH MY=  1.0000E+00, SIGMA=  5.0000E-02
TRUNCATED AT ITS
1.59E+01 %-       AND    8.41E+01 %-QUANTILES
----------------------------------------------------------------
PARAMETER NO.   6 : N O R M A L  DISTRIBUTION
WITH MY=  1.0000E+00, SIGMA=  1.0000E-02
TRUNCATED AT ITS
1.59E+01 %-       AND    8.41E+01 %-QUANTILES
----------------------------------------------------------------
PARAMETER NO.   7 : N O R M A L  DISTRIBUTION
WITH MY=  1.0000E+00, SIGMA=  1.9900E-02
```

```
TRUNCATED AT ITS
1.59E+01 %-       AND    8.44E+01 %-QUANTILES
------------------------------------------------------------
PARAMETER NO.   8 : N O R M A L  DISTRIBUTION
WITH MY=  1.0000E+00, SIGMA=  1.0000E-02
TRUNCATED AT ITS
1.59E+01 %-       AND    8.41E+01 %-QUANTILES
------------------------------------------------------------
PARAMETER NO.   9 : N O R M A L  DISTRIBUTION
WITH MY=  1.0000E+00, SIGMA=  5.0000E-02
TRUNCATED AT ITS
1.59E+01 %-       AND    8.41E+01 %-QUANTILES
------------------------------------------------------------
============================================================

FULLY DEPENDENT PARAMETERS
==========================

DEPENDENT      CORRESPONDING     GRADE-
#    PARAMETER      FREE PARAMETER    CORRELATION
1        7               6              1.0
------------------------------------------------------------

FREE PARAMETERS AND THE CORRESPONDING
COMPLETELY DEPENDENT PARAMETERS

INDEX OF      +/- INDICES OF THE CORRESPONDING
#    FREE PARAM.   COMPLETELY DEPENDENT PARAMETERS

1        1
2        2
3        3
4        4
5        5
6        6             7
7        8
8        9

REQUIRED MEASURES OF ASSOCIATION BETWEEN FREE PARAMETERS
========================================================

PAR.1 PAR.2    MEASURE    TYPE
------------------------------------------------------------

CONTROL OF THE COMPUTATION OF THE CORRELATION
OF THE TRANSFORMED NORMAL BY NUMERICAL INTEGRATION
( IF NECESSARY ) :
MAXIMUM NUMBER OF ITERATIONS           =       20
DESIRED ACCURACY OF ITERATION PROCEDURE=   2.5000E-02

P A R A M E T E R   V A L U E S   O F   T H E   D E S I G N
RUN               INDEX OF PARAMETER
         1           2           3           4
1    1.0091E+00  9.9578E-01  7.0899E-01  1.0059E+00
2    1.0074E+00  9.9795E-01 -1.4338E+00  1.0075E+00
```

3	9.9227E-01	9.9819E-01	-4.0000E-01	9.6716E-01
4	9.9512E-01	9.9123E-01	5.4987E-01	1.0345E+00
5	1.0028E+00	1.0059E+00	-9.9602E-02	1.0282E+00
6	1.0031E+00	1.0037E+00	-3.8254E-02	9.5678E-01
7	1.0088E+00	9.9115E-01	-9.7341E-01	9.8529E-01
8	1.0094E+00	1.0087E+00	-1.1079E+00	9.6143E-01
9	1.0069E+00	1.0070E+00	-2.5163E-01	1.0096E+00
10	1.0033E+00	9.9381E-01	-1.4017E+00	9.6120E-01
11	1.0062E+00	9.9526E-01	1.4128E+00	1.0109E+00
12	9.9184E-01	9.9931E-01	1.0303E-01	1.0064E+00
13	9.9569E-01	9.9791E-01	-1.1151E+00	9.8905E-01
14	1.0055E+00	1.0051E+00	2.6796E-01	1.0190E+00
15	9.9574E-01	1.0049E+00	-1.4218E+00	1.0161E+00
16	9.9818E-01	1.0060E+00	-4.6491E-01	9.9170E-01
17	1.0067E+00	9.9963E-01	-7.8914E-01	9.7399E-01
18	1.0005E+00	1.0095E+00	-5.2672E-01	9.7641E-01
19	1.0074E+00	9.9273E-01	3.7218E-01	1.0171E+00
20	9.9802E-01	9.9871E-01	2.7618E-01	1.0159E+00
21	1.0054E+00	1.0062E+00	1.5286E-01	1.0153E+00
22	1.0069E+00	9.9045E-01	-9.8377E-01	9.9923E-01
23	1.0035E+00	9.9456E-01	6.3658E-01	1.0343E+00
24	9.9590E-01	1.0079E+00	-1.6739E-01	1.0239E+00
25	1.0056E+00	1.0033E+00	-8.8277E-01	9.8952E-01
26	1.0003E+00	9.9698E-01	-1.4097E+00	9.7315E-01
27	1.0025E+00	1.0038E+00	5.4078E-01	9.7047E-01
28	1.0005E+00	1.0044E+00	-1.4193E+00	9.6151E-01
29	1.0094E+00	9.9924E-01	4.0093E-01	1.0210E+00
30	9.9513E-01	1.0017E+00	1.1163E-01	1.0199E+00
31	1.0065E+00	9.9459E-01	-1.2241E+00	1.0068E+00
32	9.9442E-01	1.0047E+00	-9.7198E-02	1.0016E+00
33	1.0033E+00	9.9341E-01	-1.4340E+00	1.0362E+00
34	1.0044E+00	9.9133E-01	1.2405E-01	1.0317E+00
35	9.9369E-01	9.9905E-01	-1.1043E+00	9.6407E-01
36	1.0025E+00	9.9175E-01	1.4810E+00	9.8630E-01
37	1.0076E+00	9.9295E-01	-8.4229E-01	9.5251E-01
38	1.0050E+00	9.9671E-01	1.3930E+00	1.0371E+00
39	1.0099E+00	9.9085E-01	5.0285E-01	9.8797E-01
40	9.9526E-01	9.9736E-01	3.1890E-01	1.0451E+00
41	9.9732E-01	9.9605E-01	-5.1195E-01	9.8416E-01
42	9.9121E-01	9.9413E-01	1.3027E+00	9.5346E-01
43	1.0032E+00	9.9341E-01	-6.9382E-01	9.9855E-01
44	1.0060E+00	9.9739E-01	-4.9315E-01	1.0191E+00
45	9.9217E-01	9.9933E-01	4.1669E-01	9.7092E-01
46	9.9692E-01	1.0045E+00	-1.0865E+00	9.7738E-01
47	1.0083E+00	1.0029E+00	-1.1937E+00	1.0198E+00
48	9.9277E-01	9.9188E-01	1.3539E+00	1.0345E+00
49	9.9534E-01	9.9415E-01	8.5235E-02	9.8243E-01
50	1.0055E+00	1.0081E+00	-1.2160E+00	1.0260E+00
51	1.0084E+00	9.9870E-01	6.5411E-01	1.0000E+00
52	9.9131E-01	1.0005E+00	-1.4297E+00	1.0001E+00
53	9.9774E-01	1.0084E+00	5.2083E-01	9.9646E-01
54	9.9584E-01	9.9031E-01	2.2974E-01	1.0369E+00
55	1.0039E+00	1.0019E+00	-7.1682E-01	1.0103E+00
56	1.0015E+00	1.0022E+00	-4.8233E-01	1.0359E+00
57	1.0046E+00	9.9238E-01	1.0862E+00	9.8143E-01

58	9.9597E-01	9.9285E-01	9.3704E-01	9.7640E-01
59	1.0072E+00	9.9456E-01	7.0515E-01	9.5786E-01
60	1.0007E+00	9.9566E-01	-1.1160E+00	9.6265E-01
61	1.0075E+00	9.9832E-01	4.8105E-01	9.6804E-01
62	9.9608E-01	1.0002E+00	1.4391E+00	9.8761E-01
63	1.0037E+00	9.9797E-01	-9.2556E-01	1.0216E+00
64	1.0065E+00	1.0079E+00	1.0424E+00	9.7370E-01
65	9.9944E-01	9.9882E-01	7.5662E-01	9.8936E-01
66	1.0024E+00	1.0048E+00	1.1548E+00	1.0164E+00
67	9.9388E-01	9.9780E-01	8.7341E-01	1.0471E+00
68	9.9782E-01	1.0099E+00	-1.1552E+00	9.9027E-01
69	9.9552E-01	1.0006E+00	-4.8103E-01	9.5240E-01
70	9.9478E-01	9.9301E-01	1.0377E+00	1.0229E+00
71	1.0002E+00	1.0061E+00	2.8691E-01	1.0173E+00
72	1.0009E+00	1.0043E+00	4.7711E-01	1.0096E+00
73	9.9154E-01	1.0063E+00	6.4357E-01	1.0100E+00
74	1.0055E+00	9.9182E-01	1.3089E+00	1.0294E+00
75	9.9504E-01	1.0070E+00	-5.2694E-01	1.0401E+00
76	1.0022E+00	1.0025E+00	8.7840E-01	1.0039E+00
77	1.0039E+00	1.0047E+00	6.6405E-01	1.0077E+00
78	1.0092E+00	9.9101E-01	-1.0129E+00	1.0347E+00
79	9.9628E-01	9.9082E-01	1.9146E-01	1.0179E+00
80	1.0065E+00	1.0077E+00	-9.5867E-01	1.0235E+00
81	1.0005E+00	1.0022E+00	-1.1187E+00	9.9107E-01
82	9.9730E-01	1.0047E+00	-2.7360E-01	1.0411E+00
83	9.9446E-01	9.9154E-01	-1.1386E+00	9.8745E-01
84	1.0047E+00	1.0042E+00	9.4720E-02	9.8136E-01
85	1.0055E+00	1.0044E+00	1.2541E+00	1.0288E+00
86	9.9231E-01	1.0060E+00	5.1777E-01	1.0062E+00
87	1.0031E+00	1.0043E+00	7.9292E-01	9.8762E-01
88	1.0074E+00	1.0076E+00	6.0472E-01	9.8573E-01
89	9.9742E-01	9.9473E-01	7.5922E-01	9.8535E-01
90	1.0006E+00	9.9726E-01	9.4857E-02	9.7161E-01
91	9.9731E-01	1.0008E+00	7.2897E-01	9.7259E-01
92	1.0009E+00	9.9090E-01	1.6013E-01	9.5061E-01
93	9.9074E-01	9.9281E-01	6.8196E-01	1.0106E+00

P A R A M E T E R V A L U E S O F T H E D E S I G N

RUN	INDEX OF PARAMETER			
	5	6	7	8
1	1.0315E+00	9.9118E-01	9.8245E-01	1.0096E+00
2	9.9904E-01	9.9399E-01	9.8807E-01	9.9487E-01
3	1.0057E+00	1.0075E+00	1.0150E+00	9.9631E-01
4	9.5441E-01	1.0072E+00	1.0145E+00	9.9964E-01
5	1.0138E+00	9.9400E-01	9.8809E-01	1.0000E+00
6	1.0025E+00	1.0014E+00	1.0028E+00	1.0040E+00
7	1.0396E+00	9.9409E-01	9.8827E-01	1.0049E+00
8	1.0227E+00	1.0071E+00	1.0143E+00	1.0065E+00
9	9.6598E-01	1.0062E+00	1.0124E+00	1.0053E+00
10	1.0053E+00	9.9498E-01	9.9003E-01	9.9589E-01
11	9.7171E-01	1.0007E+00	1.0015E+00	9.9181E-01
12	9.8158E-01	9.9523E-01	9.9054E-01	9.9272E-01
13	1.0418E+00	1.0030E+00	1.0061E+00	9.9789E-01
14	1.0064E+00	1.0066E+00	1.0133E+00	1.0093E+00
15	9.9305E-01	1.0028E+00	1.0057E+00	1.0086E+00

16	9.5861E-01	9.9457E-01	9.8922E-01	1.0096E+00
17	1.0392E+00	1.0089E+00	1.0179E+00	1.0004E+00
18	9.5519E-01	1.0077E+00	1.0154E+00	9.9326E-01
19	1.0240E+00	1.0007E+00	1.0015E+00	1.0057E+00
20	1.0003E+00	1.0061E+00	1.0122E+00	9.9186E-01
21	9.6420E-01	1.0076E+00	1.0153E+00	9.9231E-01
22	9.9827E-01	1.0008E+00	1.0017E+00	9.9641E-01
23	9.7332E-01	1.0021E+00	1.0043E+00	1.0069E+00
24	1.0226E+00	9.9407E-01	9.8822E-01	1.0023E+00
25	1.0461E+00	9.9059E-01	9.8129E-01	9.9834E-01
26	9.7303E-01	9.9275E-01	9.8558E-01	1.0092E+00
27	1.0323E+00	9.9930E-01	9.9867E-01	1.0034E+00
28	1.0215E+00	9.9776E-01	9.9559E-01	9.9888E-01
29	9.9403E-01	1.0068E+00	1.0138E+00	9.9608E-01
30	1.0412E+00	1.0038E+00	1.0076E+00	9.9787E-01
31	9.8423E-01	9.9993E-01	9.9992E-01	1.0085E+00
32	1.0193E+00	1.0016E+00	1.0034E+00	1.0036E+00
33	9.7425E-01	1.0053E+00	1.0107E+00	1.0037E+00
34	1.0020E+00	1.0087E+00	1.0175E+00	1.0049E+00
35	1.0020E+00	1.0025E+00	1.0051E+00	1.0021E+00
36	9.7359E-01	1.0081E+00	1.0162E+00	9.9682E-01
37	1.0210E+00	9.9597E-01	9.9202E-01	9.9924E-01
38	9.5647E-01	1.0047E+00	1.0094E+00	9.9028E-01
39	9.9662E-01	9.9848E-01	9.9703E-01	1.0034E+00
40	1.0420E+00	9.9965E-01	9.9936E-01	1.0052E+00
41	1.0183E+00	1.0095E+00	1.0192E+00	1.0072E+00
42	1.0244E+00	1.0040E+00	1.0081E+00	1.0039E+00
43	9.9623E-01	9.9425E-01	9.8858E-01	9.9114E-01
44	1.0314E+00	1.0058E+00	1.0117E+00	9.9480E-01
45	9.8598E-01	1.0032E+00	1.0065E+00	1.0078E+00
46	9.9021E-01	1.0040E+00	1.0080E+00	9.9616E-01
47	1.0351E+00	9.9806E-01	9.9619E-01	1.0013E+00
48	1.0169E+00	9.9933E-01	9.9873E-01	1.0032E+00
49	9.9982E-01	1.0065E+00	1.0130E+00	1.0063E+00
50	9.5925E-01	9.9849E-01	9.9704E-01	9.9183E-01
51	1.0006E+00	1.0022E+00	1.0045E+00	1.0006E+00
52	9.6979E-01	1.0066E+00	1.0132E+00	9.9309E-01
53	9.7739E-01	9.9628E-01	9.9264E-01	1.0061E+00
54	9.8312E-01	9.9985E-01	9.9976E-01	1.0004E+00
55	1.0462E+00	9.9338E-01	9.8684E-01	9.9540E-01
56	1.0044E+00	9.9711E-01	9.9429E-01	1.0012E+00
57	1.0176E+00	9.9993E-01	9.9992E-01	1.0072E+00
58	9.9728E-01	1.0053E+00	1.0107E+00	1.0071E+00
59	1.0010E+00	1.0083E+00	1.0166E+00	9.9150E-01
60	9.5138E-01	9.9318E-01	9.8646E-01	1.0027E+00
61	1.0445E+00	9.9881E-01	9.9768E-01	1.0017E+00
62	9.7179E-01	9.9849E-01	9.9705E-01	1.0013E+00
63	1.0345E+00	9.9124E-01	9.8258E-01	9.9616E-01
64	9.8425E-01	1.0041E+00	1.0083E+00	9.9694E-01
65	9.8846E-01	9.9266E-01	9.8540E-01	1.0004E+00
66	1.0057E+00	1.0042E+00	1.0084E+00	1.0086E+00
67	9.7036E-01	1.0031E+00	1.0063E+00	1.0024E+00
68	1.0068E+00	1.0055E+00	1.0110E+00	9.9921E-01
69	9.7420E-01	1.0044E+00	1.0088E+00	1.0066E+00
70	1.0111E+00	1.0069E+00	1.0138E+00	1.0037E+00

71	9.7063E-01	9.9802E-01	9.9610E-01	1.0057E+00
72	9.5459E-01	1.0098E+00	1.0198E+00	1.0035E+00
73	9.8005E-01	9.9981E-01	9.9969E-01	1.0057E+00
74	9.8359E-01	9.9256E-01	9.8521E-01	9.9011E-01
75	9.9894E-01	1.0092E+00	1.0184E+00	1.0081E+00
76	9.7017E-01	1.0020E+00	1.0041E+00	9.9121E-01
77	1.0129E+00	9.9812E-01	9.9630E-01	9.9922E-01
78	1.0101E+00	1.0078E+00	1.0156E+00	9.9020E-01
79	1.0137E+00	1.0058E+00	1.0116E+00	1.0029E+00
80	1.0439E+00	1.0036E+00	1.0072E+00	1.0062E+00
81	1.0189E+00	1.0030E+00	1.0061E+00	9.9545E-01
82	1.0456E+00	9.9960E-01	9.9926E-01	1.0029E+00
83	1.0402E+00	1.0054E+00	1.0108E+00	9.9830E-01
84	1.0498E+00	1.0034E+00	1.0068E+00	9.9831E-01
85	9.9130E-01	1.0033E+00	1.0066E+00	1.0032E+00
86	9.9917E-01	9.9775E-01	9.9556E-01	9.9328E-01
87	9.8252E-01	1.0053E+00	1.0107E+00	1.0047E+00
88	1.0310E+00	9.9025E-01	9.8061E-01	1.0033E+00
89	1.0476E+00	9.9506E-01	9.9020E-01	9.9905E-01
90	9.6736E-01	9.9473E-01	9.8953E-01	1.0023E+00
91	1.0290E+00	9.9011E-01	9.8033E-01	9.9806E-01
92	1.0405E+00	1.0047E+00	1.0095E+00	1.0071E+00
93	9.6470E-01	1.0017E+00	1.0034E+00	1.0064E+00

P A R A M E T E R V A L U E S O F T H E D E S I G N

RUN	INDEX OF PARAMETER
	9
1	1.0087E+00
2	9.7277E-01
3	1.0373E+00
4	1.0160E+00
5	1.0100E+00
6	9.8144E-01
7	9.9824E-01
8	1.0320E+00
9	9.5500E-01
10	9.6723E-01
11	9.7200E-01
12	9.8662E-01
13	1.0272E+00
14	1.0454E+00
15	9.6888E-01
16	1.0146E+00
17	9.9200E-01
18	9.8679E-01
19	1.0401E+00
20	1.0476E+00
21	9.9919E-01
22	1.0139E+00
23	1.0199E+00
24	1.0264E+00
25	1.0143E+00
26	1.0052E+00
27	9.5733E-01
28	1.0121E+00

29	9.5486E-01
30	9.8369E-01
31	1.0041E+00
32	1.0394E+00
33	9.6025E-01
34	9.5914E-01
35	9.6469E-01
36	1.0108E+00
37	1.0316E+00
38	9.8755E-01
39	1.0087E+00
40	1.0356E+00
41	9.9334E-01
42	9.9818E-01
43	1.0272E+00
44	1.0454E+00
45	9.7996E-01
46	1.0487E+00
47	1.0398E+00
48	1.0115E+00
49	1.0237E+00
50	9.7477E-01
51	1.0324E+00
52	1.0046E+00
53	9.7490E-01
54	1.0338E+00
55	1.0410E+00
56	1.0453E+00
57	1.0012E+00
58	1.0025E+00
59	1.0344E+00
60	1.0046E+00
61	9.9308E-01
62	1.0307E+00
63	1.0321E+00
64	9.6186E-01
65	1.0432E+00
66	9.8065E-01
67	9.8120E-01
68	1.0065E+00
69	9.6369E-01
70	9.5784E-01
71	9.5637E-01
72	1.0412E+00
73	1.0292E+00
74	9.8061E-01
75	1.0085E+00
76	9.7171E-01
77	1.0441E+00
78	1.0043E+00
79	9.7012E-01
80	1.0304E+00
81	1.0466E+00
82	9.8486E-01
83	1.0286E+00

```
84   9.5555E-01
85   9.7585E-01
86   9.8951E-01
87   9.9310E-01
88   1.0346E+00
89   9.9045E-01
90   1.0349E+00
91   1.0473E+00
92   1.0131E+00
93   9.6139E-01

NUMBER OF DESIGN REPETITIONS DUE TO PAR. RESTRICT.=     0
LAST DSEED=          192915327.0

DESIGN HAS BEEN GENERATED
AND WRITTEN ON OUTPUT FILE
LAST DSEED=          192915327.0
```

APPENDIX D SAMPLE.DAT

```
9 93
1.0091E+00   9.9578E-01   7.0899E-01   1.0059E+00   1.0315E+00   9.9118E-01
9.8245E-01   1.0096E+00   1.0087E+00
1.0074E+00   9.9795E-01  -1.4338E+00   1.0075E+00   9.9904E-01   9.9399E-01
9.8807E-01   9.9487E-01   9.7277E-01
9.9227E-01   9.9819E-01  -4.0000E-01   9.6716E-01   1.0057E+00   1.0075E+00
1.0150E+00   9.9631E-01   1.0373E+00
9.9512E-01   9.9123E-01   5.4987E-01   1.0345E+00   9.5441E-01   1.0072E+00
1.0145E+00   9.9964E-01   1.0160E+00
1.0028E+00   1.0059E+00  -9.9602E-02   1.0282E+00   1.0138E+00   9.9400E-01
9.8809E-01   1.0000E+00   1.0100E+00
1.0031E+00   1.0037E+00  -3.8254E-02   9.5678E-01   1.0025E+00   1.0014E+00
1.0028E+00   1.0040E+00   9.8144E-01
1.0088E+00   9.9115E-01  -9.7341E-01   9.8529E-01   1.0396E+00   9.9409E-01
9.8827E-01   1.0049E+00   9.9824E-01
1.0094E+00   1.0087E+00  -1.1079E+00   9.6143E-01   1.0227E+00   1.0071E+00
1.0143E+00   1.0065E+00   1.0320E+00
1.0069E+00   1.0070E+00  -2.5163E-01   1.0096E+00   9.6598E-01   1.0062E+00
1.0124E+00   1.0053E+00   9.5500E-01
1.0033E+00   9.9381E-01  -1.4017E+00   9.6120E-01   1.0053E+00   9.9498E-01
9.9003E-01   9.9589E-01   9.6723E-01
1.0062E+00   9.9526E-01   1.4128E+00   1.0109E+00   9.7171E-01   1.0007E+00
1.0015E+00   9.9181E-01   9.7200E-01
9.9184E-01   9.9931E-01   1.0303E-01   1.0064E+00   9.8158E-01   9.9523E-01
9.9054E-01   9.9272E-01   9.8662E-01
9.9569E-01   9.9791E-01  -1.1151E+00   9.8905E-01   1.0418E+00   1.0030E+00
1.0061E+00   9.9789E-01   1.0272E+00
1.0055E+00   1.0051E+00   2.6796E-01   1.0190E+00   1.0064E+00   1.0066E+00
1.0133E+00   1.0093E+00   1.0454E+00
9.9574E-01   1.0049E+00  -1.4218E+00   1.0161E+00   9.9305E-01   1.0028E+00
1.0057E+00   1.0086E+00   9.6888E-01
9.9818E-01   1.0060E+00  -4.6491E-01   9.9170E-01   9.5861E-01   9.9457E-01
9.8922E-01   1.0096E+00   1.0146E+00
1.0067E+00   9.9963E-01  -7.8914E-01   9.7399E-01   1.0392E+00   1.0089E+00
1.0179E+00   1.0004E+00   9.9200E-01
1.0005E+00   1.0095E+00  -5.2672E-01   9.7641E-01   9.5519E-01   1.0077E+00
1.0154E+00   9.9326E-01   9.8679E-01
1.0074E+00   9.9273E-01   3.7218E-01   1.0171E+00   1.0240E+00   1.0007E+00
1.0015E+00   1.0057E+00   1.0401E+00
9.9802E-01   9.9871E-01   2.7618E-01   1.0159E+00   1.0003E+00   1.0061E+00
1.0122E+00   9.9186E-01   1.0476E+00
1.0054E+00   1.0062E+00   1.5286E-01   1.0153E+00   9.6420E-01   1.0076E+00
1.0153E+00   9.9231E-01   9.9919E-01
1.0069E+00   9.9045E-01  -9.8377E-01   9.9923E-01   9.9827E-01   1.0008E+00
1.0017E+00   9.9641E-01   1.0139E+00
1.0035E+00   9.9456E-01   6.3658E-01   1.0343E+00   9.7332E-01   1.0021E+00
1.0043E+00   1.0069E+00   1.0199E+00
9.9590E-01   1.0079E+00  -1.6739E-01   1.0239E+00   1.0226E+00   9.9407E-01
9.8822E-01   1.0023E+00   1.0264E+00
1.0056E+00   1.0033E+00  -8.8277E-01   9.8952E-01   1.0461E+00   9.9059E-01
9.8129E-01   9.9834E-01   1.0143E+00
```

1.0003E+00 9.9698E-01 -1.4097E+00 9.7315E-01 9.7303E-01 9.9275E-01
9.8558E-01 1.0092E+00 1.0052E+00
1.0025E+00 1.0038E+00 5.4078E-01 9.7047E-01 1.0323E+00 9.9930E-01
9.9867E-01 1.0034E+00 9.5733E-01
1.0005E+00 1.0044E+00 -1.4193E+00 9.6151E-01 1.0215E+00 9.9776E-01
9.9559E-01 9.9888E-01 1.0121E+00
1.0094E+00 9.9924E-01 4.0093E-01 1.0210E+00 9.9403E-01 1.0068E+00
1.0138E+00 9.9608E-01 9.5486E-01
9.9513E-01 1.0017E+00 1.1163E-01 1.0199E+00 1.0412E+00 1.0038E+00
1.0076E+00 9.9787E-01 9.8369E-01
1.0065E+00 9.9459E-01 -1.2241E+00 1.0068E+00 9.8423E-01 9.9993E-01
9.9992E-01 1.0085E+00 1.0041E+00
9.9442E-01 1.0047E+00 -9.7198E-02 1.0016E+00 1.0193E+00 1.0016E+00
1.0034E+00 1.0036E+00 1.0394E+00
1.0033E+00 9.9341E-01 -1.4340E+00 1.0362E+00 9.7425E-01 1.0053E+00
1.0107E+00 1.0037E+00 9.6025E-01
1.0044E+00 9.9133E-01 1.2405E-01 1.0317E+00 1.0020E+00 1.0087E+00
1.0175E+00 1.0049E+00 9.5914E-01
9.9369E-01 9.9905E-01 -1.1043E+00 9.6407E-01 1.0020E+00 1.0025E+00
1.0051E+00 1.0021E+00 9.6469E-01
1.0025E+00 9.9175E-01 1.4810E+00 9.8630E-01 9.7359E-01 1.0081E+00
1.0162E+00 9.9682E-01 1.0108E+00
1.0076E+00 9.9295E-01 -8.4229E-01 9.5251E-01 1.0210E+00 9.9597E-01
9.9202E-01 9.9924E-01 1.0316E+00
1.0050E+00 9.9671E-01 1.3930E+00 1.0371E+00 9.5647E-01 1.0047E+00
1.0094E+00 9.9028E-01 9.8755E-01
1.0099E+00 9.9085E-01 5.0285E-01 9.8797E-01 9.9662E-01 9.9848E-01
9.9703E-01 1.0034E+00 1.0087E+00
9.9526E-01 9.9736E-01 3.1890E-01 1.0451E+00 1.0420E+00 9.9965E-01
9.9936E-01 1.0052E+00 1.0356E+00
9.9732E-01 9.9605E-01 -5.1195E-01 9.8416E-01 1.0183E+00 1.0095E+00
1.0192E+00 1.0072E+00 9.9334E-01
9.9121E-01 9.9413E-01 1.3027E+00 9.5346E-01 1.0244E+00 1.0040E+00
1.0081E+00 1.0039E+00 9.9818E-01
1.0032E+00 9.9341E-01 -6.9382E-01 9.9855E-01 9.9623E-01 9.9425E-01
9.8858E-01 9.9114E-01 1.0272E+00
1.0060E+00 9.9739E-01 -4.9315E-01 1.0191E+00 1.0314E+00 1.0058E+00
1.0117E+00 9.9480E-01 1.0454E+00
9.9217E-01 9.9933E-01 4.1669E-01 9.7092E-01 9.8598E-01 1.0032E+00
1.0065E+00 1.0078E+00 9.7996E-01
9.9692E-01 1.0045E+00 -1.0865E+00 9.7738E-01 9.9021E-01 1.0040E+00
1.0080E+00 9.9616E-01 1.0487E+00
1.0083E+00 1.0029E+00 -1.1937E+00 1.0198E+00 1.0351E+00 9.9806E-01
9.9619E-01 1.0013E+00 1.0398E+00
9.9277E-01 9.9188E-01 1.3539E+00 1.0345E+00 1.0169E+00 9.9933E-01
9.9873E-01 1.0032E+00 1.0115E+00
9.9534E-01 9.9415E-01 8.5235E-02 9.8243E-01 9.9982E-01 1.0065E+00
1.0130E+00 1.0063E+00 1.0237E+00
1.0055E+00 1.0081E+00 -1.2160E+00 1.0260E+00 9.5925E-01 9.9849E-01
9.9704E-01 9.9183E-01 9.7477E-01
1.0084E+00 9.9870E-01 6.5411E-01 1.0000E+00 1.0006E+00 1.0022E+00
1.0045E+00 1.0006E+00 1.0324E+00
9.9131E-01 1.0005E+00 -1.4297E+00 1.0001E+00 9.6979E-01 1.0066E+00
1.0132E+00 9.9309E-01 1.0046E+00

9.9774E-01 1.0084E+00 5.2083E-01 9.9646E-01 9.7739E-01 9.9628E-01
9.9264E-01 1.0061E+00 9.7490E-01
9.9584E-01 9.9031E-01 2.2974E-01 1.0369E+00 9.8312E-01 9.9985E-01
9.9976E-01 1.0004E+00 1.0338E+00
1.0039E+00 1.0019E+00 -7.1682E-01 1.0103E+00 1.0462E+00 9.9338E-01
9.8684E-01 9.9540E-01 1.0410E+00
1.0015E+00 1.0022E+00 -4.8233E-01 1.0359E+00 1.0044E+00 9.9711E-01
9.9429E-01 1.0012E+00 1.0453E+00
1.0046E+00 9.9238E-01 1.0862E+00 9.8143E-01 1.0176E+00 9.9993E-01
9.9992E-01 1.0072E+00 1.0012E+00
9.9597E-01 9.9285E-01 9.3704E-01 9.7640E-01 9.9728E-01 1.0053E+00
1.0107E+00 1.0071E+00 1.0025E+00
1.0072E+00 9.9456E-01 7.0515E-01 9.5786E-01 1.0010E+00 1.0083E+00
1.0166E+00 9.9150E-01 1.0344E+00
1.0007E+00 9.9566E-01 -1.1160E+00 9.6265E-01 9.5138E-01 9.9318E-01
9.8646E-01 1.0027E+00 1.0046E+00
1.0075E+00 9.9832E-01 4.8105E-01 9.6804E-01 1.0445E+00 9.9881E-01
9.9768E-01 1.0017E+00 9.9308E-01
9.9608E-01 1.0002E+00 1.4391E+00 9.8761E-01 9.7179E-01 9.9849E-01
9.9705E-01 1.0013E+00 1.0307E+00
1.0037E+00 9.9797E-01 -9.2556E-01 1.0216E+00 1.0345E+00 9.9124E-01
9.8258E-01 9.9616E-01 1.0321E+00
1.0065E+00 1.0079E+00 1.0424E+00 9.7370E-01 9.8425E-01 1.0041E+00
1.0083E+00 9.9694E-01 9.6186E-01
9.9944E-01 9.9882E-01 7.5662E-01 9.8936E-01 9.8846E-01 9.9266E-01
9.8540E-01 1.0004E+00 1.0432E+00
1.0024E+00 1.0048E+00 1.1548E+00 1.0164E+00 1.0057E+00 1.0042E+00
1.0084E+00 1.0086E+00 9.8065E-01
9.9388E-01 9.9780E-01 8.7341E-01 1.0471E+00 9.7036E-01 1.0031E+00
1.0063E+00 1.0024E+00 9.8120E-01
9.9782E-01 1.0099E+00 -1.1552E+00 9.9027E-01 1.0068E+00 1.0055E+00
1.0110E+00 9.9921E-01 1.0065E+00
9.9552E-01 1.0006E+00 -4.8103E-01 9.5240E-01 9.7420E-01 1.0044E+00
1.0088E+00 1.0066E+00 9.6369E-01
9.9478E-01 9.9301E-01 1.0377E+00 1.0229E+00 1.0111E+00 1.0069E+00
1.0138E+00 1.0037E+00 9.5784E-01
1.0002E+00 1.0061E+00 2.8691E-01 1.0173E+00 9.7063E-01 9.9802E-01
9.9610E-01 1.0057E+00 9.5637E-01
1.0009E+00 1.0043E+00 4.7711E-01 1.0096E+00 9.5459E-01 1.0098E+00
1.0198E+00 1.0035E+00 1.0412E+00
9.9154E-01 1.0063E+00 6.4357E-01 1.0100E+00 9.8005E-01 9.9981E-01
9.9969E-01 1.0057E+00 1.0292E+00
1.0055E+00 9.9182E-01 1.3089E+00 1.0294E+00 9.8359E-01 9.9256E-01
9.8521E-01 9.9011E-01 9.8061E-01
9.9504E-01 1.0070E+00 -5.2694E-01 1.0401E+00 9.9894E-01 1.0092E+00
1.0184E+00 1.0081E+00 1.0085E+00
1.0022E+00 1.0025E+00 8.7840E-01 1.0039E+00 9.7017E-01 1.0020E+00
1.0041E+00 9.9121E-01 9.7171E-01
1.0039E+00 1.0047E+00 6.6405E-01 1.0077E+00 1.0129E+00 9.9812E-01
9.9630E-01 9.9922E-01 1.0441E+00
1.0092E+00 9.9101E-01 -1.0129E+00 1.0347E+00 1.0101E+00 1.0078E+00
1.0156E+00 9.9020E-01 1.0043E+00
9.9628E-01 9.9082E-01 1.9146E-01 1.0179E+00 1.0137E+00 1.0058E+00
1.0116E+00 1.0029E+00 9.7012E-01

1.0065E+00 1.0077E+00 -9.5867E-01 1.0235E+00 1.0439E+00 1.0036E+00
1.0072E+00 1.0062E+00 1.0304E+00
1.0005E+00 1.0022E+00 -1.1187E+00 9.9107E-01 1.0189E+00 1.0030E+00
1.0061E+00 9.9545E-01 1.0466E+00
9.9730E-01 1.0047E+00 -2.7360E-01 1.0411E+00 1.0456E+00 9.9960E-01
9.9926E-01 1.0029E+00 9.8486E-01
9.9446E-01 9.9154E-01 -1.1386E+00 9.8745E-01 1.0402E+00 1.0054E+00
1.0108E+00 9.9830E-01 1.0286E+00
1.0047E+00 1.0042E+00 9.4720E-02 9.8136E-01 1.0498E+00 1.0034E+00
1.0068E+00 9.9831E-01 9.5555E-01
1.0055E+00 1.0044E+00 1.2541E+00 1.0288E+00 9.9130E-01 1.0033E+00
1.0066E+00 1.0032E+00 9.7585E-01
9.9231E-01 1.0060E+00 5.1777E-01 1.0062E+00 9.9917E-01 9.9775E-01
9.9556E-01 9.9328E-01 9.8951E-01
1.0031E+00 1.0043E+00 7.9292E-01 9.8762E-01 9.8252E-01 1.0053E+00
1.0107E+00 1.0047E+00 9.9310E-01
1.0074E+00 1.0076E+00 6.0472E-01 9.8573E-01 1.0310E+00 9.9025E-01
9.8061E-01 1.0033E+00 1.0346E+00
9.9742E-01 9.9473E-01 7.5922E-01 9.8535E-01 1.0476E+00 9.9506E-01
9.9020E-01 9.9905E-01 9.9045E-01
1.0006E+00 9.9726E-01 9.4857E-02 9.7161E-01 9.6736E-01 9.9473E-01
9.8953E-01 1.0023E+00 1.0349E+00
9.9731E-01 1.0008E+00 7.2897E-01 9.7259E-01 1.0290E+00 9.9011E-01
9.8033E-01 9.9806E-01 1.0473E+00
1.0009E+00 9.9090E-01 1.6013E-01 9.5061E-01 1.0405E+00 1.0047E+00
1.0095E+00 1.0071E+00 1.0131E+00
9.9074E-01 9.9281E-01 6.8196E-01 1.0106E+00 9.6470E-01 1.0017E+00
1.0034E+00 1.0064E+00 9.6139E-01

APPENDIX E DATA EXTRACTION

```
PROGRAM DataExtraction
      IMPLICIT double PRECISION(a-h)
      IMPLICIT INTEGER (i-z)
      PARAMETER (nmax = 93)
      CHARACTER*11 eingabedatei
      CHARACTER*14 eingabedatei2
      CHARACTER*121 zeileA
      CHARACTER*121 zeileB
      CHARACTER*121 zeileC
      INTEGER :: count1, count2
      REAL*8 ::A1, A2, B1, B2
      REAL, DIMENSION(1:36) :: PressureDropRef
      REAL, DIMENSION(1:1,1:36) :: ReferencePD
      REAL, ALLOCATABLE, DIMENSION(:,:) :: scalar
      INTEGER :: NF = 36, NJ = 93
!-------------------------------------------------------------------------
!==== REFERENCE OUTPUTS DATA EXTRACTION SECTION - START ==================
!-------------------------------------------------------------------------
!
  OPEN(201,file='reference.dat',form='formatted',status='replace',err=9001)

      DO i=1,NF
       IF (i .le. 9) THEN
         WRITE(eingabedatei(6:6), '(I1)')i
               eingabedatei(1:5) = 'P7000'
               eingabedatei(7:11) = '.out '
       ELSE IF (i .gt. 9 .AND. i .lt. 100) THEN
         WRITE(eingabedatei(6:7), '(I2)')i
               eingabedatei(1:5) = 'P7000'
               eingabedatei(8:11) = '.out'
       END IF

  OPEN(101,file=eingabedatei,form='formatted',status='old',err=9000)

  WRITE(*,*)eingabedatei,' has been opened succesfuly.'

        count1 = 0
        DO
          READ(101, '(a121)',END=300) zeileA
          IF(zeileA(37:71) .eq. 'control-block output values at time')THEN
              count1 = count1 + 1
          END IF
        END DO

300     CONTINUE

        REWIND(101)

        count2 = 0
        DO
          READ(101, '(a121)',END=301) zeileB
```

```
          IF(zeileB(37:71) .eq. 'control-block output values at time')THEN
            count2 = count2 + 1
            IF(count1 .eq. count2) THEN
               GO TO 234
            END IF
          END IF
        END DO

301     CONTINUE
234     CONTINUE

        !read useless information and dump them

        DO j=1,5
          READ(101,'(a121)',END=9000) zeileC
        END DO

        !read pressure drop data out of control-block output

        READ(101,*,END=499) A1, A2

499     CONTINUE

        PressureDropRef(i) = A2

        !scalar information stored in variable

        ReferencePD(1,i) = PressureDropRef(i)

        WRITE(201,'(f11.2)') ReferencePD(1,i)

        GO TO 500
500     CONTINUE

        END DO

        CLOSE(101)
        CLOSE(201)
!
!-------------------------------------------------------------------------
!==== UNCERTAINTY OUTPUTS DATA EXTRACTION SECTION - START ================
!-------------------------------------------------------------------------
!      OPEN(202,file='scalar.lst',form='formatted',status='replace',err=9001)
ALLOCATE (scalar(NF,NJ))
      DO k=1,NF
         DO l=1,NJ

           IF (k .le. 9 .AND.  l .le. 9) THEN
              WRITE(eingabedatei2,101) k,l
101           FORMAT("P7000",i1,"_",i1,".out")
           ELSE IF (k .le. 9 .AND.  l .gt. 9) THEN
              WRITE(eingabedatei2,102) k,l
102           FORMAT("P7000",i1,"_",i2,".out")
           ELSE IF (k .gt. 9 .AND.  l .le. 9) THEN
              WRITE(eingabedatei2,103) k,l
```

```
103           FORMAT("P7000",i2,"_",i1,".out")
            ELSE IF (k .gt. 9 .AND.  l .gt. 9) THEN
               WRITE(eingabedatei2,104) k,l
104            FORMAT("P7000",i2,"_",i2,".out")
            END IF
           OPEN(102,file=eingabedatei2,form='formatted',status='old',err=9000)

WRITE(*,*)eingabedatei2,' has been opened succesfully.'

        count1 = 0
        DO
          READ(102, '(a121)',END=302) zeileA
          IF(zeileA(37:71) .eq. 'control-block output values at time')THEN
             count1 = count1 + 1
          END IF
            END DO

302     CONTINUE
        REWIND(102)

        count2 = 0
        DO
          READ(102, '(a121)',END=303) zeileB
          IF(zeileB(37:71) .eq. 'control-block output values at time')THEN
            count2 = count2 + 1
            IF(count1 .eq. count2) THEN
              GO TO 235
            END IF
          END IF
        END DO

303      CONTINUE
235      CONTINUE

         !read useless information and dump them

         DO m=1,5
           READ(102,'(a121)',END=9000) zeileC
         END DO

         !read pressure drop data out of control-block output

         READ(102,*,END=498) B1, B2

498      CONTINUE

         scalar(k,l) = B2

         END DO
         END DO

         DO l=1,NJ
           WRITE(202,'(100f11.2)') (scalar(k,l) , k=1,NF)
         END DO
```

```
        CLOSE(102)
        CLOSE(202)
        GO TO 9999

9000  CONTINUE
      WRITE(*,*) '*     ** ERROR: Could not open file on unit 101'
      GO TO 9998
9001  CONTINUE
      WRITE(*,*) '*** ERROR: Could not open file on unit',eingabedatei
      GO TO 9998
9998  CONTINUE
      WRITE(*,*)'Program termination due to errors'
      GO TO 9999
9999  CONTINUE
      WRITE(*,*)'finished'

      END
```

APPENDIX F EQUUS.PRN

```
Uncertainty and Sensitivity Analysis


 DATE: 2012/03/30
 TIME:  09:51

 CURRENT SAMPLE SIZE            =    93
 CURRENT NUMBER OF CONSEQUENCES =    36

 NUMBER OF SELECTED CONSEQUENCES :
    1
 INDICES OF SELECTED CONSEQUENCES :
    1

 NUMBER OF SELECTED DISTRIBUTIONS TO BE FITTED
    4
 INDICES OF SELECTED DISTRIBUTIONS :
     3 : NORMAL
     4 : LOGNORMAL
     5 : UNIFORM
     8 : LOG-TRIANGULAR

EMPIRICAL QUANTILES OF CONSEQUENCE NO.    1
*****************************************
        CURRENT SAMPLE SIZE =     93

                            MINIMUM =    1.0617E+03
   #   INDEX
   1       1      1.00 %-QUANTILE =    1.0617E+03
   2       2      2.00 %-QUANTILE =    1.0698E+03
   3       3      3.00 %-QUANTILE =    1.0700E+03
   4       4      4.00 %-QUANTILE =    1.0719E+03
   5       5      5.00 %-QUANTILE =    1.0754E+03
   6       6      6.00 %-QUANTILE =    1.0754E+03
   7       7      7.00 %-QUANTILE =    1.0760E+03
   8       8      8.00 %-QUANTILE =    1.0769E+03
   9       9      9.00 %-QUANTILE =    1.0783E+03
  10      10     10.00 %-QUANTILE =    1.0802E+03
  11      11     11.00 %-QUANTILE =    1.0805E+03
  12      12     12.00 %-QUANTILE =    1.0852E+03
  13      13     13.00 %-QUANTILE =    1.0853E+03
  14      14     14.00 %-QUANTILE =    1.0876E+03
  15      14     15.00 %-QUANTILE =    1.0876E+03
  16      15     16.00 %-QUANTILE =    1.0884E+03
  17      16     17.00 %-QUANTILE =    1.0907E+03
  18      17     18.00 %-QUANTILE =    1.0908E+03
  19      18     19.00 %-QUANTILE =    1.0935E+03
  20      19     20.00 %-QUANTILE =    1.0935E+03
  21      20     21.00 %-QUANTILE =    1.0936E+03
  22      21     22.00 %-QUANTILE =    1.0937E+03
  23      22     23.00 %-QUANTILE =    1.0948E+03
```

24	23	24.00	%-QUANTILE =	1.0953E+03
25	24	25.00	%-QUANTILE =	1.0968E+03
26	25	26.00	%-QUANTILE =	1.0970E+03
27	26	27.00	%-QUANTILE =	1.0970E+03
28	27	28.00	%-QUANTILE =	1.0978E+03
29	27	29.00	%-QUANTILE =	1.0978E+03
30	28	30.00	%-QUANTILE =	1.1000E+03
31	29	31.00	%-QUANTILE =	1.1003E+03
32	30	32.00	%-QUANTILE =	1.1005E+03
33	31	33.00	%-QUANTILE =	1.1008E+03
34	32	34.00	%-QUANTILE =	1.1008E+03
35	33	35.00	%-QUANTILE =	1.1009E+03
36	34	36.00	%-QUANTILE =	1.1014E+03
37	35	37.00	%-QUANTILE =	1.1021E+03
38	36	38.00	%-QUANTILE =	1.1068E+03
39	37	39.00	%-QUANTILE =	1.1082E+03
40	38	40.00	%-QUANTILE =	1.1095E+03
41	39	41.00	%-QUANTILE =	1.1107E+03
42	40	42.00	%-QUANTILE =	1.1113E+03
43	40	43.00	%-QUANTILE =	1.1113E+03
44	41	44.00	%-QUANTILE =	1.1116E+03
45	42	45.00	%-QUANTILE =	1.1124E+03
46	43	46.00	%-QUANTILE =	1.1126E+03
47	44	47.00	%-QUANTILE =	1.1143E+03
48	45	48.00	%-QUANTILE =	1.1159E+03
49	46	49.00	%-QUANTILE =	1.1161E+03
50	47	50.00	%-QUANTILE =	1.1164E+03
51	48	51.00	%-QUANTILE =	1.1169E+03
52	49	52.00	%-QUANTILE =	1.1188E+03
53	50	53.00	%-QUANTILE =	1.1191E+03
54	51	54.00	%-QUANTILE =	1.1194E+03
55	52	55.00	%-QUANTILE =	1.1205E+03
56	53	56.00	%-QUANTILE =	1.1208E+03
57	54	57.00	%-QUANTILE =	1.1219E+03
58	54	58.00	%-QUANTILE =	1.1219E+03
59	55	59.00	%-QUANTILE =	1.1223E+03
60	56	60.00	%-QUANTILE =	1.1229E+03
61	57	61.00	%-QUANTILE =	1.1233E+03
62	58	62.00	%-QUANTILE =	1.1242E+03
63	59	63.00	%-QUANTILE =	1.1242E+03
64	60	64.00	%-QUANTILE =	1.1285E+03
65	61	65.00	%-QUANTILE =	1.1295E+03
66	62	66.00	%-QUANTILE =	1.1296E+03
67	63	67.00	%-QUANTILE =	1.1296E+03
68	64	68.00	%-QUANTILE =	1.1306E+03
69	65	69.00	%-QUANTILE =	1.1307E+03
70	66	70.00	%-QUANTILE =	1.1316E+03
71	67	71.00	%-QUANTILE =	1.1318E+03
72	67	72.00	%-QUANTILE =	1.1318E+03
73	68	73.00	%-QUANTILE =	1.1347E+03
74	69	74.00	%-QUANTILE =	1.1353E+03
75	70	75.00	%-QUANTILE =	1.1354E+03
76	71	76.00	%-QUANTILE =	1.1355E+03
77	72	77.00	%-QUANTILE =	1.1359E+03
78	73	78.00	%-QUANTILE =	1.1381E+03

```
  79      74     79.00 %-QUANTILE =    1.1392E+03
  80      75     80.00 %-QUANTILE =    1.1427E+03
  81      76     81.00 %-QUANTILE =    1.1429E+03
  82      77     82.00 %-QUANTILE =    1.1437E+03
  83      78     83.00 %-QUANTILE =    1.1453E+03
  84      79     84.00 %-QUANTILE =    1.1457E+03
  85      80     85.00 %-QUANTILE =    1.1457E+03
  86      80     86.00 %-QUANTILE =    1.1457E+03
  87      81     87.00 %-QUANTILE =    1.1495E+03
  88      82     88.00 %-QUANTILE =    1.1513E+03
  89      83     89.00 %-QUANTILE =    1.1542E+03
  90      84     90.00 %-QUANTILE =    1.1544E+03
  91      85     91.00 %-QUANTILE =    1.1554E+03
  92      86     92.00 %-QUANTILE =    1.1572E+03
  93      87     93.00 %-QUANTILE =    1.1619E+03
  94      88     94.00 %-QUANTILE =    1.1697E+03
  95      89     95.00 %-QUANTILE =    1.1762E+03
  96      90     96.00 %-QUANTILE =    1.1812E+03
  97      91     97.00 %-QUANTILE =    1.1828E+03
  98      92     98.00 %-QUANTILE =    1.1843E+03
  99      93     99.00 %-QUANTILE =    1.1869E+03
                        MAXIMUM =    1.1869E+03

         SAMPLE MEAN               =    1.1175E+03
         SAMPLE STANDARD DEVIATION =    2.8699E+01

FITTED DISTRIBUTION TO DATA OF CONSEQUENCE NO.   1
**************************************************
 N O R M A L  DISTRIBUTION
 WITH MY =  1.1175E+03, SIGMA =  2.8699E+01
 ( NOT TRUNCATED )

RESULTS OF THE KOLMOGOROV-SMIRNOV-TEST FOR GOODNESS-OF-FIT
----------------------------------------------------------
(PARAMETERS ESTIMATED FROM THE SAME SAMPLE !!!)
 KOLMOGOROV-SMIRNOV-D-STATISTICS =   8.1345E-02
 CORRESPONDING LEVEL OF SIGNIFICANCE =   5.6962E-01

 SELECTED QUANTILES OF THE FITTED DISTRIBUTION
 ---------------------------------------------
  1.00 %-QUANTILE =    1.0508E+03
  5.00 %-QUANTILE =    1.0703E+03
 10.00 %-QUANTILE =    1.0808E+03
 20.00 %-QUANTILE =    1.0934E+03
 30.00 %-QUANTILE =    1.1025E+03
 40.00 %-QUANTILE =    1.1103E+03
 50.00 %-QUANTILE =    1.1175E+03
 60.00 %-QUANTILE =    1.1248E+03
 70.00 %-QUANTILE =    1.1326E+03
 80.00 %-QUANTILE =    1.1417E+03
 90.00 %-QUANTILE =    1.1543E+03
 95.00 %-QUANTILE =    1.1647E+03
 99.00 %-QUANTILE =    1.1843E+03

FITTED DISTRIBUTION TO DATA OF CONSEQUENCE NO.   1
```

```
**************************************************
 L O G N O R M A L  DISTRIBUTION
 WITH MY =  7.0186E+00, SIGMA =  2.5574E-02
 ( NOT TRUNCATED )

RESULTS OF THE KOLMOGOROV-SMIRNOV-TEST FOR GOODNESS-OF-FIT
------------------------------------------------------------
(PARAMETERS ESTIMATED FROM THE SAME SAMPLE !!!)
 KOLMOGOROV-SMIRNOV-D-STATISTICS =   7.9045E-02
 CORRESPONDING LEVEL OF SIGNIFICANCE =   6.0653E-01

 SELECTED QUANTILES OF THE FITTED DISTRIBUTION
 ---------------------------------------------
  1.00 %-QUANTILE =    1.0526E+03
  5.00 %-QUANTILE =    1.0712E+03
 10.00 %-QUANTILE =    1.0812E+03
 20.00 %-QUANTILE =    1.0934E+03
 30.00 %-QUANTILE =    1.1023E+03
 40.00 %-QUANTILE =    1.1100E+03
 50.00 %-QUANTILE =    1.1172E+03
 60.00 %-QUANTILE =    1.1244E+03
 70.00 %-QUANTILE =    1.1323E+03
 80.00 %-QUANTILE =    1.1415E+03
 90.00 %-QUANTILE =    1.1544E+03
 95.00 %-QUANTILE =    1.1652E+03
 99.00 %-QUANTILE =    1.1857E+03

FITTED DISTRIBUTION TO DATA OF CONSEQUENCE NO.   1
**************************************************
 U N I F O R M  DISTRIBUTION
 BETWEEN   1.0603E+03 AND   1.1883E+03

RESULTS OF THE KOLMOGOROV-SMIRNOV-TEST FOR GOODNESS-OF-FIT
------------------------------------------------------------
(PARAMETERS ESTIMATED FROM THE SAME SAMPLE !!!)
 KOLMOGOROV-SMIRNOV-D-STATISTICS =   1.9308E-01
 CORRESPONDING LEVEL OF SIGNIFICANCE =   1.9475E-03

 SELECTED QUANTILES OF THE FITTED DISTRIBUTION
 ---------------------------------------------
  1.00 %-QUANTILE =    1.0616E+03
  5.00 %-QUANTILE =    1.0667E+03
 10.00 %-QUANTILE =    1.0731E+03
 20.00 %-QUANTILE =    1.0859E+03
 30.00 %-QUANTILE =    1.0987E+03
 40.00 %-QUANTILE =    1.1115E+03
 50.00 %-QUANTILE =    1.1243E+03
 60.00 %-QUANTILE =    1.1371E+03
 70.00 %-QUANTILE =    1.1499E+03
 80.00 %-QUANTILE =    1.1627E+03
 90.00 %-QUANTILE =    1.1755E+03
 95.00 %-QUANTILE =    1.1819E+03
 99.00 %-QUANTILE =    1.1870E+03

FITTED DISTRIBUTION TO DATA OF CONSEQUENCE NO.   1
```

```
*****************************************************
 L O G - T R I A N G U L A R  DISTRIBUTION
 BETWEEN   1.0617E+03 AND   1.1869E+03 WITH EXP(LOG-PEAK) AT   1.1065E+03

RESULTS OF THE KOLMOGOROV-SMIRNOV-TEST FOR GOODNESS-OF-FIT
-----------------------------------------------------------
(PARAMETERS ESTIMATED FROM THE SAME SAMPLE !!!)
 KOLMOGOROV-SMIRNOV-D-STATISTICS =   7.3853E-02
 CORRESPONDING LEVEL OF SIGNIFICANCE =   6.9082E-01

 SELECTED QUANTILES OF THE FITTED DISTRIBUTION
 ---------------------------------------------
  1.00 %-QUANTILE =    1.0689E+03
  5.00 %-QUANTILE =    1.0779E+03
 10.00 %-QUANTILE =    1.0847E+03
 20.00 %-QUANTILE =    1.0944E+03
 30.00 %-QUANTILE =    1.1019E+03
 40.00 %-QUANTILE =    1.1083E+03
 50.00 %-QUANTILE =    1.1150E+03
 60.00 %-QUANTILE =    1.1223E+03
 70.00 %-QUANTILE =    1.1308E+03
 80.00 %-QUANTILE =    1.1409E+03
 90.00 %-QUANTILE =    1.1542E+03
 95.00 %-QUANTILE =    1.1637E+03
 99.00 %-QUANTILE =    1.1765E+03
```

APPENDIX G SAMOS.PRN

```
Uncertainty and Sensitivity Analysis


 DATE: 2012/03/30
 TIME:     09:59

 CURRENT NUMBER OF PARAMETERS   =     9
 CURRENT SAMPLE SIZE            =    93
 CURRENT NUMBER OF CONSEQUENCES =    36

 NUMBER OF ADMITTED CONSEQUENCES :
    1
 INDICES OF ADMITTED CONSEQUENCES :
    1
 INDEX OF TRANSFORMATION OF ADMITTED CONSEQUENCES :
    0

 NUMBER OF ADMITTED PARAMETERS :
    8
 INDICES OF ADMITTED PARAMETERS :
    1    2    3    4    5    6    8    9

 NUMBER OF SENSITIVITY MEASURES TO BE PLOTTED :
    0


TRANSFORM.-TYPE=  0 , CONSEQUENCE NO.=   1

ORDERED SENSITIVITY MEASURES FROM ORDINARY CORRELATIONS
------------------------------------------------------------
 CURRENT NUMBER OF PARAMETERS =    8
 CURRENT SAMPLE SIZE          =   93

       ORDINARY           PARTIAL            STD.REGR.
  #    CC         PAR.NO  CC         PAR.NO  FROM CC   PAR.NO

  1   -7.4877E-01    6   -9.9920E-01    6   -6.1222E-01    6
  2    6.2070E-01    9    9.9838E-01    9    4.3565E-01    9
  3    5.2325E-01    5    9.9688E-01    5    3.2136E-01    5
  4    2.8104E-01    2    9.9627E-01    2    2.7800E-01    2
  5   -2.5170E-01    3   -9.5269E-01    8   -7.6084E-02    8
  6    1.3701E-01    1   -9.4883E-01    3   -7.4161E-02    3
  7   -8.3884E-02    4    2.0496E-01    4    5.0635E-03    4
  8   -8.0042E-02    8    1.4600E-03    1    3.5640E-05    1

 R**2  OF THE CORRELATION-MATRIX  =   9.9944E-01
```

APPENDIX H DAKOTA REPORT

General

Error Handling	Ignore model check errors
Total Tasks	93
Successful Tasks	93
Random Seed	666674 (system-generated)
Sampling Method	Monte-Carlo
Order	1
Probability	95.0%
Confidence	95.0%

Results Matrix

ASV1
1833.249267578125
1930.962158203125

1.1 Response Function: ASVI1

Mean	1880.6939645
Standard Deviation	23.930941073
Coefficient of Variance	0.01272452697

95% Confidence Intervals

Mean	1875.7654456	1885.6224833
Standard Deviation	20.916625043	27.968357118

Cumulative Distribution Function

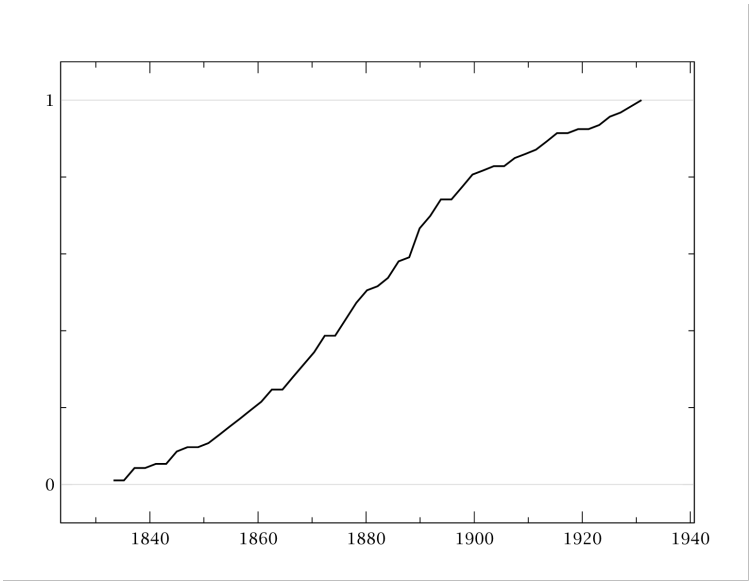

Response Correlations

	Simple	Partial	Simple Rank	Partial Rank
d1	0.763973	0.995819	0.759661	0.968054
d2	-0.0294279	0.144264	-0.00532661	0.0893693
d3	-0.113314	-0.79554	-0.11641	-0.369488
d4	0.636032	0.994048	0.630793	0.95478
d5	0.0450883	0.00679033	0.01125	-0.147751

Variable	Nominal	Distribution	Type	Adjustment	Parameters
spacer k loss factor	1.2	d1	Normal	Scalar	μ:1.2, σ:0.06, [1.14, 1.26]
wall rougness	2.5E-6	d2	Normal	Scalar	μ:2.5E-6, σ:1.25E-7, [2.38E-6, 2.53E-6]
inlet temperature	311.65	d3	Normal	Scalar	μ:311.65, σ:1.5, [310.15, 313.15]
mass flow	4.0277	d4	Normal	Scalar	μ:4.0277, σ:0.040277, [3.9875, 4.068]
outlet Pressure	2.0E5	d5	Normal	Scalar	μ:2.0E5, σ:2000.0, [1.98E5, 2.02E5]

Variate Data 1

Task	d1	d2	d3	d4	d5
1	1.159147282	2.41350726e-006	311.6157123	4.01805752	199679.2688
2	1.140580281	2.440686607e-006	310.5791366	4.01042388	198311.7162
3	1.183774516	2.467981742e-006	311.66213	4.008888063	200753.8198

Task	d1	d2	d3	d4	d5
4	1.254567857	2.397312291e-006	312.9951083	4.05421478	200725.8836
5	1.179015528	2.498942033e-006	310.8305097	4.014652344	201374.4395
6	1.217183749	2.381640664e-006	312.2962954	3.999774429	200646.8523
7	1.244098294	2.433406079e-006	310.419832	4.047694926	199748.4991
8	1.249676058	2.400160633e-006	311.7279177	4.056662259	201110.3817
9	1.191915532	2.428348731e-006	311.018016	4.008243881	199420.4141
10	1.196343206	2.447372578e-006	311.450467	4.031451431	201926.9268
11	1.210231613	2.419942869e-006	310.2469775	4.022415989	200012.6859
12	1.207410841	2.445885685e-006	310.4539735	4.042560128	198041.8542
13	1.169521818	2.381265429e-006	311.7022163	4.005767541	199470.6716
14	1.196277034	2.442382506e-006	310.70055	4.009077772	199672.0975
15	1.228678798	2.480529445e-006	310.5757818	4.013589268	199266.5988
16	1.158642504	2.464062971e-006	312.6503333	4.053142891	201365.2021
17	1.226548821	2.516986142e-006	311.652484	4.025791021	198765.1706
18	1.231635709	2.437499846e-006	312.5422494	4.019450335	199916.9608
19	1.225497991	2.516020578e-006	310.7045158	4.016074893	198823.5882
20	1.17228859	2.457294839e-006	311.1941262	3.997157162	201609.272
21	1.23947838	2.450469555e-006	310.5512761	4.062337962	200542.7174
22	1.210998283	2.490109423e-006	311.872142	4.051785577	198310.4498
23	1.254310581	2.482112245e-006	311.7417967	4.01077094	200003.3182
24	1.232111576	2.457043241e-006	310.7696093	4.037061209	199824.8352
25	1.202083796	2.522679596e-006	311.8212604	4.024132226	199330.8478
26	1.202299707	2.502838457e-006	311.7050961	3.996853469	199124.615
27	1.240500989	2.488351494e-006	310.4896208	4.031020564	200741.5426
28	1.161956351	2.463548047e-006	312.2665848	4.002305522	198809.0911
29	1.15002278	2.414515161e-006	310.5565587	4.051105899	201010.664
30	1.228788002	2.462730946e-006	311.9759123	4.002465142	198048.4394
31	1.172507784	2.439979243e-006	310.3445121	4.045835455	200929.8451
32	1.16274216	2.436677945e-006	310.8495717	4.052950386	198641.8908
33	1.163404786	2.448952579e-006	312.5822833	4.055311234	200710.9627
34	1.19363736	2.4407332e-006	310.7386866	4.04440186	201337.7593
35	1.156385116	2.443376736e-006	311.8955817	4.002870577	201142.5775
36	1.229423861	2.484883852e-006	311.3271903	4.000504766	198420.624
37	1.230494371	2.439937582e-006	311.7844628	4.03095448	199689.6207
38	1.249186462	2.526691404e-006	312.5467961	4.028011815	200876.8773
39	1.1673434	2.486111064e-006	312.7224697	4.020497728	198988.6399
40	1.16423133	2.522221303e-006	312.4896303	4.049045499	199894.4426
41	1.178605923	2.470474519e-006	310.3619594	4.007358948	198846.1086

Task	d1	d2	d3	d4	d5
42	1.204764185	2.521025227e-006	310.2319293	4.056213847	200053.1158
43	1.23830385	2.493262945e-006	311.7110348	4.04915204	201195.4523
44	1.218549784	2.416811688e-006	310.5333318	4.014152869	199978.6343
45	1.200021797	2.450077201e-006	312.3524759	4.050320317	199519.9327
46	1.221765269	2.499322638e-006	312.8781127	4.03964463	201312.8011
47	1.211701304	2.518066864e-006	311.3942794	4.022256282	198041.8849
48	1.252444682	2.448642923e-006	311.7656376	4.048493204	200997.5058
49	1.174019596	2.420912562e-006	311.5015568	4.027505964	199923.8011
50	1.220077612	2.486782123e-006	311.3040702	4.026990518	200591.0934
51	1.180490223	2.395853495e-006	311.8770006	4.000823229	199240.1799
52	1.208376032	2.524637061e-006	310.6062005	4.005596217	201133.0435
53	1.225807226	2.515448503e-006	312.9513124	3.995255399	198552.7244
54	1.199700711	2.410784885e-006	310.3280243	4.026027434	199924.0856
55	1.151178144	2.431500469e-006	312.9397554	4.053789588	199530.9724
56	1.221949562	2.393842915e-006	311.5173876	4.012490291	200774.8046
57	1.194827188	2.443084275e-006	312.1149313	4.024035773	201431.4216
58	1.216611366	2.44225905e-006	312.5725676	4.065433359	198700.887
59	1.178958521	2.480195941e-006	310.3771229	4.066184681	199449.9095
60	1.254198012	2.395136977e-006	313.0961165	4.038898077	199720.0463
61	1.212774039	2.384986595e-006	311.6093553	4.01914102	198464.9359
62	1.245112926	2.383704995e-006	311.7856871	4.005556055	200890.4162
63	1.196573187	2.382105708e-006	310.6735401	4.006064372	200280.7129
64	1.177365087	2.467890752e-006	311.784395	4.001455371	201508.6504
65	1.195789659	2.392392496e-006	312.7900573	4.047265836	200137.1734
66	1.221721993	2.474430903e-006	311.8934408	4.021992312	200460.6741
67	1.236427478	2.474353577e-006	311.5493739	3.988591843	200465.2532
68	1.242977798	2.435275776e-006	311.1100819	4.023985526	198295.216
69	1.188578191	2.49716266e-006	311.6175088	4.009136206	200986.7938
70	1.200070251	2.512374927e-006	312.6671969	4.011062819	200670.4871
71	1.171520062	2.450486078e-006	313.0965151	4.063208392	200204.9271
72	1.252990503	2.381264575e-006	311.3799446	4.048431681	198725.0763
73	1.245641287	2.441558862e-006	311.2924641	4.038497292	198598.6882
74	1.220183188	2.435540174e-006	311.4759517	3.993550924	200084.7291
75	1.207060719	2.393156398e-006	311.155557	4.040436454	199941.8642
76	1.225528296	2.503549564e-006	312.2459477	4.017101359	198853.6507
77	1.168121787	2.514209322e-006	312.7066144	3.995907751	199403.9034
78	1.173906934	2.435796224e-006	311.43329	4.013397955	198180.3021
79	1.204945456	2.509581228e-006	312.7614165	4.031807069	199016.9069

Task	d1	d2	d3	d4	d5
80	1.140466754	2.455592014e-006	310.9456994	4.049376788	200571.6432
81	1.185470414	2.3873701e-006	311.9450572	4.043927376	200100.6533
82	1.166923317	2.44067852e-006	311.6792041	4.02554793	198372.2961
83	1.241680803	2.429272926e-006	310.3971516	4.032208829	201432.7699
84	1.232028194	2.523661735e-006	310.1836821	4.06106545	200855.7882
85	1.177913604	2.473537202e-006	312.0595841	4.013136751	198408.4456
86	1.18142858	2.450264936e-006	311.9427259	4.063318637	198664.0121
87	1.203976444	2.484549815e-006	310.6574562	3.994142626	200297.2561
88	1.21735519	2.504901872e-006	311.8075461	4.014718318	201785.7967
89	1.173233238	2.433296083e-006	312.5010559	4.011062844	201055.5127
90	1.246597486	2.416417399e-006	312.7670575	4.009882403	199281.5335
91	1.20733848	2.458149972e-006	310.5739985	4.041158782	198261.7171
92	1.244646178	2.425144579e-006	311.070924	4.009238202	200815.2835
93	1.184760093	2.476395829e-006	312.3601637	4.064502643	199616.7621

DAKOTA Input File

The input file used in a -pre_run DAKOTA invocation to generate the random variates.

```
strategy,
   single_method

method,
   nond_sampling,
        samples = 93
        # stub response levels
        response_levels = 0.0 1.0
        sample_type random
        distribution cumulative

variables,
   normal_uncertain     = 5
        descriptors      = 'd1'  'd2'  'd3'  'd4'  'd5'
        means            = 1.2  2.5E-6  311.65  4.0277  2.0E5
        std_deviations   = 0.06  1.25E-7  1.5  0.040277  2000.0
        lower_bounds     = 1.14  2.38E-6  310.15  3.9875  1.98E5
        upper_bounds     = 1.26  2.53E-6  313.15  4.068  2.02E5

interface,
   system
        analysis_driver = '<not used>'

responses,
   num_response_functions = 1
   no_gradients
   no_hessians
```

NRC FORM 335
(12-2010)
NRCMD 3.7

U.S. NUCLEAR REGULATORY COMMISSION

BIBLIOGRAPHIC DATA SHEET

(See instructions on the reverse)

1. REPORT NUMBER
(Assigned by NRC, Add Vol., Supp., Rev., and Addendum Numbers, if any.)

NUREG/IA-0462

2. TITLE AND SUBTITLE

Uncertainty and Sensitivity Investigations with TRACE-SUSA and TRACE-DAKOTA by Means of Post-test Calculations of NUPEC BFBT Experiments

3. DATE REPORT PUBLISHED

MONTH	YEAR
August	2017

4. FIN OR GRANT NUMBER

5. AUTHOR(S)

Wadim Jaeger, Victor Hugo Sanchez Espinoza*

Francisco Javier Montero Mayorga, Cears Queral**

6. TYPE OF REPORT

Technical

7. PERIOD COVERED (Inclusive Dates)

8. PERFORMING ORGANIZATION - NAME AND ADDRESS (If NRC, provide Division, Office or Region, U. S. Nuclear Regulatory Commission, and mailing address; if contractor, provide name and mailing address.)

*Karlsruher Institute of Technology (KIT)
Institute for Neutron Physics and Reactor Technology (INR)
Hermann-von-Helmholtz-Platz 1
76344, Eggenstein-Leopoldshafen, Germany

**Universidad Politecnica de Madrd
Departamento de Sistemas Energeticos ETSI Minas
28003 Madrid, Alenza 4, Spain

9. SPONSORING ORGANIZATION - NAME AND ADDRESS (If NRC, type "Same as above", if contractor, provide NRC Division, Office or Region, U. S. Nuclear Regulatory Commission, and mailing address.)

Division of Systems Analysis
Office of Nuclear Regulatory Research
U.S. Nuclear Regulatory Commission
Washington, DC 20555-0001

10. SUPPLEMENTARY NOTES

K.Tien, NRC Project Manager

11. ABSTRACT (200 words or less)

Uncertainty and sensitivity investigations are performed with TRACE-SUSA and with TRACE-DAKOTA for thermal hydraulic simulations of selected BWR related experimental scenarios based on the NUPEC BFBT data base. Steady state as well as transient scenarios are selected to conduct a comprehensive investigation of BWR like phenomena. The steady state investigations include single and two phase flow pressure drop analyses, axial void fraction profiles and critical power predictions. The pressure losses and the void fractions are also predicted during two postulated BWR transients; a turbine trip and a trip of a re-circulation pump. The average error for the pressure losses, the void fractions and the critical power scenarios is in the order of ± 5 %. Parameters of the input and of the source code are selected for the uncertainty and sensitivity study. By means of sensitivity coefficients, a quantitative way of evaluating the system response is given. The analysis shows that even small variations can cause a rather large spread of the output parameter(s). The investigations show also that the width of the predicted uncertainty band is a function of parameters like the inlet sub cooling or the hydraulic diameter. In addition, shortcomings of the thermal hydraulic code/modeling or of the uncertainty and sensitivity tool(s) are given in order to help to improve the prediction capabilities.

12. KEY WORDS/DESCRIPTORS (List words or phrases that will assist researchers in locating the report.)

Atomic Energy Authority Winfrith (AEAW)
BWR Full-size Fine mesh Bundle Test (BFBT)
Design Analysis Kit for Optimization and Terascale Application (DAKOTA)
Software system for Uncertainty and Sensitivity Analysis (SUSA)
Code Scaling, Applicability and Uncertainty (CSAU)
Deutscher Akademischer Austausch Dienst (DAAD)
Nuclear Power Engineering Corporation (NUPEC)
Uncertainty Methodology based on Accuracy Extrapolation (UMAE)

13. AVAILABILITY STATEMENT

unlimited

14. SECURITY CLASSIFICATION

(This Page)
unclassified

(This Report)
unclassified

15. NUMBER OF PAGES

16. PRICE

Federal Recycling Program

UNITED STATES
NUCLEAR REGULATORY COMMSSION
WASHINGTON, DC 20555-0001

OFFICIAL BUSINESS

NUREG/IA-0462

Uncertainty and Sensitivity Invetigations with TRACE-SUSA and TRACE-DAKOTA by Means of Post-test Calculations of NUPEC BFBT Experiments

August 2017